



BINDING SERVICES
Tel +44 (0)29 2087 4949
Fax +44 (0)29 20371921
e-mail bindery@cardiff.ac.uk

**INVESTIGATION OF FACTORS
AFFECTING SKIN PENETRATION
*IN VITRO***

by

Darren Michael Green

A thesis submitted to the University of Wales in
accordance with the requirements for the degree of
Doctor of Philosophy

Welsh School of Pharmacy,
Cardiff University
October 2005

UMI Number: U207220

All rights reserved

INFORMATION TO ALL USERS

The quality of this reproduction is dependent upon the quality of the copy submitted.

In the unlikely event that the author did not send a complete manuscript and there are missing pages, these will be noted. Also, if material had to be removed, a note will indicate the deletion.



UMI U207220

Published by ProQuest LLC 2013. Copyright in the Dissertation held by the Author.
Microform Edition © ProQuest LLC.

All rights reserved. This work is protected against
unauthorized copying under Title 17, United States Code.



ProQuest LLC
789 East Eisenhower Parkway
P.O. Box 1346
Ann Arbor, MI 48106-1346

Acknowledgements

I would like to sincerely thank my employers, An-eX analytical services ltd., for providing me with the opportunity to pursue this research on a part-time basis.

I am indebted to my supervisor, Dr Keith R. Brain, for providing guidance and personal support over many challenging years. I would also like to extend my thanks to both current and former colleagues at An-eX: Kenneth A. Walters, Adam. C. Watkinson, Sally I. Brain, Brenda Williams and the late Valerie J. James.

I would also like to thank OmniPharm Research International Inc. for providing several novel compounds assessed in this research, and Cutest systems ltd. for providing skin surface biopsies.

Special thanks go to my wife, Jo, and my parents for so wonderfully looking after my children, Jamie and Abby, whilst I was occupied with writing this thesis. I must also thank Jo for proof reading the final draft.

Finally, I would like to thank Professor Paul Spencer, OBE, who first suggested applying to An-eX for a summer post, whilst I was an undergraduate. Without this intervention, I would not have found a career that has kept my interest for the past 11 years.

This work is dedicated to my fantastic wife, Jo.

Abstract

In vitro human skin permeation evaluations have received more widespread international scientific acceptance due to the recent publication of OECD guideline 428. However many significant issues remain unresolved. When desirable retardation of skin penetration of toxic compounds such as pesticides and chemical warfare agents was evaluated using model permeants, retardation was observed under certain conditions, but was not predictable. It was concluded that generic penetration modulation was not a realistic goal. Investigations into skin surface sampling techniques highlighted the difficulties of minimising variability, and comparison of *in vitro* tape stripping with published *in vivo* data for a clobetasol propionate cream demonstrated the significance of formulation inhomogeneity. Determination of orally administered doxycycline in the stratum corneum using *in vivo* skin surface biopsies suggested that it was unlikely that this technique could be of value for most orally administered drugs. Evaporative loss of volatile permeants, such as fragrances, during skin penetration studies makes it impossible to achieve full mass balance. Direct capture of evaporating material was occlusive and significantly affected the amount that permeated through the skin membranes. A simple novel method was therefore developed to allow estimation of evaporative loss under the experimental conditions. Pre-study skin water permeability coefficient (k_p) is frequently used as a membrane integrity check and it is generally assumed that skin of higher water permeability will be of higher permeability for subsequently applied compounds, regardless of differing physicochemical properties. However, it was shown that k_p did not correlate with subsequent test compound permeation for twelve compounds of moderate to high lipophilicity. Furthermore the k_p limit used to reject 'damaged' skin (2.5×10^{-3} cm/h) did not provide discrimination between normal and damaged membranes, and raised significant issues as to what should be considered 'normal' barrier function.

Abbreviations

ACN	Acetonitrile
ANOVA	Analysis of variance
ATR-FTIR	Attenuated Total Reflectance Fourier transform Infra-Red spectroscopy
Azone	Laurocapram, 1-dodecylaza-cycloheptan-2-one
b.p.	Boiling point
^{14}C	Carbon-14
CP	Clobetasol propionate
d^{25}	Density at 25°C
DEET	N,N-diethyl- <i>m</i> -toluamide
δ	Solubility parameter
DPM	Disintegrations per minute
DPPC	Dipalmitoyl phosphatidylcholine
EHD	2-ethyl-1,3-hexanediol
EPBS	25% (v/v) ethanol/PBS
ER	Enhancement ratio
FL	Fluorescence
HC	Hydrocortisone
$^3\text{H}_2\text{O}$	Tritiated water
HPLC	High performance liquid chromatography
IMS	Industrial methylated spirit
IPM	Isopropylmyristate
$K_{o/w}$	n-octanol/water partition coefficient
k_p	Permeability coefficient
LSC	Liquid scintillation counting
M	Molar
m.p.	Melting point
ME	Methyl eugenol
MP	Mobile phase
M_w	Molecular weight

n	Number of replicates
PBS	Phosphate buffered saline (pH 7.4)
PG	Propylene glycol
PTFE	Polytetrafluoroethylene
r	Correlation coefficient (linear fit)
RSD	Relative standard deviation
SC	Stratum corneum
SE	Standard error
SEPA 0009	Soft Enhancement of Percutaneous Absorption compound 0009
SSB	Skin surface biopsies
t	Time
TA	Triamcinolone acetonide
TEWL	Transepidermal water loss
TFA	Trifluoroacetic acid
UV	Ultraviolet
UV-Vis	Ultraviolet-Visible
v/v	Volume/volume ratio
w/v	Weight/volume ratio
w/w	Weight /weight ratio

Contents

Declaration	i
Acknowledgements	ii
Dedication	iii
Abstract	iv
Abbreviations	v
Contents	vii

Chapter 1

General Introduction

1.1	Introduction	1
1.2	Structure of human skin	2
1.2.1	Hypodermis	3
1.2.2	Dermis	3
1.2.3	Epidermis	4
1.2.3.1	Basal layer	5
1.2.3.2	Spinous layer	5
1.2.3.3	Granular layer	6
1.2.3.4	Stratum lucidum	6
1.2.3.5	Transition layer	6
1.2.3.6	Cornified layer (Stratum corneum (SC))	6
1.2.4	Skin appendages	9
1.2.4.1	Sweat glands	9
1.2.4.2	Pilosebaceous units	10
1.3	Routes of percutaneous penetration	10
1.3.1	Introduction	10
1.3.2	Intercellular route	12
1.3.3	Transcellular route	12
1.3.4	Transappendageal route	13

1.4	Theoretical concepts in percutaneous penetration	14
1.4.1	Diffusional calculations	15
1.4.2	Partition coefficient	17
1.4.3	Thermodynamic activity	17
1.4.4	Solubility parameters	18
1.4.5	Predictive models of skin permeation	19
1.5	Measurement of skin penetration <i>in vitro</i>	20
1.5.1	Diffusion cells	21
1.5.2	Skin membranes	23
1.5.3	Receptor media	25
1.5.4	Assessment of skin distribution of a permeant	26
1.5.5	Application of compounds to the skin surface	27
1.5.6	<i>In vivo in vitro</i> correlations	27
1.6	Variations in skin permeability	28
1.6.1	Inter-species differences in skin permeability	28
1.6.2	Variations in human skin permeability	29
1.7	Modification of skin penetration	30
1.8	Study objectives	31
1.9	References	32

Chapter 2

Chemical enhancement and retardation of skin permeation

2.1	Introduction	37
2.2	Specifically designed chemical enhancers	39
2.2.1	Azone and its analogues	39
2.2.2	SEPA	45
2.3	Specifically designed chemical retarders	46
2.3.1	MacroDerm compounds	46
2.3.2	TopiCare Delivery Compounds	47
2.3.3	Novel penetration retarders co-developed in our laboratory	48
2.4	References	50

Chapter 3

Investigations into the effect of retarder 4-F2 using the model permeant DEET

3.1	Introduction	53
	3.1.1 DEET	53
3.2	Assessment of the effect of skin pre-treatment with retarder 4-F2 on the human skin permeation and distribution of DEET	55
	3.2.1 Materials and equipment	55
	3.2.2 Methods	55
	3.2.2.1 Receptor phase preparation	55
	3.2.2.2 Vehicle preparation	56
	3.2.2.3 Skin preparation	57
	3.2.2.4 Diffusion cells	58
	3.2.2.5 Membrane integrity assessment	58
	3.2.2.6 Skin pre-treatment with 4-F2	59
	3.2.2.7 Application of DEET solution	59
	3.2.2.8 Determination of skin permeation	60
	3.2.2.9 Determination of skin distribution and DEET recovery	60
	3.2.2.10 Sample analysis and assay validation	61
	3.2.3 Results and discussion	65
3.3	Assessment of the effect of a reduced pre-treatment dose of retarder 4-F2 on the permeation of DEET through human skin	71
	3.3.1 Materials and equipment	72
	3.3.2 Methods	72
	3.3.2.2 Vehicle preparation	72
	3.3.2.3 Skin preparation	72
	3.3.2.5 Membrane integrity assessment	72
	3.3.2.6 Skin pre-treatment with 4-F2	73
	3.3.2.7 Application of DEET solution	73

3.3.2.8	Determination of skin permeation	73
3.3.2.9	Determination of skin distribution and DEET recovery	73
3.3.2.10	Sample analysis and assay validation	74
3.3.3	Results and discussion	74
3.4	Assessment of the effect of pre-treatment and co-administration of retarder 4-F2 on the permeation of DEET through human skin	78
3.4.1	Materials and equipment	79
3.4.2	Methods	79
3.4.2.2	Vehicle preparation	79
3.4.2.3	Skin preparation	80
3.4.2.5	Membrane integrity assessment	80
3.4.2.6	Skin pre-treatment with 4-F2	80
3.4.2.7	Application of DEET solutions	80
3.4.2.8	Determination of skin permeation	81
3.4.2.9	Determination of skin distribution and DEET recovery	81
3.4.2.10	Sample analysis and assay validation	81
3.4.3	Results and discussion	81
3.5	Examination of correlation between water permeability and DEET permeation	86
3.6	Conclusions	89
3.7	References	91

Chapter 4

Further investigations into the effect of retarder compounds using three model permeants

4.1	Introduction	92
4.1.1	Selected permeants study 1: glyphosate and water	93

4.2	Assessment of the effect of pre-treatment with retarders 4-F2, 2-F1, ORI-PR2 and ORI-PR3 on the human skin permeation of glyphosate and water	94
4.2.1	Materials and equipment	94
4.2.2	Methods	96
4.2.2.1	Receptor phase preparation	96
4.2.2.2	Vehicle preparation	96
4.2.2.3	Skin preparation	98
4.2.2.4	Diffusion cells	98
4.2.2.5	Membrane integrity assessment	99
4.2.2.6	Skin pre-treatment	100
4.2.2.7	Application of 0.1% ¹⁴ C-glyphosate in ³ H ₂ O solution	100
4.2.2.8	Determination of skin permeation	100
4.2.2.9	Determination of skin content and radiolabel recovery	100
4.2.3	Results and discussion	101
4.2.3.1	Glyphosate permeation data	101
4.2.3.2	Water permeation data	105
4.2.4	Conclusions	108
4.3	Assessment of the effect of pre-treatment with 4-F2 and 2-F1 on the human skin permeation of hydrocortisone and co-application of 4-F2 with hydrocortisone	109
4.3.1	Hydrocortisone	109
4.3.2	Materials and equipment	111
4.3.3	Methods	111
4.3.3.1	Receptor phase preparation	111
4.3.3.2	Vehicle preparation	111
4.3.3.3	Skin preparation	112
4.3.3.5	Membrane integrity assessment	113
4.3.3.6	Skin pre-treatment	113
4.3.3.7	Application of hydrocortisone in PG suspension	113

4.3.3.8	Determination of skin permeation	114
4.3.3.9	Sample analysis and assay validation	114
4.3.4	Results and discussion	119
4.4	Overall conclusions	124
4.5	References	125

Chapter 5

Investigation of skin surface sampling techniques

5.1	Introduction	127
5.2	Comparison of stripping efficiency for 3M Magic Tape and D-Squame	130
5.2.1	Introduction	130
5.2.2	Materials and equipment	131
5.2.3	Methods	132
5.2.3.1	Receptor phase preparation	132
5.2.3.2	Donor solution activity	132
5.2.3.3	Skin preparation and diffusion cells	132
5.2.3.4	Group allocation and skin treatment	132
5.2.3.5	Measurement of water permeation	133
5.2.4	Results and discussion	134
5.3	Tape stripping following application of a clobetasol propionate formulation	137
5.3.1	Introduction	137
5.3.2	Materials and equipment	138
5.3.3	Analytical method development and validation	138
5.3.4	Pilot <i>in vitro</i> stripping study	142
5.3.4.1	Methods	142
5.3.4.2	Results and discussion	143
5.3.5	<i>In vivo</i> tape stripping following application of Dermovate and assessment of formulation variability	144
5.3.5.1	<i>In vivo</i> tape stripping experiment 1	145

5.3.5.2	<i>In vivo</i> tape stripping experiment 2	146
5.3.5.3	Assessment of homogeneity of Dermovate formulation	147
5.3.5.4	<i>In vivo</i> tape stripping experiment 3	148
5.3.6	Conclusions	149
5.4	Weight of tissue removed by D-Squame	150
5.4.1	Methods	150
5.4.2	<i>In vivo</i> versus <i>in vitro</i> assessment 1	151
5.4.3	<i>In vivo</i> versus <i>in vitro</i> assessment 2	151
5.4.4	Conclusions	152
5.5	Skin surface biopsies (SSB)	153
5.5.1	Materials and equipment	155
5.5.2	Analytical method development and sample analysis	155
5.5.2.1	Analysis using UV-Vis detection	155
5.5.2.2	Analysis using fluorescence detection	158
5.5.2.3	Further analysis using UV-Vis detection	159
5.6	Overall conclusions	161
5.7	References	163

Chapter 6

Estimation of evaporative loss for volatile permeants

6.1	Introduction	165
6.2	Published reports on assessment of evaporative loss	166
6.3	Experimental methods for capturing evaporating material	168
6.3.1	Introduction	168
6.3.2	Materials and equipment	169
6.3.3	General methods	169
6.3.3.1	Vehicle preparation	169
6.3.3.2	Skin preparation	170
6.3.3.3	Diffusion cells and receptor phase	170

6.3.4	Evaporative loss trapping method 1	171
6.3.4.1	Trapping device and diffusion cell preparation	171
6.3.4.2	ME application and measurement of skin permeation	172
6.3.4.3	Recovery of applied ME from the skin, diffusion cell and trapping device	172
6.3.4.4	Results for trapping method 1	173
6.3.5	Evaporative loss trapping method 2	174
6.3.5.1	Trapping device and diffusion cell preparation	174
6.3.5.2	ME application and measurement of skin permeation	174
6.3.5.3	Recovery of applied ME from the skin, diffusion cell and trapping device	174
6.3.5.4	Results for trapping method 2	174
6.3.6	Evaporative loss trapping method 3	176
6.3.6.1	Trapping device and diffusion cell preparation	176
6.3.6.2	ME application and measurement of skin permeation	176
6.3.6.3	Recovery of applied ME from the skin, diffusion cell and trapping device	176
6.3.6.4	Results for trapping method 3	176
6.3.7	Evaporative loss trapping methods 4	178
6.3.7.1	Trapping device and diffusion cell preparation	178
6.3.7.2	ME application and measurement of skin permeation	179
6.3.7.3	Recovery of applied ME from the skin, diffusion cell and trapping device	179
6.3.7.4	Results for trapping methods 4	179
6.3.8	Conclusions	182
6.4	Simultaneous collection of evaporating material from several cells	183
6.5	Methods of estimating evaporative loss	184
6.5.1	Introduction	184

6.5.2	Materials and equipment	185
6.5.3	Evaporative loss method 1	185
6.5.3.1	Diffusion cell preparation and ME dosing	185
6.5.3.2	Cell sampling	185
6.5.3.3	Results for evaporative loss method 1	186
6.5.4	Evaporative loss method 2	186
6.5.4.1	Diffusion cell preparation and ME dosing	186
6.5.4.2	Cell sampling	186
6.5.4.3	Results for evaporative loss method 2	187
6.5.5	Evaporative loss method 3	187
6.5.5.1	Diffusion cell preparation and ME dosing	187
6.5.5.2	Cell sampling	188
6.5.5.3	Results for evaporative loss method 3	188
6.6	Comparison of the final estimation of evaporative loss method with fragrance material skin permeation	189
6.6.1	Fragrance 1 (very volatile)	190
6.6.2	Fragrance 2 (moderately volatile)	192
6.7	Conclusions	194
6.8	References	195

Chapter 7

Comparison between the pre-study water permeability of human skin membranes and subsequent permeation of alternative test compounds

7.1	Introduction	196
7.2	Review of published data	196
7.3	Comparison of water permeability and test compound permeation for studies in our laboratory	200
7.3.1	Methods of measurement of water permeability and test compound permeation	201
7.3.2	Methods of comparison	202

7.3.3	Results	205
7.3.3.1	Compounds of moderate to high lipophilicity	205
7.3.3.2	Compounds of low lipophilicity	209
7.3.3.3	Compounds applied in formulations containing a permeation enhancer	209
7.4	Conclusions	211
7.5	References	213

Chapter 8

General discussion

8.1	General discussion	214
-----	---------------------------	-----

Chapter 1

General Introduction

1.1 Introduction

Skin is the largest organ in the human body, amounting to more than 10% of body weight (Walters and Brain, 2001). It also has a large surface area of approximately 1.80 m² for a 65kg adult (Schaefer and Redelmeier, 1996a), although that is only a small proportion of the surface area of the lungs or intestines (~100 and ~300 m², respectively). The primary purpose is to provide a protective barrier to both the unwanted exit of internal fluids and the entry of external stimuli such as chemicals, micro-organisms and radiation. There are also many other important functions, including thermoregulation and excretion of waste products, and skin allows humans to interact with the environment through touch and the sense of heat and pain.

Whilst skin provides an effective and complex barrier, research into the nature of this barrier has helped lead to the availability of a wide range of drug treatments applied to the skin, for local or systemic effect. Whilst there would be benefits in delivering many drugs transdermally (for systemic effect), particularly due to the avoidance of first-pass metabolism, only a small proportion are capable of permeating through the skin to a therapeutic degree. Compounds that most efficiently penetrate the skin generally have relatively low molecular weight (typically less than 500 Daltons) and are both lipid and water soluble. Many potentially toxic compounds also fit these criteria, so the study of skin penetration is also of great importance in allowing the prevention of harmful exposure to external agents.

Although the physicochemical properties of the applied compound are of great significance in the skin absorption process, the effects of the formulation/vehicle are frequently large, and complex interactions between formulations and skin occur.

The penetration of exogenous compounds into, and permeation through, the skin, is controlled for most compounds by the stratum corneum (SC), the outermost layer of the skin. As the SC is non-viable, skin penetration can be accurately assessed *in vitro* for many compounds providing suitable protocols are used.

1.2 Structure of human skin

The skin (Figure 1.1) consists of three layers, the epidermis (including the outermost stratum corneum (SC)), dermis, and subcutaneous tissues (hypodermis). Skin morphology can best be described from the innermost layer out so that the process of SC formation can be followed. There are also a number of appendages, including hair follicles and sweat glands, associated with the skin.

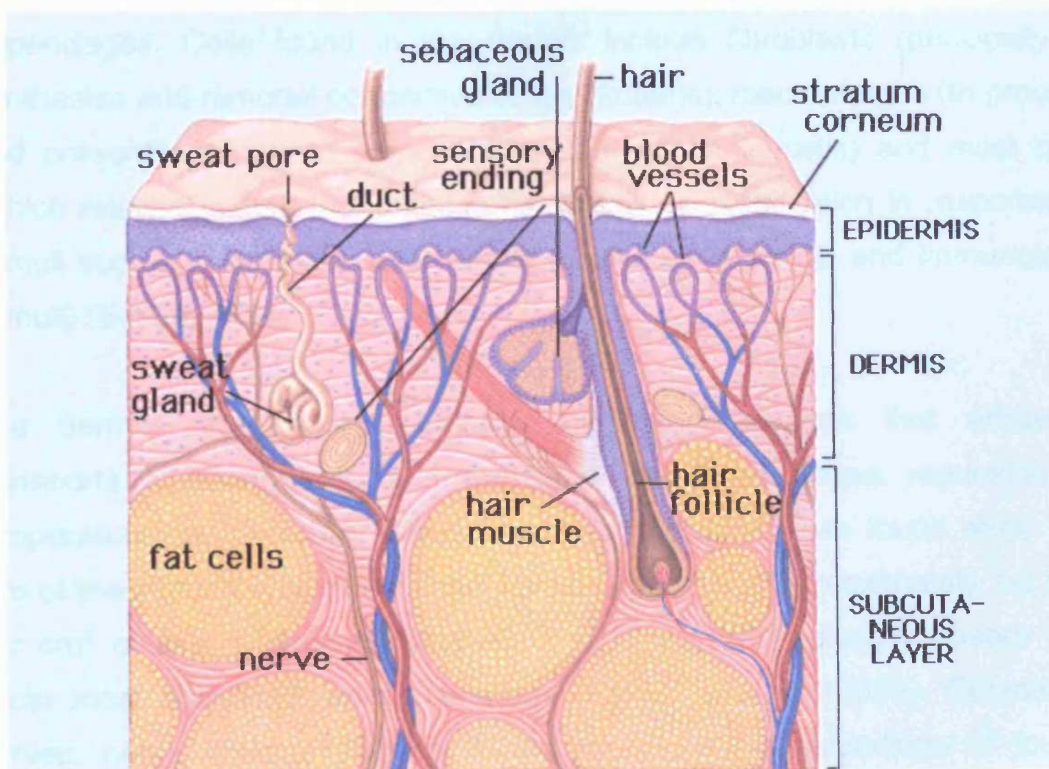


Figure 1.1 Structure of the skin (Madigan et al, 1997)

1.2.1 Hypodermis

The hypodermis mainly contains adipocytes (which specialise in storing energy as fat), and provides a cushion between the dermis and internal structures, such as muscle and bone, as well as insulating the body (Eckert, 1992). Collagen fibres provide flexible linkages between the dermis and underlying structures (Barry, 1983a). The thickness of the hypodermis varies greatly in thickness from site to site, individual to individual, and according to nutritional status.

1.2.2 Dermis

The dermis principally consists of a matrix of connective tissue woven from fibrous proteins and mucopolysaccharides (Barry, 1983a). It is typically 2-5 mm thick and provides physical support for the epidermis and skin appendages. Cells found in the dermis include fibroblasts (principally to synthesise and remodel connective tissue proteins), macrophages (to process and present antigens to immunocompetent lymphoid cells) and mast cells (which release factors that initiate chemotaxis or vasodilation in response to stimuli such as cold and acute trauma as well as chemical and immunologic stimuli) (Eckert, 1992).

The dermis contains an extensive circulatory network that efficiently transports compounds to and from the skin, and allows regulation of temperature and pressure. Blood vessels of the dermis are found within 0.2 mm of the surface and, with a vascular surface area of approximately 1-2 cm² per cm² of skin surface (Scheuplein and Blank 1971), readily absorb and dilute most chemicals which penetrate the SC (Barry, 1983a). Cutaneous nerves, nerve endings and capillaries modulate the sensations of touch, temperature and pain (Barry, 1983a).

The uppermost surface of the dermis contains protrusions (papillae) that intercalate with downward protrusions in the epidermis at the basal lamina,

the dermo-epidermal junction. The basal lamina can control the passage of very large molecules and diseases which operate at this level can markedly reduce epidermis/dermis adhesion (Barry, 1983a).

1.2.3 Epidermis

The epidermis is a complex multi-layered region of the skin, where the major cell type (>90%), keratinocytes, undergoes a programmed process of differentiation in which proliferative, metabolically active, basal cells are converted to highly differentiated non-dividing cells of dead, keratinized protein (corneocytes) (Eckert, 1992, Barry, 1983a). Several layers or zones are distinguishable (Figure 1.2), and these will be discussed below.

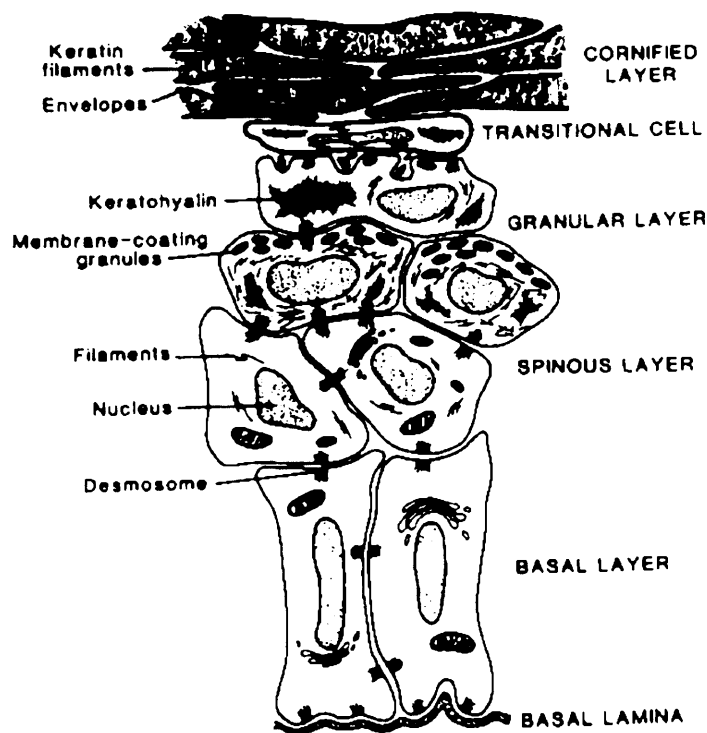


Figure 1.2 Structure of the epidermis (Eckert, 1992)

Epidermal thickness varies between about 60 and 800 μm (eyelid and soles, respectively) depending on cell size and number of layers, with a typical value of $\sim 100 \mu\text{m}$. The cornified layer, the SC, is 10-20 μm thick, consisting of 15-25 flattened and stacked cells (Walters and Brain, 2001).

The epidermis contains no vascular network, with cell nutrients supplied to the lower layers through diffusion from the dermis. The epidermis is under continual change, with cells typically proceeding from the basal layer to the surface over a period of three to four weeks (Odland, 1983), with the outmost layer being constantly shed. For the rapidly proliferating epidermis observed in psoriasis, this process can be as fast as 4 days (Barry, 1983a).

1.2.3.1 Basal layer

The basal cells are nucleated, columnar, with their long axis at right angles to the dermoepidermal junction (Barry, 1983a). Basal cells are anchored to the basal lamina via numerous hemidesmosomes, whilst desmosomes link the basal cells. Basal cells are constantly undergoing mitosis (cell nuclear division plus cytokinesis, which produces two identical daughter cells). The basal layer also contains melanocytes, which produce melanin in reaction to radiation exposure (e.g. sunlight), as the protective process of pigmentation. Melanocytes lose their activity in vitiligo, and hyperactive melanocytes produce tanning, freckles, moles and malignant melanomas (Barry, 1983a).

Basal cell proliferation is controlled by a variety of intrinsic and extrinsic factors (including epidermal growth factor, progesterone, vitamins A and D), and the dermis can also have a direct influence (observed following grafting) (Eckert, 1992).

1.2.3.2 Spinous layer

Immediately above the basal layer is the spinous layer, with cells containing spines (or prickles) caused by bundles of tonofilaments (tonofibrils) (Elias, 1989). Cells within the spinous layer are responsible for the synthesis of lamella granules, which are secretory organelles between 0.2 and 0.3 μm in length and are responsible for the production of the intercellular lipid matrix of the SC (Elias, 1989).

1.2.3.3 Granular layer

Cells in the stratum granulosum are in the final stage of differentiation prior to death. The layer is peppered with electron dense keratohyalin granules (Eckert, 1992). In the upper layers of the stratum granulosum, these lamellar granules migrate to the cell surface, fuse with the membrane and release their lipid content. Concurrently, cell nuclei shrink, and the cells become more flattened.

1.2.3.4 Stratum lucidum

The layer is only present in the palm and sole of the foot. It is thin and translucent and located immediately above the granular layer.

1.2.3.5 Transition layer

This is the point at which keratinocytes become corneocytes. The activity of proteases and nucleases destroys most of the cellular organelles, DNA and RNA (Eckert, 1992), cells lose their nuclei, and the lipid content of the lamellar bodies are extruded into the intercellular space. Keratin filaments are restructured to a more stable form and the cornified envelope is formed around them (Eckert, 1992).

1.2.3.6 Cornified layer (Stratum corneum (SC))

The stratum corneum (SC) is the outermost layer of the epidermis and is composed of corneocytes that are parallel to the SC surface (van Hal et al, 1996) embedded in a complex intercellular lipid (Elias, 1989). The SC is commonly simplified to an interlocking bricks and mortar model, where the corneocytes make up the bricks and the lipid bilayers are the mortar, although sweat glands and hair follicles puncture the wall. The corneocytes approximately 40 μm long and approximately 0.5 μm thick (Schaefer and Redelmeier, 1996a). The keratin rich corneocytes are flattened polyhedrons

held to adjacent corneocytes by modified desmosomes and an interdigitating system of ridges and grooves (Eckert, 1992). The majority of intracellular protein is found as bundled keratin filaments, with about 30 family members of keratin present, and it is likely that disulphide bonds are important for the formation of the bundles (Schaefer and Redelmeier, 1996b). The cornified envelope consists of a highly cross-linked protein complex that is very insoluble and chemically resistant (Schaefer and Redelmeier, 1996b, Walters and Brain, 2001). The degradation of desmosomes leads to desquamation, where lipid soaked horny flakes are lost from the skin surface at a whole body rate of 0.5 – 1g per day (Eckert, 1992).

The intercellular lipid matrix is arranged in continuous, stable, bilayers, and the lipid content (Table 1.1, Walters and Brain, 2001 adapted from Wertz and Downing, 1989) mainly consists of cholesterol, cholesterol derivatives, and ceramides (Figure 1.3), with a lack of the phospholipids found in many other biological membranes. The lipid lamellae provide a significant and tortuous barrier to chemical permeation.

Table 1.1 Composition of human stratum corneum lipids (Walters and Brain, 2001 adapted from Wertz and Downing, 1989)

Lipid	% w/w	mol %
Cholesterol esters	10.0	7.5 ^a
Cholesterol	26.9	33.4
Cholesterol sulfate	1.9	2.0
<i>Total cholesterol derivatives</i>	<i>38.8</i>	<i>42.9</i>
Ceramide 1	3.2	1.6
Ceramide 2	8.9	6.6
Ceramide 3	4.9	3.5
Ceramide 4	6.1	4.2
Ceramide 5	5.7	5.0
Ceramide 6	12.3	8.6
<i>Total ceramides</i>	<i>41.1</i>	<i>29.5</i>
Fatty acids	9.1	17.0 ^a
Others	11.1	10.6 ^b

^a based on C₁₆ alkyl chain

^b based on M_w of 500

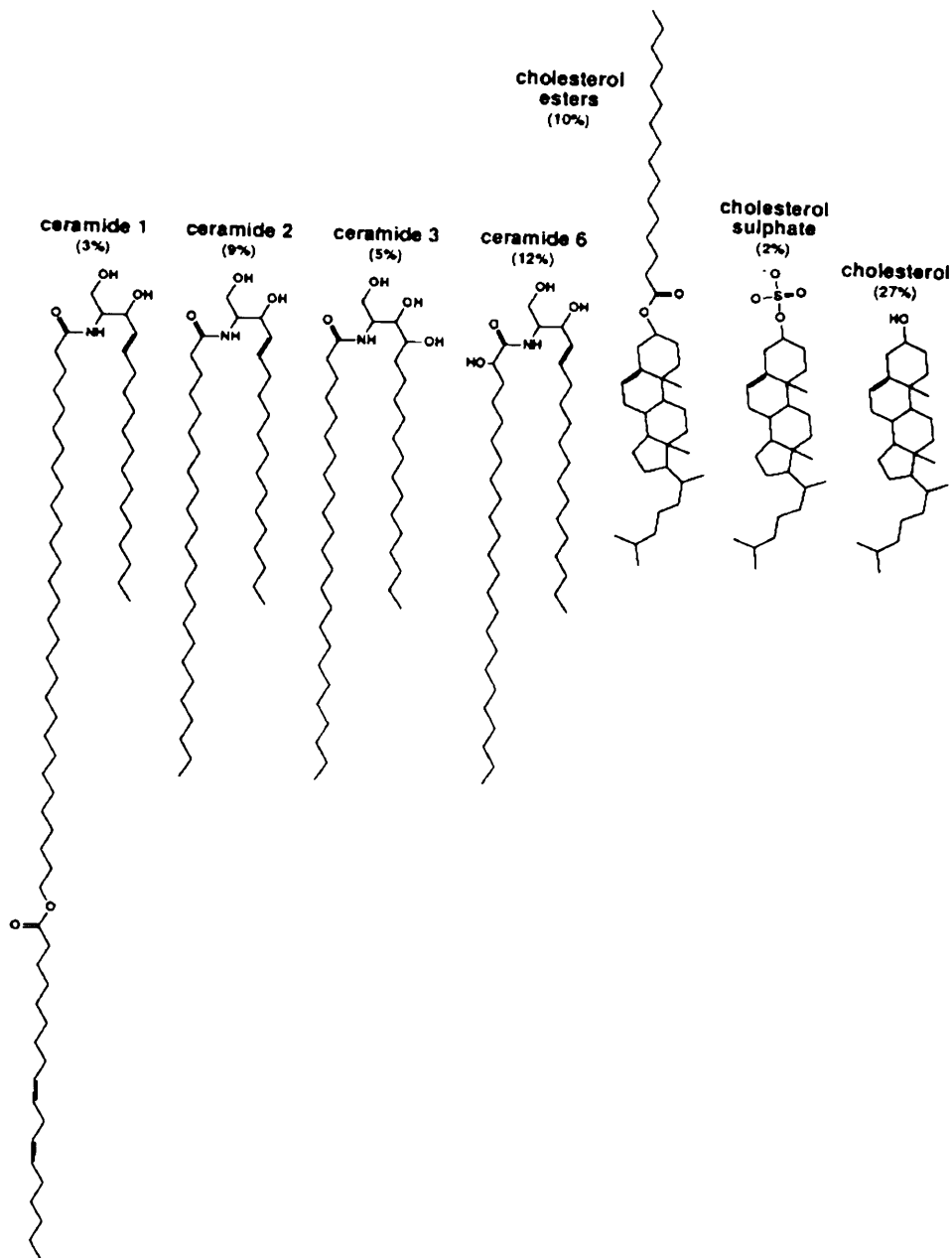


Figure 1.3 Major lipids of the intercellular regions of the human stratum corneum (Brain and Walters, 1993)

The water content of the SC can vary greatly and hydration has a large effect on permeability. Water is necessary for proper functioning of the SC and is present in normal SC at 5-20%, mainly located in intracellular keratin bundles (Scheuplein and Blank, 1971), but occlusion can increase this water content to approximately 50% (Potts, 1986). Generally, increased hydration causes swelling of the corneocytes and promotes the uptake of water into the intercellular lipid domains (Bucks and Maibach, 1999). This can cause

increased permeation, although not in all cases (especially for compounds with low K_{ow}), with degree of enhancement appearing compound specific and, perhaps, also dependent on the occlusive system used (Bucks and Maibach, 1999). Prolonged occlusion can also cause local irritation. Bucks and Maibach (1999) noted that increased hydration does not just simply increase fluidity of the intercellular lipid bilayers, as this would manifest itself in an increase in permeation for all compounds. They postulated that SC hydration alters the SC/viable epidermis partitioning step, with the SC becoming more hydrophilic in nature as the polar head group area between the bilayers absorbs water. Whilst the permeant will still distribute between the hydrophobic bilayer interiors and polar head groups, the reduction in difference between the SC and more aqueous viable epidermis facilitates transfer of the permeant. Other workers, including Ruland et al. (1994) and Scheuplein and Blank (1971), have proposed the existence of aqueous pores that provide easy passage of very polar compounds.

1.2.4 Skin appendages

1.2.4.1 Sweat glands

Eccrine sweat glands develop over most of the body, with between 2 and 5 million (Barry, 1983a) providing a secretory heat control function that can also be activated by the nervous system. A watery solution is manufactured from plasma in a secretory coil located in the dermis and subcutaneous tissue, connected to the intraepidermal sweat duct unit, exiting the surface as a visible pore. The daily output of sweat varies greatly, ranging from 1 litre to 12 litres under maximal stimulation, and accounts for about 80% of the water lost through the skin, the remainder being via transepidermal water loss (Ebling 1963 in Barry, 1983a).

Apocrine sweat glands are present in the embryo as part of the pilosebaceous unit, but most disappear so that, in adults, they are only located in the axilla, mammary areola and perianal area. They are 10 times larger than eccrine

sweat glands and produce a milky or oily secretion that can be metabolised to produce the characteristic body smell (Barry, 1983a).

1.2.4.2 Pilosebaceous units

The pilosebaceous unit is principally comprised of the hair shaft, follicle and sebaceous gland. Hair is comprised of three concentric rings of tightly fused horny cells containing 'hard' keratin, which has a higher sulphur content than the 'soft' keratin in corneocytes (Barry, 1983a). The follicle is enclosed by epidermis and anchors to a stud of dermis at the base, the follicular papilla. The arrector pili muscle attaches the follicle wall to the dermoepidermal junction and when contracted moves the hair upright. Sebaceous glands are located beneath the epidermis and secrete an oily substance (sebum) into the neck of hair follicles via the sebaceous ducts. Sebum may function as an antibacterial and antifungal agent and also help prevent water loss (Barry, 1983a) by sealing the follicle. It consists of triglycerides, free fatty acids, wax esters, squalene, cholesterol and cholesterol esters although the exact content varies according to anatomical location (Greene and Downing, 1970). It is generally accepted that the pilosebaceous unit (and sebum) is not usually involved in skin absorption processes (although delivery to the follicle can occur), and it accounts for only ~0.1 % of surface area.

1.3 Routes of percutaneous penetration

1.3.1 Introduction

The SC is regarded as the rate-limiting barrier for most compounds (except for the most lipophilic) applied to the skin. Diffusion across the SC is usually via a passive process following a concentration gradient from the skin surface (e.g. drug contained in a formulation) to the low or zero concentration zone of the dermis (where permeating compound is efficiently removed via the extensive circulatory network).

There are a number of processes that must occur during percutaneous absorption (Figure 1.4) and only a relatively small proportion of molecules are able to do so to a therapeutically useful degree.

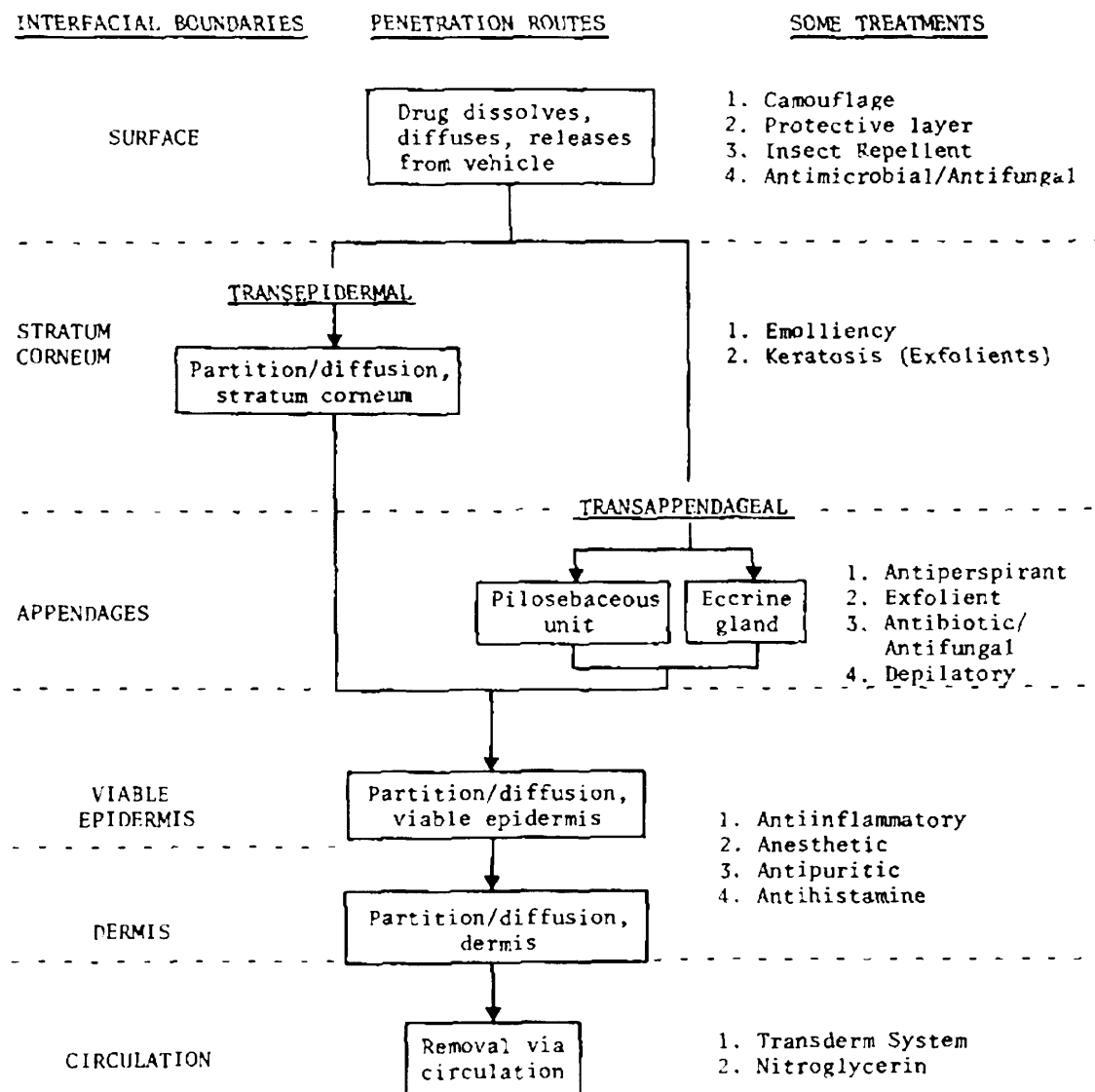


Figure 1.4 Routes of skin penetration and examples of treatments (Barry, 1983a)

There are three SC penetration routes (Figure 1.5) considered feasible: intercellular, transcellular and transappendageal (shunt route).

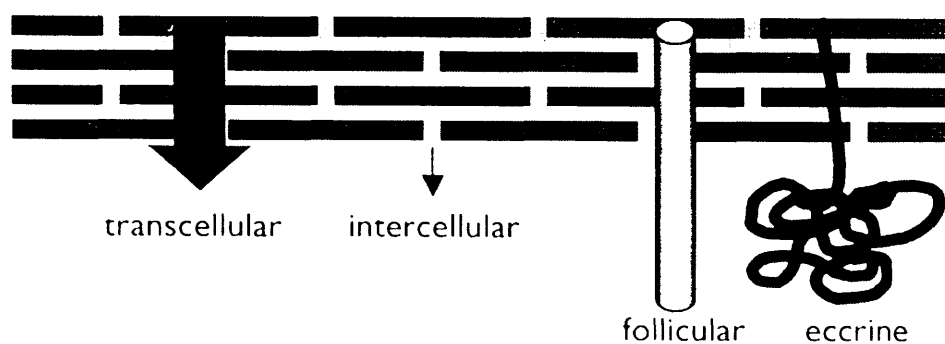


Figure 1.5 Routes of SC penetration (Hadgraft, 2001)

1.3.2 Intercellular route

This is believed to be the most likely route by which most molecules cross the SC. Molecules transfer along the lipid bilayers, repeatedly partitioning into, and diffusing across, the structured layers. The route around the essentially impermeable corneocytes is highly tortuous, and calculations suggested a diffusional pathlength for methyl nicotinate of 350 μm (Albery and Hadgraft, 1979), and 750 μm for water (Potts and Francouer, 1991), approximately 20-50 times the thickness of the SC.

The visualisation of mercury chloride in intercellular channels using electron microscopy (Boddé et al, 1991), and the observation that delipidisation of the SC causes increased skin permeation (Menczel, 1995), provide further support for this route.

1.3.3 Transcellular route

This route, whilst direct, would require molecules to repeatedly cross both corneocytes and lipid bilayers. Corneocytes (section 1.2.3.6) are considered relatively impermeable, and significant transfer of molecules through both corneocytes and the lipid bilayers would be considered unfavoured due to the disparate physiochemical properties required.

1.3.4 Transappendageal route

The appendages offer a potential route (shunt route) that bypasses normal SC permeation processes. However, they are thought to be of limited importance. Sweat glands and hair follicles, whilst large in number, cover only a small proportion of the skin surface area.

The role of sweat glands in skin absorption *in vivo* is considered unimportant, as molecules would have to overcome the considerable outward flow of sweat, a highly aqueous environment, and sweat pores may close when not in use via a valve mechanism at the opening of the gland (Hadgraft, 1983).

Hair follicles cover ~0.1% of skin surface area and it is believed can provide a limited route of absorption for some molecules. The pilosebaceous unit provides a far greater surface area for absorption than that presented on the outside skin surface. The delivery of compounds to the follicle itself may be of benefit for some dermatological treatments, and liposomal formulations can be beneficial in this respect (reviewed by Agarwal et al, 2000). Polymeric nanoparticles have been shown to preferentially accumulate in the follicular openings (Alvarez-Roman et al, 2004), with 20 μm particles entering the follicles to a greater extent than 200 μm particles. However, follicular accumulation does not mean that the material will become absorbed systemically as molecules must diffuse through the sebaceous lipids, whilst sebum excretion is a potential route of elimination.

A study applying fluorescent model substances of varying lipophilicity to human scalp skin, measured using confocal laser scanning microscopy after 18 hours, showed greatest penetrated amount for the medium lipophilicity tracer, but greatest accumulation in parts of the hair follicle for the high lipophilicity tracer (Grams and Boustra, 2002). The actual route of transport to the follicle could not be determined, but the work did confirm different selectivities for the skin and hair follicle.

1.4 Theoretical concepts in percutaneous penetration

The principal barrier, the intercellular lipid bilayers within the SC, provides a discriminating route where penetration of a molecule is largely based upon physicochemical characteristics. The ability of the molecule to partition into the lipid bilayers is of vital importance and molecular weight and size have a large effect.

The actual rate at which a compound permeates a skin membrane is affected by the concentration applied, the degree of partitioning of the molecule between the vehicle and SC, and the diffusivity of the molecule within the SC (Walters and Brain, 2001). The absolute amounts of molecule permeating are also greatly affected by inter- and intra-regional variations in skin permeability (discussed later). The mathematical principles of diffusion and derivation of mathematical models for skin absorption have been discussed in detail (Barry, 1983b, Walters and Brain, 2001) and important points will be summarised below.

The ionisation state of the applied molecule is also an important consideration for many compounds, with charged species far less able to partition into the SC. Many drugs are ionisable, and it is usually best to apply the non-ionised form of the drug, although skin pH control will ultimately determine the state of permeating species. However, in a non-aqueous vehicle, organic salts (charged drug plus organic counter-ion) can penetrate in the form of ion-pairs and have surprisingly high fluxes (US EPA, 1992).

A typical absorption process following application of a drug solution to the skin surface is shown in Figure 1.6. If drug concentration is measured either systemically (*in vivo*) or in the receptor phase under a skin membrane (*in vitro*), there is a delay prior to appearance of the drug (lag time). Frequently a period of steady state diffusion will then be observed. Eventually, the rate of permeation will begin to plateau, often due to the depletion of donor phase concentration (including, perhaps, deliberate removal of remaining applied

drug) or the presence of high levels of permeant in the receptor phase (*in vitro*) resulting in sink conditions no longer applying.

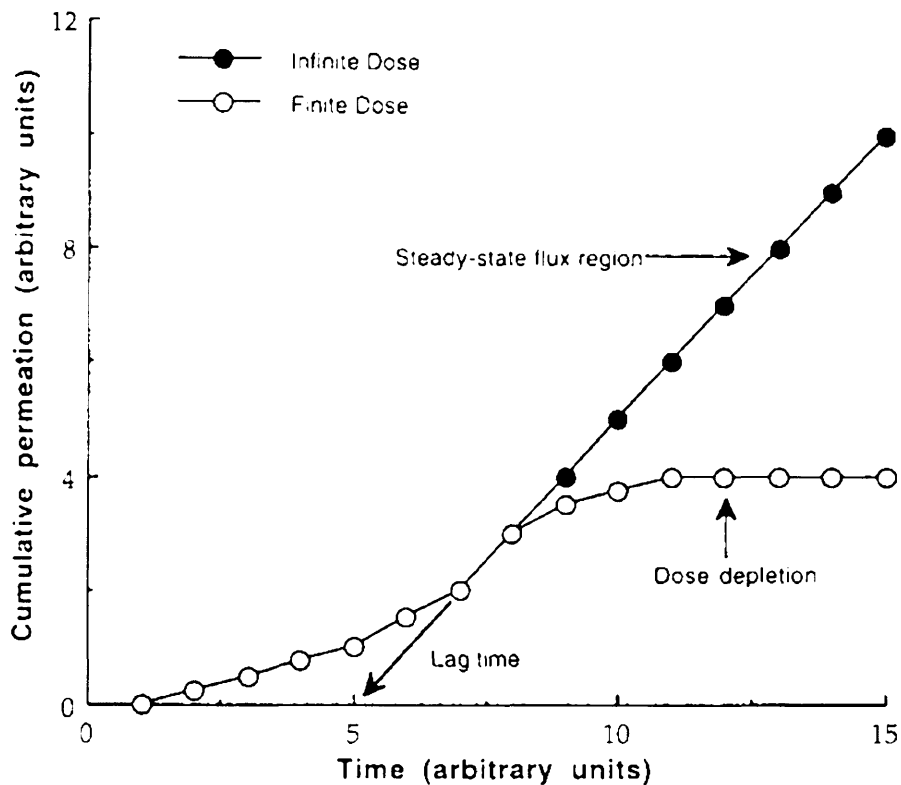


Figure 1.6 Typical permeation profiles (Brain et al, 2002)

1.4.1 Diffusional calculations

Fick's laws of diffusion were derived by Adolf E. Fick 150 years ago, and the 1st law relates the steady state flux (rate of transfer per unit area) of diffusing substance, J , to the diffusion coefficient, D , the concentration of the diffusing substance, C , and the position, x , in the membrane being traversed. The diffusion coefficient depends upon interactions between the permeant and membrane.

Equation 1.1
$$J = -D (\partial C / \partial x)$$

The equation is not in a form suitable for use in calculation of skin permeation. Therefore, it is expressed as equation 1.2, where K is the membrane-vehicle

partition coefficient, C_v is the permeant concentration in the vehicle and h is the diffusional pathlength (not the membrane thickness for skin due to the convoluted permeation route). C_v can usually be used rather than the term ΔC , the difference between concentrations in the vehicle and skin (C_s), as $C_v - C_s$ usually approximates to C_v due to the low concentration in the skin.

Equation 1.2 $J = (DKC_v)/h$

The diffusion coefficient, D , membrane-vehicle partition coefficient, K , and diffusional pathlength, h , are difficult to determine for the heterogeneous skin membrane, therefore the term permeability coefficient, k_p , (equation 1.3) is used.

Equation 1.3 $k_p = (DK)/h$

Therefore, flux can most simply be described by equation 1.4. For skin permeation, typical units are: J (μg per cm^2 per hour), k_p (cm per hour) and C_v (μg per cm^3).

Equation 1.4 $J = k_p C_v$

The flux can be measured in vitro and used together with a known C_v to calculate k_p . The amount absorbed, Q , over the entire application area, A , over time, T , can be estimated using equation 1.5, which takes into account the lag time, **lag**, prior to steady state conditions.

Equation 1.5 $Q = k_p C_v A (T - \text{lag})$

1.4.2 Partition coefficient

The determination of membrane-vehicle partition coefficient, K , is difficult to perform for skin, as it would require measurement of the concentration in the SC lipids. Therefore, estimation is made using a relatively easy to measure, experimentally determined parameter, the n-octanol-water partition coefficient, $K_{o/w}$, with octanol representing SC lipid uptake of the permeant. $\log K_{o/w}$ is usually presented and has been measured for many compounds, as it is widely used parameter to enable estimation of uptake into many membranes and strata.

Optimal lipophilicity for a skin permeant, described using $\log K_{o/w}$ values, appears to range between 1 and 3 (Walters and Brain, 2001), although there are many additional physicochemical factors to consider. Permeants with $\log K_{o/w}$ values higher than 3 may exhibit decreased permeation due to inability to diffuse into the more hydrophilic regions of the epidermis. For reference, the reported $\log K_{o/w}$ of octanol itself ranges between 2.8 and 3.15 (1-octanol puriss, $\geq 99.5\%$, Sigma-Aldrich material safety data sheet).

1.4.3 Thermodynamic activity

The concentration gradient described above is a simplification of the exact physicochemical parameters that drive diffusion and, more precisely, the chemical potential gradient, $\partial\mu/\partial x$, should be used (Walters and Brain, 2001). This would indicate that the flux of a drug, from a single vehicle containing varying amounts of drug, will be maximal when saturated, with the flux at half saturation being half that of the saturated solution. Once saturation has been achieved, the addition of excess drug does not increase flux. This means that saturated solutions of a drug in different vehicles should produce the same flux, as long as there is no interaction between the vehicle and membrane. However, this is generally not true for skin, where vehicle components often alter the membrane properties.

Supersaturation, an unstable state where the solubility of the drug in the vehicle is greater than the saturated solubility, has enabled greater flux, with the 2, 3 and 4 degrees of supersaturation (ratio of solubility achieved to the saturated solubility) corresponding reasonably well (Figure 1.7) with the increased flux for piroxicam (Pellett et al, 1997). Supersaturation can be achieved by various means and can, for instance, occur following evaporation of volatile vehicle components, for example in an ethanolic gel, and it is possible to prolong the state of supersaturation through the inclusion of anti-nucleating polymers.

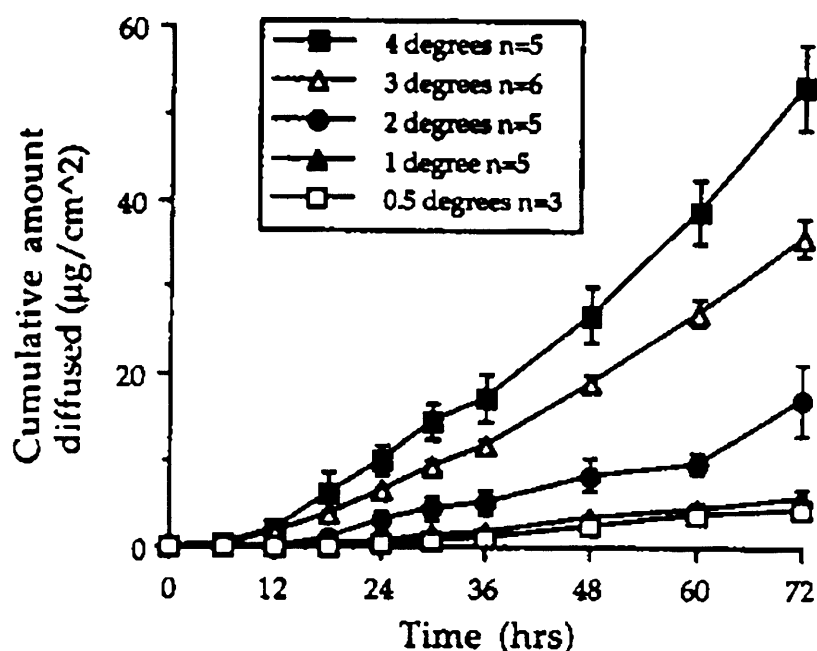


Figure 1.7 How the degree of supersaturation affects the permeation of piroxicam through human epidermal membranes in vitro; n is the number of replicates (Pellett, 1997)

1.4.4 Solubility parameters

The solubility parameter, δ , (equation 1.6) allows comparison of cohesive energy of a material, with materials of similar δ able to dissolve more easily in each other. The cohesive energy, c , is derived from the molar heat of vaporisation, which provides a measurement of the energy required to break

all inter-molecular attractions. ΔH is the heat of vaporisation, R is the gas constant, T is temperature (K) and V_m the molar volume.

Equation 1.6
$$\delta = \sqrt{c} = [(\Delta H - RT)/V_m]^{1/2}$$

Solubility parameters can be calculated in units of $(\text{cal}/\text{cm}^3)^{1/2}$ (cohesive energy density) or the SI unit of $\text{MPa}^{1/2}$ (cohesive pressure) with values approximately twice the non SI unit.

The value of solubility parameters in terms of skin penetration considerations may be to provide a way to optimise formulations/vehicle content in order that interaction/solubility within the skin ($\delta \sim 10 (\text{cal}/\text{cm}^3)^{1/2}$, Liron and Cohen, 1984) may be maximised. However, the value of this approach has yet to be proven, and other physicochemical parameters, for example, M_w and lipophilicity, are believed to predominate.

1.4.5 Predictive models of skin permeation

Several equations have been developed that aim to predict the skin permeability coefficients, k_p , of an applied compound using a limited number of physicochemical properties. These equations were developed using published data for permeation from aqueous solution for a limited number of compounds. A commonly used model (equation 1.7), developed by Potts and Guy (1992), relates k_p (cm/h) to the permeant's n-octanol-water partition coefficient, $K_{o/w}$ and molecular weight, M_w , both important determinants of skin permeation.

Equation 1.7
$$\log k_p = 0.71 \log K_{o/w} - 0.0061 M_w - 2.72$$

The data set used by Potts and Guy contained over 90 compounds with $\log K_{o/w}$ values in the range -3 to 6 , and M_w from 18 to >750 . Other models have applied further factors related to the hydrogen bonding capacity of the

permeant, the sum of atomic partial charges, and melting point, and these have been discussed by Pugh et al (1998). However, all of these predicted k_p values apply to permeation from aqueous solution and not to real formulations, applied under in-use conditions, where factors such as skin/formulation interactions and finite dose conditions are important.

Comparison of predicted k_p to experimental k_p values (for formulations or non-aqueous solutions) can show great differences, with the predicted k_p for methyl dodecyl-nitrosamine four orders of magnitude greater than the experimental values for an IPM solution and an oil-in-water emulsion (Walters and Brain, 2001; Walters et al, 1997). However, the models can be of some value, for example, in selection of candidates for further investigation from large libraries of compounds.

1.5 Measurement of skin penetration *in vitro*

The best prediction of human skin absorption of compounds *in vivo* can usually be achieved through the use of human skin *in vitro*. Due to the removal of the circulatory network present *in vivo*, *in vitro* measurements must be performed under appropriate experimental conditions, and these vary somewhat depending upon the permeant's physicochemical properties.

Measurements of human skin absorption *in vitro* are usually preferable to using animal models *in vivo* and excised animal skin *in vitro*, as many animal models show much higher absorption due to a significantly lower barrier function. Permeability differences between species will be discussed later.

For *in vitro* studies, skin membranes are mounted in diffusion cells, and a receptor phase of suitable composition accepts permeating compound that has been applied to the surface of the membrane.

Many guidance documents for skin penetration studies have been published (Skelly et al, 1987; SCCNFP 2003; OECD, 2004a). OECD test guideline 428

(OECD 2004a), together with the associated guidance document for the conduct of skin absorption studies, OECD series on testing and assessment number 28 (OECD, 2004b), generally encapsulate current best practice. However, determination of the exact experimental parameters for a particular study still requires careful scientific consideration due to the generic nature of these guidelines. It should also be noted that there are debatable points in OECD test guidance documents, and certain suggestions, for example suitable receptor phases, may conflict with guidelines from other bodies (e.g. SCCNFP, 2003). Indeed, studies that are performed for submission to a regulatory body should be performed to the appropriate guideline. The recommended number of replicates also vary, from four to twelve and, due to the inherent variability of skin, the higher number is preferable, particularly when comparing two similar formulations.

1.5.1 Diffusion cells

There are two types of diffusion cell that are commonly used, static horizontal cells and flow-through cells, and both have benefits and limitations. These cells, together with an example of a side-by-side diffusion cell, often used for saturated solution studies with non-skin membranes, are shown in Figure 1.8 (Walters and Brain, 2001). Cells are usually made from glass, but other inert materials such as polytetrafluoroethylene (PTFE) can be used.

Static diffusion cells have the benefit of relatively low receptor phase volume, for example different cell types in our laboratory range between 2 and 5 ml. The removal of samples from this receptor medium at various time-points can allow low amounts of permeating compound to be quantified using common sensitive analytical techniques, such as high performance liquid chromatography (HPLC). However, for compounds that permeate well, this low volume can become rate limiting if the receptor phase does not offer sufficient solubility, and different receptor media must be used to overcome this.

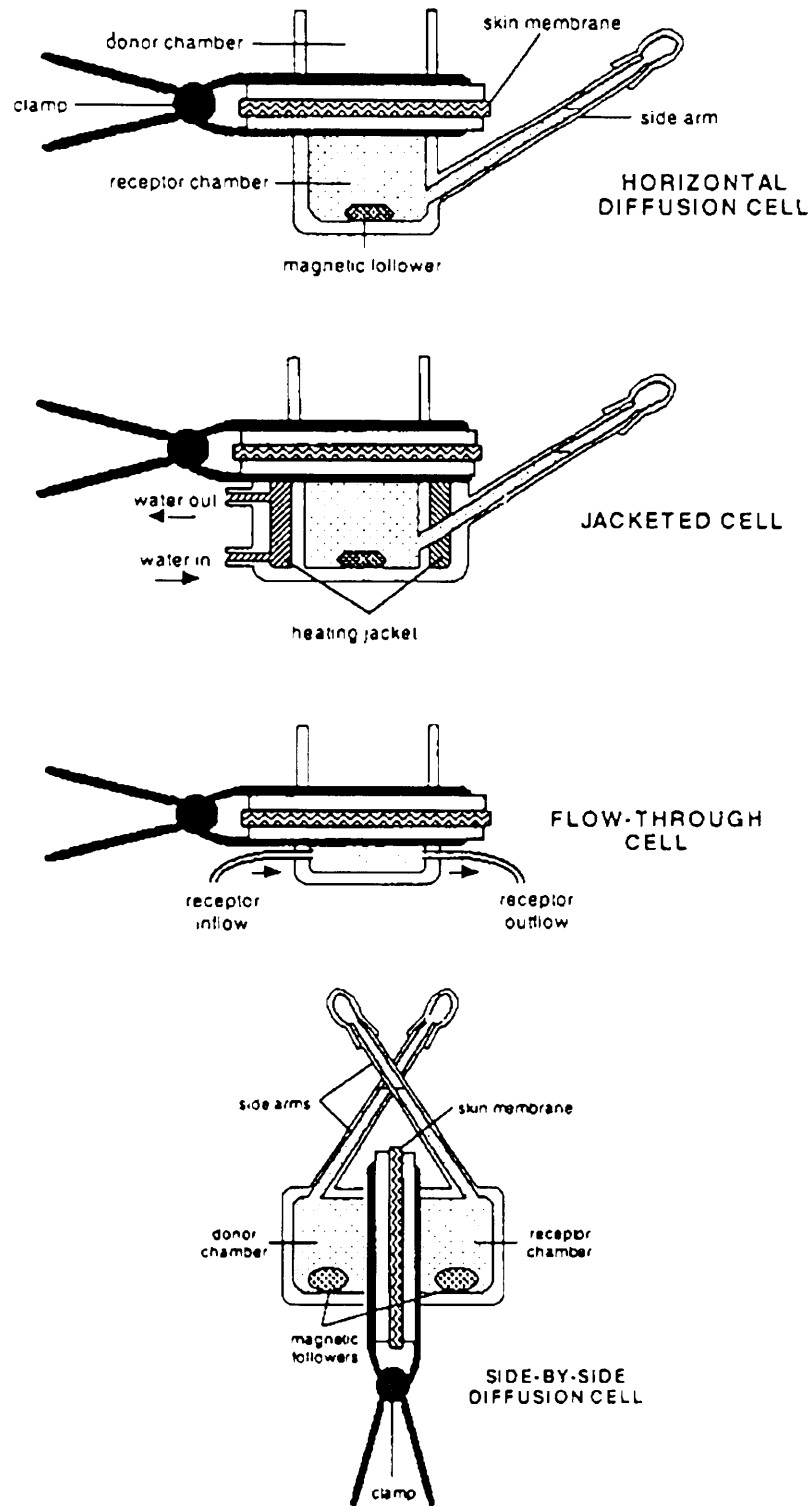


Figure 1.8 Diffusion cells designs (Brain et al, 2002)

Flow-through cells use a continual flow (often 1-5 ml per hour) of receptor medium in an attempt to provide sink conditions at all times, although a physiological buffer receptor medium can still become rate limiting for lipophilic compounds, with media modification required. These cells also

produce large volumes of receptor fluid that, for many permeants, require a concentration step (using, for example, solid phase extraction), prior to analysis, which adds complexity and cost and will increase variability.

Diffusion cells must be used under temperature-controlled conditions, in order to mimic the *in vivo* skin surface temperature of 32°C (as temperature affects permeation rates). Typically this involves placing the cells in a waterbath at 37°C, although jacketed cells containing integral water circulation are also used. Submersible magnetic stirrer beds help provide sink conditions by ensuring that the contents of the receptor chamber are continuously agitated by a magnetic follower.

1.5.2 Skin membranes

The type of skin membrane that is appropriate for a study depends principally upon permeant lipophilicity. For human skin, four skin preparations are possible; full thickness membranes (consisting of dermis, epidermis and stratum corneum), dermatomed membranes (where a portion of the dermis has been removed, with a membrane thickness of 300, 500 or 1000 µm often produced), epidermal membranes (where the dermis has been fully removed following heating to 60°C for 55-60 seconds) and stratum corneum membranes (where the viable epidermis has been enzymatically removed from epidermal membranes using a 0.0001% trypsin solution).

For hydrophilic permeants, full thickness or dermatomed membranes are appropriate as the dermis is not considered to be rate limiting. However, more lipophilic permeants should be assessed using epidermal membranes. SC membranes are generally too fragile for general use. Epidermal and SC membranes require physical support, for example, on filter paper or a PTFE mesh. All the membrane types contain the principal barrier to permeation, the SC.

Preparation techniques can cause damage to the SC, especially for epidermal and SC membranes, and it is good practice to measure membrane integrity prior to application of test permeants, where possible. This can be achieved by measuring parameters such as the permeation of a marker compound (such as tritiated water), transepidermal water loss, or skin resistance. Water permeation and transepidermal water loss increase for damaged membranes, whilst skin resistance decreases. The water permeation membrane integrity check is discussed in detail in chapter 7.

Skin, from either cadavers or, preferably, surgical procedures, is frequently stored frozen (-20°C) for up to one year prior to use, with little reported change in the permeability (Harrison et al, 1984). However, the skin should not be purposely hydrated prior to freezing as this may change subsequent permeation characteristics (Walters and Brain, 2001). A benefit of immediate usage, especially of skin from surgical sources, can be the maintenance of metabolic activity. Some molecules, for instance ester pro-drugs, can be metabolised in the skin, principally in the epidermis and dermis, and therefore metabolically active skin is required to correctly measure the skin absorption and fate of the applied material. Wester et al (1998), showed that anaerobic metabolism (where glucose is converted to lactose) for dermatomed cadaver skin was highest during the 18 hours following donor death, decreased approximately 3-fold by day 2, but then maintained steady-state activity through to day 8. They also assessed the effect of the heat treatment process used to produce epidermal membranes and found, unsurprisingly, a large reduction in viability for the epidermis and dermis. Therefore, only full thickness and dermatomed sections are suitable for 'viable' skin studies.

Skin from surgical sources is usually from the abdominal or breast regions, whereas cadaver sites can be more variable. The site can have a large effect on permeability (discussed later).

Artificial skin constructs are commercially available, and suitable for use in some toxicological screening models. However, they are of limited value for

skin penetration studies due to the much reduced barrier function (Schmook et al, 2001).

1.5.3 Receptor media

An ideal receptor medium is a physiological pH buffer, such as pH 7.4 phosphate buffered saline (PBS). However, as discussed above, this medium must be modified for many permeants to enable sufficient solubility (no greater than 10% of the saturated solubility, discussed further below) for the permeating species. Physiological pH should generally be used so that the more hydrophilic lower epidermal layers are maintained at the correct pH, as alteration of this pH can profoundly change the partitioning and flux of weakly ionisable permeants (Kou et al, 1993).

Increased solubility of lipophilic permeants is typically achieved through the addition of ethanol, a non-ionic surfactant such Oleth-20 (Polyoxyethylene 20 oleyl ether; trade names include Volpo N20 (Croda Oleochemicals Ltd.) and Brij-98 (ICI Americas, Inc.)), or bovine serum albumin (BSA). Additions to PBS of 25% (v/v) ethanol, up to 6% (w/v) Oleth-20, or up to 4% BSA (w/v), are considered to have relatively little effect on the permeability characteristics of skin and are widely used. The selection of most suitable receptor phase should be made according to solubility and analytical considerations, with Oleth-20 and BSA containing large number of compounds that can interfere with techniques such as HPLC.

The provision of sufficient solubility is widely recognised (Skelly et al, 1987, SCCNFP, 2003) as requiring the permeant to reach no greater than 10% of the saturated solubility. Concentrations greater than 10% would potentially limit proper diffusion processes, with back-diffusion and the lack of sink conditions reducing measured flux. For poorly soluble compounds, it may only be possible to confirm that the 10% criterion was not surpassed post-experimentally.

Receptor media that do not use physiological pH buffer include 50/50 (v/v) ethanol/water, polyethylene glycol (PEG)/water mixtures and propylene glycol (PG)/water mixtures. These media may offer increased solubility of very lipophilic compounds, but their use may cause large changes to the skin barrier and results obtained will probably not reflect the *in vivo* situation.

The sampling of each diffusion cell receptor phase, and replacement of the volume removed with fresh temperature-equilibrated receptor medium, should be carefully performed using techniques that do not cross-contaminate.

1.5.4 Assessment of skin distribution of a permeant

Following the completion of skin permeation measurements, typically after 24 or 48 hours, the distribution of applied material can be measured on and in the skin membrane. A typical procedure would involve wiping or washing the skin surface to remove surface material, tape stripping the SC using adhesive tape, then extracting the remaining tissue, with the epidermis separated from the dermis for full thickness and dermatomed membranes. Full mass balance studies would also include a donor chamber wash, and extraction of the tissue support for epidermal membranes. Tape stripping is discussed in details in chapter 5.

The analysis of skin distribution samples can require the development of extraction methods that can vary greatly in complexity. However, the inclusion of radiolabelled permeants (typically ^{14}C or ^3H) into the formulation/vehicle can simplify analysis greatly, with samples simply dissolved in dedicated tissue solubilisers, such as OptiSolve (Wallac, UK), then counted for radiolabel. However, for formulated products such as creams, the radiolabelled permeant should be incorporated during formulation construction to ensure correct phase dispersion. For example, the majority of the active may be located in the oil phase of an oil-in-water cream. If the radiolabel is subsequently mixed into this pre-prepared formulation, the radiolabel will not be distributed in the same manner as the bulk active, and subsequent skin

penetration measurements may not be representative of the true penetration of the active. However, formulation construction can be difficult to achieve when processes and quantitative excipient lists are not in the public domain. Additional concerns for investigations using radiolabels are the presence of radiochemical impurities, and tritium exchange where the label is in a labile position. Both can cause uncertainty in the measured data, especially when low concentrations of permeant are detected, sometimes requiring additional analytical procedures to confirm identity of the detected compound.

1.5.5 Application of compounds to the skin surface

Skin penetration and permeation studies are performed using either a finite or infinite dose. Finite doses are most frequently used for assessing drug formulations and for dermal risk assessments under in-use conditions, and have the most relevance to human exposure *in vivo*. A finite dose is chosen to mimic in-use application amounts and usually ranges between 2 and 5 mg/cm², and up to 10 µl/cm² for liquids. Infinite doses can be particularly useful for examining skin penetration of compounds in simple vehicles and can allow elucidation of skin permeation parameters without the complex interactions of a formulation and with a reduced likelihood of donor depletion effects.

1.5.6 *In vivo in vitro* correlations

Direct comparison of data generated *in vitro* with *in vivo* data can be difficult for reasons such as the non-existence of *in vivo* data and the different conditions (e.g. dose, site, formulation) in which compounds are applied. Where direct comparison can be made, and differences exist it has been noted that it is just as likely that the *in vivo* data is incorrect (Kligman, 1983 in Bronaugh, 1989). The relatively low amounts of compound that permeate through skin, together with the large systemic compartment, significant metabolism and slow excretion kinetics, make *in vivo* studies technically difficult and can favour falsely low results (Schaefer and Redelmeier, 1996c).

However, in a recent *in vivo in vitro* comparative study where conditions were tightly controlled, good correlation was found for the pesticide propoxur (van der Sandt et al, 2000).

1.6 Variations in skin permeability

1.6.1 Inter-species differences in skin permeability

Correctly performed *in vitro* studies using human skin are often considered the best predictor of the *in vivo* human situation. However, human tissue is a limited resource and many researchers have used animal skin models, both *in vitro* and *in vivo*. Whilst a knowledge of the differences in permeability between species can help when considering extrapolation to humans, there is no consistent relationship between permeability in humans and the various animal models. It is also possible that data generated in animals could, for instance during formulation optimisation studies, incorrectly predict interactions and rank orders of permeation due to the differing skin structures.

Literature suggests that the weanling pig and rhesus monkey provide the best animal models for *in vivo* human data, with rabbit and rat providing much higher absorption (Wester and Maibach, 1989). Anatomical variation exists for animals, as well as for human, with dorsal skin reported to be more permeable than abdominal skin for rat but less permeable for hairless mouse (Wester and Maibach, 1989).

Most animal skin models contain a higher follicular density than human skin and this can exclude the preparation of epidermal membranes for *in vitro* use, probably limiting the value of animal models for very lipophilic compounds where dermatomed sections would still be rate limiting. Unfortunately, models such as hairless mouse contain skin strata only a fraction of the thickness of human skin and provide data of limited value.

In vivo animal models still have a role in predicting human exposure for toxic molecules, especially in addition to human *in vitro* data, and allow a greater confidence in the generation of safety data. *In vivo* rat studies are still widely used for pesticide safety assessments to ensure acceptable risk to humans (operators, workers, bystanders) (SANCO, 2003).

1.6.2 Variations in human skin permeability

Anatomical variations in skin permeability are large (Table 1.2, Wester and Maibach, 1999), and this can be exploited for drug delivery, for example, by dosing regions of high permeability. However, it also has implications for the testing of chemicals both *in vivo* and *in vitro*. Testing should ideally be performed at (*in vivo*), or using skin from (*in vitro*), the in-use site of application. However, for *in vitro* testing using surgical skin samples, only breast and abdominal tissue is normally available, and the implications of a different site of application should be considered. A related issue is the difficulty of correctly modelling diseased skin, such as psoriatic skin, *in vitro*.

Table 1.2 Regional variation in human skin absorption (adapted from Wester and Maibach, 1999)

Anatomical site	Absorption index (arm=1)			
	HC*	Pesticides**	Pyrene***	PAH****
Genitals	40	12		
Arm	1	1	1	1
Hand	1	1	0.8	0.5
Leg/ankle	0.5	1	1.2	0.8/0.5
Trunk/shoulder	2.5	3	1.1	/2.0
Head/neck	5	4	/1.3	1.0

* - hydrocortisone; ** parathion and malathion; ***1-OH-pyrene in urine after coal tar ointment application; **** PAH absorption rate constants after coal tar ointment application

In vitro intra-donor variation within samples from the same region can be fairly high, as can inter-donor variation. An *in vitro* intra-donor variability of 45% relative standard deviation (RSD), and inter-donor variability of 65%RSD, was

reported by Barry and Southwell (Barry, 1983c) following analysis of their own and published data. The comparative *in vivo* variations were 30 and 45%RSD, respectively, and it was concluded that even well controlled *in vitro* experiments increase variability compared to well performed *in vivo* procedures. Reported variations due to age and race appear inconclusive, but may vary with permeant. A review of the limited published data on age and race variation can be found in Walters and Brain (2001).

1.7 Modification of skin penetration

The amount of an applied drug that penetrates into, and permeates through, the skin can be improved by methods such as formulation/vehicle optimisation and thermodynamic control (including supersaturation). Formulations directly applied to the skin are usually of the semi-solid type; creams (oil-in-water and water-in-oil), gels, or ointments (anhydrous). There are wide ranges of excipients for semi-solid formulation and Walters and Brain (2001) review these in detail.

In addition to formulation optimisation, it is possible to alter the intrinsic permeability of a compound by various means. These include chemical modification of the drug (pro-drugs and eutectic mixtures), physical modification of the skin (iontophoresis, electroporation, phonophoresis and microporation) and chemical modification of the skin (enhancers and retarders).

Numerous compounds have been shown to increase the permeability of skin, such that applied drugs can be delivered more efficiently. Their mode of action is generally thought to be through disruption of the lipid bilayers in the SC, and these compounds are classed as enhancers. It is also possible that the integrity of the lipid bilayers can be improved though the application of retarder compounds which intercalate with the bilayers. A detailed discussion of chemical enhancers and retarders is presented in chapter 2.

1.8 Study objectives

The research presented in this thesis was performed over several years of part-time study. Initial general objectives were refined, as significant issues in the study of *in vitro* percutaneous penetration became apparent.

The first section of the presented research (chapters 2 to 4) investigates the hypothesis that 'specifically designed compounds may be able to retard the skin penetration of xenobiotics'.

The remainder of the presented research addresses a number of important issues that must be resolved if *in vitro* skin penetration studies are to be accepted as a true reflection of the *in vivo* situation.

The specific objectives addressed are:

- a) to investigate the potential effect of novel skin penetration retarders using several model permeants;
- b) to investigate skin surface sampling techniques;
- c) to investigate methods of estimating evaporative loss of volatile compounds during skin penetration studies;
- d) to evaluate whether there is a relationship between pre-study water permeability of human skin membranes and subsequent permeation of alternative test compounds.

1.9 References

Agarwal, R., Katare, O.P. and Vyas, S.P. (2000). The pilosebaceous unit: a pivotal route for topical drug delivery. *Methods Find Exp. Clin. Pharmacol.*, **22**, 129-133.

Albery, W.J. and Hadgraft, J. (1979). Percutaneous absorption: in vivo experiments. *J. Pharm. Pharmacol.*, **31**, 140-147.

Alvarez-Roman, R., Naik, A., Kalia, Y.N., Guy, R.H. and Fessi, H.J. (2004). Skin penetration and distribution of polymeric nanoparticles. *J. Control. Rel.*, **99**, 53-62.

Baden, H.P. (1979), Keratinization in the epidermis. *Pharm Ther.*, **7**, 393-411.

Barry, B.W. (1983a). Structure, function, diseases and topical treatment of human skin, in *Dermatological formulations; percutaneous absorption*, pp. 1-48. Marcel Dekker Inc., New York, USA.

Barry, B.W. (1983b). Basic principles of diffusion through membranes, in *Dermatological formulations; percutaneous absorption*, pp. 49-94. Marcel Dekker Inc., New York, USA.

Barry, B.W. (1983c). Methods for studying percutaneous absorption, in *Dermatological formulations; percutaneous absorption*, pp. 234-295. Marcel Dekker Inc., New York, USA.

Bodde, H., van den Brink, E.I., Koerten, H.K. and de Haan, F.H.N. (1991). Visualization of in vitro percutaneous penetration of mercuric chloride; transport through intercellular space versus cellular uptake through desmosomes. *J. Control. Rel.*, **15**, 227-236

Brain, K.R. and Walters, K.A. (1993). In *Pharmaceutical skin penetration enhancement*, Walters, K.A. and Hadgraft, J. (eds) pp. 389-416. Marcel Dekker Inc., New York, USA.

Brain, K.R., Walters, K.A. and Watkinson, A.C. (2002). Methods for studying percutaneous absorption, *Dermatological and transdermal formulations*, pp. 197-270. Marcel Dekker Inc., New York, USA.

Bronaugh, R.L. (1989). Determination of percutaneous absorption by in vitro techniques, in *Percutaneous Absorption: mechanisms – methodology – drug delivery*, 2nd Ed. Bronaugh, R.L. and Maibach H.I., (eds), pp 239-258. Marcel Dekker Inc., New York, USA.

Bucks, D and Maibach, H.I. (1999). Occlusion does not uniformly enhance penetration in vivo, in *Percutaneous absorption: drugs – cosmetics – mechanisms - methodology*, 3rd Ed. Bronaugh, R.L and Maibach H.I. (eds) pp 81-105. Marcel Dekker Inc., New York, USA.

Ebling, F.J. (1963). In *Handbook of cosmetic science*. Hibbott, H.J. (ed). Pergamon Press, Elmsford, New York, USA.

Elias, J. L. (1989). The microscopic structure of the epidermis and its derivatives, in *Percutaneous absorption: mechanisms – methodology - drug delivery*, 2nd Ed. Bronaugh, R.L and Maibach H.I. (eds). pp. 3-12. Marcel Dekker Inc., New York. USA

Erkert, R.L. (1992). The structure and function of skin, in *Pharmacology of the skin*. Muktar, H. (ed), pp 3-12. CRC Press Inc., Boca Raton, USA.

Grams, Y.Y. and Bouwstra, J.A. (2002). Penetration and distribution of three lipophilic probes in vitro in human skin focusing on the hair follicle. *J. Control. Rel.*, **83**, 253-262.

Greene, R.S. and Downing, D.T. Pochi, P.E. and Strauss, J.S. (1970). Anatomical variation in the amount and composition of human skin surface lipid. *J. Invest. Dermatol.*, **54**, 240-247.

Hadgraft, J. (1983). Percutaneous absorption: possibilities and problems. *Int. J. Pharm.*, **16**, 255-270.

Hadgraft, J. (2001). Skin, the final frontier. *Int. J. Pharm.*, **224**, 1-18.

Harrison, S.M., Barry, B.W. and Dugard (1984). Effects of freezing on human skin permeability. *J. Pharm. Pharmacol.*, **36**, 261-262.

Kligman, A.M. (1983). A biological brief on percutaneous absorption. *Drug Dev. Ind. Pharm.*, **9**, 521-560.

Kou, J.H., Roy, S.D., and Du, J. (1993). Effect of receiver fluid pH on in vitro skin flux of weakly ionizable drugs. *Pharm. Res.*, **10**, 986-90. Erratum in: *J. Pharm. Res.*, (1994), **11**, 1222.

Liron, Z. and Cohen, S. (1984). Percutaneous absorption of alkanolic acids II: application of regular solution theory. *J. Pharm. Sci.*, **73**, 538-542.

Madigan, M.T., Martinko, J.M. and Parker, J. (1997). *Brock Biology of Microorganisms*, 8th Ed. Prentice Hall, Upper Saddle River, NJ, USA

Menczel, E. (1995). Assessment of delipidization as an enhancing factor in percutaneous penetration. *Curr Probl Dermatol.*, **22**, 189-194.

Noonan, P.K. and Wester, R.C. (1989). Cutaneous metabolism of xenobiotics, in *Percutaneous Absorption: mechanisms – methodology – drug delivery*, 2nd Ed. Bronaugh, R.L. and Maibach H.I., (eds), pp 53-75. Marcel Dekker Inc., New York, USA.

Odland, G.F., (1983). Structure of the skin, in *Biochemistry and Physiology of the skin*. Goldsmith, L.A. (ed), p 3. Oxford University Press, New York, USA.

OECD (2004a). OECD guideline for the testing of chemicals; Test guideline 428. Skin absorption: *in vitro* method. OECD, Paris.

OECD (2004b). OECD series on testing and assessment number 28. Guidance document for the conduct of skin absorption studies. OECD, Paris.

Pellett, M.A., Castellano, S., Hadgraft, J. and Davis, A.F. (1997). The penetration of supersaturated solutions of piroxicam across silicone membranes and human skin *in vitro*. *J. Control. Rel.*, **46**, 205-214.

Potts, R.O. (1986). Stratum corneum hydration: experimental techniques and interpretation of results. *Journal of the Society of Cosmetic Chemists*, **37**, 9-33.

Potts, R.O. and Francouer, M.L. (1991). The influence of stratum-corneum morphology on water permeability. *J. Invest. Dermatol.*, **96**, 495-499.

Potts, R. O. and Guy, R. H. (1992). Predicting skin permeability. *Pharm. Res.*, **9**, 663-669.

Pugh, W.J., Hadgraft, J. and Roberts, M.S. (1998). Physicochemical determinants of stratum corneum permeation, in *Dermal absorption and toxicity assessment*. Roberts, M.S. and Walters, K.A. (eds), pp 245-268. Marcel Dekker Inc., New York, USA.

Ruland, A., Rohr, U. and Kreuter, J. (1994). Transdermal delivery of the tetrapeptide hisetal (melanotropin(6-9)) and amino-acids - their contribution to the elucidation of the existence of an aqueous pore pathway. *Int. J. Pharm.*, **107**, 23-28.

SANCO guideline (2004). Guidance Document on Dermal Absorption, Sanco/222/2000 rev. 7. European commission health & consumer protection directorate-general.

SCCNFP (2003). Basic criteria for the *in vitro* assessment of dermal absorption of cosmetic ingredients, SCCNFP/0750/03. SCCNFP, Brussels.

Schaefer, H. and Redelmeier, T. E. (1996a). Structure and dynamics of the skin barrier, in *Skin barrier: principles of percutaneous absorption*. pp 1-42. S. Karger AG, Basel, Switzerland.

Schaefer, H. and Redelmeier, T. E. (1996b). Composition and structure of the stratum corneum, in *Skin barrier: principles of percutaneous absorption*. pp 43-86. S. Karger AG, Basel, Switzerland.

Schaefer, H. and Redelmeier, T. E. (1996c). The practical application of techniques to measure percutaneous absorption, in *Skin barrier: principles of percutaneous absorption*. pp 213-262. S. Karger AG, Basel, Switzerland.

Scheuplein, R.J. and Blank, I.H. (1971). Permeability of the Skin. *Physiological Reviews*, **51**, 702-747.

Schmook, F.P., Meingassner, J.G. and Billich, A. (2001). Comparison of human skin or epidermis models with human and animal skin in in-vitro percutaneous absorption. *Int J. Pharm.*, **215**, 51-56.

Skelly, J.P., Shah, V.P., Maibach, H.I., Guy, R.H., Wester, R.C., Flynn, G., et al., (1987). FDA and AAPS report of the workshop on principles and practices of in vitro percutaneous penetration studies: Relevance to bioavailability and bioequivalence. *Pharm. Res.* **4**, 265–267.

US EPA (1992), report EPA/600/8-91/011B, Dermal Exposure Assessment: Principles and Applications. Through: http://risk.lsd.ornl.gov/homepage/DERM_EXP.PDF, accessed 24/09/05.

Van de Sandt, J.J.M., Meuling, W.J.A., Elliot, G.R., Cnubben, N.H.P. and Hakkert, B.C. (2000). Comparative in vivo-in vitro percutaneous absorption of the pesticide propoxur. *Tox. Sci.*, **58**, 15-22.

Van Hal, D.A., Jeremiasse, E., Junginger, H.E., Spies, F. and Bouwstra, J.A. (1996). Structure of fully hydrated human stratum corneum: A freeze fracture electron microscopy study. *J. Invest. Dermatol.*, **106**, 89-95.

Walters K.A. and Brain K.R. (2001). Topical and transdermal delivery, in *Pharmaceutical preformulation and formulation: a practical guide from candidate drug selection to commercial dosage form*. Gibson, M. (ed), pp 515-579. Interpharm Press, Englewood, CO, USA.

Walters, K.A., Brain, K.R., Dressler, W.E., Green, D.M., Howes, D., James, V.J., Kelling, C.K., Watkinson, A.C. and Gettings, S.D. (1997). Percutaneous penetration of N-nitroso-N-methyldodecylamine through human skin in vitro: application from cosmetic vehicles. *Food Chem. Toxicol.*, **35**, 705-712.

Wertz, P.W. and Downing, D.T. (1989). Stratum corneum: biological and biochemical considerations, in *Transdermal drug delivery*. Hadgraft, J. and Guy, R.H. (eds), pp 1-22. Marcel Dekker Inc., New York, USA.

Wester, R.C. and Maibach, H.I. (1989). In vivo animal models for percutaneous absorption, *Percutaneous Absorption: mechanisms – methodology – drug delivery*, 2nd Ed. Bronaugh, R.L. and Maibach H.I., (eds), pp 215-238. Marcel Dekker Inc., New York, USA.

Wester, R.C. and Maibach, H.I. (1999). Regional variation in percutaneous absorption, in *Percutaneous absorption: drugs – cosmetics – mechanisms - methodology*, 3rd Ed. Bronaugh, R.L and Maibach H.I. (eds) pp 107-116. Marcel Dekker Inc., New York, USA.

Wester, R.C., Christoffel, J., Hartway, T., Poblete, N., Maibach, H.I. and Forsell, J. (1998). Human cadaver skin viability for in vitro percutaneous absorption: storage and detrimental effects of heat-separation and freezing. *Pharm. Res.* **15**, 82-4.

Chapter 2

Chemical enhancement and retardation of skin permeation

2.1 Introduction

This chapter discusses the effect, and possible mechanisms, of skin penetration and permeation modifiers such as Azone[®], SEPA[®] and N-0915 and how this knowledge helped design the novel penetration retarders assessed in chapters 3 and 4.

Chemical enhancers are compounds that cause a reduction in the skin barrier function, such that greater delivery of an active drug into and/or through the skin can be achieved. Chemical retarders act in the opposite way, augmenting the skin barrier.

Many compound types can perform as enhancers, including surfactants, solvents, fatty acids, pyrrolidones, terpenes, and simple and long-chain alkyl esters. Several of these compound types can be found in formulations applied to the skin, where they are often considered as non-active excipients and fragrances. There have been several comprehensive reviews of penetration enhancers including those by Williams and Barry (2004) and those contained in the book edited by Walters and Hadgraft (1993).

It has been stated that the ideal enhancer should have the following wide-ranging attributes (modified from Barry, 1983):

- A. The material should be pharmacologically inert.
- B. The material should not be toxic, irritating or allergenic.
- C. On application, the onset of penetration enhancing-action should be immediate, and the duration of effect predictable and suitable.
- D. When the material is removed from the skin, the tissue should immediately and fully recover its normal barrier property.

- E. The barrier function of the skin should reduce in one direction only so that loss of endogenous materials does not change.
- F. The enhancer should be chemically and physically compatible with a wide range of drugs and formulation excipients.
- G. The substance should be an excellent solvent for drugs.
- H. The substance should spread well on the skin and possess a suitable skin 'feel'.
- I. The chemical should formulate into lotions, suspensions, ointments, creams, gels, aerosols and skin adhesives.
- J. It should be inexpensive, odourless, tasteless and colourless so as to be cosmetically acceptable.

The entire list of attributes will be physically impossible to achieve, particularly as no chemical enhancement process can simply be turned on and off like a switch. However, there is great opportunity to increase the skin penetration of drugs such that therapeutic treatment, or improvements in current applications, can be achieved. However, many compounds/solvents that are able to significantly enhance skin absorption cannot be used clinically due to skin irritation or damage. This resulted in the design of specific enhancer compounds that, it is hoped, have low irritancy and toxicity.

The possibility of reducing the skin penetration of harmful and potentially toxic compounds, such as chemical warfare agents and agrochemicals, is also an exciting prospect. The application of barrier creams can provide a physical layer of limited protection. However, reducing skin permeability generally, or to a particular compound or group of compounds, for a period of time would be beneficial in many circumstances.

One important commercial consideration is the regulatory hurdle that will be placed on specifically designed penetration modifiers. As they will generally be new chemical entities, comprehensive safety data will be required, and simple addition to existing licensed products will not be possible.

2.2 Specifically designed chemical enhancers

The most extensively studied specifically designed enhancers are probably Azone and SEPA (specifically SEPA 0009). Many analogues of these compounds have been produced and their effects investigated both *in vitro* and *in vivo*. They are believed to act by disruption of the lipid bilayers in the SC, and evidence for this will be discussed below. It should also be noted that many other enhancers, such as oleic acid and terpenes, might act in a similar manner.

2.2.1 Azone and its analogues

Stoughton (1982) reported the skin permeation enhancement of several compounds of varying lipophilicity by Azone (1-dodecylaza-cycloheptan-2-one, laurocapram, Figure 2.1). Many investigations into the effect of application solvent, concentration and drug applied subsequently followed. Azone is a colourless, odourless liquid (m.p. -7°C , $\log K_{o/w}$ 6.2) with low-irritancy and toxicity (oral LD50 in rat 9 g/kg) and it is soluble in most organic solvents (Williams and Barry, 2004).

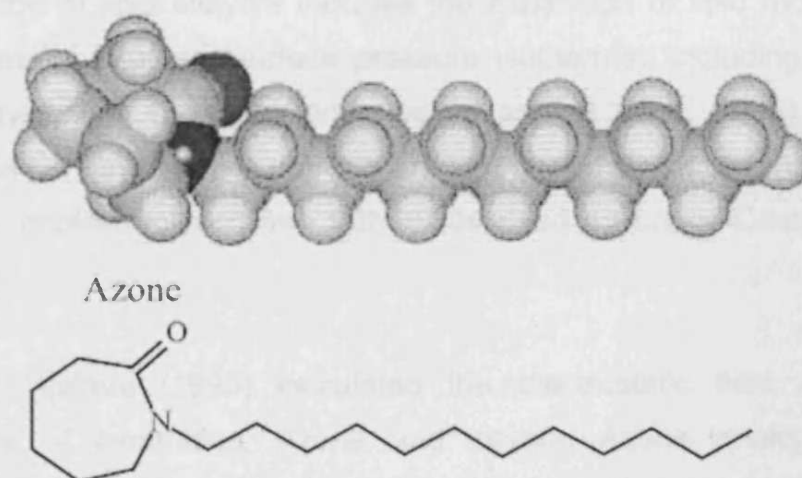


Figure 2.1 The chemical structure and configuration of Azone (Williams and Barry, 2004)

Pure Azone has been shown to be poorly absorbed by the skin, and the amounts that were absorbed were fairly quickly eliminated (Wiechers et al, 1987). Azone appears to be most effective at concentrations between 0.1 and 5% (Williams and Barry, 2004), either as a formulated product or in a solvent such as propylene glycol. Compounds enhanced by Azone are disparate and include 5-fluorouracil, verapamil, triamcinolone acetonide, flurbiprofen, naproxen and 4-cyanophenol. However, not all compounds are enhanced by Azone and investigations are still ongoing regarding in-use safety. Gyurik (1997) suggested that nitrogenous enhancers could interact with DNA and RNA cycles of building and repair, and therefore their mutagenicity and carcinogenicity should be studied in depth.

The proposed 'soup-spoon' configuration of Azone (Figure 2.1) was believed to interact with the skin lipids, with the seven-membered ring lying in the plane of the polar head groups, forcing them apart, disrupting packing in the head region, as well as intercalating with the lower acyl chain region (Hoogstraate et al, 1991). It was suggested that the dodecyl chain length allowed optimal insertion into the lipid (Hoogstraate et al, 1991). Several studies into other enhancing chemicals, such as fatty acids, have also found similar chain lengths (C₁₀ - C₁₂) effective (Aungst et al, 1986; Aungst, 1989). Evidence for the disruption of lipid bilayers includes the expansion of lipid monolayers in Langmuir trough studies (surface pressure isotherms), including dipalmitoyl phosphatidylcholine (DPPC) monolayers (Hadgraft et al, 1996) and, more relevant (as human SC does not contain phospholipids), mixed monolayers of ceramides, cholesterol and free fatty acids used by Lopez-Castellano et al (2000).

Brain and Walters (1993) calculated the electrostatic field around the headgroups of ceramides, Azone and several Azone analogues. They suggested that the electropositive and electronegative regions on opposite sides of the ceramide headgroups may be involved in binding with surrounding ceramide headgroups. The spoon shaped Azone molecule was calculated to have an electronegative site at the carbonyl moiety, but no

complementary positive side, leading to an unbalanced interaction with the ceramide headgroups and potentially a permeable defect. One Azone analogue, N-0915 (found to act as a retarder, see below), was shown to have a negative and positive side, and thus may be able to beneficially interact with the ceramides headgroups.

Many *in vitro* skin penetration and permeation studies have shown an enhancement effect with Azone using both pre-treatment and co-application conditions. Enhancement is usually demonstrated by comparison with a control group (not containing Azone), although it should be noted that the inclusion of Azone into a formulation could simply alter the thermodynamic activity of the measured permeant, rather than having an effect on the skin. Whilst skin penetration experiments show whether enhancement is occurring, they provide limited information regarding the mode of action. Harrison et al (1996a) used Attenuated Total Reflectance Fourier transform Infra-Red (ATR-FTIR) spectroscopy together with flux measurement with static diffusion cell experiments to examine the mechanism of enhancement of the model permeant, 4-cyanophenol, using Azone and Transcutol. It was found that the two enhancers probably exerted their effect by different mechanisms, with Azone reducing the diffusional resistance of the SC whilst Transcutol increased the solubility of the penetrant in this barrier. In a separate study using perdeuterated Azone (Harrison et al, 1996b), ATR-FTIR was used to monitor SC fluidity through measurement of the C-H₂ symmetric stretching frequency (2850 cm⁻¹). The applied perdeuterated Azone did not interfere with SC measurements as the C-D stretching bands were at ~2100 cm⁻¹. Results indicated that Azone may increase SC fluidity at physiological temperature, and that Azone is homogeneously distributed throughout the SC lipids (Harrison et al, 1996b).

When a group of Azone analogues (Figure 2.2) were tested on skin permeation of metronidazole, all but one (N-0915) enhanced permeation compared to a control treatment, with Azone providing greatest enhancement (Hadgraft et al, 1996). Comparison between each enhancer and control

treatment was performed with four replicates from the same donor. However, inspection of the data for all of the control groups (6 groups each with 4 replicates), showed that variability between the control groups was large, with a twenty-fold difference in average metronidazole permeation between some control groups. The total number of donors was not stated (but must have been 6 or less), and large inter-donor variability is not particularly uncommon for skin experiments. However, there are limitations in making comparisons with samples from only one donor, as it may not be representative of the wider population. It is also the case that the much more permeable donors would have been less susceptible to enhancement, as approximately 25% of the applied dose had permeated by 48 hours for these control groups. The enhancement factor of 6.7 seen for Azone (at 40 hours) would not be possible for these groups. Interestingly, the significant retardation seen for N-0915 (enhancement factor 0.2) was using one of the more permeable donors.

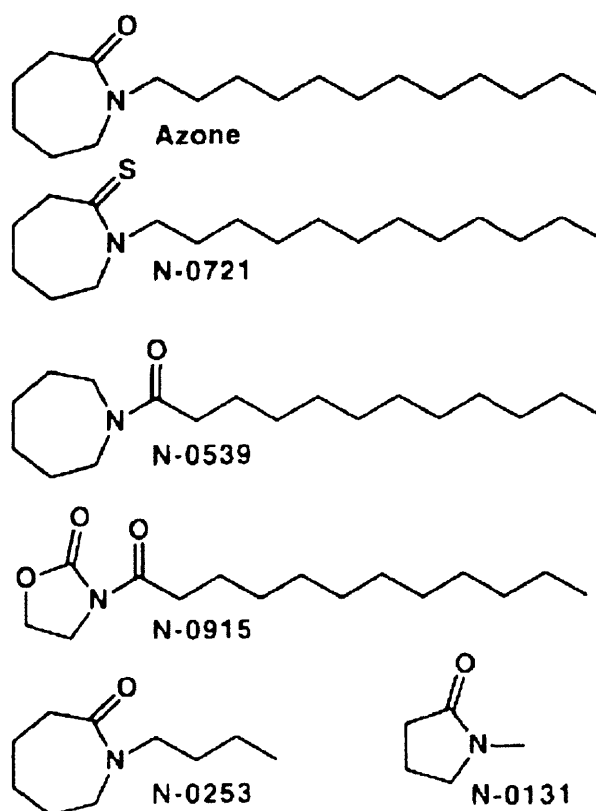


Figure 2.2 Chemical structures of selected Azone analogues (Hadgraft et al, 1996)

In Langmuir trough studies of the Azone analogues (Figure 2.2), N-0915 condensed DPPC monolayers and increased phase transition temperatures (the opposite effects to Azone), suggesting that skin lipids might also be condensed and become less permeable (Hadgraft et al, 1996). It was calculated that the 'soup-spoon' structure of Azone was not the minimum energy conformation form, and it was suggested that the enhancing effect of Azone was due to competition with skin lipids for hydrogen bonding sites, rather than spatial disruption effects. This was disputed by Milleman et al (1997), and recalculation of the conformation suggested by Hadgraft et al (1996) showed higher energy than the global minimum, which corresponded with a spoon shape. Perhaps this disparity confirms the drawbacks of particular computer algorithms in general, as they are only predictive in nature based on their training data set and their accuracy cannot be guaranteed.

The addition of a methyl group to the caprolactam ring (Milleman, 1997), to produce 3-methyl, 4-methyl, 5-methyl, 6-methyl and 7-methyl Azone analogues, reduced flux enhancement for hydrocortisone compared to Azone, using mouse skin. The same calculated minimum energy 'soup-spoon' configurations were found for the methyl analogues and it was concluded that the change in the caprolactam ring charge density and steric bulk caused decreased effectiveness.

A large series of Azone analogues were prepared and studied by Michniak and co-workers (1993a, 1993b, 1994a, 1995) using the model drug hydrocortisone 21-acetate applied in propylene glycol. The skin penetration and permeation studies used hairless mouse skin and many of the prepared compounds were not strict analogues of Azone, although they followed the same basic principles of lipophilic chain with polar head group. In several cases, 'Azone analogues' were superior to Azone in enhancing flux. A related investigation using different application vehicles (Michniak et al, 1994b) showed interesting results, with vehicle having a large effect on flux modification. Pre-treatment with Azone in the lipophilic vehicle isopropylmyristate (IPM) was no more effective than IPM alone. Some of the

analogues assessed also retarded hydrocortisone 21-acetate flux in some vehicles, compared to pre-treatment with vehicle alone, although the vehicles chosen enhanced flux compared to no pre-treatment, so the implications of retardation under some conditions were unclear. Co-administration produced reduced enhancement compared to pre-treatment.

The use of animal skin for many of the *in vitro* permeation studies of Azone and its analogues may mean that the effectiveness of enhancement has been overestimated in many cases, and it is quite possible that different rank orders would have occurred with human skin. This was appreciated by some authors, with a cautionary statement regarding extrapolation to humans (Michniak et al, 1993b).

A double-blind, randomised, vasoconstriction study comparing a 0.05% triamcinolone acetonide (TA)/Azone formulation (TNX) with that of standard 0.1% TA creams was performed with 61 healthy adult volunteers (Cato et al, 2001a). The subjects' forearms were exposed to formulations for 6 or 16 hours, and blanching assessed 2 hours after removal of formulations. The TNX formulation was significantly better than the 0.1% TA formulations after 6 hours ($p < 0.001$) and 16 hours ($p < 0.02$) exposure. One subject had an adverse reaction, erythema at the 6 hour site for TNX formulation, but this was not observed at the 16 hour site. The TNX formulation (Durham Pharmaceuticals Ltd, South Caroline, USA) then underwent a randomised clinical effectiveness trial for the treatment of atopic dermatitis (Cato et al, 2001b) and significant improvement in disease symptoms and status were observed compared to TA and control formulations. The company website (www.durhampharma.com, accessed 051005) suggested that the formulation was awaiting final approval from the FDA and market launch was expected in 2002. However, this does not yet appear to have occurred. A methotrexate/Azone formulation also appears to be under development by the same company for psoriasis vulgaris (Sutton et al, 2001).

2.2.2 SEPA

SEPA (Soft Enhancement of Percutaneous Absorption) is a family of patented (MacroChem Corp., Lexington, USA) enhancer compounds that feature a dioxane or dioxolane ring system and various side chains. SEPA 0009 (2-n-nonyl,1,3-dioxolane, Figure 2.3) was selected for development following initial *in vitro* studies that showed it had the broadest spectrum of activity and was one of the best enhancers in the SEPA family. SEPA 0009 is a clear, colourless oil (m.p. 0 °C, b.p. 89-90 °C) with a M_w of 200.31.

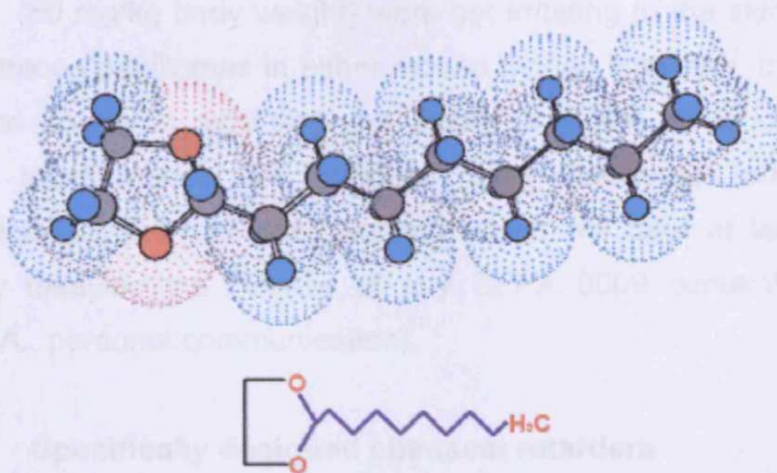


Figure 2.3 The chemical structure and configuration of SEPA 0009 (MacroChem, 2005)

It has been claimed by the developers that SEPA 0009 has superior enhancing capability compared to other enhancers, with a reliable, broad spectrum of activity (for both polar and non-polar compounds), and that it is safe for humans (especially as it is a non-nitrogenous enhancer) and easy to formulate (Gyurik, 1997). Thorough, positive, safety assessments have been performed in humans and animals (Gyurik, 1997) and several clinical trials have been undertaken for a testosterone formulation containing SEPA 0009 (Opterone[®], MacroChem, for the treatment of hypogonadism), and a nail lacquer formulation containing econazole and SEPA 0009 (EcoNail[™], MacroChem, for the treatment of onychomycosis).

SEPA 0009 mode of action is believed to be similar to that discussed above for Azone, with lipid bilayer disordering perhaps creating both aqueous and lipoidal conduits in the SC (Gyurik, 1997).

A recent study (Fuhrman et al, 2005), where SEPA 0009 was applied to the skin of both genetically engineered mice (with reduced tumour suppresser gene activity for carcinogen identification) and non-transgenic mice, has raised questions over safety. At high doses (1500 mg/kg body weight), SEPA 0009 induced tumorigenesis in genetically engineered mice, and it was proposed that this was a result of the preceding severe and chronic irritation. Low doses (50 mg/kg body weight) were not irritating to the skin and did not cause squamous papillomas in either mouse model. However, these findings raised some concerns regarding the safety of SEPA 0009. Although the transgenic mice model can produce false positives, further lifetime carcinogenicity studies are now required which will take at least 2 years, significantly delaying the release of any SEPA 0009 containing products (Walters K.A., personal communication).

2.3 Specifically designed chemical retarders

There are only a few reports of specifically designed retarders, and these include MacroDerm compounds (MacroChem Corp., USA), TopiCare Delivery Compounds (Penederm Inc., USA) and compounds prepared in collaboration with our laboratory. The retarder N-0915 (an Azone analogue not specifically designed to act as a retarder) is discussed in section 2.2.1.

2.3.1 MacroDerm compounds

MacroDerms (Figure 2.4) are low to moderate molecular weight polymers that can be synthesised to exhibit lipophilic, amphiphilic, or hydrophilic characteristics.

It is claimed that MacroDerms have an affinity for the SC such that they are able to retain any active moieties in the upper layers of the skin (MacroChem Corp.) and impede dermal penetration. However, it is also claimed that they do not readily penetrate the skin, so limited safety assessments would be required. Evidence of a reduction in skin absorption of the insect repellent DEET, and a reduction in epidermis and dermis levels of the sunscreen octyl dimethyl PABA were reported on their website, but not as yet in a scientific journal. It might be the case that these molecules may partially act by reducing the release of active compounds from the formulation into the SC.

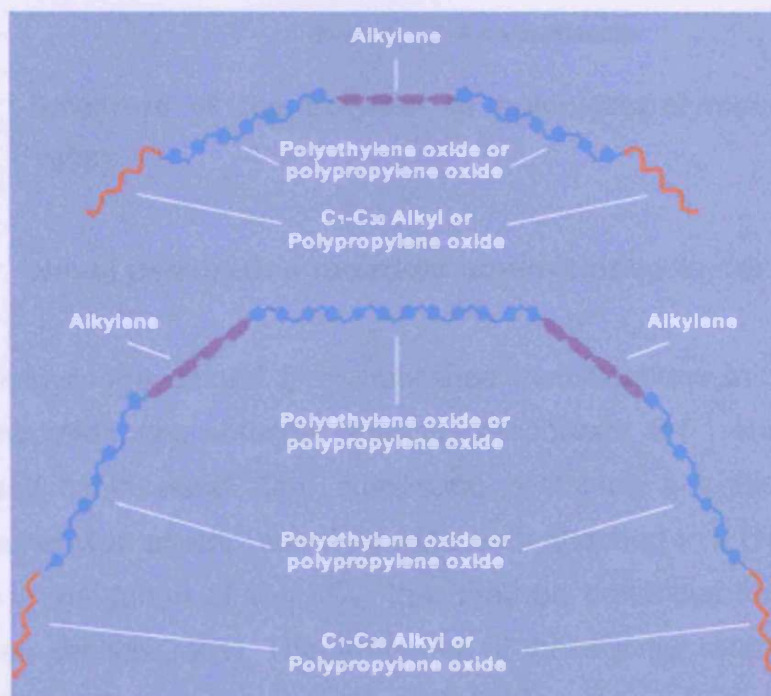
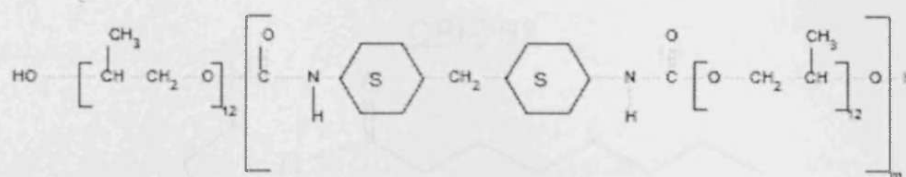


Figure 2.4 Example MacroDerm molecules (MacroChem Corp.)

2.3.2 TopiCare Delivery Compounds

The patented TopiCare Delivery Compounds (Penederm Inc.) are liquid polymer mixtures that are incorporated into topical formulations to help retain solubilised drugs, such as tretinoin, on the skin surface and in the upper layers of the skin (Skov et al, 1997). A marketed tretinoin gel (0.025%, Avita cream, Mylan, USA) contains the TopiCare Delivery Compound polyolprepolymer-2 (PP-2). *In vitro* human skin penetration studies and clinical

trial data showed benefits for inclusion of PP-2 compared to another marketed formulation. PP-2 is a clear, non-volatile viscous liquid of low toxicity, with a weight-average M_w of ~ 4000 , but a number-average molecular weight (NAM_w) of ~ 2000 (NICNAS, 1996). It appears that PP-2 consists of 80% polymer (Figure 2.5) plus an obligatory 20% propylene glycol by-product.



where $m = 1-4$ predominantly

Figure 2.5 Structure of the polymer in polyolprepolymer-2 (NICNAS, 1996)

2.3.3 Novel penetration retarders co-developed in our laboratory

Using the knowledge gained from published investigations into Azone and related compounds, two potential retarder compounds, 2-F1 and 4-F2, were designed and synthesised. One compound contained a cyclic polar head group, the other was acyclic, and they were both attached to a C_{11} alkyl chain, which was in the range of $C_{10} - C_{12}$ that may be beneficial for lipid bilayer insertion (see section 2.2.1). The structures of these initial retarders and two subsequently synthesised analogues, ORI-PR2 and ORI-PR3 are shown in Figure 2.6.

Three of the potential retarder compounds, 2-F1, ORI-PR2 and 4-F2 are liquid at skin temperature, whilst ORI-PR3 is a waxy solid. Molecular weights are 267.4, 221.3, 285.4 and 255.4 for 2-F1, ORI-PR2, ORI-PR3 and 4-F2, respectively.

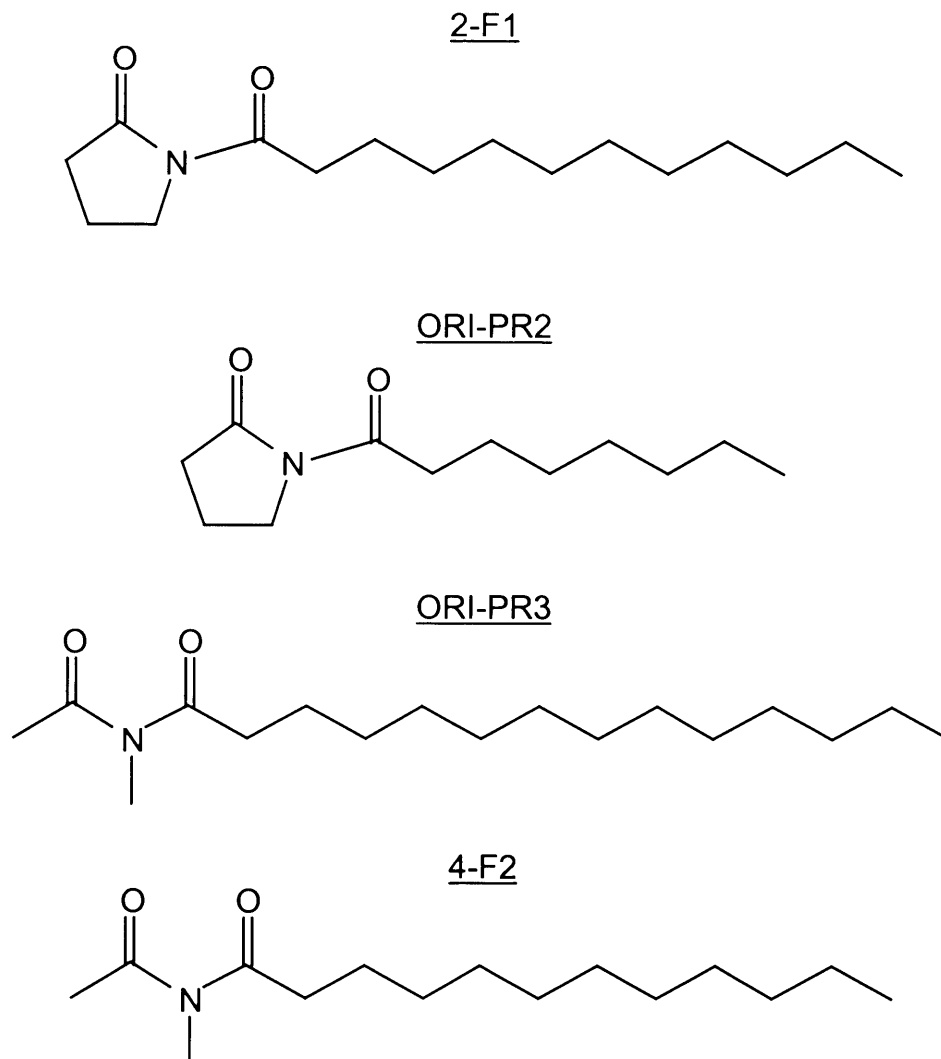


Figure 2.6 Chemical structures of potential penetration retarders

Compounds 2-F1 and 4-F2 were investigated in preliminary *in vitro* studies (Brain et al, 1996), and shown to retard the skin permeation of DEET, whilst Azone increased the permeation compared to the control. The permeation of hydrocortisone was assessed in the same study and showed the same effects at the only time-point where hydrocortisone was detected (48 hours). Retarder 4-F2 appeared the most promising of the two penetration retarders from this initial data.

Compound 4-F2 was investigated further in chapter 3, and all four potential retarder compounds (Figure 2.6) were assessed in chapter 4.

2.4 References

Aungst, B.J. (1989). Structure-effects studies of fatty acid isomers as skin penetration enhancers and skin irritants. *Pharm. Res.* **6**, 244– 247.

Aungst, B.J., Rogers, N.J. and Shefter, E. (1986). Enhancement of naloxone penetration through human skin in vitro using fatty acids, fatty alcohols, surfactants, sulfoxides and amides, *Int. J. Pharm.* **33**, 225– 234.

Barry, B.W. (1983). Properties that influence percutaneous absorption, in *Dermatological formulations; percutaneous absorption*, pp. 127-233. Marcel Dekker Inc., New York, USA.

Brain, K.R. and Walters, K.A. (1993). Molecular modelling of skin permeation enhancement by chemical agents, in *Pharmaceutical skin penetration enhancement*. Walters K.A. and Hadgraft, J (eds), pp. 389-416. Marcel Dekker Inc., New York, USA.

Brain, K.R., Green, D.M., James, V.J., Walters, K.A., Watkinson, A.C., Allan, G. and Hammond, J. (1996). Preliminary evaluation of novel penetration retarders, in *Prediction of Percutaneous Penetration*, Vol. 4B. Brain, K.R., James, V.J. and Walters, K.A. (eds) pp. 131-132. STS publishing, Cardiff, UK.

Cato, A., Sutton, L., Manning, G.N. and Kaplan, A.S. (2001a). Activity of a 0.05% Triamcinolone Acetonide/Laurocapram Formulation: Double-Blind, Randomized Comparison with Standard 0.1% Triamcinolone Acetonide Creams and with Mild (Class VI) to Potent (Class III) Topical Corticosteroids. *Curr. Ther. Res.*, **4**, 231-235.

Cato, A., Swinehart, J.M., Griffin, E.I., Sutton, L. and Kaplan, A.S. (2001b). Azone enhances clinical effectiveness of an optimized formulation of triamcinolone acetonide in atopic dermatitis. *Int. J. Dermatol.*, **40**, 232-236.

Fuhrman, J., Shafer, L., Repertinger, S., Chan, T. and Hansen, L.A. (2005). Mechanisms of SEPA 0009-Induced Tumorigenesis in v-ras(Ha) Transgenic Tg.AC Mice. *Toxicol. Pathol.* **33**, 623-630.

Gyurik, R.J. (1997). The future of chemical enhancers, in *Perspectives in Percutaneous Penetration*, Vol. 5B. Brain, K.R., James, V.J. and Walters, K.A. (eds) pp. 17-23. STS publishing, Cardiff, UK.

Hadgraft, J., Peck, J., Williams, D.G., Pugh, W.J. and Allan, G. (1996). Mechanisms of action of skin penetration enhancers/retarders: Azone and analogues. *Int. J. Pharm.*, **141**, 17-25.

Harrison, J.E., Watkinson, A.C., Green, D.M., Hadgraft, J. and Brain, K. (1996a). The relative effect of Azone and Transcutol on permeant diffusivity and solubility in human stratum corneum. *Pharm. Res.*, **13**, 542-546.

Harrison, J.E., Groundwater, P.W., Brain, K.R., and Hadgraft, J. (1996b). Azone induced fluidity in human stratum corneum. A fourier transform infrared spectroscopy investigation using the perdeuterated analogue. *J. Control. Rel.*, **41**, 283-290.

Hoogstraate, A.J., Verhoef, J., Brussee, J., Ijzerman, A.P., Spies, F. and Boddé, H.E. (1991). Kinetics, ultrastructural aspects and molecular modelling of transdermal peptide flux enhancement by N-alkylazacycloheptanones. *Int. J. Pharm.*, **76**, 37-47.

Lopez-Castellano, A., Cortell-Ivars, C., Lopez-Carballo, G. and Herraiz-Dominguez, M. (2000). The influence of Span20 on stratum corneum lipids in langmuir monolayers: comparison with Azone. *Int. J. Pharm.* **203**, 245-253.

Michniak, B.B., Player, M.R., Chapman, Jr., J.M. and Sowell, Sr., J.W. (1993a). In vitro evaluation of a series of Azone analogs as dermal penetration enhancers. I. *Int. J. Pharm.*, **91**, 85-93.

Michniak, B.B., Player, M.R., Fuhrman, L.C., Christensen, C.A., Chapman, Jr., J.M. and Sowell, Sr., J.W. (1993b). In vitro evaluation of a series of Azone analogs as dermal penetration enhancers. II. (Thio)amides. *Int. J. Pharm.*, **94**, 203-210.

Michniak, B.B., Player, M.R., Fuhrman, L.C., Christensen, C.A., Chapman, Jr., J.M. and Sowell, Sr., J.W. (1994a). In vitro evaluation of a series of Azone analogs as dermal penetration enhancers. III. Acyclic amides. *Int. J. Pharm.*, **110**, 231-239.

Michniak, B.B., Player, M.R., Chapman, Jr., J.M. and Sowell, Sr., J.W. (1994b). Azone analogues as penetration enhancers: effect of different vehicles on hydrocortisone acetate skin permeation and retention. *J. Control. Rel.*, **32**, 147-154.

Michniak, B.B., Player, M.R., Godwin, D.A., Phillips, C.A. and Sowell, Sr., J.W. (1995). In vitro evaluation of a series of Azone analogs as dermal penetration enhancers. IV. Amines. *Int. J. Pharm.*, **116**, 201-209.

Milleman E.J., Danker, W.A., Chapman, J.M. and Michniak, B.B. (1997). Addition of a methyl group to the caprolactam ring on Azone: the effect on dermal penetration enhancement, in *Perspectives in Percutaneous Penetration*, Vol. 5B. Brain, K.R., James, V.J. and Walters, K.A. (eds) pp. 153-156. STS publishing, Cardiff, UK.

NICNAS (1996), Australian National Industrial Chemicals Notification and Assessment Scheme, full public report on polymer in Polyolprepolymer-2, File No. NA/378. Through;
<http://www.nicnas.gov.au/publications/CAR/new/NA/NAFULLR/NA0300FR/NA378FR.pdf>, accessed 04/10/05.

Skov, M.J., Quigley, J.W. and Bucks, D.A. (1997). Topical delivery system for tretinoin: research and clinical implications. *J. Pharm. Sci.*, **86**, 1138-1143.

Stoughton, R.B. (1982). Enhanced percutaneous penetration with 1-dodecylazacycloheptan-2-one. *Arch. Dermatol.*, **118**, 474-477.

Sutton, L., Swinehart, J.M., Cato, A. and Kaplan, A.S. (2001). Safety of 1% methotrexate/Azone (MAZ) gel applied topically once daily in patients with psoriasis vulgaris. *Int. J. Dermatol.*, **40**, 464-467.

Walters K.A. and Hadgraft, J (1993). *Pharmaceutical skin penetration enhancement*. Walters K.A. and Hadgraft, J (eds). Marcel Dekker Inc., New York, USA.

Wiechers, J.W., Drenth, B.F., Jonkman, J.H. and de Zeeuw, R.A. (1987). Percutaneous absorption and elimination of the penetration enhancer Azone in humans. *Pharm. Res.*, **4**, 519-23.

Williams, A.C. and Barry, B.W. (2004). Penetration enhancers. *Adv. Drug Deliv. Rev.*, **56**, 603-618

Chapter 3

Investigations into the effect of retarder 4-F2 using the model permeant DEET

3.1 Introduction

The results of a preliminary evaluation of the novel penetration retarders 2-F1 and 4-F2 (Brain et al, 1996) indicated that significant retardation of both DEET and hydrocortisone had been achieved. However, those experiments were of fairly limited scope and further investigation into the effects of these retarders was required

Fresh samples of 4-F2 (see section 2.3.3) were synthesised in 2002/3 by OmniPharm Research International Inc., enabling reinvestigation of the previously observed retardation.

The first experiment reported in this chapter utilised very similar conditions to the DEET data reported in 1996, but with the addition of some controls (such as inclusion of a membrane integrity check) to increase confidence in the data produced. Additionally, the skin distribution of DEET 24 hours after dosing was assessed.

3.1.1 DEET

The permeant assessed in this work was DEET (CAS No. 134-62-3, Figure 3.1), N,N-diethyl-*m*-toluamide. DEET has a molecular weight of 191.27 Daltons, is a liquid ($d^{25} \sim 0.997$, b.p. 160°C), has a low solubility in water (<1 mg/ml), but is freely miscible with ethanol. The reported log octanol/water partition coefficient, log $K_{O/W}$ of DEET varies between 1.44 (Stinecipher, 1998) and 2.18 (Sangster, 2004).

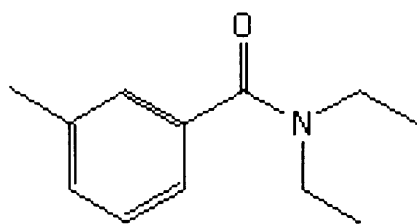


Figure 3.1 Structure of DEET

DEET is an effective broad spectrum repellent against insects developed by the U.S. Army in 1946, and first registered in the USA in 1957. There are many different types of product used, and DEET concentrations range from ~4 to 100% (US Environmental Protection Agency, 1998). It is believed that DEET repels mosquitoes by inhibiting host identifying lactic acid receptors on their antennae (Davis, 1976). A study comparing duration of action *in vivo* with *in vitro* evaporation indicated that a minimum DEET evaporation rate of $1.2 \pm 0.3 \mu\text{g}/\text{cm}^2\cdot\text{h}$ was required to repel *Aedes aegypti* mosquitoes (Reifenrath, 1982).

Although the general safety of DEET has been established by long term human use and extensive animal studies, both local and systemic adverse effects have been observed, especially in the young. Cases of death, toxic encephalopathy, and cardiovascular and dermal toxicity have been reported (Qui, 1998). Efforts have been made to formulate DEET in controlled release formulations in order to reduce potential dermal absorption. 3M developed a polymer based product containing 33% DEET in 1984 and this was adopted by the U.S. military as the main product used by the time of the first Gulf War (Cecchine, 2000).

The effect of ethanol on the permeation of DEET has been assessed by several groups, with reported enhancement of steady state flux of DEET for 40-50% ethanol solutions, relative to neat technical grade DEET (Qui, 1998 and Stinecipher, 1998). On the other hand 75% and neat ethanol were reported to produce a reduction in DEET permeation relative to technical grade (Qui, 1998) using large DEET doses and rat skin. Work in this chapter

used DEET solutions in 96% (v/v) ethanol, but for the small, finite doses applied, the ethanol would be expected to act principally as a rapidly evaporating application vehicle.

3.2 Assessment of the effect of skin pre-treatment with retarder 4-F2 on the human skin permeation and distribution of DEET

3.2.1 Materials and equipment

Compound 4-F2 (4 x 100 mg samples, batch no. 1) was supplied by OmniPharm Research International Inc., Buffalo, USA. DEET (98%) was from Sigma-Aldrich Ltd. Tritiated water ($^3\text{H}_2\text{O}$) was from Amersham Pharmacia Biotech, Little Chalfont, UK, and diluted with distilled water to a specific activity of 10 $\mu\text{Ci/ml}$. Water was distilled in all glass apparatus and solvents and buffer salts were of AnalaR grade or better (BDH). OptiPhase 'HiSafe' 3 liquid scintillation cocktail and OptiSolve tissue solubiliser were from Wallac (UK) Ltd. Radioactive samples were dispersed in 3 ml scintillation cocktail and counted for radioactivity using a Wallac 1409 liquid scintillation counter. Weight measurements were made on a Sartorius BP211D 5-place semi-micro analytical balance equipped with a statistical printer. Vortexing was performed using a Vortex Genie 2 (Scientific Industries, USA), and sonication using an ultrasonic bath (model U300T, Ultrawave Ltd, Cardiff, UK). D-Squame adhesive tape was from CuDerm Corporation (Dallas, USA).

3.2.2 Methods

3.2.2.1 Receptor phase preparation

Phosphate buffered saline (pH 7.4; PBS) was prepared by dissolving the following salts in water: 2.1 g/l $\text{NaH}_2\text{PO}_4 \cdot 2\text{H}_2\text{O}$, 19.1 g/l $\text{Na}_2\text{HPO}_4 \cdot 12\text{H}_2\text{O}$ and 4.4 g/l NaCl. The pH of the buffer was confirmed to be 7.4 ± 0.1 .

DEET had a measured solubility at 23°C in PBS of 5.7 ± 0.1 mg/ml (mean \pm standard error, SE, $n=3$, 2.0%RSD, determined by HPLC). Solubility was difficult to assess due to the tendency of DEET to form an emulsion, or fine droplet dispersion, in PBS (and water) at concentrations close to, and above, the saturated solubility. Reported water solubility varies greatly (~10-fold), possibly due to contamination of the analysed sample with excess DEET. The optimal developed method was as follows. Vials containing PBS and excess DEET were shaken for 24 hours. The vials were allowed to stand unshaken for 30 minutes, allowing excess DEET to rise to separate on the surface. Samples of the lower layer were transferred to a small separating funnel using a Pasteur pipette, and the middle cut of the PBS layer placed in a vial prior to 1 in 1000 dilution with PBS and analysis. Direct sampling of the lower layer without the use of the separating funnel caused DEET contamination and highly variable results. To confirm the validity of the measured values above, two additional methods were assessed: (i) a 1.5 ml centrifuged sample of a saturated solution was centrifuged for 10 minutes at 12,000 rpm, and the tube frozen (upright) overnight. The bottom 0.5 ml of the tube was cut-off whilst frozen, the solution defrosted, vortexed and diluted as above prior to analysis (6.10 mg/ml by HPLC) (ii) a new vial containing excess DEET was placed on a roller shaker for 3 hours at room temperature. Granular activated charcoal (for gas adsorption) was added to the vial (charcoal equivalent to ~30% of solution volume) and excess DEET appeared to adsorb to the charcoal. A portion of the PBS solution was centrifuged (to remove fine charcoal particles) and a sample diluted and analysed by HPLC. The measured DEET concentration was 6.75 mg/ml, and it is likely that the higher result was due to the warming of the PBS solution following addition of the charcoal, thus causing higher solubility.

3.2.2.2 Vehicle preparation

A 0.5% (w/v) DEET solution in ethanol (96% (v/v), AnalaR, measured d_{25} 0.803 g/ml) was prepared by transferring 31.43 mg DEET (measured d_{25} 0.997 g/ml) to a 20 ml glass vial using a Pasteur pipette, and adding 5.049 g ethanol (= 6.288 ml). The vial was immediately capped and the contents

shaken prior to storage at room temperature in the dark. If ideal mixing is assumed, then the calculated solution concentration was 4.97 mg/ml DEET.

A 2% (w/v) 4-F2 solution in ethanol (96% (v/v), AnalaR) was prepared by transferring 26.60 mg 4-F2 (gently warmed to produce a homogeneous oil) to a 1.5 ml glass vial using a warmed Pasteur pipette, and adding 1.068 g ethanol (= 1.330 ml). The vial was immediately capped and the contents shaken prior to storage at room temperature in the dark. The melting point of 4-F2 was around room temperature and therefore, when transferring pure 4-F2, vials were hand warmed to ensure homogeneous transfer. If ideal mixing and a 4-F2 density of 1 g/ml were assumed, then the calculated solution concentration was 19.61 mg/ml 4-F2. Small-scale preparation of the 4-F2 solution was necessary due to the small amount of material available.

3.2.2.3 Skin preparation

Human epidermal membranes were prepared using a standard procedure. Full-thickness human female abdominal and breast skin, obtained from cosmetic surgery and stored at -20°C, was thawed at room temperature for processing. Following removal of the subcutaneous fat by blunt dissection, individual portions of skin were immersed in water at 60°C for 55 seconds. The epidermis (comprising stratum corneum and epidermis) was then gently removed from the underlying dermis. The latter was discarded and the epidermal membrane floated onto the surface of water and taken up onto aluminium foil. The membranes were thoroughly dried and stored flat at -20°C until used.

On the day of use, the epidermal membranes were floated onto water from the aluminium foil and taken up onto 25 mm diameter filter paper supports. The membranes were then mounted onto diffusion cells. Membranes from three different donors were prepared and the donors were distributed as evenly as possible between the experimental groups.

3.2.2.4 Diffusion cells

The skin membranes were mounted as a barrier between the halves of greased (high vacuum grease, Dow Corning, USA) horizontal Franz-type diffusion cells (Figure 3.2), with the stratum corneum facing the donor chamber. The area available for diffusion was about 1.2 cm², with the exact area being measured for each diffusion cell.

The receptor chambers of the diffusion cells were initially filled with a known volume of PBS and capped. The diffusion cells were immersed in a constant temperature water bath such that the receptor chambers were maintained at 37.0±0.5°C throughout the experiment. This ensured that the skin surface temperature was maintained at 32.0±1°C. Receptor chamber contents were continuously agitated by small PTFE-coated magnetic followers driven by submersible magnetic stirrers. The cells were allowed to temperature equilibrate for 30 minutes before subsequent treatment.

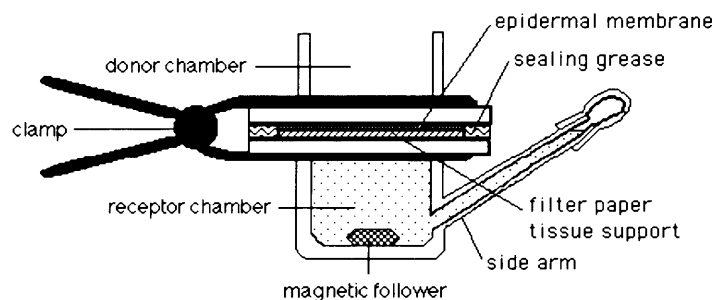


Figure 3.2 Horizontal glass diffusion cell

3.2.2.5 Membrane integrity assessment

The integrity of each membrane was assessed prior to pre-treatment with 4-F2. The permeation of tritiated water was determined by applying 500 µl of 10 µCi/ml ³H₂O to the skin surface and removing a 200 µl sample from the receptor phase twenty minutes later. The sample was counted using liquid scintillation counting (LSC). The skin surface was subsequently washed six times with water and the receptor chambers three times with PBS, prior to

refilling with PBS. The cells were then allowed to re-equilibrate to the correct temperature.

Of 18 cells prepared, twelve cells exhibited a water permeability coefficient, $k_p < 2.5 \times 10^{-3}$ cm/h, a cut-off point for typical permeability (Bronaugh, 1986). The failed cells were mainly from one donor, suggesting that the skin from this donor failed to heat separate properly. Due to the high risk of damage to the two remaining (potentially weak) membranes during the rinsing procedure (to remove remaining tritiated water), all cells from this donor were rejected, as each dosed cell generated significant analytical cost due to the large number of samples for analysis.

3.2.2.6 Skin pre-treatment with 4-F2

Following the membrane integrity assessment, cells were separated into two groups for pre-treatment (prior to application of DEET). Group 1 cells received a $50 \mu\text{l}/\text{cm}^2$ dose of 2% 4-F2 in ethanol. Group 2 (control) cells received an identical dose of ethanol alone. The pre-treatments were applied using a $50 \mu\text{l}$ Hamilton syringe and the cells were left undisturbed in the waterbath for 2 hours. It was observed that the pre-treatment vehicle had completely evaporated in less than 40 minutes.

3.2.2.7 Application of DEET solution

All cells (groups 1 and 2) received a target dose of $10 \mu\text{l}/\text{cm}^2$ 0.5% DEET in ethanol, applied using a $25 \mu\text{l}$ Hamilton syringe. Cells were rotated in a circular motion to ensure that the applied solutions spread evenly over the entire skin surface. For each cell, the exact time of application was noted and that time represented zero time for that cell. The diffusion cell donor chambers were not occluded.

3.2.2.8 Determination of skin permeation

200 µl samples were taken (using a digital pipette) from each receptor chamber 15 minutes prior to dosing and 2, 4, 8, 12 and 24 hours after dosing. Each sample was placed into a 200 µl micro-vial (Chromacol Ltd, Welwyn Garden City, UK) and immediately frozen (-20°C) pending analysis. The liquid removed by each sample was replaced with fresh temperature equilibrated blank receptor medium.

3.2.2.9 Determination of skin distribution and DEET recovery

Following removal of the 24 hour receptor phase samples, the remaining receptor phases were removed, placed in 20 ml glass vials (Chromacol, UK), the vials tightly capped and frozen (-20°C). Material remaining on the skin surface was removed by gentle wiping with dry cotton buds. The cotton bud wipes for each cell were placed into 20 ml glass vials, the vials were tightly capped and then frozen pending extraction and analysis. The diffusion cells were then dismantled and the epidermal membranes secured onto a small disc of thin plastic using cyanoacrylate adhesive. Each epidermal membrane was tape stripped 10 times using D-Squame[®] adhesive tape discs. The tape strips were grouped (placed in the same vial) as follows: strip 1, strips 2-3, strips 4-6 and strips 7-10. Vials were frozen as above. The remaining samples of skin (epidermis plus any remaining stratum corneum) were then placed into individual glass vials and the vials frozen as above.

Surface wipe and tape strip 1, strips 2-3, 4-6 and 7-10 samples were extracted into suitable volumes (7, 2, 1, 1 and 2 ml respectively) of 50/50 (v/v) acetonitrile/water with vortexing and sonication. An aliquot of the extract was centrifuged for 3 minutes at 10,000 rpm prior to analysis. For remaining skin samples, a different extraction procedure was required due to significant assay interference when using acetonitrile/water extraction. These samples were extracted into 2 ml of distilled water with 30 minutes shaking at 60°C. This method was modified from that used to extract aciclovir from skin

samples (Volpato et al, 1997). The single skin extraction procedure was found to efficiently recover the majority of the DEET, as a second extraction process performed for one cell recovered less than 10% of that measured in the first extract.

3.2.2.10 Sample analysis and assay validation

A sensitive high performance liquid chromatography (HPLC) method for the quantitation of DEET was developed for this study. The chromatographic equipment used was as follows; TSP SCM1000 vacuum membrane degasser, P4000 quaternary pump, AS3000 autosampler, UV6000LP UV/Vis detector and SN4000 controller interface. Data collection and integration were conducted using PC1000 Ver. 3.5.1 software (TSP Ltd., Stoke-On-Trent, UK). Separation was performed on a Genesis C18 (Jones) 4 μm , 150 x 4.6 mm column protected with C18 security guard cartridges (Phenomenex). The injection volume was 50 μl (Pushloop injection).

Mobile phase (MP) A consisted of 50/50 acetonitrile/water, and MP B was 100% acetonitrile. The acetonitrile used throughout this work was of HiPerSolv far UV grade. The flow rate was 1 ml/min and quantitation was by UV detection at 208 nm (a local lambda maximum/inflexion), with UV scans (200-320 nm) also collected. The integration wavelength was chosen as the best compromise between maximising the detection limit for DEET and minimising the influence of chromatically interfering compounds. The gradient elution program shown in Table 3.1 was used for all samples except receptor phase samples. This gradient program was developed to produce a flat baseline during the elution of the DEET peak (~5.2 minutes) and included a column rinse period to remove skin and adhesive compounds prior to the next injection. For receptor phase samples, a seventeen minute runtime, 100% MP A isocratic method was used.

Table 3.1 HPLC gradient elution program – used for all non-receptor phase samples

Time (min)	% MP A	% MP B
0.0	100	0
5.5	100	0
8.0	30	70
18.0	30	70
21.0	100	0
35.0	100	0

Five level linear calibration plots were constructed (within PC1000) using DEET standard solutions prepared in PBS, water and 50/50 acetonitrile/water (as all samples used one of these injection solvents). The calibration concentration ranges varied between solvents and samples analysed but fell between 0.020 and 20 µg/ml DEET. Sample concentrations above 20 µg/ml were outside the linear calibration region and required dilution prior to analysis. An example calibration (Figure 3.3, 0.02 to 5 µg/ml DEET in 50/50 acetonitrile/water) and a chromatogram (Figure 3.4, 12 h sample cell 1) are shown below. The calibration plot correlation coefficient, r , was typically 1.0000 and the software calculated reliability value was >99.98%.

Injection reproducibility was assessed using three replicate injections of each 50/50 acetonitrile/water standard solution (Table 3.2). Inter-day variability was good, with a variation of 0.92% RSD for the 50/50 acetonitrile/water injection solvent standards (assessed using the calibration gradients, $n=3$ for each injection solvent). Injection reproducibility appeared similar for the other injection solvents but was not formally assessed.

Mode: Reprocessed Data
 Original Results: C:\TSP\DG_11_03\Data\Standards5.RES
 Reprocessed Results: C:\TSP\DG_11_03\Data\Standards5.RMS

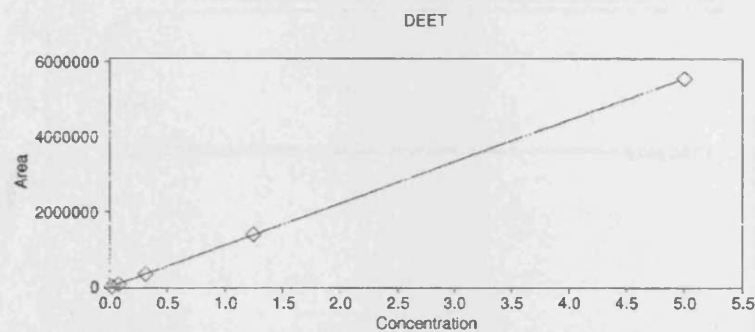
Page 1
 Reported On: 11-01-05 13:38:49

Calibration Report

Calculation Type: External Standard (Area)
 Number of Calibration Levels: 5
 Fit Type: Linear Fit
 Weighting: None

Signal 1: UV6000LP B 208 nm

Vial Name	Vial	Injections
Calibration 01	B01	1
Calibration 02	B02	1
Calibration 03	B03	1
Calibration 04	B04	1
Calibration 05	B05	1



AREA = B * CONC + C
 B = 1.10956e+06, C = 7.6291e+03, RELIABILITY = 99.999%, CORR COEFF = 1.0000

Component	RT (min)	Linear Coeff	Const Coeff	%Rel	Corr
DEET	5.058	1.10956e+06	7.62906e+03	99.999	1.0000

System: Reprocess	Analyst: dg	PC1000 Ver 3.5.1
Acquisition Method: C:\TSP\DG_11_03\Methods\dg1.AQM		02-06-03 13:10:38
Calculation Method: C:\TSP\DG_11_03\Methods\dg1_MP_208.CAM		09-06-03 13:24:48
Report Method: C:\TSP\DG_11_03\Methods\dg1.RPM		11-04-03 11:19:10

Figure 3.3 Typical DEET calibration (5 level, 0.02 to 5 µg/ml DEET in 50/50 acetonitrile/water)

Table 3.2 Injection reproducibility

DEET concentration (µg/ml)	peak area variability (% RSD)
0.0195	1.06
0.0781	0.74
0.3125	0.64
1.25	0.45
5	0.91

Mode: Acquired Data
Original Results: C:\TSP\DG_11_03\Data\12hr_samples1.RMS

Page 1
Reported On: 11-01-05 16:00:20

Analysis Report

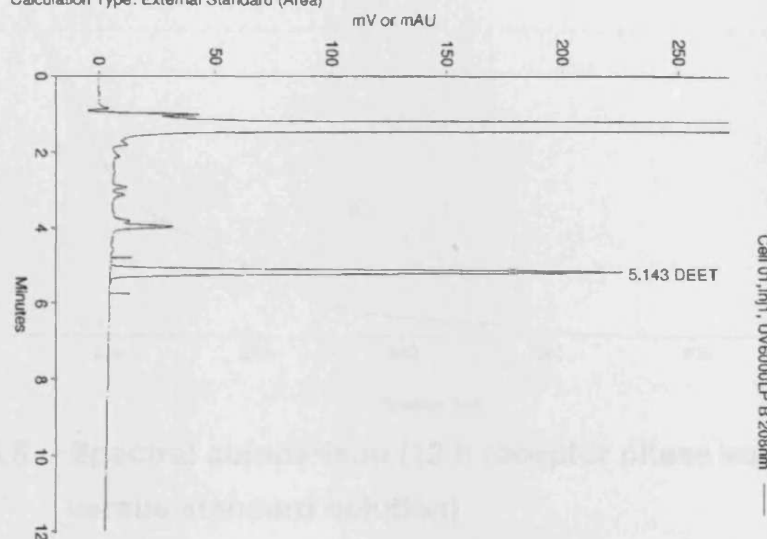
Name: Cell 01
Type: Sample
Injection Volume: 50.0 μ L

Vial: B01
Injection: 1 of 1
Injected On: 15-04-03 13:32:07

Acquisition Log
Column Pressure (PSI): 1174
Noise (microAU): 2e+02
Run-Time Messages: None

Column Temperature (C): N/A
Drift (microAU/min): 5e+02
Pump Flow Stability: 3.2

Signal 1: UV6000LP B 208 nm
Calculation Type: External Standard (Area)



Component	RT(min)	Area	Height	ug/ml	Peak Type
DEET	5.143	1726267	221997	1.7907	Modified
Totals		1726267	221997	1.7907	

Figure 3.4 Example chromatogram (12 h receptor phase sample, cell 1)

As there were no control cells that were not dosed with DEET, the spectral purity of the DEET peaks for several cells was compared to that for a standard solution, enabling confirmation that there were no co-eluting compounds. The spectral purity comparison was performed in Spectacle, a program associated with the PC1000 HPLC operating program. An example of the comparison (Figure 3.5) between a 12 h receptor phase sample (signal A) and a similar concentration standard solution (signal B) over a wide wavelength range (200 to 320 nm) produced an excellent correlation of value of 999.8 (of a possible 1000).

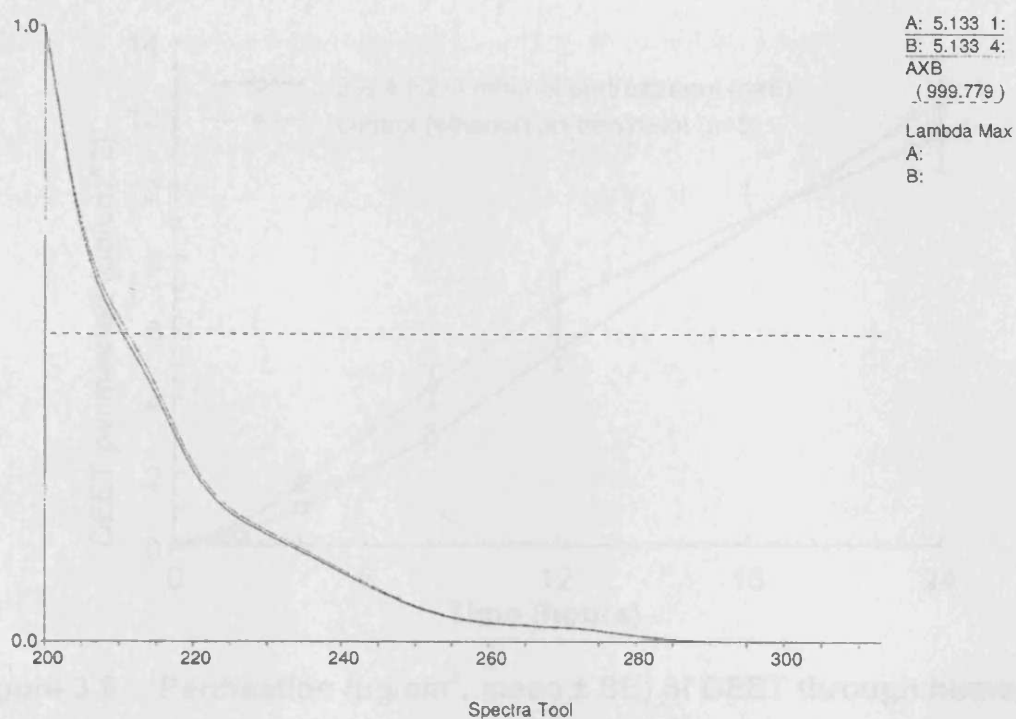


Figure 3.5 Spectral comparison (12 h receptor phase sample cell 1 versus standard solution)

3.2.3 Results and discussion

Data are expressed as the mean \pm standard error (SE) amount ($\mu\text{g}/\text{cm}^2$) and % of the applied dose. Statistical comparisons were performed using single factor ANOVA in Microsoft Excel 5.0.

The average DEET doses were 50.0 ± 0.3 and $49.8 \pm 0.5 \mu\text{g}/\text{cm}^2$ for the 4-F2 and ethanol pre-treated groups, respectively. Five cells from two skin donors were run for each group.

The permeation of DEET through the human skin membranes, and into the receptor phases, is shown in Figure 3.6. At 24 hours, a mean of 12.4 ± 1.1 and $11.5 \pm 1.0 \mu\text{g}/\text{cm}^2$ DEET had permeated for 4-F2 and ethanol pre-treated groups respectively. Following normalisation for the exact dose applied to each cell, the 24 h permeation values corresponded to 24.8 ± 2.1 and $22.9 \pm 1.9\%$ of the applied dose (Figure 3.7).

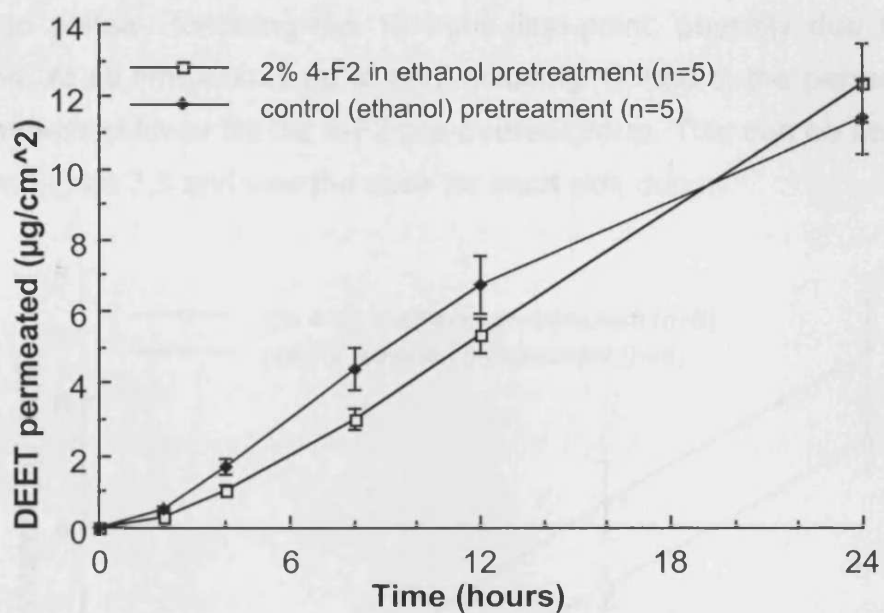


Figure 3.6 Permeation ($\mu\text{g}/\text{cm}^2$, mean \pm SE) of DEET through human membranes from a 0.5% solution in ethanol

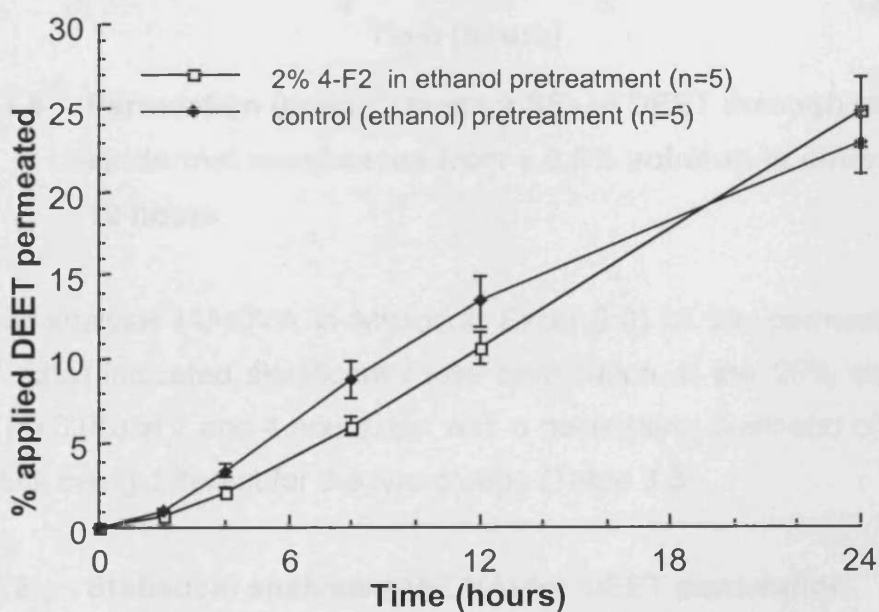


Figure 3.7 Permeation (% applied dose, mean \pm SE) of DEET through human epidermal membranes from a 0.5% solution in ethanol

For the ethanol pre-treatment group, the penetration rate appeared to have started to plateau following the 12 hour time-point, possibly due to donor depletion. At all time-points up to and including 12 hours, the permeation of DEET appeared lower for the 4-F2 pre-treated group. This can be seen more clearly in Figure 3.8 and was the case for each skin donor.

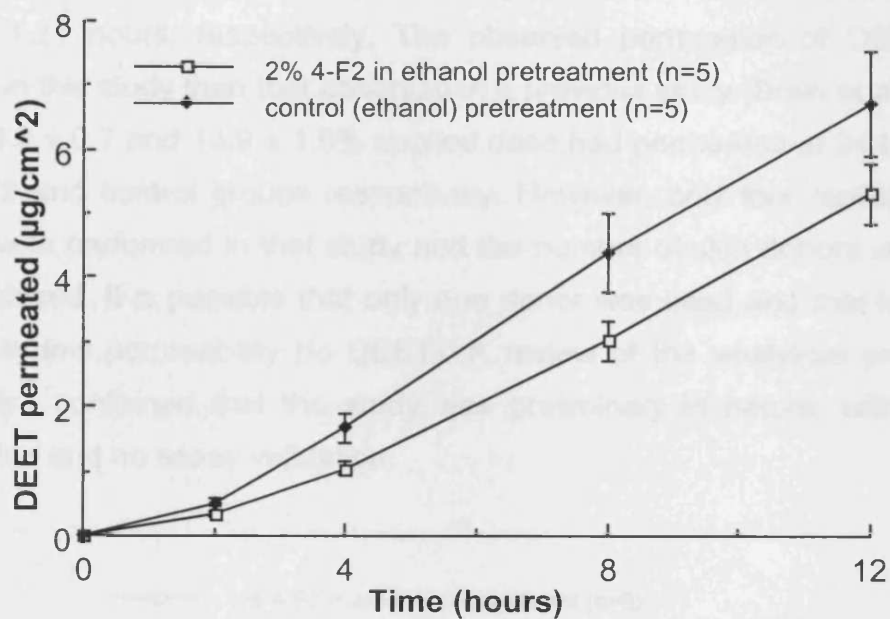


Figure 3.8 Permeation ($\mu\text{g}/\text{cm}^2$, mean \pm SE) of DEET through human epidermal membranes from a 0.5% solution in ethanol up to 12 hours

Statistical analysis (ANOVA in Microsoft Excel 5.0) of the permeation data ($\mu\text{g}/\text{cm}^2$ data) indicated significantly less permeation at the 95% confidence interval ($p < 0.05$) at 2 and 4 hours, but with a decreasing likelihood of the later time points being different for the two groups (Table 3.3).

Table 3.3 Statistical analysis (ANOVA) for DEET permeation

Time (hours)	4-F2 pre-treatment ($\mu\text{g}/\text{cm}^2$)	Control pre-treatment ($\mu\text{g}/\text{cm}^2$)	p-value
2	0.326 \pm 0.034	0.509 \pm 0.064	0.035
4	1.04 \pm 0.102	1.67 \pm 0.22	0.031
8	3.02 \pm 0.2	4.40 \pm 0.62	0.076
12	5.32 \pm 0.48	6.72 \pm 0.82	0.18
24	12.4 \pm 1.1	11.5 \pm 1.0	0.54

Linear fits ($r^2=0.999$) of the permeation data (mean group data fitted) are shown in Figure 3.9, with 4 to 24 hour data fitted for 4-F2 pre-treatment and 2 to 12 hour data fitted for the control pre-treatment. Pre-treatment with 4-F2 produced a small reduction (~9%) in the apparent steady state DEET permeation rate, 0.572 versus 0.629 $\mu\text{g}/\text{cm}^2\cdot\text{h}$ for the control pre-treatment (p-value 0.56). However, the apparent lag time was doubled to 2.49 hours versus 1.21 hours, respectively. The observed permeation of DEET was greater in this study than that observed in a previous study (Brain et al, 1996), where 6.8 ± 0.7 and $13.9 \pm 1.8\%$ applied dose had permeated at 24 hours for the 4-F2 and control groups respectively. However, only four replicates per group were performed in that study and the number of skin donors used was not disclosed. It is possible that only one donor was used and that is was of unusually low permeability (to DEET). A review of the analytical procedure used also confirmed that the study was preliminary in nature, with limited calibration and no assay validation.

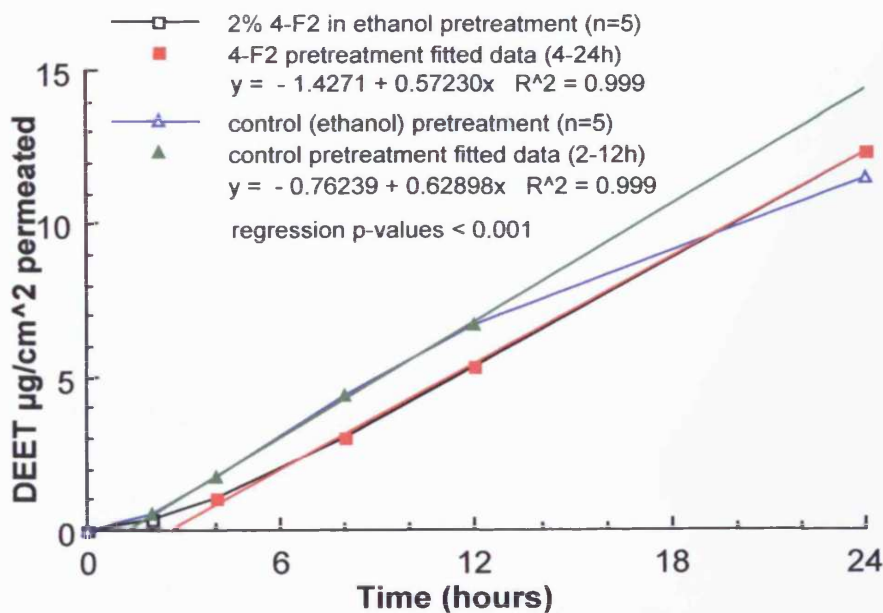


Figure 3.9 Permeation ($\mu\text{g}/\text{cm}^2$) of DEET through human epidermal membranes from a 0.5% solution in ethanol – fitted data

Analysis of the skin distribution samples showed some large differences between the two groups (Figure 3.10), particularly in the surface wipes and strip 1. The surface wipes at 24 hours contained 21.2 ± 1.9 and $11.9 \pm 1.6\%$ of the applied DEET dose for the 4-F2 and control groups respectively. These differences between the groups were similar for the other analysed compartments. The combined totals in the tape strips amounted to 4.90 ± 1.47 and 2.72 ± 0.28 , and the epidermis recoveries were 2.32 ± 0.69 and $1.45 \pm 0.22\%$ of the applied DEET dose for the 4-F2 and control groups respectively. The individual tape strip group values are shown, together with all other distribution and permeation data at 24 hours, in Table 3.4. Overall recoveries of applied DEET were low for both groups at 53.1 ± 2.4 and $39.1 \pm 1.6\%$ of the applied dose for the 4-F2 and control groups respectively. DEET is a volatile compound, so low recoveries were not unexpected. The possible reasons for the significant difference (p -value = 0.001) in overall recoveries between the two groups are discussed later.

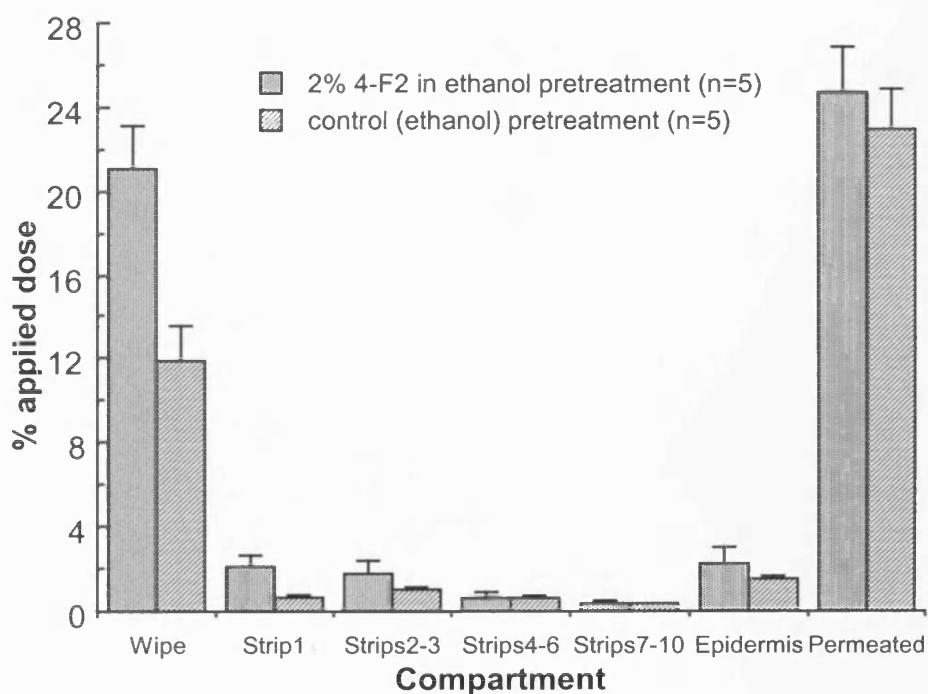


Figure 3.10 Distribution (% of the applied dose, mean \pm SE) of DEET between all compartments from a 0.5% solution in ethanol

Table 3.4 DEET distribution data (% of the applied dose, mean \pm SE) at 24h

Compartment	4-F2 pre-treatment	control pre-treatment	p-value
Wipe	21.2 \pm 1.9	11.39 \pm 1.6	0.006
Strip 1	2.09 \pm 0.53	0.684 \pm 0.122	0.031
Strips 2-3	1.79 \pm 0.55	1.07 \pm 0.104	0.23
Strips 4-6	0.674 \pm 0.265	0.657 \pm 0.068	0.95
Strips 7-10	0.336 \pm 0.140	0.315 \pm 0.057	0.89
Epidermis	2.32 \pm 0.69	1.45 \pm 0.22	0.26
Permeated	24.8 \pm 2.1	23.0 \pm 1.9	0.55
Overall recovery	53.1 \pm 2.4	39.1 \pm 1.6	0.001

Average amount of DEET per tape strip data ($\mu\text{g}/\text{cm}^2$ per strip, Figure 3.11) were generated by dividing the amount of DEET ($\mu\text{g}/\text{cm}^2$) in each tape strip group by the number of tape strips in that group. These data showed that the amount of DEET recovered clearly decreased with skin depth. Although the contents of the first tape strip group might be regarded substantially as surface material, the general shape of this profile was a reflection of the 'concentration gradient' of DEET within the epidermal membrane.

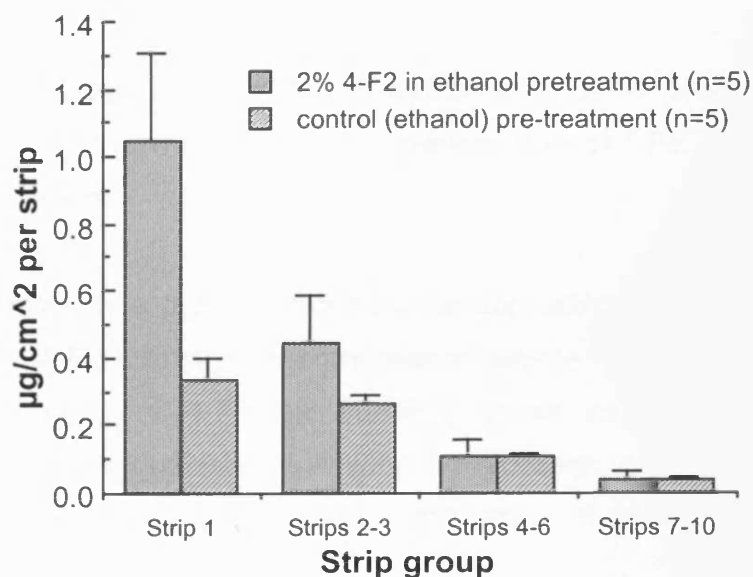


Figure 3.11 Distribution ($\mu\text{g}/\text{cm}^2$ per strip, mean \pm SE) of DEET within each tape strip group following normalisation for the number of strips

The marked differences in surface wipe, tape strip and skin content between the 4-F2 and control (ethanol only) pre-treated groups may indicate interaction between the 4-F2 and DEET such that the evaporation rate from the skin surface was reduced. The low recovery of applied DEET from the skin surface for the control groups also confirmed that the likely reason that the permeation rate began to plateau was donor depletion. The dosing regimen for this experiment was chosen to closely match earlier work on this compound (Brain et al, 1996). The pre-treatment dose of 4-F2 was 1 mg/cm², whilst only 50 µg/cm² DEET was applied. This large differential in concentration could result in 4-F2 providing mainly a physical barrier to DEET at early time-points, with much of the applied 4-F2 still residing at the skin surface after 2 hours pre-treatment. This may have resulted in the potential intercalation of 4-F2 with skin lipids not being the most significant process in the observed retardation of DEET permeation at early time-points. However, if there was sustained significant interaction between DEET and 4-F2 at the skin surface, it might be expected that the steady state permeation rate would reduce, due to a decrease in the surface availability of 'free' DEET. This did not appear to be the case as the apparent steady state permeation rates for both 4-F2 pre-treated and control groups were similar.

3.3 Assessment of the effect of a reduced pre-treatment dose of retarder 4-F2 on the permeation of DEET through human skin

The subsequent investigation into the potential retardation of skin permeation of DEET by 4-F2 focused on comparison between groups pre-treated with different amounts of 4-F2. In addition, these experiments investigated diffusion chamber occlusion following evaporation of the ethanol vehicle following DEET application, to reduce the effect of donor depletion through evaporative loss of DEET.

3.3.1 Materials and equipment

As described in section 3.2.1

3.3.2 Methods

As described in section 3.2.2 except as indicated below.

3.3.2.2 Vehicle preparation

A fresh 2% (w/v) 4-F2 solution in ethanol (96% (v/v), AnalaR) was prepared by transferring 35.25 mg 4-F2 (gently warmed to produce a homogeneous oil) to a 20 ml glass vial using a warmed Pasteur pipette, and adding 1.415 g ethanol (= 1.762 ml). The vial was immediately capped and the contents shaken prior to storage at room temperature in the dark. If ideal mixing is assumed, then the calculated solution concentration was 19.61 mg/ml 4-F2.

The 0.5% (w/v) DEET solution described in section 3.2.2.2 was also used in this experiment.

3.3.2.3 Skin preparation

As described in section 3.2.2.3 except that four donors were used (two of these donors were also used in section 3.2.2.3).

3.3.2.5 Membrane integrity assessment

As described in section 3.2.2.5, except a total of 24 cells were prepared, and the 21 cells used exhibited water permeability coefficients, k_p , of less than 2.5×10^{-3} cm/h.

3.3.2.6 Skin pre-treatment with 4-F2

Following the membrane integrity assessment, cells were separated into three groups (seven cells per group) for pre-treatment (prior to application of DEET). Group 1 cells received a 50 $\mu\text{l}/\text{cm}^2$ dose of 2% 4-F2 in ethanol. Group 2 cells received a 10 $\mu\text{l}/\text{cm}^2$ dose of 2% 4-F2 in ethanol. Group 3 (control) cells received a 50 $\mu\text{l}/\text{cm}^2$ dose of ethanol alone. The pre-treatments were applied using Hamilton syringes and the cells left undisturbed in the waterbaths for 2 hours.

3.3.2.7 Application of DEET solution

As described in section 3.2.2.7 except that the diffusion cell donor chambers were occluded using greased glass coverslips 15 minutes after application of the DEET solutions. The ethanol donor vehicle appeared to have evaporated in that time-period.

3.3.2.8 Determination of skin permeation

As described in section 3.2.2.8 except that 200 μl samples were taken from each receptor chamber 2, 4, 8, 19 and 24 hours after dosing.

3.3.2.9 Determination of skin distribution and DEET recovery

Following removal of the 24 hour receptor phase samples, the remaining receptor phases were removed, placed in 20 ml glass vials (Chromacol, UK), the vials tightly capped and frozen (-20°C). Material remaining on the skin surface and condensed on the underside of the coverslip was removed by gentle wiping with dry cotton buds. The cotton bud wipes for each cell were placed into 20 ml glass vials, the vials were tightly capped and then frozen pending extraction and analysis. The diffusion cells were then dismantled and the epidermal membranes placed into individual glass vials and the vials frozen as above.

Surface wipes were extracted into 8 ml of 50/50 (v/v) acetonitrile/water with vortexing and sonication. An aliquot of the extract was centrifuged for 3 minutes at 10,000 rpm prior to analysis. Skin samples were extracted into 6 ml of distilled water with 30 minutes shaking at 60°C. Only a single extraction of the skin samples was deemed necessary as a second extract (two cells assessed using a 3 ml extraction volume) contained <6% of the DEET recovered in the first extract (equivalent to <0.5% of the applied dose).

3.3.2.10 Sample analysis and assay validation

As described in section 3.2.2.10 except that the wavelength used to quantify DEET was changed to 254 nm as this offered improved range due to decreased sensitivity (compared to 208 nm) at the higher concentrations observed in this experiment. Samples were diluted into range as appropriate using digital pipettes.

3.3.3 Results and discussion

The data from two diffusion cells were rejected as they were visually observed to have leaked following the tritiated water removal procedure, indicating that membrane integrity had been compromised. Data from those cells confirmed these observations with 30 and 47% of the applied DEET dose having permeated by 2 hours. Therefore, data from a total of 6, 7 and 6 replicates were available for the 50 $\mu\text{l}/\text{cm}^2$ 2% 4-F2 (group 1), 10 $\mu\text{l}/\text{cm}^2$ 2% 4-F2 (group 2) and 50 $\mu\text{l}/\text{cm}^2$ ethanol (group 3) control pre-treatment groups respectively. The DEET dose for all cells was 50 $\mu\text{g}/\text{cm}^2$.

The permeation of DEET through the human skin membranes, and into the receptor phases, is shown in Figures 3.12 and 3.13. At 24 hours, a mean of 23.9 ± 2.2 , 19.8 ± 2.3 and 20.6 ± 1.8 $\mu\text{g}/\text{cm}^2$ DEET had permeated for 50 and 10 $\mu\text{l}/\text{cm}^2$ 2% 4-F2 and 50 $\mu\text{l}/\text{cm}^2$ ethanol pre-treated groups, respectively. These 24 h permeation values corresponded to 47.7 ± 4.4 , 39.6 ± 4.5 and $41.2 \pm 3.7\%$ of the applied dose respectively.

The rate of DEET permeation for the control group again started to plateau earlier than for 4-F2 pre-treated cells, possibly due to greater loss of applied DEET during the period of vehicle evaporation (prior to occlusion). Inspection of the data up to 8 hours (Figure 3.14) showed the following trend for DEET permeation following pre-treatment: control > 50 $\mu\text{l}/\text{cm}^2$ 2% 4-F2 > 10 $\mu\text{l}/\text{cm}^2$ 2% 4-F2. Statistical analysis of the permeation data (Table 3.5) confirmed that the 10 $\mu\text{l}/\text{cm}^2$ 2% 4-F2 group was most different to the control, with a p-value of 0.13 at 2 hours, gradually becoming less different over time (p-values 0.31 and 0.80 at 8 and 24h, respectively). Differences between the two doses of 4-F2 gradually increased over the 24 hours (p-value 0.23 at 24 h), possibly indicating that DEET evaporation was reduced (during the period of vehicle evaporation) by the greater 4-F2 dose.

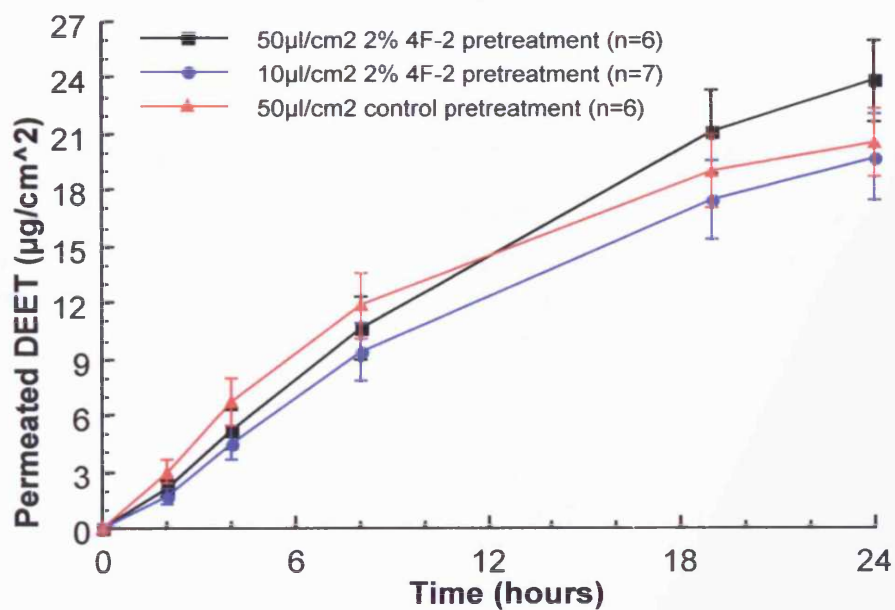


Figure 3.12 Permeation ($\mu\text{g}/\text{cm}^2$, mean \pm SE) of DEET through human epidermal membranes from a 0.5% solution in ethanol

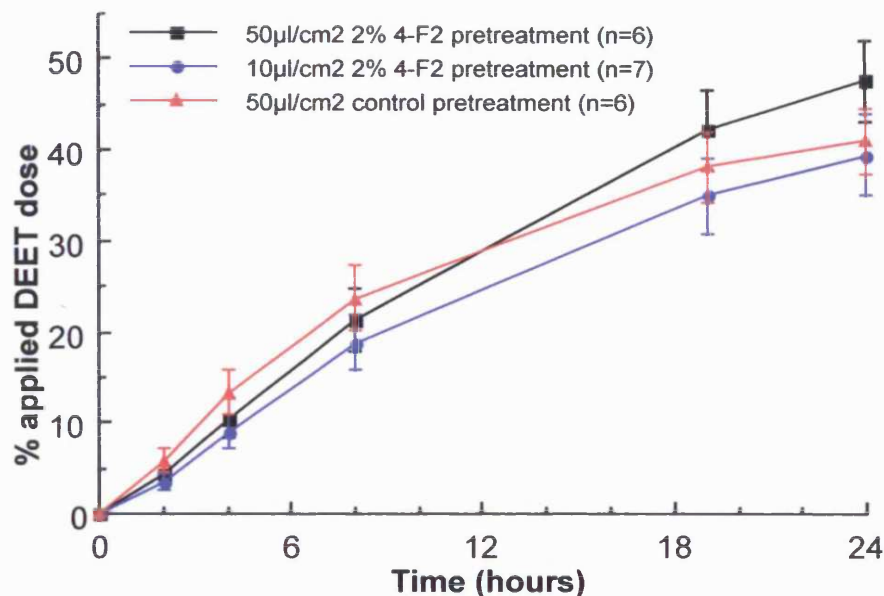


Figure 3.13 Permeation (% applied dose, mean \pm SE) of DEET through human epidermal membranes from a 0.5% solution in ethanol

Table 3.5 Statistical analysis (ANOVA) for DEET permeation ($\mu\text{g}/\text{cm}^2$ data) following 2 hours pre-treatment

Time (hours)	50µl 2% 4-F2 vs. control (p-value)	10µl 2% 4-F2 vs. control (p-value)	50µl 2% 4-F2 vs. 10µl 2% 4-F2 (p-value)
2	0.311	0.127	0.545
4	0.393	0.178	0.613
8	0.629	0.312	0.599
12	0.509	0.603	0.267
24	0.277	0.802	0.229

The permeation rate of DEET was increased by the occlusive conditions, with both higher apparent steady state permeation rates (1.42, 1.28 and 1.87 $\mu\text{g}/\text{cm}^2\cdot\text{h}$ for 50 and 10 $\mu\text{l}/\text{cm}^2$ 2% 4-F2 and 50 $\mu\text{l}/\text{cm}^2$ ethanol pre-treated groups respectively, Figure 3.15) and shorter lag times (0.43, 0.59 and 0.42 h respectively) than those observed under the non-occlusive conditions reported in section 3.4.1.

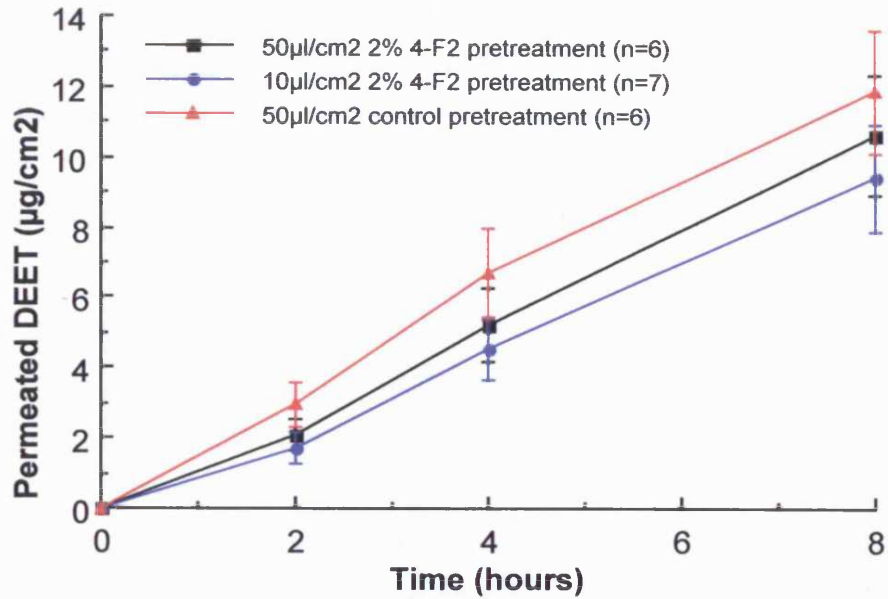


Figure 3.14 Permeation ($\mu\text{g}/\text{cm}^2$, mean \pm SE) of DEET through human epidermal membranes from a 0.5% solution in ethanol up to 8 hours

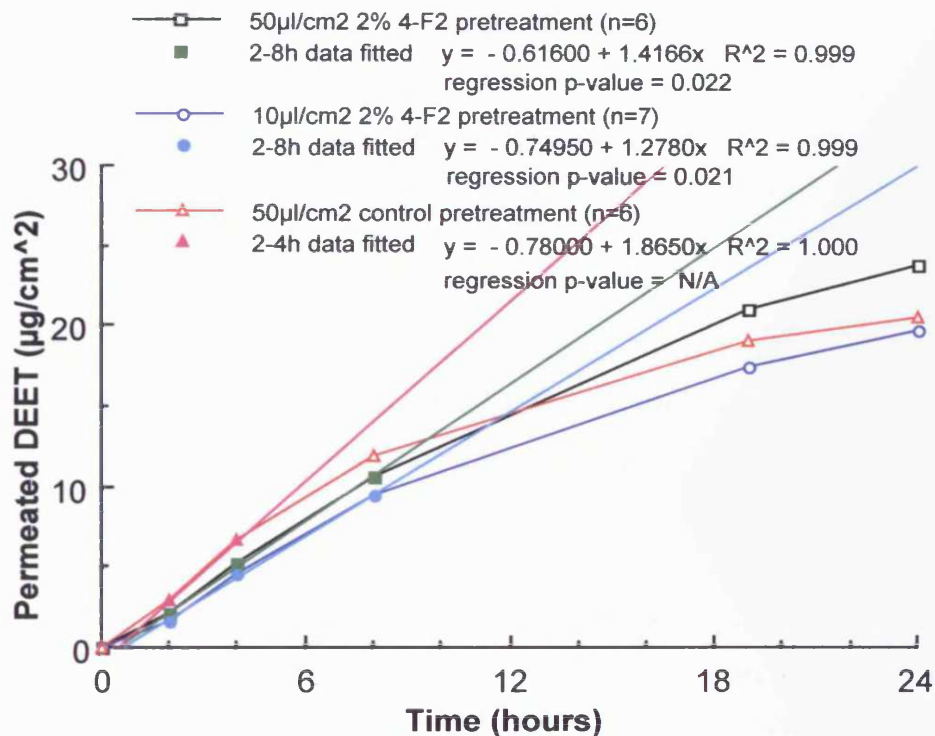


Figure 3.15 Permeation ($\mu\text{g}/\text{cm}^2$) of DEET through human epidermal membranes from a 0.5% solution – fitted data

The recoveries of DEET from the wipes (skin surface and coverslip used to occlude the donor chamber) were lower than expected at 8.28 ± 1.78 , 7.75 ± 1.00 and $4.35 \pm 1.01\%$ of the applied DEET dose for the 50 and 10 $\mu\text{l}/\text{cm}^2$ 2% 4-F2 and 50 $\mu\text{l}/\text{cm}^2$ ethanol pre-treated groups respectively. Recoveries from the epidermal membrane (including stratum corneum) were 13.5 ± 1.5 , 8.72 ± 1.47 and $6.71 \pm 0.77\%$ of the applied DEET dose respectively. Overall recoveries were greatest for the 4-F2 pre-treated cells with values of 69.5 ± 2.4 , 56.1 ± 3.8 and $52.2 \pm 3.8\%$ of the applied DEET dose respectively. It is likely that significant evaporation of the applied DEET occurred whilst the vehicle was allowed to evaporate (15 minutes) prior to occlusion, especially as ethanol increases the evaporation of volatile organic compounds (Mazza, 2000). Interaction between DEET and 4-F2 was still likely given the higher recoveries for the 4-F2 pre-treated cells, especially for the higher dose. However, the lower 4-F2 pre-treatment dose, 10 $\mu\text{l}/\text{cm}^2$ 2% 4-F2, equating to 200 $\mu\text{g}/\text{cm}^2$ 4-F2, may have been more effective (p-values 0.5 to 0.6 for 2, 4 and 8 hour data) in retarding the permeation of DEET at early time-points. Further investigations with this lower dose appeared warranted.

3.4 Assessment of the effect of pre-treatment and co-administration of retarder 4-F2 on the permeation of DEET through human skin

The conditions utilised in this assessment were designed to more rigorously assess the potential retardation of DEET permeation by 4-F2, through a combination of the lower 4-F2 pre-treatment dose (200 $\mu\text{g}/\text{cm}^2$) and a non-occlusive application of a higher DEET dose more representative of in-use conditions. Additionally, co-administration of DEET and 4-F2, rather than pre-treatment, was assessed to determine whether 4-F2 could rapidly exert a permeation rate modifying effect from a formulation. This study focused on the permeation of DEET up to 8 hours after application. Little or no observation of donor depletion through evaporation would be expected over this experimental time-frame due to the greater DEET dose.

3.4.1 Materials and equipment

As described in section 3.2.1

3.4.2 Methods

As described in section 3.2.2 except as indicated below.

3.4.2.2 Vehicle preparation

A 15% (w/w) DEET solution in ethanol (96% (v/v)) was prepared by transferring 0.30919 g DEET to a 20 ml glass vial using a Pasteur pipette, and adding ethanol until a combined weight of 2.06120 g was achieved. The vial was immediately capped and the contents shaken prior to storage at room temperature in the dark. If ideal mixing is assumed, this solution was equivalent to ~124.1 mg/ml DEET.

A solution containing 4% (w/w) 4-F2 solution and 15% (w/w) DEET in ethanol (96% (v/v), AnalaR) was prepared by transferring 35.25 mg 4-F2 (gently warmed to produce a homogeneous oil) to a 20 ml glass vial using a warmed Pasteur pipette, adding 0.11376 g DEET and 0.61651 g ethanol (total solution weight 0.76065 g). The vial was immediately capped and the contents shaken prior to storage at room temperature in the dark. If ideal mixing is assumed, this solution was equivalent to ~124.7 mg/ml DEET and ~33.30 mg/ml 4-F2. This solution contained ~4% (w/w) 4-F2 and not 2% (w/v) due to the lower application dose (~5 $\mu\text{l}/\text{cm}^2$) compared to the pre-treatment dose (~10 $\mu\text{l}/\text{cm}^2$).

The 2% (w/v) 4-F2 solution described in section 3.3.2.2 was also used in this experiment.

3.4.2.3 Skin preparation

As described in section 3.3.2.3.

3.4.2.5 Membrane integrity assessment

As described in section 3.2.2.5 except that a total of 25 cells were prepared, and 17 cells exhibited a water permeability coefficient, k_p , of lower than 2.5×10^{-3} cm/h (a nominal cut-off point for accepted normal permeability). These 17 cells and one additional cell which was close to this cut-off point was included (k_p 2.72×10^{-3} cm/h) to allow six replicates per group. Subsequent data from this additional cell was closely examined to determine whether the membrane permeability for DEET was abnormal.

3.4.2.6 Skin pre-treatment with 4-F2

Following the membrane integrity assessment, cells were separated into three groups (six cells per group) for pre-treatment (prior to application of DEET). Group 1 cells received a $10 \mu\text{l}/\text{cm}^2$ dose of 2% (w/v) 4-F2 in ethanol. Group 2 (control) and group 3 (to be subsequently dosed with 4-F2) received a $10 \mu\text{l}/\text{cm}^2$ dose of ethanol alone. The pre-treatments were applied using Hamilton syringes and the cells left undisturbed in the waterbaths for 2 hours.

3.4.2.7 Application of DEET solutions

The DEET solutions (15% (w/w) DEET for groups 1 and 2 and 15% (w/w) DEET + 4% (w/w) 4-F2 for group 3) were applied to the skin surface at a target dose of $5 \mu\text{l}/\text{cm}^2$, in the following manner. The diffusion cell was placed on a 5 place electronic balance (supported on a glass beaker) and the balance tared. The appropriate target volume was applied to the skin surface using a digital pipette, and the actual weight applied immediately recorded. The weight applied was suitable for direct use in data calculations, as the DEET solutions were prepared on a w/w basis. This weighing method was

necessary, as pipetting very small volumes of highly ethanolic solutions using air displacement pipettes is inaccurate (due to surface tension effects). Cells were rotated to ensure that the applied solutions spread evenly over the entire skin surface. For each cell, the exact time of application was noted and that time represented zero time for that cell. The diffusion cell donor chambers were not occluded.

3.4.2.8 Determination of skin permeation

As described in section 3.2.2.8 except that 200 μl samples were taken from each receptor chamber 1, 2, 4, 6 and 8 hours after dosing.

3.4.2.9 Determination of skin distribution and DEET recovery

No skin distribution or DEET recovery samples were collected for this experiment.

3.4.2.10 Sample analysis and assay validation

As described in section 3.3.2.10.

3.4.3 Results and discussion

The data from one diffusion cell was rejected as ~10 times more DEET had permeated in the first hour compared to the rest of the group, indicating that membrane integrity had been compromised by the tritiated water removal procedure (measured water permeability coefficient, k_p , for that cell prior to rinsing was 1.86×10^{-3} cm/h). Data from a total of 5, 6 and 6 replicates were therefore available for the 10 $\mu\text{l}/\text{cm}^2$ 2% 4-F2 (group 1), 10 $\mu\text{l}/\text{cm}^2$ ethanol (group 2) control and 10 $\mu\text{l}/\text{cm}^2$ ethanol (group 3, prior to co-administration of 4-F2 with DEET) pre-treatment groups respectively.

The permeation of DEET through the human skin membranes and into the receptor phases is shown in Figures 3.16 and 3.17. For this higher DEET dose, both 4-F2 treated groups appeared to have potentially enhanced DEET permeation compared to the control group. At 8 hours, a mean of 86.1 ± 13.5 , 62.7 ± 5.4 and $101 \pm 23 \mu\text{g}/\text{cm}^2$ DEET had permeated for the $10 \mu\text{l}/\text{cm}^2$ 2% 4-F2 and $10 \mu\text{l}/\text{cm}^2$ ethanol control pre-treated and co-administered 4-F2/DEET groups respectively. These 8 h permeation values corresponded to 12.9 ± 2.0 , 8.70 ± 0.89 and $14.8 \pm 3.1\%$ of the applied dose respectively. There were no indications of donor depletion effects over the experimental time-frame (8 hours).

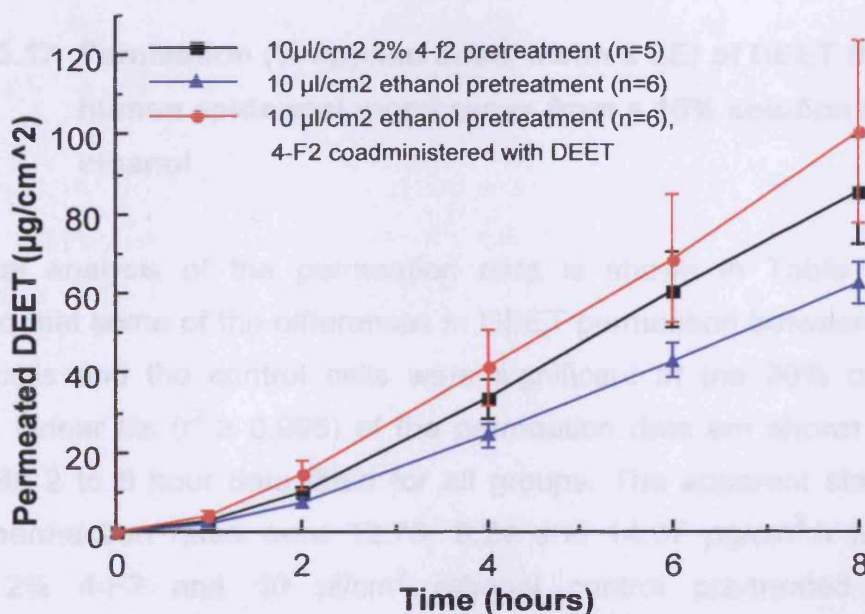


Figure 3.16 Permeation ($\mu\text{g}/\text{cm}^2$, mean \pm SE) of DEET through human epidermal membranes from a 15% solution in ethanol

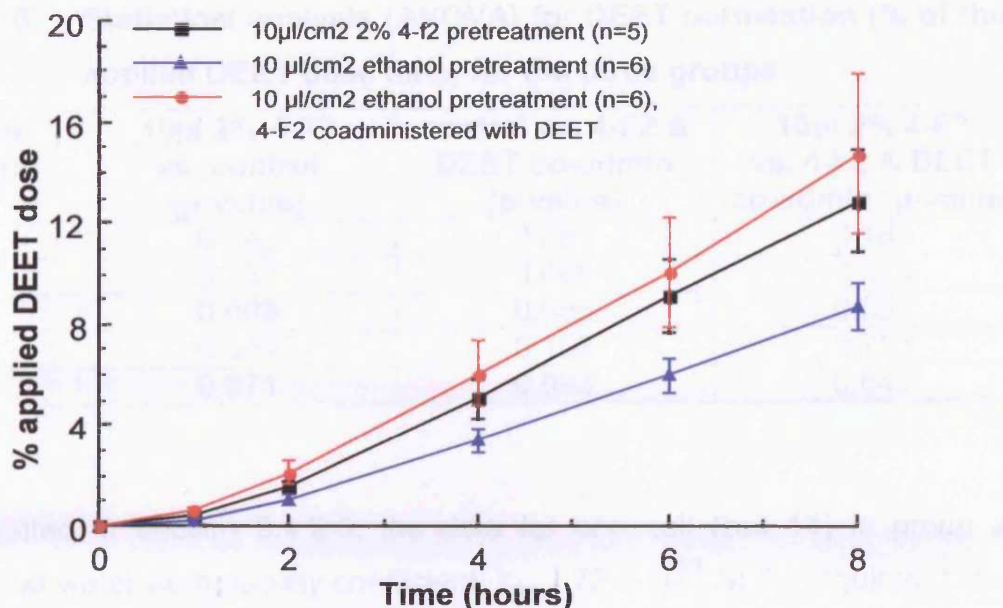


Figure 3.17 Permeation (% applied dose, mean \pm SE) of DEET through human epidermal membranes from a 15% solution in ethanol

Statistical analysis of the permeation data is shown in Table 3.6. This indicated that some of the differences in DEET permeation between the 4-F2 dosed cells and the control cells were significant at the 90% confidence interval. Linear fits ($r^2 \geq 0.998$) of the permeation data are shown in Figure 3.18, with 2 to 8 hour data fitted for all groups. The apparent steady state DEET permeation rates were 12.78, 9.24 and 14.37 $\mu\text{g}/\text{cm}^2\cdot\text{h}$ for the 10 $\mu\text{l}/\text{cm}^2$ 2% 4-F2 and 10 $\mu\text{l}/\text{cm}^2$ ethanol control pre-treated and co-administered 4-F2/DEET groups respectively. The apparent lag times were similar for all groups at 1.27, 1.29 and 1.08 hours respectively.

Table 3.6 Statistical analysis (ANOVA) for DEET permeation (% of the applied DEET dose data) for the three groups

Time (hours)	10µl 2% 4-F2 vs. control (p-value)	control vs. 4-F2 & DEET co-admin (p-value)	10µl 2% 4-F2 vs. 4-F2 & DEET co-admin (p-value)
1	0.242	0.053	0.183
2	0.137	0.065	0.328
4	0.098	0.088	0.551
6	0.064	0.102	0.738
8	0.071	0.093	0.645

As indicated in section 3.4.2.5, the data for one cell (cell 14) in group 3 (measured water permeability coefficient, k_p , 2.72×10^{-3} cm/h) required close inspection prior to inclusion. DEET permeation data for this cell was the highest for the group, but by only a small margin (from a cell with a k_p of 2.30×10^{-3} cm/h). Data from cell 14 also showed a normal permeation profile, and whilst removal from the group dropped averages close to those for group 1 (4-F2 pre-treatment), this cell could not be described as an outlier and was not rejected from the data interpretation.

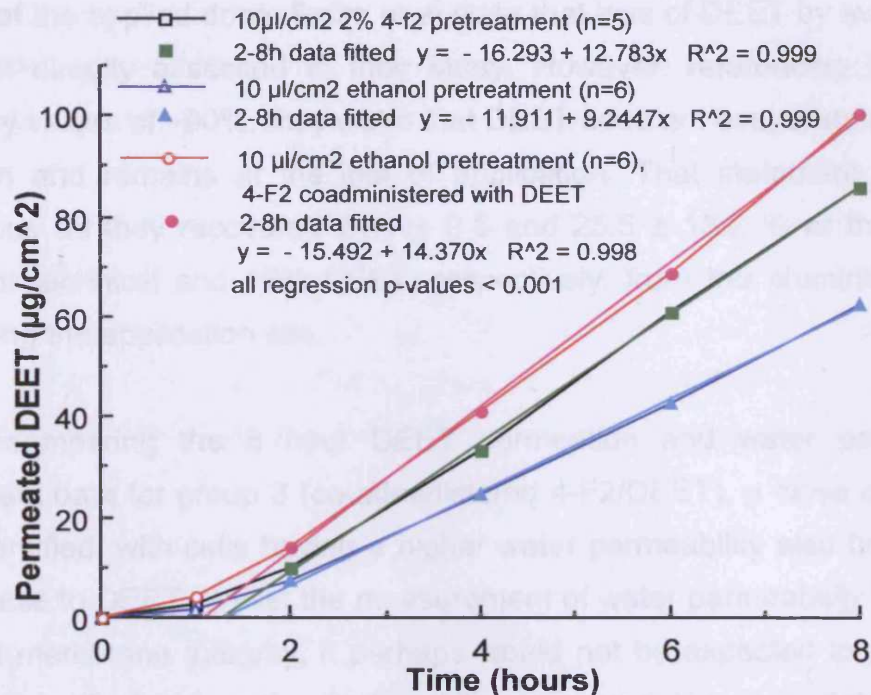


Figure 3.18 Permeation ($\mu\text{g}/\text{cm}^2$, mean \pm SE) of DEET through human epidermal membranes from a 15% solution in ethanol – fitted data

The permeation of DEET from a 15% (w/w) solution in ethanol has previously been assessed *in vivo* by Selim et al (1995). They applied a smaller dose (15 μl to 6 x 4 cm) of either technical DEET (98.8%) or 15% (w/w) DEET in ethanol, spiked with ^{14}C -DEET, to the forearm of volunteers for 8 hours followed by a rinse-off procedure with propan-2-ol. The application site was protected with an aluminium dome containing air holes. The 15 μl dosing volume was selected purely due to the propensity of larger volumes to migrate outside the dosing area. Blood samples from the ipsilateral arm (the arm where the dose was applied) showed rapid permeation, and measured radioactivity was fairly constant between 4-8 hours. Interestingly, samples from the contralateral (non-application) arm were below the limit of quantitation (2 times background) at all time-points, indicating very rapid metabolism and elimination. Mean recovery (for the 15% DEET group) in the urine (the main route of excretion) was $8.32 \pm 3.62\%$ of the applied dose, which compared well with the control group in experiment 3 (above) at $8.70 \pm$

0.89% of the applied dose. Selim et al state that loss of DEET by evaporation was not directly assessed in their study. However, referencing their total recovery values of ~90%, they claim that DEET does not evaporate readily off the skin and remains at the site of application. That statement is clearly erroneous as they recovered 21.1 ± 9.5 and 25.5 ± 13.2 % of the applied dose for technical and 15% DEET, respectively, from the aluminium dome protecting the application site.

Whilst comparing the 8 hour DEET permeation and water permeability coefficient data for group 3 (co-administered 4-F2/DEET), a close correlation was identified, with cells having a higher water permeability also being more permeable to DEET. Whilst the measurement of water permeability is used to confirm membrane integrity, it perhaps would not be expected to mirror the permeation of a larger and more lipophilic compound. However, data reported by Bronaugh et al (1986) indicated that skin samples of higher water permeability (compared to less permeable control samples) did show higher permeation for all of the seven varied compounds assessed (n=5 for each compound). Although, it was noted that the increase in water permeability was significantly different at the 95% confidence interval to the increase in permeation of two test compounds, cortisone and DDT. The very limited reporting of data and lack of details regarding methods in that section of their paper limits proper exploration of the correlation between water permeability and test compound permeation in that study.

3.5 Examination of correlation between water permeability and DEET permeation

The possible correlation between water and DEET permeability observed above (section 3.4.3) was initially investigated for all groups by dividing the % DEET permeated data (at 8 hours) by the water k_p for each cell. The average (mean \pm SE) results were 9.90 ± 0.92 (20.7 %RSD), 6.44 ± 1.19 (45.3 %RSD) and 7.98 ± 0.66 (18.4 %RSD) for the $10 \mu\text{l}/\text{cm}^2$ 2% 4-F2 and $10 \mu\text{l}/\text{cm}^2$ ethanol control pre-treated and co-administered 4-F2/DEET groups respectively. The significance of the above results was that dividing DEET

permeation by the membrane water permeability for the 4-F2 groups decreased data variability whereas for the control group the variability was increased. Therefore, it appeared that the correlation between DEET and water permeability was only apparent for both the 4-F2 treated groups (and not the ethanol alone pre-treated group). This correlation can be seen better in Figure 3.19. The linear fit correlation coefficient, r , was highest for group 3 (co-administration of 4-F2 and DEET) with $r^2=0.918$, and the intercept was fairly close to the origin. Group 1 (4-F2 pre-treatment) also showed some correlation with $r^2=0.790$. No correlation was observed for the control group ($r^2=0.089$).

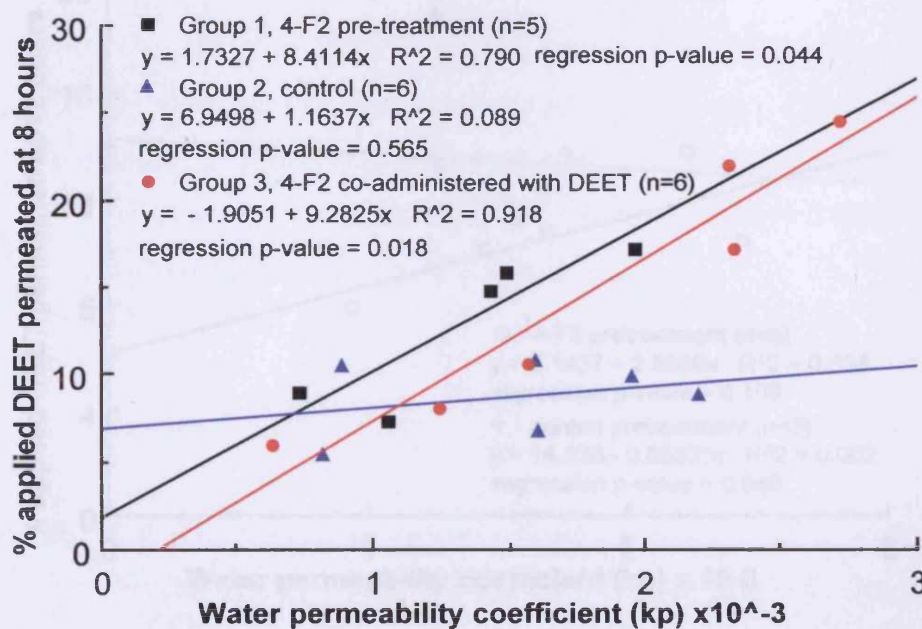


Figure 3.19 Correlation of DEET permeation at 8 hours (% applied dose) and water permeability coefficient, k_p

The correlation between DEET permeation and water permeability coefficient was also retrospectively assessed for the first two studies, although it should be noted that the DEET dose was much smaller than that used above (section 3.3). For the first study (50 $\mu\text{g}/\text{cm}^2$ DEET dose, non-occlusive conditions), the 12 hour permeation data (% applied dose) was used as this was the last time-point before the rate of DEET permeation began to plateau

for the control group. The results of the comparison (Figure 3.20), again indicated no correlation for the control cells, but possibly limited correlation ($r^2=0.538$) for the 4-F2 dosed cells. For the second study (Figure 3.21, 50 $\mu\text{g}/\text{cm}^2$ DEET dose, occlusive conditions following vehicle evaporation), DEET permeation data at only 4 hours was fitted (again due to the permeation rate beginning to plateau for some cells) and there may have been a loose correlation between DEET permeation and water permeability for all groups (the best correlation, $r^2=0.831$, was for the lower 4-F2 pretreatment volume).

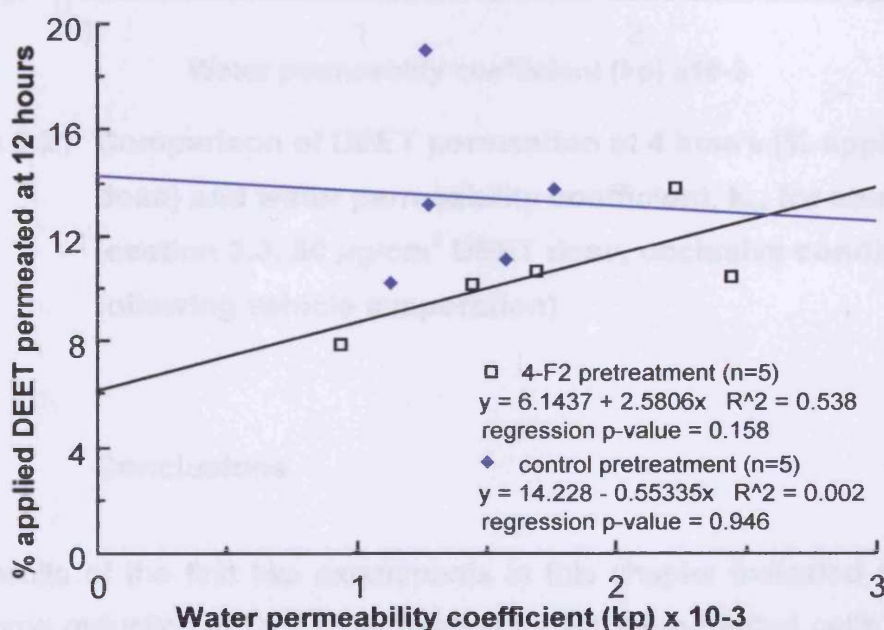


Figure 3.20 Comparison of DEET permeation at 12 hours (% applied dose) and water permeability coefficient, k_p , for study 1 (section 3.2, 50 $\mu\text{g}/\text{cm}^2$ DEET dose, non-occlusive conditions)

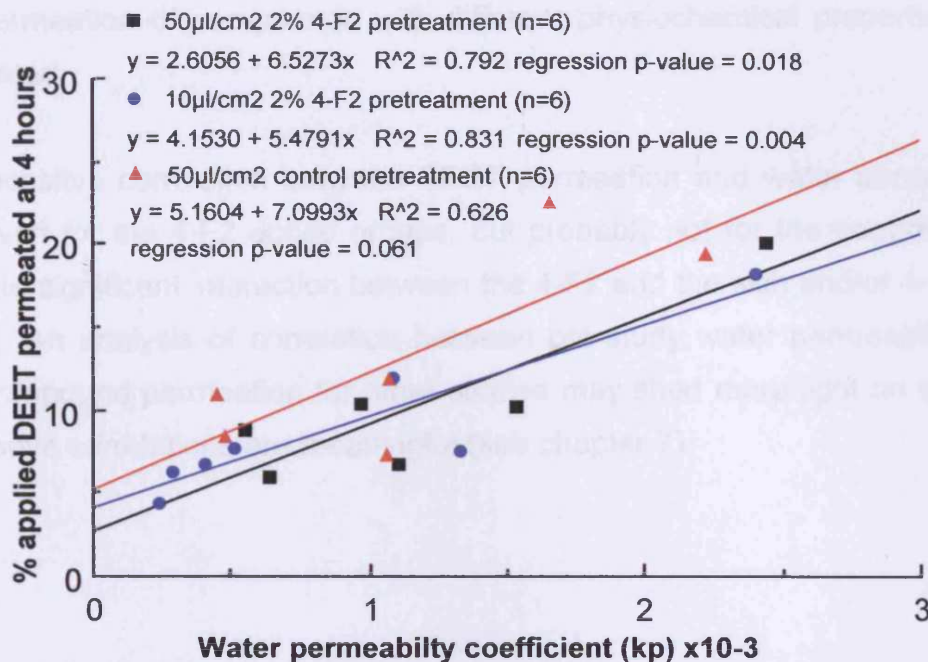


Figure 3.21 Comparison of DEET permeation at 4 hours (% applied dose) and water permeability coefficient, k_p , for study 2 (section 3.3, 50 μ g/cm² DEET dose, occlusive conditions following vehicle evaporation)

3.6 Conclusions

The results of the first two experiments in this chapter indicated that there was some reduction in DEET permeation for 4-F2 pre-treated cells, although this was only at relatively early time-points. The third experiment used a more realistic dose of DEET (15% w/w, representing the lower-end of DEET containing products) and both 4-F2 pre-treatment and co-administration appeared to enhance DEET permeation. For all experiments, there was evidence of interaction of 4-F2 with either the skin and/or applied DEET, with 4-F2 altering both DEET permeation profiles and the recoveries of applied DEET in various skin strata.

The degree of DEET permeation modification by 4-F2 was not particularly great, or consistent. However, investigation into the potential effect of 4-F2 on

the permeation of compounds with different physiochemical properties was warranted.

The possible correlation between DEET permeation and water permeability observed for the 4-F2 dosed groups, but probably not for the controls, may indicate significant interaction between the 4-F2 and the skin and/or 4-F2 and DEET. An analysis of correlation between pre-study water permeability and test compound permeation for other studies may shed more light on whether the above correlations are meaningful (see chapter 7).

3.7 References

Brain, K.R., Green, D.M., James, V.J., Walters, K.A., Watkinson, A.C., Allan, G. and Hammond, J. (1996). Preliminary evaluation of novel penetration retarders, in *Prediction of Percutaneous Penetration, Vol. 4B*. Brain, K.R., James, V.J. and Walters, K.A. (eds) pp. 131-132. STS publishing, Cardiff, UK.

Bronaugh R.L., Stewart, R.F. and Simon, M. (1986). Methods for in vitro percutaneous absorption studies VII: use of excised human skin. *J. Pharm Sci*, **75**, 1094-1097.

Cecchine, G., Golomb, B.A., Hilborne, L.H., Specktor, D.M. and Anthony, C.R. (2000). Chapter 5: DEET in *A review of the scientific literature as it pertains to Gulf War illnesses, Volume 8: Pesticides*. National Defense Research Institute, RAND, USA. MR-1018/8-OSD.

Davis, E.E. and Sokolove, P.G. (1976). Lactic acid receptors on the antennae of the mosquito, *Aedes aegypti*. *J. Comp. Physiol.*, **105**, 43-54.

Mazza, P. (2000). Ethanol: fueling rural economic revival; Through; http://www.harvestcleanenergy.org/pdfs/Ethanol_Report.pdf, accessed 19/8/05.

Qui, H., McCall, J.W. and Jun, H.W. (1998). Formulation of topical insect repellent N,N-diethyl-*m*-toluamide (DEET): vehicle effects on DEET in vitro permeation. *Int. J. Pharm*, **163**, 167-176.

Reifenrath, W.G. and Robinson, P.B. (1982). In vitro skin evaporation and penetration characteristics of mosquito repellents. *J. Pharm. Sci.*, **71**, 1014-1018.

Sangster, J. (2004). LOGKOW databank. Sangster Research Laboratory, Montreal, Canada.

Selim, S., Hartnagel, J.R., Osimitz, T.G., Gabriel, K.L. and Schoenig, G.P. (1995). Absorption, metabolism, and excretion of N,N-diethyl-*m*-toluamide following dermal application to human volunteers. *Fund. Appl. Toxicol.*, **25**, 95-100.

Stinecipher, J. and Shah, J. (1998) Percutaneous permeation of the *meta*, *ortho* and *para* isomers of N,N-diethyltoluamide. *Int. J. Pharm*, **160**, 31-41.

US Environmental Protection Agency (1998). Reregistration Eligibility Decision (RED) EPA738-R-98-010.

Volpato, N.M., Santi, P., Laureri, C. and Colombo, P. (1997). Assay of aciclovir in human skin layers by high-performance liquid chromatography. *J. Pharm. and Biomed. Anal.*, **16**, 515-520.

Chapter 4

Further investigations into the effect of retarder compounds using three model permeants

4.1 Introduction

Following the detailed evaluation of the modification of permeation of DEET by the potential retarder 4-F2 (discussed in chapter 3), it was considered appropriate to investigate the effect of 4-F2 on the human skin permeation of permeants with different physicochemical characteristics to DEET. Additionally, further potential retarder compounds (2-F1, ORI-PR2 and ORI-PR3; see section 2.3.3) were synthesised by OmniPharm Research International Inc., which allowed potential structure/retardation effects to be probed.

The first study reported in this chapter assessed the effect of pre-treating human skin membranes with ethanolic solutions of each potential retarder on the permeation of a radiolabelled pesticide, ^{14}C -glyphosate (compound details given in section 4.1.1 below). The permeation of the application vehicle, water, was simultaneously measured by incorporation of tritiated water ($^3\text{H}_2\text{O}$) in the vehicle.

The second study assessed the effect of pre-treatment with ethanolic solutions of the retarders, 4-F2 (batches 1 and 2; assessed separately) and 2-F1 on the skin permeation of a non-ionisable compound, hydrocortisone (compound details given in section 4.3.1). One retarder, 4-F2 batch 2, was also applied in propylene glycol to allow comparison with both the ethanolic pre-treatment and a published study (Fuhrman Jr et al, 1997) on several novel penetration enhancers, applied in a similar manner, in this vehicle.

4.1.1 Selected permeants study 1: glyphosate and water

The permeants assessed in this section were glyphosate and water. Glyphosate (CAS No. 1071-83-6, Figure 4.1, N-(phosphonomethyl)-glycine), has a molecular weight of 169.07 Daltons, is a white crystalline solid (m.p. 230°C), has a reasonably good solubility in water (12 mg/ml at 25°C), but a low solubility in organic solvents. It is an ionisable compound with reported pK_as at 2.32, 5.86 and 10.86, and log K_{OW} of between -2.8 and -1.7 (WHO, 1994 and Wester et al, 1991, respectively).

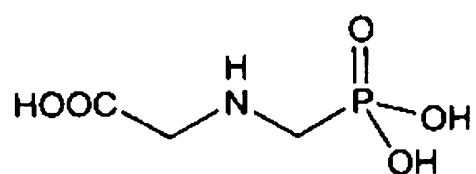


Figure 4.1 Structure of Glyphosate (Merck Index XIII Edition)

Glyphosate is typically formulated as the highly water soluble isopropylamine (e.g. Roundup™, Monsanto) or trimethylsulfonium salt, and is one of the most widely used non-specific herbicides. It is used to control grasses, broadleaf weeds, woody plants and aquatic weeds, both industrially and by the public. It is also used to desiccate plants such as cotton and cereals prior to harvest and, at low doses, as a plant growth regulator. Glyphosate is absorbed through leaves and is distributed throughout the plant. Little absorption occurs through roots due to high soil affinity. In plants, it is believed that glyphosate inhibits the shikimic acid pathway of aromatic amino acid synthesis, photosynthesis, plant respiration, plant nucleic acid synthesis and the metabolism of phenolic compounds (Eldon and Oehme, 1992). This pathway exists only in plants and micro-organisms and not in mammals (Malik et al., 1989). Roundup is frequently formulated for professional use as 41% isopropylamine salt, and is sprayed as a liquid with ground and aerial equipment. Due to the extensive use of glyphosate (~8500 tonnes annually) under various conditions, there is a potential for occupational exposure via the dermal route as well as exposure for the general public via food and water

(U.S. EPA, 1993). It is therefore a particularly relevant permeant with regard to retardation evaluation.

Glyphosate is relatively low in toxicity (mammal) and classed in the U.S. as a Group E carcinogen (evidence of no carcinogenic effects). However, glyphosate products are considered a leading cause of eye and skin irritation in mixer/loader/applicators in California (U.S. EPA, 1993). Formulation excipients, especially surfactants, play an important role in the higher irritation potential of some products.

The permeation of glyphosate through human skin has been reported by Wester et al (1991, 1996). A review of that work, and comparison with data produced here, is presented in the results and discussion section (4.2.3).

The permeation of water through human skin has been measured by many researchers throughout the world, and it is the 'typical' permeation rate that is used by many laboratories as a skin membrane integrity confirmation tool (see chapter 7). The incorporation of tritiated water into the applied 0.1% ^{14}C -glyphosate in water vehicle allowed the effect of the retarders on the permeation of water, under infinite dose and occlusive conditions, to be investigated simultaneously.

4.2 Assessment of the effect of pre-treatment with retarders 4-F2, 2-F1, ORI-PR2 and ORI-PR3 on the human skin permeation of glyphosate and water

4.2.1 Materials and equipment

Compounds 4-F2 (batch numbers 1 and 2), 2-F1, ORI-PR2 and ORI-PR3 were supplied by OmniPharm Research International Inc., Buffalo, USA. The compounds were characterised by OmniPharm and were used as received.

^{14}C -Glyphosate (glycine-2- ^{14}C , ARC1312, 50 mCi/mmol, 50 μCi , 99% purity by TLC) was from American Radiolabeled Chemicals Inc. (ARC). Due to a

dispensing error by ARC, the radiolabelled glyphosate was received in two shipments containing 9.25 μCi and 41.75 μCi . Unlabelled glyphosate (product code; P5671, purity 96%, 1g) was obtained from Sigma-Aldrich Ltd.

Tritiated water ($^3\text{H}_2\text{O}$) was from Amersham Pharmacia Biotech (Little Chalfont, UK) and diluted with distilled water to a specific activity of 10 $\mu\text{Ci}/\text{ml}$. Water was distilled in all-glass apparatus and solvents and buffer salts were of AnalaR grade or better (BDH). OptiPhase HiSafe 3 liquid scintillation cocktail and OptiSolve tissue solubiliser were from Wallac (UK) Ltd. Radioactive samples were dispersed in 3 ml scintillation cocktail (HiSafe 3, Wallac) using disposable 6 ml diffuse plastic scintillation vials (Zinser Analytic) and counted for radioactivity using a Wallac 1409 liquid scintillation counter. Weight measurements were made on a Sartorius BP211D 5-place semi-micro analytical balance equipped with a statistical printer.

The liquid scintillation counter operating program was Wallac 1400 DSA version 2.2. Radioactivity was quantified as disintegration per minute (DPM), and data were transferred electronically to Microsoft Excel worksheets for subsequent calculations. Accurate dual label analysis (^3H and ^{14}C) is possible through the use of a digital overlay technique (dual label DOT DPMTM) and the use of spectrum libraries. The technique reconstructs a standard spectrum for each isotope at the same quench level and intensity as the unknown sample (which produces a composite spectrum), and then, following a successful fit to library spectra, the isotope ratios and intensities are calculated and used to produce DPM values. The technique uses an external standard (^{152}Eu) automatically moved into place directly beneath each sample for a period of 10 seconds, enabling counting efficiency to be determined for each sample. The DOT DPM technique eliminates the usual requirement for specific isotope combination quench curves to be prepared, and the DPM values are not dependent on isotope ratios. There is also no sample volume dependence and unsuccessful spectrum fit, for example due to phase separation, results in sample rejection.



Chemiluminescence frequently occurs in samples of biological origin during the hydrolysis of long macromolecules in the scintillation fluid. These chemiluminescence events release a single photon whilst normal decay releases several photons. The two detectors on opposite sides of the sample measure decay photons virtually simultaneously, but this is not the case for the chemiluminescence photon. However, extensive chemiluminescence results in multiple single photons, and if the photons arrive at both detectors within the detector coincidence resolving time (a few nanoseconds), it would appear as a decay event. However, high levels of chemiluminescence produce a large delayed spectrum (non-coincidental detection) that was also (separately) recorded by the counter. The chemiluminescence correction option (ChemiStrip™), used for all sample counting, subtracted the chemiluminescence spectrum, if any, channel by channel from the combined sample plus chemiluminescence spectrum prior to subsequent calculation.

4.2.2 Methods

4.2.2.1 Receptor phase preparation

Phosphate buffered saline (pH 7.4; PBS) was prepared by dissolving the following salts in water: 2.1 g/l $\text{NaH}_2\text{PO}_4 \cdot 2\text{H}_2\text{O}$, 19.1 g/l $\text{Na}_2\text{HPO}_4 \cdot 12\text{H}_2\text{O}$ and 4.4 g/l NaCl. The pH of the buffer was confirmed to be 7.4 ± 0.1 .

Glyphosate has high water solubility (12 mg/ml) and PBS was used in previous permeation studies (Wester et al, 1996). Nevertheless, sufficient solubility in the receptor phase was confirmed visually with 7.86 mg glyphosate dissolving in 2 ml PBS (3.93 mg/ml) within 20 minutes.

4.2.2.2 Vehicle preparation

A 0.1% (w/v) ^{14}C -glyphosate solution in tritiated water ($^3\text{H}_2\text{O}$) was prepared as followed; 15.56 mg unlabelled glyphosate (purity 96% therefore equivalent to 14.94 mg pure compound) was directly weighed into a 20 ml glass vial. 250 μl ^{14}C -glyphosate stock solution was added (containing a calculated 0.08 mg

glyphosate), followed by 3 ml 9.19 $\mu\text{Ci/ml}$ $^3\text{H}_2\text{O}$ and 11.75 ml distilled water. The final calculated solution activities were 1.67 $\mu\text{Ci/ml}$ ^{14}C -glyphosate (0.1001% glyphosate) and 1.84 $\mu\text{Ci/ml}$ $^3\text{H}_2\text{O}$. However, the measured ^{14}C -glyphosate activity (see below) was 24.6% of that expected. The remaining ^{14}C -glyphosate stock solution was sampled and found to be of low activity. Investigations by ARC discovered a dispensing error prior to shipment, and the outstanding quantity of radiolabel was shipped at a later date. The utilised ^{14}C -glyphosate stock solution may have contained only a quarter of the expected glyphosate concentration but, even if this was the case, the final glyphosate concentration would have been little different at 0.0997% (w/v).

Four 50 μl samples of the donor solution (0.1% (w/v) ^{14}C -glyphosate in $^3\text{H}_2\text{O}$) were analysed by liquid scintillation counting (LSC) and indicated homogeneous distribution of the radiolabels in the donor solution. For ^{14}C -glyphosate, the mean DPM/ μg was 910.1 (0.47%RSD) and for $^3\text{H}_2\text{O}$ the mean DPM/mg was 4175 (0.37%RSD).

Solutions of the retarder compounds at target concentrations of 2% (w/v) in ethanol (96% (v/v), AnalaR) were prepared on a small scale due to the small amounts of material available. Samples of retarder compounds were transferred to 1.5 ml glass vials, and appropriate volumes of ethanol added (by weight and subsequently converted to volume using the measured density). Vials were immediately capped and the contents shaken prior to storage at room temperature in the dark. All retarder compounds, except ORI-PR3, were transferred as liquids (4-F2 was gently hand warmed to produce a homogeneous oil) using Pasteur pipettes. ORI-PR3, a waxy solid, was transferred using a micro-spatula. All mixtures appeared to form homogeneous solutions, except ORI-PR3, which formed a cloudy suspension. If ideal mixing and retarder compound densities of 1 g/ml were assumed, then the calculated solution concentrations were 19.54, 19.50, 19.53, 18.35 and 19.54 mg/ml for 4-F2 batch 1, 2-F1, ORI-PR2, ORI-PR3 and 4-F2 batch 2 respectively.

4.2.2.3 Skin preparation

Human abdominal and breast skin, obtained following cosmetic reduction surgery, was initially prepared by removal of the subcutaneous fat and connective tissue by dissection, prior to storage at -20°C . On the day of use, the skin membranes, comprising stratum corneum, epidermis and dermis, were thawed at room temperature, then trimmed to an appropriate size for mounting in diffusion cells. Three different donors were prepared and distributed evenly throughout the test groups.

Full thickness skin membranes were suitable for use in this study due to the highly water-soluble nature of glyphosate, whilst the second permeant was water itself. The presence of the dermis adds no additional (permeation rate) barrier for such permeants compared to stratum corneum or epidermal membranes.

4.2.2.4 Diffusion cells

The skin membranes were mounted as a barrier between the halves of greased (high vacuum grease, Dow Corning, USA) horizontal Franz-type diffusion cells, with the stratum corneum facing the donor chamber. The area available for diffusion was about 1.2 cm^2 , with the exact area being measured for each diffusion cell. A schematic of the diffusion cell can be seen in section 3.2.2.4, and the experimental set-up is shown in Figure 4.2.

The receptor chambers of the diffusion cells were filled with PBS (nominally 3.3 ml, accurately measured for each cell) and capped. The diffusion cells were immersed in a constant temperature water bath such that the receptor chambers were maintained at $37.0\pm 0.5^{\circ}\text{C}$ throughout the experiment. This ensured that the skin surface temperature was maintained at $32.0\pm 1^{\circ}\text{C}$. Receptor chamber contents were continuously agitated by small PTFE-coated magnetic followers driven by submersible magnetic stirrers. The cells were allowed to temperature equilibrate for 30 minutes.



Figure 4.2 The experimental diffusion cell set-up

4.2.2.5 Membrane integrity assessment

The integrity of each membrane was not assessed prior to pre-treatment with retarder compounds for two reasons. Firstly, full thickness membranes do not undergo the occasionally damaging process of heat separation used to produce epidermal membranes (as used in Chapter 3). Secondly, the membrane integrity test used in our laboratory assesses the permeation of tritiated water, which was one of the permeants to be assessed following pre-treatment with retarder compounds, and it was inevitable that some tritium carryover would have occurred. The permeation rate of water (from the ^{14}C -glyphosate in $^3\text{H}_2\text{O}$ vehicle) through each membrane was therefore assessed post-experimentally. This indicated that there were no cells with significantly compromised barrier function.

4.2.2.6 Skin pre-treatment

Cells were separated into six groups of 6 cells for pre-treatment (prior to application of ^{14}C -glyphosate in $^3\text{H}_2\text{O}$). Cells received a $50\ \mu\text{l}/\text{cm}^2$ dose of either 2% retarder compound in ethanol or ethanol alone. The pre-treatments were applied using a $50\ \mu\text{l}$ Hamilton syringe and the cells were left undisturbed in the waterbath for 2 hours. It was observed that the pre-treatment vehicle had completely evaporated in less than 1 hour.

4.2.2.7 Application of 0.1% ^{14}C -glyphosate in $^3\text{H}_2\text{O}$ solution

Following pre-treatment, all cells (groups 1 to 6) received a target dose of $300\ \mu\text{l}/\text{cm}^2$ 0.1% ^{14}C -glyphosate in tritiated water, applied using a digital pipette. For each cell, the exact time of application was noted and that time represented zero time for that cell. The diffusion cell donor chambers were occluded using greased coverslips to prevent evaporation of the tritiated water.

4.2.2.8 Determination of skin permeation

$200\ \mu\text{l}$ samples were taken (using a digital pipette) from each receptor chamber 1, 2, 4, 6, 8, 12 and 24 hours after dosing. Each sample was placed directly into scintillation fluid and analysed for ^{14}C and ^3H by LSC. The liquid removed by each sample was replaced with fresh temperature equilibrated blank receptor medium.

4.2.2.9 Determination of skin content and radiolabel recovery

Following removal of the 24 hour receptor phase samples, the remaining receptor phases were removed to waste. For each cell, the donor phase was removed using a digital pipette and placed in a 20 ml glass vial (Chromacol, UK). Any condensation droplets on the occlusive glass coverslip were also collected using the digital pipette. The donor chamber and skin surface was then washed, with aspiration, four times with 1 ml aliquots of water, with

washings added to the removed donor phase. Diffusion cells were then dismantled and the circular dosed section of skin plus a ~2 mm border excised using a scalpel. Each full thickness skin sample was placed in a 20 ml glass vial, 4 ml OptiSolve™ (Wallac), a toluene and quaternary ammonium based tissue solubiliser, added and the vial capped. The vial was shaken using a Stuart Scientific Gyro-Rocker (Fisher, UK) at room temperature for 72 hours, which dissolved each skin sample entirely.

The 24 hour wash and dissolved skin sample vials were vortexed prior to sampling (200 µl) and counting for ¹⁴C and ³H by LSC.

4.2.3 Results and discussion

Data are expressed as the mean ± standard error (SE) amount (µg/cm² for glyphosate, mg/cm² for water) and % of the applied dose. Statistical comparisons were performed using single factor ANOVA in Microsoft Excel Version X (Mac OS X).

The 2 hour pre-treatment doses ranged from 49.5 to 50.5 µl/cm² for each cell, with average doses for each group close to 50.0 µl/cm². The ¹⁴C-glyphosate/³H₂O doses ranged from 298 to 303 µl/cm² with average doses for each group close to 300 µl/cm². Six cells from three skin donors (2 per donor) were run for each group.

4.2.3.1 Glyphosate permeation data

The permeation of glyphosate through the human skin membranes and into the receptor phases is shown in Figure 4.3. Glyphosate permeation rates began to plateau for all groups at between 8 and 12 hours, possibly due to donor phase depletion, even though average group recoveries in the receptor phase at 24 hours only ranged from 6.3 to 7.8% of the applied dose. This issue is discussed further later in this section.

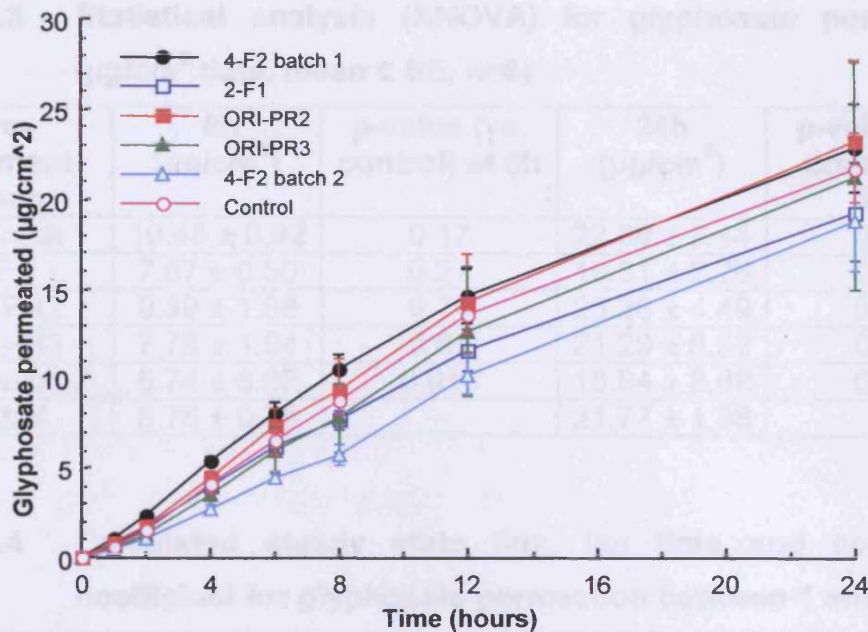


Figure 4.3 Permeation ($\mu\text{g}/\text{cm}^2$, mean \pm SE, $n=6$) of glyphosate through human skin from a 0.1% ^{14}C -glyphosate in tritiated water

Total amounts permeated ($\mu\text{g}/\text{cm}^2$ data) for each retarder pre-treated group were compared statistically to those for the control pre-treated group at both 8 and 24 hours (Table 4.3). Limited differences were observed at 24 hours (p -values ≥ 0.41). However, at 8 hours, where possible donor depletion had no apparent influence on any group, glyphosate permeation for 4-F2 batch 2 pre-treated cells was significantly lower at the 95% confidence interval ($p < 0.05$) than for the control group. Surprisingly, the greatest permeation at 8 hours was observed for 4-F2 batch 1 pre-treated cells (p -value 0.17 versus control) and statistical comparison of glyphosate permeation data for the two batches of 4-F2 produced a p -value of 0.001.

For each pre-treatment group the apparent steady state flux value for glyphosate permeation between 1 and 8 hours (prior to the permeation rate beginning to plateau), estimated lag time and the linear fit correlation coefficient squared (r^2) are presented in Table 4.4 and Figure 4.4.

Table 4.3 Statistical analysis (ANOVA) for glyphosate permeation ($\mu\text{g}/\text{cm}^2$ data, mean \pm SE, n=6)

Pre-treatment group	8h ($\mu\text{g}/\text{cm}^2$)	p-value (vs. control) at 8h	24h ($\mu\text{g}/\text{cm}^2$)	p-value (vs. control) at 24h
4-F2 batch 1	10.45 \pm 0.82	0.17	22.89 \pm 2.44	0.72
2-F1	7.67 \pm 0.50	0.27	19.31 \pm 2.76	0.48
ORI-PR2	9.39 \pm 1.68	0.74	23.26 \pm 4.49	0.77
ORI-PR3	7.78 \pm 1.94	0.65	21.29 \pm 6.32	0.94
4-F2 batch 2	5.74 \pm 0.62	0.013	18.84 \pm 2.88	0.41
control	8.76 \pm 0.78	-	21.77 \pm 1.88	-

Table 4.4 Calculated steady state flux, lag time and correlation coefficient for glyphosate permeation between 1 and 8 h

Pre-treatment group	Flux (1-8 h) ($\mu\text{g}/\text{cm}^2 \cdot \text{h}$)	Estimated lag time (h)	Correlation coefficient, r^2
4-F2 batch 1	1.36	0.19	0.998
2-F1	1.02	0.22	0.994
ORI-PR2	1.27	0.47	0.997
ORI-PR3	1.08	0.68	0.997
4-F2 batch 2	0.780	0.50	0.997
control	1.20	0.61	0.999

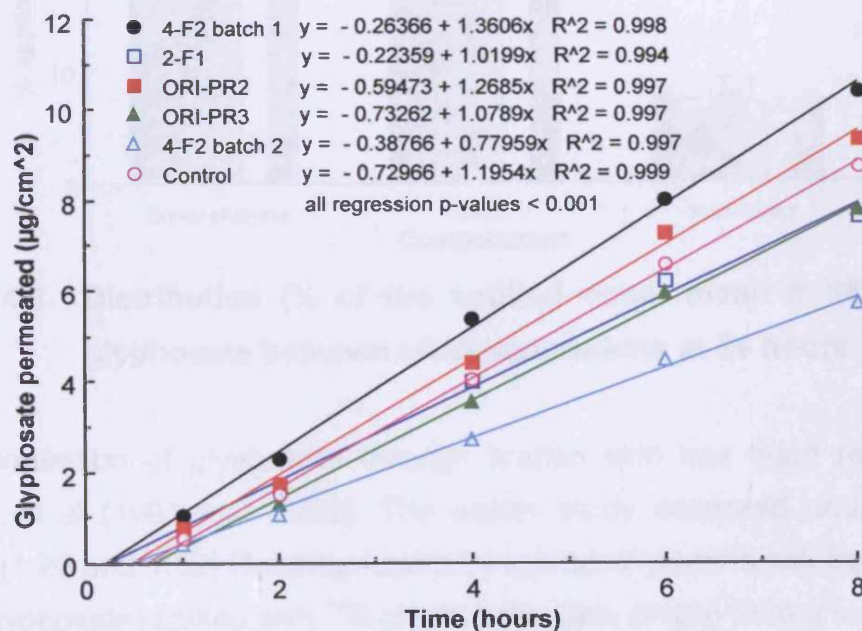


Figure 4.4 Linear fits of glyphosate permeation data ($\mu\text{g}/\text{cm}^2$, n=6) up to 8 hours after application

Distribution of glyphosate in the 24 hour wash (donor chamber plus skin surface) and the dissolved full thickness human skin membranes appeared similar for all groups (Figure 4.5). Statistical analysis was performed for several of the most disparate data sets, and resultant p-values were all ≥ 0.31 . On average, only 41-45% of the applied dose was recovered from the solution or the skin surface, whilst the skin membranes contained, on average, 37-43% of the applied dose. This significant reduction in donor phase glyphosate concentration could account for the reduction in the permeation rate at later time-points. Overall recoveries of applied glyphosate were good, and group averages ranged from 87 – 93%.

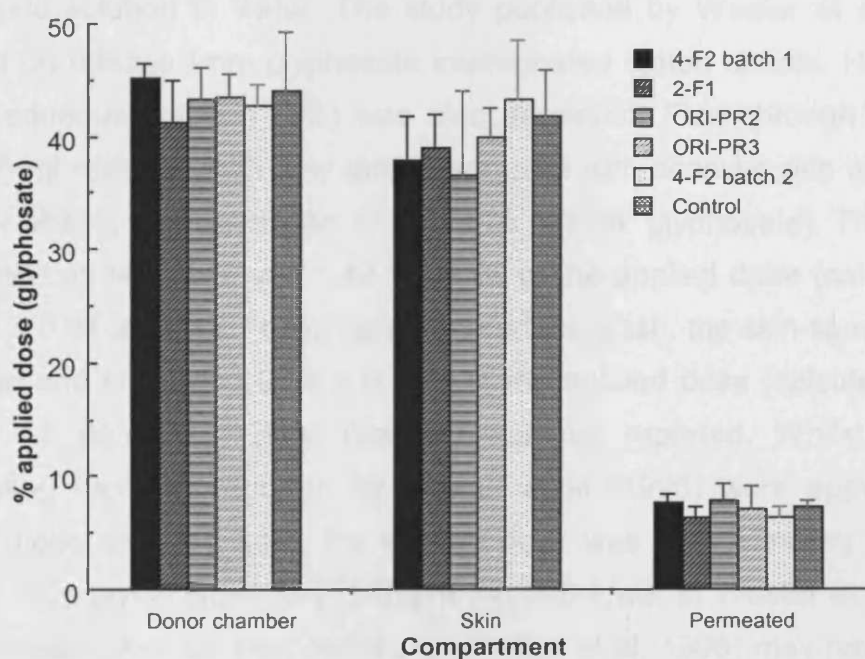


Figure 4.5 Distribution (% of the applied dose, mean \pm SE, n=6) of glyphosate between all compartments at 24 hours

The permeation of glyphosate through human skin has been reported by Wester et al (1991 and 1996). The earlier study assessed undiluted and diluted (1:20 and 1:32) Roundup (containing isopropylamine salt equivalent to 1.1% glyphosate) spiked with ^{14}C -glyphosate. Skin (thigh) from a single donor was used (within 5 days of autopsy, stored at 4°C in Eagle's minimum essential cell culture medium) in flow-through diffusion cells (1 cm², 3 ml human plasma receptor phase at 3 ml/h). Application volumes were 14, 70

and $140 \mu\text{l}/\text{cm}^2$ combined with exposure periods of 30 min, 4, 8 and 16 h (although not 16 h for undiluted product). Cells were not occluded so it was likely that vehicle evaporation would have been an issue at later time-points. Measured permeation was low (maximum $2.2 \pm 0.5\%$ of the applied dose) but quite variable, with absorption values for different exposure periods of the same solution varying in a somewhat random manner. This may have been due to a sensitivity issue when collecting aliquots of the flow-through receptor phase for counting and a limitation of the 3 replicates used per group. The largest amount of glyphosate permeated was $0.62 \mu\text{g}/\text{cm}^2$ ($140 \mu\text{l}/\text{cm}^2$ dose of undiluted formulation with the 8 h exposure period, $0.4 \pm 0.2\%$ applied dose), $\sim 7\%$ of the permeation observed here from an infinite dose of a glyphosate solution in water. The study published by Wester et al in 1996 focused on release from glyphosate impregnated cotton sheets. However, a simple aqueous solution (1%) was also assessed. Flow through cells (0.8 cm^2 , 3.5 ml with a 3 ml/h flow rate) were used with cadaver skin and a PBS receptor phase. The dose was 300 μl ($3.75 \text{ mg}/\text{cm}^2$ glyphosate). The amount permeated at 24 hours was $1.42 \pm 0.25\%$ of the applied dose (calculated to be $53.3 \pm 0.94 \mu\text{g}/\text{cm}^2$). Following a skin surface wash, the skin samples were analysed and contained $0.56 \pm 0.13\%$ of the applied dose (calculated to be $21.0 \pm 4.9 \mu\text{g}/\text{cm}^2$). Overall recovery was not reported. Whilst amounts permeating ($\mu\text{g}/\text{cm}^2$) reported by Wester et al (1996) were approximately double those reported here, the applied dose was approximately ten times greater. Skin levels were very different (~ 6 fold lower in Wester et al, 1996). The skin wash method (not defined by Wester et al, 1996) may have been a factor, together with the skin type/source. Another possibility is that the ethanol pre-treatment may have markedly increased the subsequent permeation of glyphosate.

4.2.3.2 Water permeation data

The permeation of water from the 0.1% ^{14}C -glyphosate in tritiated water donor solution is shown in Figure 4.6. For all groups the permeation rate began to plateau after 12 hours, although only to a limited degree. At all time-points water permeation was lowest for the control group (blank ethanol pre-treated),

and, for some groups, actual enhancement of water permeation by the retarder compound appeared likely. Statistical analysis of the total amounts permeated (mg/cm^2 data) at both 12 and 24 hours are presented in Table 4.5, with the greatest differences (p-values 0.16 and 0.17 at 12 and 24 hours, respectively) between 4-F2 batch 1 and the control pre-treatments. In contrast to the data for glyphosate, differences between the two batches of 4-F2 were small for water permeation, with p-values of 0.59 and 0.61 at 12 and 24 hours, respectively.

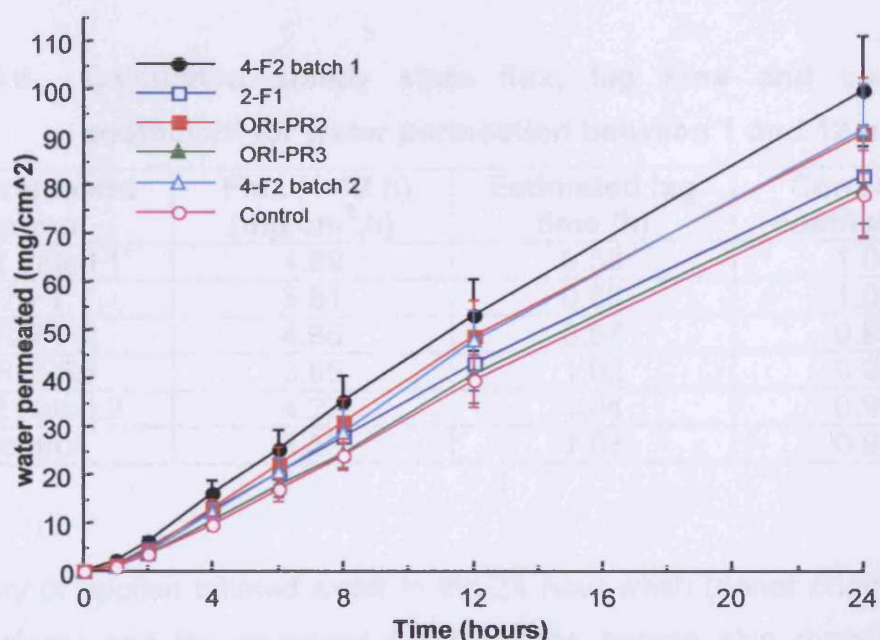


Figure 4.6 Permeation ($\mu\text{g}/\text{cm}^2$, mean \pm SE, $n=6$) of water through human skin from a 0.1% ^{14}C -glyphosate in tritiated water

Table 4.5 Statistical analysis (ANOVA) for water permeation ($\mu\text{g}/\text{cm}^2$ data, mean \pm SE, $n=6$)

Pre-treatment group	12h (mg/cm^2)	p-value (vs. control) at 12h	24h (mg/cm^2)	p-value (vs. control) at 24h
4-F2 batch 1	53.1 \pm 7.2	0.16	100.0 \pm 11.6	0.17
2-F1	43.1 \pm 5.7	0.66	82.5 \pm 10.1	0.77
ORI-PR2	48.7 \pm 7.3	0.34	91.1 \pm 11.8	0.41
ORI-PR3	40.9 \pm 5.9	0.86	79.8 \pm 10.2	0.92
4-F2 batch 2	47.8 \pm 6.4	0.34	92.1 \pm 9.3	0.32
control	39.5 \pm 5.4	-	78.4 \pm 9.1	-

For each pre-treatment group the apparent steady state flux value for water permeation between 1 and 12 hours (prior to the permeation rate beginning to plateau), estimated lag time and the linear fit correlation coefficient squared (r^2) are presented in Table 4.6. The flux of water for 4-F2 batch 1 pre-treated cells was 33% greater than for the control. The permeation rate of water for all groups was higher than typically observed (up to 2.5 mg/cm².h), possibly due to a reduction in barrier function caused by the glyphosate donor solution acidity (measured pH = 2.50) and/or the 50 µl/cm² ethanol pre-treatment, and the completely occlusive conditions employed.

Table 4.6 Calculated steady state flux, lag time and correlation coefficient for water permeation between 1 and 12 hours

Pre-treatment group	Flux (1-12 h) (mg/cm ² .h)	Estimated lag time (h)	Correlation coefficient, r^2
4-F2 batch 1	4.69	0.58	1.000
2-F1	3.81	0.68	1.000
ORI-PR2	4.36	0.87	0.999
ORI-PR3	3.65	1.02	0.998
4-F2 batch 2	4.27	1.04	0.997
control	3.53	1.03	0.997

Recovery of applied tritiated water in the 24 hour wash (donor chamber plus skin surface) and the dissolved full thickness human skin membranes is shown together with permeated values in Figure 4.7. Groups where higher permeation was observed appeared to show a commensurate reduction in recovery in the surface washes. Levels in the skin appeared similar (4.0 to 5.8% of the applied dose) for all groups, and no groups were significantly different to the control (p-values ranged 0.46-0.78). Overall recoveries of applied tritiated water were high, with group averages ranging between 85 and 92%.

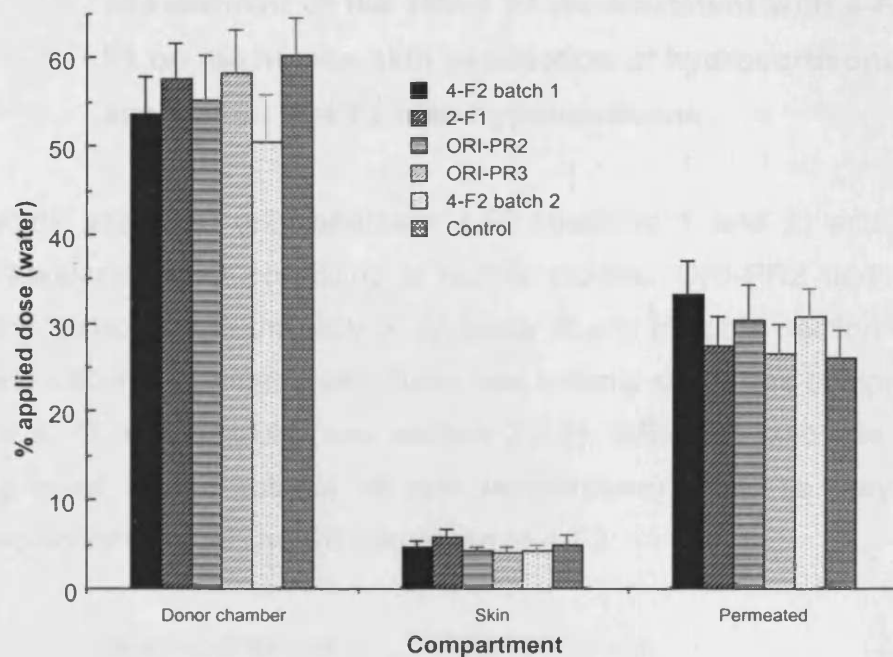


Figure 4.7 Distribution (% of the applied dose, mean \pm SE, n=6) of tritiated water between all compartments at 24 hours

4.2.4 Conclusions

Modification (retardation or enhancement) of glyphosate permeation by any of the assessed retarder compounds was very limited and there was little difference between the behaviour of the different retarders. There was some evidence of retardation of glyphosate permeation after pre-treatment with one retarder, 4-F2 batch 2, over a limited period of time. However, in contrast, batch 1 of the same retarder may have slightly enhanced the permeation of glyphosate.

The effects of pre-treatment with the retarder compounds on the permeation of water ranged from none to slight enhancement. All water permeability values were somewhat high, indicating that the relatively low pH of the donor glyphosate solution may have had a detrimental effect on skin barrier integrity. It is possible that any such disruption of the lipid bilayer structure could result in a matrix that was resistant to modulation by the retarders.

4.3 Assessment of the effect of pre-treatment with 4-F2 and 2-F1 on the human skin permeation of hydrocortisone and co-application of 4-F2 with hydrocortisone

This study assessed only retarders 4-F2 (batches 1 and 2) and 2-F1, as these appeared most promising in earlier studies. ORI-PR2 and ORI-PR3 were not tested due to the lack of evidence of any effect in section 4.2. ORI-PR2 and ORI-PR3 probably also have less optimal structures compared to 2-F1 and 4-F2, respectively (see section 2.3.3). ORI-PR3 also has a higher melting point (solid material at skin temperature) and this may indicate reduced ability to enter the SC compared to 4-F2.

4.3.1 Hydrocortisone

Hydrocortisone (HC, cortisol, CAS No. 50-23-7, Figure 4.8, (11 β)-11,17,21-trihydroxypregn-4-ene-3,20-dione) is an endogenous glucocorticoid (the principal glucocorticoid produced by the adrenal cortex).

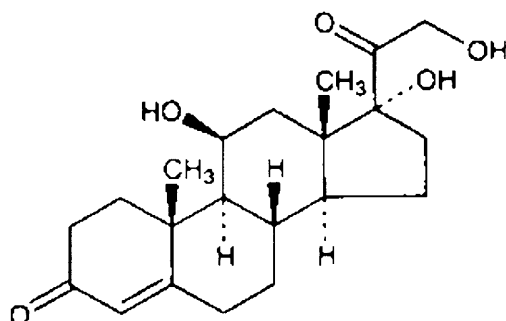


Figure 4.8 Structure of hydrocortisone (Merck Index XIII Edition)

Hydrocortisone has a molecular weight of 362.46 Daltons, is a bitter-tasting crystalline solid (m.p. 217-220°C), has a fairly low water solubility (0.28 mg/ml at 25°C), but a good solubility in ethanol (15 mg/ml at 25°C) and propylene glycol (12.7 mg/ml at 25°C) [Merck Index, XIII edition]. The reported log K_{OW} of HC is 1.61 (EDETOX database).

HC is a vital part of the body's response to inflammation and trauma such as disease or surgery. In unphysiologically high concentrations, HC suppresses

all phases of the inflammatory reaction (i.e. the organism defensive measures against foreign or noxious matter). Short term use of HC is virtually without side effects, but long term use, especially of higher doses given orally, can mimic the effects of Cushing's Syndrome (endogenous over production of HC) with many negative side effects including lowered resistance to infection and delayed healing, and also (due to mineralcorticoid activity) osteoporosis, skin atrophy and salt and fluid retention. To limit potential for developing Cushing's Syndrome, HC derivatives with lower mineralcorticoid activity are usually administered, and local application is preferred, although skin atrophy and mucosal colonisation with candida fungi can still occur (Lullmann et al, 2000). For long term use, a just sufficient dose is typically given, although the inhibitory feedback mechanism can lower production of endogenous HC following administration of exogenous glucocorticoid.

Hydrocortisone has been applied topically since the 1950s, often formulated in ointment or cream bases at concentrations up to 1%, and can produce dramatic suppression of inflammation in cases of eczema and dermatitis. The application of occlusive film/dressing (e.g. plastic sheet) aids penetration of topical steroids, although if large areas of skin have been treated systemic absorption can be an issue. Several ester prodrugs of HC are also applied topically (e.g. valerate).

The reported skin permeation of HC varies greatly depending upon application vehicle, dose and the conditions used (particularly occlusive state). The reported permeation of HC under similar conditions to those employed in this study is discussed in section 4.9. HC was also assessed in the preliminary investigation of the 4-F2 and 2-F1 (Brain et al, 1996), although the conditions used were different to those used here, and that study was of limited scope.

4.3.2 Materials and equipment

As described in section 4.2.1 except that hydrocortisone (98.4% purity) was supplied by Sigma-Aldrich and propylene glycol (PG, B.P. grade) by VWR (Lutterworth, UK).

4.3.3 Methods

As described in section 4.2.2 except as indicated below.

4.3.3.1 Receptor phase preparation

Phosphate buffered saline (pH7.4; PBS) was prepared as described in 4.3.1. 25% ethanol PBS (EPBS) was subsequently prepared by mixing 25/75 (v/v) ethanol/PBS. The ethanol was of 96% v/v AnalaR grade (VWR).

Hydrocortisone solubility in PBS, EPBS and 0.9% NaCl (aq) was initially assessed visually by addition of increasing volumes of solvent to small quantities of HC. Solubility in PBS and saline appeared fairly poor (<107 and ~120 µg/ml respectively), but significantly greater in EPBS (>200 µg/ml). Therefore, EPBS was selected as the receptor phase. The solubility of HC in EPBS at 25°C was subsequently determined by HPLC and found to be 1.84 mg/ml.

4.3.3.2 Vehicle preparation

Previous retarder solutions were prepared by weight due to the inability of air displacement pipettes to accurately transfer solvent mixtures with properties different to water (e.g. density, viscosity, vapour pressure and surface tension). New positive displacement pipettes with disposable capillaries and pistons allowed more accurate transfer by volume and therefore slightly different preparation methods were used.

Fresh solutions of 2% (w/v) 4-F2 batches 1 and 2, and 2-F1 in ethanol (96%) were prepared as follows. Samples of 4-F2 were gently hand warmed to produce yellow liquid. 2-F1 did not require warming (already a pale liquid). 10 μ l samples of the retarders were transferred using a positive displacement pipette to tared vials and the weight delivered recorded. If accurate pipetting was assumed then retarder densities were 0.89, 0.90 and 0.93 g/ml for 4-F2 batches 1 and 2 and 2-F1, respectively. Ethanol (490 μ l, weight delivered recorded) was added, the vials capped and shaken forming clear solutions. If ideal mixing was assumed, then the calculated solution concentrations were 2.00, 2.06 and 2.06 % (w/v), respectively.

A more concentrated solution of 4-F2 batch 2 in propylene glycol was prepared in a similar manner by mixing 5.50 mg 4-F2 batch 2 and 43.95 μ l PG. The resultant concentration was 0.430 Molar (M; equivalent to ~10.98% w/v). The target concentration of 0.4M was chosen to match that used by Fuhrman et al (1997) for the assessment of several novel penetration enhancers.

Visual investigation of HC solubility in PG indicated a solubility of >10.4 mg/ml at 25°C, and Fuhrman et al (1997) reported a value of 0.03M at 32 \pm 0.5°C (equivalent to 10.9 mg/ml). As the HC donor solution should remain saturated throughout the experiment, excess HC should be included. Fuhrman et al (1997) did not specify what excess they included. Therefore, a saturated solution of hydrocortisone in PG that included excess solid was prepared by mixing 42.04 mg HC with 2 ml PG (weight delivered equivalent to 1.994 ml) producing a suspension containing 21.1 mg/ml. The suspension was stirred overnight at 32°C.

4.3.3.3 Skin preparation

As described in section 4.2.2.3 except that four donors were used.

4.3.3.5 Membrane integrity assessment

As described in section 3.2.2.5 except that cells were sampled after one hour and were refilled with EPBS. Of the 30 cells prepared, 27 exhibited a water permeability coefficient of lower than 2.5×10^{-3} cm/h (the typical rejection value, see Chapter 7). The three cells with higher permeability coefficient ($2.69 \geq k_p \times 10^{-3} \leq 5.24$) were used in the study due to the shortage of available tissue, but subsequent data from these cells were closely inspected and are discussed further in the results and discussion section.

4.3.3.6 Skin pre-treatment

Following the membrane integrity assessment, cells were separated into six groups (five cells per group) for pre-treatment (prior to application of HC in PG). Groups 1 to 4 received a $50 \mu\text{l}/\text{cm}^2$ dose of 2% 4-F2 batch 1 in ethanol, 2% 2-F1 in ethanol, 2% 4-F2 batch 1 in ethanol and blank ethanol, respectively. Groups 5 and 6 received a $5 \mu\text{l}/\text{cm}^2$ dose of 0.43M 4-F2 batch 2 in PG and blank PG, respectively. The $50 \mu\text{l}/\text{cm}^2$ pre-treatments were applied using Hamilton syringes and the $5 \mu\text{l}/\text{cm}^2$ pre-treatments using a positive displacement pipette. Cells were left undisturbed in the waterbaths for 2 hours, but it was observed that ethanol based pre-treatments had evaporated within 45 minutes. The 4-F2 batch 2 in PG pre-treated cells gradually lost all visible surface material (probably through absorption rather than evaporation due to the relatively low volatility of PG), whereas all the control PG pre-treated cells still had surface material present at 2 hours. This suggested that the presence of 4-F2 may have increased the skin absorption of PG.

4.3.3.7 Application of hydrocortisone in PG suspension

All cells (groups 1 to 6) received a target dose of $20 \mu\text{l}/\text{cm}^2$ HC in PG suspension, applied using a positive displacement pipette. The suspension was shaken immediately prior to the removal of each aliquot to try to ensure equal application of excess HC. For each cell, the exact time of application was noted and that time represented zero time for that cell. The diffusion cell

donor chambers were occluded using greased coverslips to match conditions assessed by Fuhrman et al (1997). Occlusive conditions would be expected to maximise permeation.

4.3.3.8 Determination of skin permeation

200 µl samples were taken (using a digital pipette) from each receptor chamber 5, 10, 19, 24, 32 and 48 hours after dosing. Each sample was placed into a 200 µl micro-vial (Kinesis Ltd, Bolnhurst, UK) and immediately frozen (-20°C) pending analysis. The liquid removed by each sample was replaced with fresh temperature equilibrated blank receptor medium.

Following removal of the 48 hour receptor phase samples, the remaining receptor phases were removed, placed in individual 20 ml glass vials (Kinesis), capped and frozen (-20°C). These samples were used for assay validation purposes.

4.3.3.9 Sample analysis and assay validation

A sensitive high performance liquid chromatography (HPLC) method for the quantitation of hydrocortisone was developed for this study. The chromatographic equipment used was as follows; LDC vacuum membrane degasser, LDC CM3500 and 3200 pumps, TSP AS3000 autosampler, LDC SM5000 photo diode array detector and SN4000 controller interface. Data collection and integration were conducted using PC1000 Ver. 3.0.1 software (TSP Ltd., Stoke-On-Trent, UK). Separation was performed on a Genesis C18 (Jones) 4 µm, 150 x 4.6 mm column protected with C18 security guard cartridges (Phenomenex). The injection volume was 20 µl (Pushloop injection).

The mobile phase was 35/65 (v/v) acetonitrile/water (acetonitrile of far UV grade), flow rate 1 ml/min and quantitation was by UV detection at 245 nm (the observed lambda maximum). The retention time of HC was ~4.6 minutes, and the total runtime twenty minutes. UV scans (210-310 nm) were

collected during assay development to allow selection of the most suitable wavelength and the spectral purity of the HC peak for receptor phase samples was compared to that for a standard solution, enabling confirmation that there were no co-eluting compounds. An example of the spectral comparison (Figure 4.9) between a 48 h receptor phase sample and standard solution, over a wide wavelength range (210 to 310 nm), produced an excellent correlation of value of 999.3 (of a possible 1000).

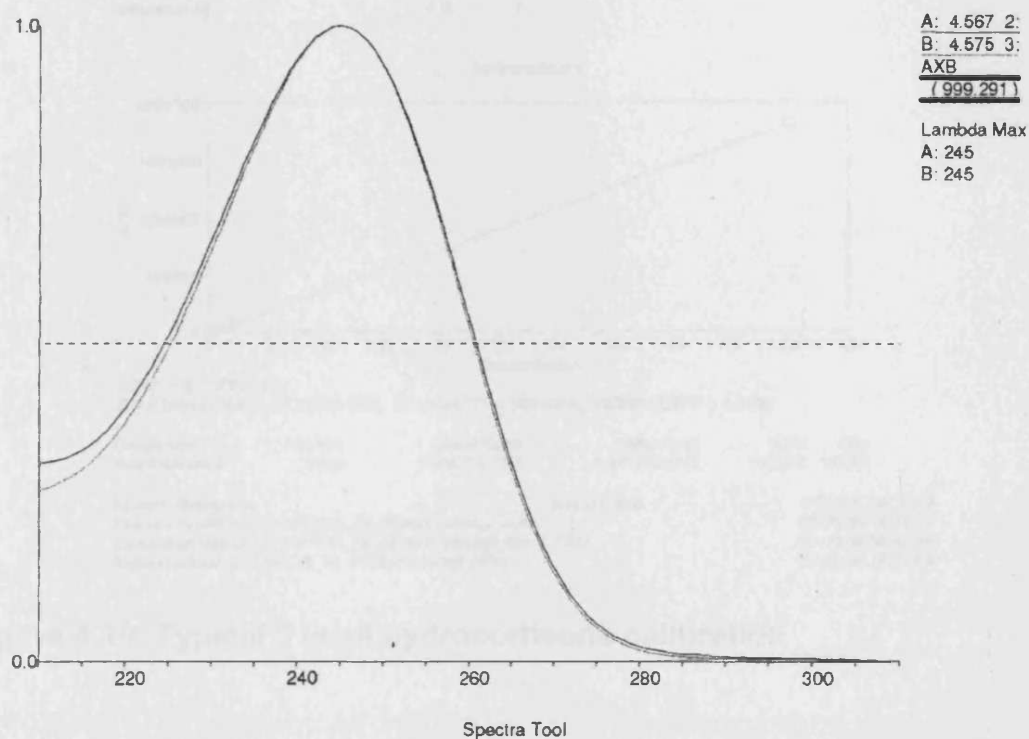


Figure 4.9 Spectral comparison (48 h receptor phase sample versus standard solution)

Five and six level linear calibration plots were constructed (within PC1000) using HC standard solutions prepared in EPBS. The calibration concentration ranges for the five and six level calibrations were 0.08 to 50 and 0.08 to 150 $\mu\text{g/ml}$, respectively. Sample concentrations above 50 $\mu\text{g/ml}$ were processed using the 6 level calibration, and no sample fell above the highest calibration point. An example 5 level calibration (Figure 4.10) and a chromatogram (Figure 4.11, 19 hour sample cell 1) are shown below. Calibration plot correlation coefficients, r , were always 1.0000 and the software calculated reliability values $\geq 99.999\%$.

Mode: Reprocessed Data
 Original Results: C:\TSP\DG_15_05\Data\Standards1.RES
 Reprocessed Results: C:\TSP\DG_15_05\Data\Standards1.RMS

Page 1

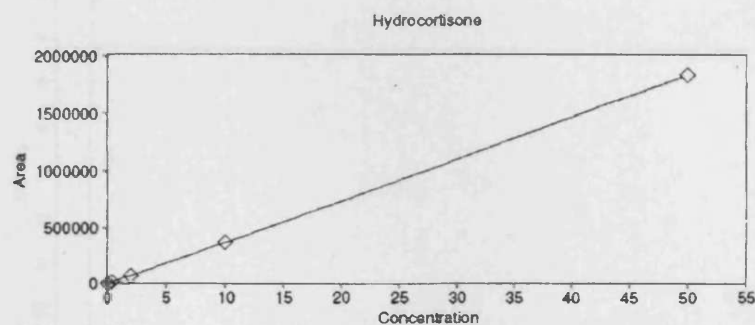
Reported On: 28-06-05 08:52:34

Calibration Report

Calculation Type: External Standard (Area)
 Number of Calibration Levels: 5
 Fit Type: Linear Fit
 Weighting: None

Signal 1: UV3000/FOCUS/SM5000 A 245 nm

Vial Name	Vial	Injections
Calibration 01	A11	1
Calibration 02	A12	1
Calibration 03	A13	1
Calibration 04	A14	1
Calibration 05	A15	1



AREA = B * CONC + C

B = 3.6601e+004, C = 5.3576e+002, RELIABILITY = 100.000%, CORR COEFF = 1.0000

Component	RT(min)	Linear Coeff	Const Coeff	%Rel	Corr
Hydrocortisone	4.620	3.66012e+004	5.35763e+002	100.000	1.0000

System: Reprocess

Analyst: dmg

PC1000 Ver 3.0.3

Acquisition Method: C:\TSP\DG_15_05\Methods\dg2.AQM

27-06-05 16:24:10

Calculation Method: C:\TSP\DG_15_05\Methods\dg2_5level.CAM

28-06-05 08:52:04

Report Method: C:\TSP\DG_15_05\Methods\dg2.RPM

27-06-05 12:17:08

Figure 4.10 Typical 5 level hydrocortisone calibration

Two 48 hour receptor phase samples (cell 6 pre-treated with 2-F1 in ethanol and cell 21 pre-treated with 4-F2 batch 2 in PG) were spiked with known concentrations of HC (25 µg/ml). Both unspiked and spiked samples were analysed and spike recoveries calculated. Recoveries were 101.5 and 101.0%, respectively.

Mode: Reprocessed Data
 Original Results: C:\TSP\DG_15_05\Data\19h_samples1.RES
 Reprocessed Results: C:\TSP\DG_15_05\Data\19h_samples1.RMS

Page 1
 Reported On: 30-06-05 09:47:33

Analysis Report

Name: Cell 1
 Type: Sample
 Injection Volume: 20.0 uL

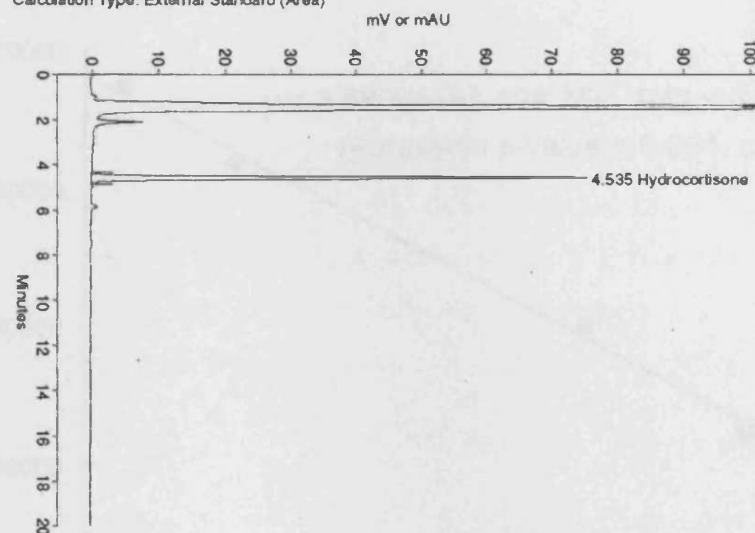
Vial: B01

Injection: 1 of 1
 Injected On: 29-06-05 12:08:19

Acquisition Log

Column Pressure (PSI): 933 Column Temperature (C): 26 Pump Flow Stability: N/A
 Noise (microAU): 8e+001 Drift (microAU/min): -8e+001
 Run-Time Messages: None

Signal 1: UV3000/FOCUS/SM5000 A 245 nm
 Calculation Type: External Standard (Area)



Component	RT(min)	Area	Height	ug/ml	Peak Type
Hydrocortisone	4.535	607225	75572	17.095	Modified
Totals		607225	75572	17.095	

System: Reprocess Analyst: dmg PC1000 Ver 3.0.3
 Acquisition Method: C:\TSP\DG_15_05\Methods\dg2.AQM 27-06-05 16:24:10
 Calculation Method: C:\TSP\DG_15_05\Methods\dg2_5level.CAM 29-06-05 13:22:48
 Report Method: C:\TSP\DG_15_05\Methods\dg2.RPM 27-06-05 12:17:08

Figure 4.11 Example chromatogram (19 h receptor phase sample, cell 1)

Some instability of HC was observed at room temperature and, to a more limited degree, for frozen samples. For samples of standard solutions that remained at room temperature (26-28°C during the period of analysis), a degradation peak was observed at ~3.8 minutes, and the increasing area of this peak accounted for the majority of the observed decrease in the HC peak. Spectral comparison (210 to 310 nm) of the HC and degradation peaks produced a correlation value of 998.7, indicating that the UV absorbing moiety was essentially the same. This degradation peak was itself unstable over prolonged periods leading to a reduction in the combined peak area.

Repeated analysis of a 10 µg/ml standard solution (at room temperature) over a period of 36 hours showed an apparently linear ($r^2=0.997$) decrease in HC peak area (Figure 4.12). The longest period of time that any samples were in the autosampler prior to analysis was 15 hours, and this time was minimised wherever possible. The 10 µg/ml solution of HC would have degraded by ~3.4% over that period of time.

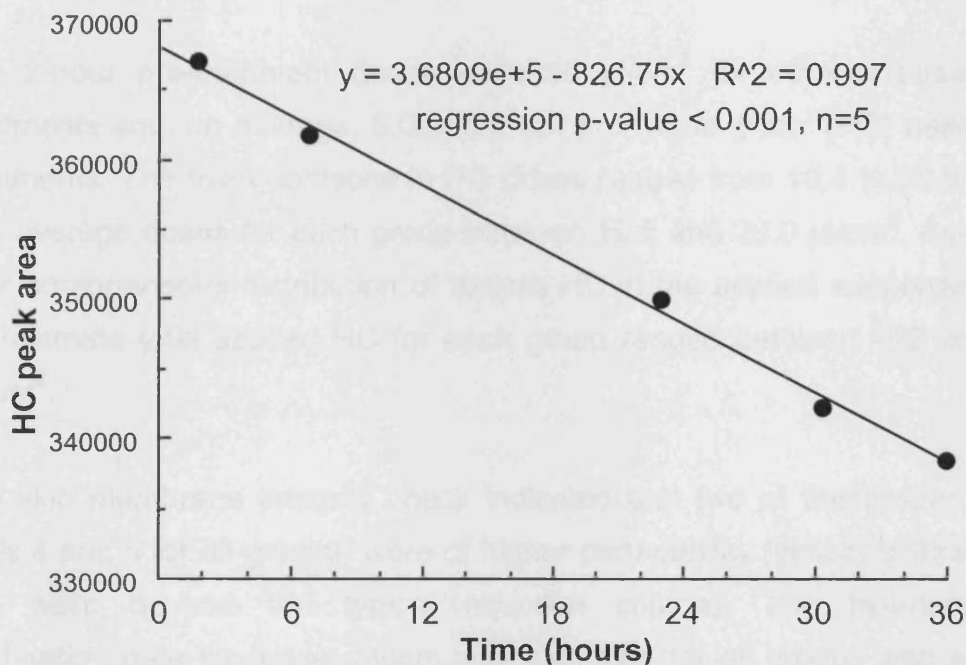


Figure 4.12 Decrease in hydrocortisone peak area for a 10 µg/ml solution in EPBS stored at 25-27°C

The observed degradation of standard solutions frozen immediately after preparation, defrosted and vortexed at room temperature prior to analysis was lower, at 3.5% after 3 days. The inter-day variability, assessed using defrosted standard solutions, was reasonable, with a variation of 1.95% RSD (using the 6 level calibration gradients, $n=3$). Samples from the skin permeation study were analysed within 2-6 days, again limiting degradation.

In the light of the large differences in the permeation of HC for the different groups assessed, the effect of HC degradation in the autosampler (room temperature), the receptor phase itself (37°C), and the freeze-thaw cycle were considered to be of minor significance.

4.3.4 Results and discussion

Data are expressed as the mean \pm standard error (SE) amount ($\mu\text{g}/\text{cm}^2$) hydrocortisone and % of the applied dose, assuming homogeneous distribution of excess HC in the applied suspension. Statistical comparisons were performed using single factor ANOVA in Microsoft Excel Version X (Mac OS X).

The 2-hour pre-treatment doses were $50 \mu\text{l}/\text{cm}^2$ for ethanol based pre-treatments and, on average, $5.0 \mu\text{l}/\text{cm}^2$ for propylene glycol (PG) based pre-treatments. The hydrocortisone in PG doses ranged from 18.4 to $20.0 \mu\text{l}/\text{cm}^2$ with average doses for each group between 19.5 and $20.0 \mu\text{l}/\text{cm}^2$. Assuming near homogeneous distribution of excess HC in the applied suspension, the approximate total applied HC for each group ranged between 412 and $421 \mu\text{g}/\text{cm}^2$.

The skin membrane integrity check indicated that two of the tissue donors (cells 4 and 5 for all groups) were of higher permeability (including three cells that were beyond the typical rejection criteria). The hydrocortisone permeation data for these donors was also high for all groups with a much shorter lag time than for the other two donors. Therefore, data have been presented both for all cells ($n=5$ per group), and following exclusion of the two higher permeability donors ($n=3$ per group). Complete rejection of all data from these donors was not considered valid, as 9 of the 12 cells appeared to have effectively normal water permeability.

The permeation of HC through the human skin membranes, and into the receptor phases, is shown in Figures 4.13 ($n=5$ per group) and 4.14 ($n=3$ per group). For both sets of data, substantial enhancement of HC permeation was observed for all retarder pre-treated cells.

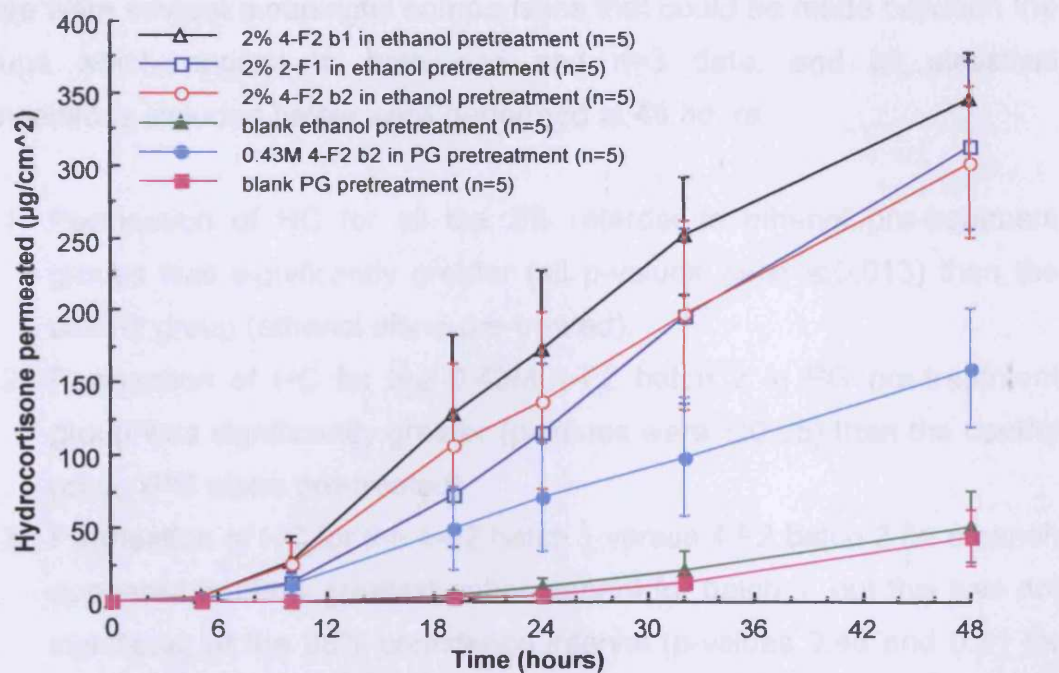


Figure 4.13 Permeation ($\mu\text{g}/\text{cm}^2$, mean \pm SE) of HC through human skin membranes from a saturated solution in PG – all donors

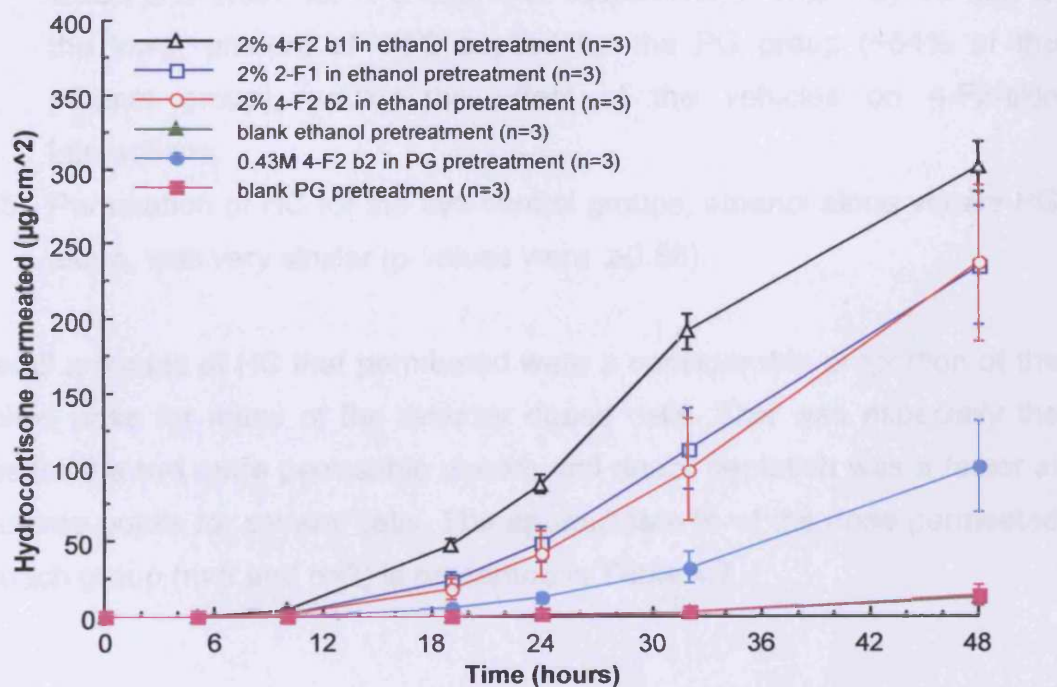


Figure 4.14 Permeation ($\mu\text{g}/\text{cm}^2$, mean \pm SE) of HC through human skin membranes from a saturated solution in PG – two donors excluded

There were several meaningful comparisons that could be made between the groups which applied to both n=5 and n=3 data, and all statistical comparisons included below were performed at 48 hours:

1. Permeation of HC for all the 2% retarder in ethanol pre-treatment groups was significantly greater (all p-values were ≤ 0.013) than the control group (ethanol alone pre-treated).
2. Permeation of HC for the 0.43M 4-F2 batch 2 in PG pre-treatment group was significantly greater (p-values were ≤ 0.05) than the control group (PG alone pre-treated).
3. Permeation of HC for the 4-F2 batch 1 versus 4-F2 batch 2 (in ethanol) appeared to show greatest enhancement for batch 1, but this was not significant at the 95% confidence interval (p-values 0.48 and 0.31 for n=5 and n=3, respectively).
4. Permeation of HC for 4-F2 batch 2 in ethanol versus 4-F2 in PG showed greater enhancement for the ethanol vehicle (p-values were 0.065 and 0.087 for n=5 and n=3, respectively). This may be due to the lower amount of 4-F2 applied for the PG group (~54% of the ethanol group), and/or the effect of the vehicles on 4-F2/skin interactions.
5. Permeation of HC for the two control groups, ethanol alone versus PG alone, was very similar (p-values were ≥ 0.86).

Overall amounts of HC that permeated were a considerable proportion of the applied dose for many of the retarder dosed cells. This was especially the case for the two more permeable donors and donor depletion was a factor at later time-points for several cells. The approximate % of the dose permeated for each group (n=5 and n=3) is presented in Table 4.7.

Table 4.7 Permeation of HC at 48 hours (% applied dose assuming homogeneous distribution of excess HC, mean \pm SE)

Pre-treatment group	48h ~% permeated (n=3)	48h ~% permeated (n=5)
4-F2 batch 1/ethanol	71.6 \pm 4.1	83.0 \pm 7.5
2-F1/ethanol	56.2 \pm 9.6	76.9 \pm 14.0
4-F2 batch 2/ethanol	56.3 \pm 12.4	71.9 \pm 12.4
Ethanol control	2.86 \pm 0.41	12.6 \pm 6.0
4-F2 batch 2/PG	23.8 \pm 7.3	38.2 \pm 9.7
PG control	3.22 \pm 1.63	10.7 \pm 4.7

If it was assumed that there were no changes in vehicle volume or constituents over the experimental period, then the excess HC (included in the donor vehicle) would have been consumed after ~49% of the applied HC had been absorbed by the skin. After that point the vehicle would no longer be saturated and donor depletion would have become an issue. However, donor phase volume was visually inspected at various time-points, and it was noticed that the volume increased, reaching ~ double the applied volume at 48 hours. Due to the hygroscopic nature of PG, it is likely that the additional volume was due to water absorption from the skin. This gradual absorption of water by the donor phase would have reduced the solubility of HC in the vehicle such that depletion may not have been an issue for most cells.

The skin permeation of HC from a saturated solution in PG was much greater than that from a saturated solution in water (Brain et al, 1996). For example, the average permeation for the ethanol pre-treated control group was $0.62 \pm 0.15 \mu\text{g}/\text{cm}^2$, and this compares to 51.4 ± 24.6 (n=5) and 12.1 ± 1.7 (n=3) $\mu\text{g}/\text{cm}^2$ for the current study. Bendas et al (1995), during investigations into binary solvent mixtures (water/PG), concluded that the enhancement effect of PG on HC permeation was one of solvent drag. Large enhancement of estradiol permeation from a 100% PG vehicle (100-fold increase in flux compared to that from saturated water) was observed by Megrab et al (1995). They investigated PG uptake from PG/water mixtures into fully hydrated stratum corneum and found a drop in water content (w/w) that was mirrored by an increase in PG content (w/w). However, when the values were recalculated as mmol/mg dry stratum corneum they discovered that the

overall number of solvent molecules in the stratum corneum with pure PG was reduced 6-fold compared to pure water. It was believed that water content affects packing of the polar head groups in the lipid bilayers and the hydrophilic PG with two hydroxyl groups might interact with these head groups in a similar fashion. They concluded that despite probably dehydrating the skin and decreasing drug diffusivity (due to tighter packing of the lipid bilayers), the large increase in estradiol skin solubility due to the presence of PG allows enhancement of flux. It was therefore not unexpected that the retarders did not behave the same in PG.

Fuhrman et al (1997), in an inter-species comparison of the effect of various enhancers on the permeation of HC, used the same pre-treatment doses as above for the PG vehicle pre-treatment groups, but for a 1 h pre-treatment time. Although the applied volumes ($20 \mu\text{l}/\text{cm}^2$) for the HC in PG doses were the same as used here, the excess HC included was not quantified/disclosed. A single human donor was used (cadaver, 56 years, thigh), and no integrity check was performed. Permeation was monitored (at undisclosed time-points) up to only 24 hours. No permeation plots were shown, only receptor phase concentrations at 24 h and calculated permeability coefficients. The cell dimensions were used to calculate values for comparison with data produced in this chapter. The control group receptor phase concentrations at 24h were $50 \pm 13 \mu\text{g}/\text{cm}^2$ (mean \pm SD, $n=5$), and the highest enhanced group (DMEA, N-dodecyl-N-(2-methoxyethyl)acetamide) was $670 \pm 90 \mu\text{g}/\text{cm}^2$ (enhancement ratio 13.4). These values were much greater than those observed here using abdominal and breast tissue from elective surgery. Equivalent values at 24 h for the PG pre-treated control group were 4.97 ± 2.48 ($n=5$) and 1.02 ± 0.47 ($n=3$) $\mu\text{g}/\text{cm}^2$ (mean \pm SE). Corresponding values for the 0.43M 4-F2 batch 2 in PG pre-treated group were 80.0 ± 37.3 ($n=5$) and 11.9 ± 3.4 ($n=3$) $\mu\text{g}/\text{cm}^2$, producing enhancement ratios (ER) of 14.3 and 11.7 for the $n=5$ and $n=3$ data respectively, ratios that were similar to several enhancers assessed by Fuhrman et al (1997).

In a study comparing skin constructs with normal skin (human, pig and rat) for percutaneous absorption of four topical drugs (Schmook, 2001), a HC flux of

$0.023 \pm 0.007 \mu\text{g}/\text{cm}^2\cdot\text{h}$ was reported for human skin (abdominal cadaver, single donor, $n=3$). The donor solution was 1% HC in PG (10 mg/ml), dose $\sim 118\mu\text{l}/\text{cm}^2$ (unoccluded), and receptor phase 25% ethanol/PBS. No permeation profiles or further permeation data were presented, but even if a zero lag time was apparent, the maximum permeated was $\sim 1.10 \mu\text{g}/\text{cm}^2$ over 48 hours. By comparison, values at 48 h for the PG pre-treated control group in this study were 44.2 ± 19.2 ($n=5$) and 13.4 ± 7.0 ($n=3$) $\mu\text{g}/\text{cm}^2$ (mean \pm SE). One could conclude that differences might have been partially due to inter-donor variation together with the effect of PG pre-treatment and dosing with a saturated plus excess HC vehicle.

4.4 Overall conclusions

The results of the second study in this chapter indicated that there was great enhancement of hydrocortisone permeation following pre-treatment with 4-F2 (batches 1 and 2) and 2-F1.

The results of first study indicated that any modification (retardation or enhancement) of glyphosate permeation, by any of the assessed retarder compounds, was limited, and that the effect on the permeation of water ranged from none to slight enhancement.

It was necessary, therefore, to conclude that the 'retarders' examined could not be classed as generic skin permeation retarders that would reliably reduce permeation of a range of compounds applied in different vehicles. There was evidence of some retardation of DEET permeation at early time-points under certain application conditions (chapter 3). However, the remaining evidence pointed to either no effect or, for some compounds, actual enhancement of permeation. It is probable that these unexpected data were a result of the complexity of the skin barrier matrix, and the multifaceted nature of vehicle interactions with permeants and matrix components.

Further investigations into the retarders are planned but will focus on new variations of the non-cyclic (4-F2 type) molecules.

4.5 References

Bendas, B., Schmalfuß, U. and Neubert, R. (1995). Influence of propylene glycol as cosolvent on mechanisms of drug transport from hydrogels. *Int. J. Pharm.*, **116**,19-30.

Brain, K.R., Green, D.M., James, V.J., Walters, K.A., Watkinson, A.C., Allan, G. and Hammond, J. (1996). Preliminary evaluation of novel penetration retarders. In *Prediction of Percutaneous Penetration, Vol. 4B*. Brain, K.R., James, V.J. and Walters, K.A. (eds) pp. 131-132. STS publishing: Cardiff, UK.

EDETOX database; Evaluations and predictions of dermal absorption of toxic chemicals (EDETOX). EU Framework V: Quality of Life, Environment and Health Key Action Funding. Project Number: QLKA-2000-00196. www.ncl.ac.uk/edetox/index.html, accessed 210205

Eldon, S.A. and Oehme, F.W. (1992). The biological activity of glyphosate to plants and animals: a critical review. *Vet. Hum. Toxicol.* **34**, 531-43.

Fuhrman, Jr., L.C., Michniak, B.B., Behl, C.R. and Malick, A.W. (1997). Effect of novel penetration enhancers on the transdermal delivery of hydrocortisone: an in vitro species comparison. *J. Control. Rel.* **45**, 199-206.

Lullmann, H., Mohr, K., Ziegler, A. and Biegler, D. (2000). *Color Atlas of Pharmacology*, 2nd Edition. Georg Thieme Verlag, Stuttgart, Germany. ISBN 3-13-781702-1 (GTV).

Malik J., Barry G. and Kishore G (1989). The herbicide glyphosate. *Biofactors* **2**, 17-25.

Merck Index XIII Edition. *The Merck Index: An Encyclopedia of Chemicals, Drugs, and Biologicals*, 13th Edition (2001). O'Neil, M.J. (Senior Editor). ISBN: 0-911910-13-1. Merck and Co. Inc., Whitehouse Station, NJ, USA.

Megrab, N.A., Williams, A.C. and Barry, B.W. (1995). Oestradiol permeation through human skin and silastic membrane: effects of propylene glycol and supersaturation. *J. Contr. Rel.* **36**, 277-294.

Schmook, F.P., Meingassner, J.G. and Billich, A. (2001). Comparison of human skin or epidermis models with human and animal skin in in-vitro percutaneous absorption. *Int. J. Pharm.* **215**, 51-56

U.S. EPA (1993). Re-registration eligibility decision (RED) document for glyphosate. EPA-738-F-93-011, Washington, DC.

WHO (1994). *Environmental Health Criteria*, 159. Glyphosate. 177P. WHO: Geneva, Switzerland. ISBN 92-4-157159-4:177.

Wester R.C., Melendres J, Sarason R, McMaster J, Maibach H.I. (1991). Glyphosate skin binding, absorption, residual tissue distribution and skin decontamination. *Fundam. Appl. Toxicol.* **16**, 725-32.

Wester R.C., Quan, D. and Maibach H.I. (1996). *In Vitro* percutaneous absorption of model compounds glyphosate and malathion from cotton fabric into and through human skin. *Food and Chem. Toxicol.* **34**, 731-735.

Chapter 5

Investigation of skin surface sampling techniques

5.1 Introduction

Skin surface sampling can be performed both *in vivo* and *in vitro*, and is usually performed by tape stripping the skin surface. This process involves sequential application of adhesive tape to and removal from the skin surface, gradually removing the stratum corneum (Pinkus, 1951 through Tsai, 1991b). The stratum corneum *in vivo* can be removed entirely after 100-120 consecutive strips with sellotape (Ohman and Vahlquist, 1994). A technique used solely *in vivo*, that is approximately 10 times more efficient than tape stripping (Ohman and Vahlquist, 1994), involves the removal of skin surface biopsies (SSB), using cyanoacrylate glue, and this will be discussed later (section 5.5).

Tape stripping is a relatively non-invasive procedure that has been used *in vivo* to measure levels of topically applied compounds (for example, corticosteroids) in the upper layers of the skin at specific time-points. These measurements can provide data regarding chemical penetration into skin, chemical permeation through the skin, chemical elimination from the skin, pharmacodynamic parameters and clinical parameters (Surber et al, 1999).

Whilst it is generally recognised that the amount of tissue removed changes with each consecutive strip, drug concentrations in the tape strips have been used to estimate total skin absorption (Depuis et al, 1984). A skin blanching bioassay also correlated reasonably well with measured levels of betamethasone dipropionate in tape strips (Pershing, 1992). The FDA/AAPS (Shah et al, 1998) provided guidance on how tape stripping studies might be used to provide evidence of bioequivalence of topical dermatological dosage forms. However, this approach was later abandoned due to the variability of tape stripping methods and lack of appropriate validation.

Tape stripping data performed *in vitro* is often included in studies for risk assessment purposes, enabling calculation of permeant levels in the stratum corneum. There is some disagreement as to whether all material taken up into the SC actually reaches the systemic compartment. Due to the continual turnover and shedding (desquamation) of the stratum corneum, one regulatory body, the Scientific Committee on Cosmetic Products and Non-Food Products Intended For Consumers (SCCNFP), does not consider levels in the SC tape strips to be ultimately absorbed (SCCNFP, 2003). Further uses of tape stripping include assessment of drug concentration gradients in the skin when comparing formulated products during development stages, and measurement of drug levels for topically active compounds such as retinoids. However the removal of stratum corneum in tape strips must be both substantial and reproducible for this to be of real value.

Whilst many researchers have published tape stripping data, there is no generally agreed standardised tape or method. Several Client studies performed in our laboratory (data not in public domain) used 3M Magic Tape. However, the introduction of D-Squame skin surface sampling discs, (CuDerm Corporation, Dallas, USA) which were specifically designed for tape stripping (to quantify levels of scaliness) meant comparison of their performance with that of the 3M Magic Tape was appropriate. D-Squame uses a fully cured medical grade synthetic polyacrylate ester adhesive on a high clarity polymeric film, and the pre-cut discs are easy to handle.

3M Magic Tape was assessed by Tsai et al (1991a) in a study of three tapes produced by 3M Company, cellulose backed No. 810 (Magic Tape), polyester backed No. 850, and polypropylene backed No. 845. Type 810 and 845 were similarly good at removing stratum corneum from skin (hairless mouse) prior to mounting in diffusion cells, measured by increases in transepidermal water loss (TEWL), following incremental removal of strips. In contrast, tape No. 850 removed virtually no stratum corneum. The measurement of weight of tissue removed was not possible for 3M Magic Tape due to its reported hygroscopicity, as strips were allowed to dry for several days prior to weighing. A subsequent experiment, using tapes 810 and 845, stripped

hairless mouse skin 2, 12 and 24 hours after dosing with a minoxidil solution (dose $71 \mu\text{l}/\text{cm}^2$). This showed poor stripping performance for both tapes at 12 and 24 hours. Strips 1 and 2 removed large amounts of tissue/radiolabel at those time-points, but then further stripping had little benefit. The reason for this was investigated in a subsequent study (Tsai, 1991b), where a solvent mixture of 20/60/20 (v/v/v) propylene glycol/ethanol/water was shown to have a great effect on the efficiency of harvesting stratum corneum by tape No. 845. The longer the contact time, the greater the weight of tissue removed, with strips 1 and 2 removing the entire stratum corneum and epidermis for some cells (> 12 hours), indicating a great reduction in cohesiveness of the dermo-epidermal junction, a recognised weak point in the skin structure (Tregear, 1966 in Tsai et al, 1991b). The dose applied ($71 \mu\text{l}/\text{cm}^2$), was high, compared to the standard finite dose of $5 \text{ mg}/\text{cm}^2$ used for most *in vitro* tape stripping studies, and this may have been a factor in the efficiency of tape stripping at later time-points. The effect on human skin, which is structurally different, may also be much less marked.

A more recent study (Henn et al, 1993) attempted to measure the quantity of tissue removed by D-Squame discs using Lowry protein determination. Unfortunately, the assay suffered from interference from components of D-Squame and, although the determination did work for a cellulose tape (Cellux), there was a reported lack of sensitivity (5 sections of tape were required per determination). Weight of tissue removed was compared for human and hairless mouse skin *in vivo* (n=10), and showed good performance for D-Squame. Both tapes removed significantly greater amounts of tissue for hairless mouse skin compared to human, confirming the structural differences for mouse skin.

Dreher et al (2005) have examined 5 mm diameter sections of D-Squame discs using an adapted Lowry assay in 96-well plates. A benefit of this technique would be to allow the removal of a small section of each strip for protein assay, and the remaining disc could be extracted for active. However, they concluded that the analysed sections were not predictive of the entire

strip i.e. removal of SC by D-Squame is not homogeneous (Dreher et al, 2005).

Work by Weigmann et al (2003, 2005) indicated that a visible wavelength spectroscopic method could be used to determine the amount of SC removed. Absorbance in the visible range allowed determination of the absolute mass of corneocyte aggregates on the strips removed, and identical results were achieved in two institutions performing clinical investigations (Weigmann et al, 2003).

The published assessments of tape stripping above showed that there was no simple, single method to determine tape stripping efficiency. Therefore, conditions that are considered important when tape stripping in our laboratory were used to compare D-Squame with Magic Tape. Additionally, it is often important that *in vitro* stripping data is a meaningful reflection of that expected *in vivo*. Therefore, a comparison between *in vitro* tape stripping using D-Squame, and a published *in vivo* study, using clobetasol propionate 0.05% cream was performed.

5.2 Comparison of stripping efficiency for 3M Magic Tape and D-Squame

5.2.1 Introduction

The efficiency and reproducibility of stratum corneum removal by adhesive tapes is likely to be affected by several factors, including skin hydration and surface condition (including the presence of applied formulations or residual wash solvent), method of strip application and removal (including variability due to operator differences). Following initial use of D-Squame to strip skin samples following 24 hours exposure to a topical formulation, it was noted that removal of stratum corneum may have been more efficient compared to the previously used 3M Magic Tape. It was believed that the D-Squame tape

might have been less affected by either the presence of small amounts of residual formulation, or an increase in skin hydration.

In order to investigate possible differences in stripping efficiency between the two tapes, the effect of tape stripping (10 strips) the skin surface on the permeation of tritiated water was assessed. In this first section of the study, cells were either stripped with 3M Magic Tape or D-Squame discs or left unstripped (controls) prior to mounting in diffusion cells and measuring water permeation. For the second section of the study, skin samples were mounted in diffusion cells for 24 hours prior to stripping, cell re-assembly and measurement of water permeation. This was to replicate the typical study exposure period of 24 hours prior to stripping, and enabled hydration and/or potential changes in the stratum corneum cohesiveness to be modelled.

The permeation of water through human skin and its measurement are discussed in some detail in Chapters 3, 4 and 7. Removal of 10 stratum corneum tape strips would be expected to increase water permeability due to the reduction in skin barrier function caused by the surface 'damage'. Ten strips would not be expected to remove the entire stratum corneum under normal conditions.

5.2.2 Materials and equipment

Tritiated water ($^3\text{H}_2\text{O}$) was obtained from Amersham International (Little Chalfont, UK) and diluted with distilled water to a specific activity of 2 $\mu\text{Ci/ml}$. Water was distilled in all glass apparatus and solvents and buffer salts were of AnalaR grade or better (BDH). OptiPhase 'HiSafe' 3 liquid scintillation cocktail and OptiSolve tissue solubiliser were from Wallac. Radioactive samples were dispersed in 3 ml scintillation cocktail (HiSafe 3, Wallac) using disposable 6 ml diffuse plastic scintillation vials (Zinser Analytic) and counted for radioactivity using a Wallac 1409 liquid scintillation counter (see section 4.2.1).

D-Squame skin sampling discs were purchased directly from CuDerm Corporation (Dallas, USA) and 3M Magic Tape from Viking Direct Ltd (Leicester, UK).

5.2.3 Methods

5.2.3.1 Receptor phase preparation

Phosphate buffered saline (pH 7.4; PBS) was prepared as described previously (section 3.2.2.1).

5.2.3.2 Donor solution activity

Four 50 μ l samples of the donor solution ($\sim 2 \mu\text{Ci/ml } ^3\text{H}_2\text{O}$) were analysed by liquid scintillation counting (LSC) which indicated homogeneous distribution of the radiolabel, with a mean DPM/ μ l of 4564 (0.76%RSD).

5.2.3.3 Skin preparation and diffusion cells

Human abdominal skin, obtained during autopsy, was stored at -20°C and prepared as detailed in section 4.2.2.3. Nine different donors were prepared and distributed throughout the test groups. Details of the diffusion cells used can be found in section 4.2.2.4.

5.2.3.4 Group allocation and skin treatment

A total of six groups ($n=5$) were prepared. Three groups were allocated for immediate treatment, and three groups for 24 hours hydration in diffusion cells prior to treatment. The treatment process is outlined in Table 5.1. For skin samples requiring stripping, the diffusional area was stripped 10 times with either D-Squame or 3M Magic Tape. Tape was applied to the skin surface and pressed with a thumb, using moderate pressure, prior to rapid

removal (with the aid of forceps for D-Squame). A single operator stripped all cells and consistent technique was used throughout.

Table 5.1 Group allocation and skin treatment (5 replicates per group)

Group	Treatment prior to mounting skin in diffusion cells	Procedure at 0 hours	Treatment at 24 hours	Procedure at 24 hours
1	None, controls A (C-A)	Measure water permeation	None, end of experiment	N/A
2	3M Magic Tape stripped (MT-A)	Measure water permeation	None, end of experiment	N/A
3	D-Squame stripped (DS-A)	Measure water permeation	None, end of experiment	N/A
4	None	hydration for 24 hours	None, controls B (C-B)	Measure water permeation
5	None	hydration for 24 hours	3M Magic Tape stripped (MT-B)	Measure water permeation
6	None	hydration for 24 hours	D-Squame stripped (DS-B)	Measure water permeation

5.2.3.5 Measurement of water permeation

All cells (groups 1 to 6) received an infinite dose of 500 μ l tritiated water, applied using a digital pipette, at the appropriate time (either $t=0$ or $t=24$ hours). For each cell, the exact time of application was noted and that time represented zero time for that cell. The diffusion cell donor chambers were occluded using tightly fitting plastic vial caps, to limit evaporation of the tritiated water.

200 μ l samples were taken (using a digital pipette) from each receptor chamber 1, 2, 3, 4, and 24 hours after dosing. Each sample was placed directly into scintillation fluid and analysed for ^3H by LSC. The liquid removed by each sample was replaced with fresh temperature equilibrated blank receptor medium.

5.2.4 Results and discussion

Data are expressed as the mean \pm standard error (SE) amount (mg/cm^2) permeated. Statistical comparisons were performed using single factor ANOVA in Microsoft Excel Version X (Mac OS X). One cell (Group 5, 24 h hydration, 3M Magic Tape stripped) was rejected as it showed very high water permeation due to severe damage during stripping. This can occasionally occur for cells that are stripped after removal from diffusion cells, and could be the result of sideways pressure accidentally applied to the skin surface.

The permeation of water for the control groups (with and without 24 hours hydration) was very similar (Figure 5.1), which indicated that, as might be expected, the 24 hour hydration period had little effect on water permeability.

The permeation of water for the groups with no hydration period is shown in Figure 5.2, and large differences in stripping efficiency were apparent. For skin that was immediately stripped (no hydration period), 3M Magic Tape caused significant, but very variable, reduction in barrier function. The water permeation rate started to decrease at some point beyond 4 hours (possibly due to depletion of the applied dose) and comparison to the control group indicated a 30-fold increase in water permeation at 4 hours, reducing to 8-fold by 24 hours. Statistical comparison showed that, despite the apparent large increase in water permeation for the 3M Magic Tape group, permeation was not significantly greater than the control, at the 95% confidence interval, until the 24 hour time-point (p-value 0.046, 0.12 to 0.18 at earlier time-points) due to the high variability. In contrast, D-Squame only roughly doubled water permeation compared to the control, but in a more reproducible manner, with the increase varying between 2 and 3-fold at all time-points assessed. Statistical analysis versus control showed, perhaps surprisingly, lower p-values between 1 and 4 hours (p-values 0.065 to 0.13), than for 3M Magic Tape versus control. At 24 hours, the comparison for D-Squame produced a p-value of 0.14, indicating that permeation was not significantly greater than control, at the 95% confidence interval.

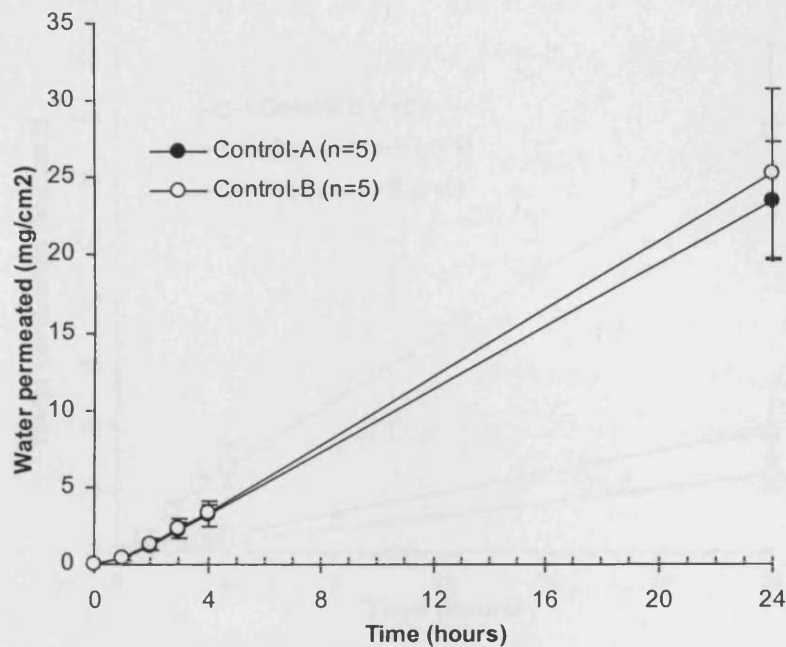


Figure 5.1 Water permeation for control groups (A = no hydration period, B= 24 hour hydration period)

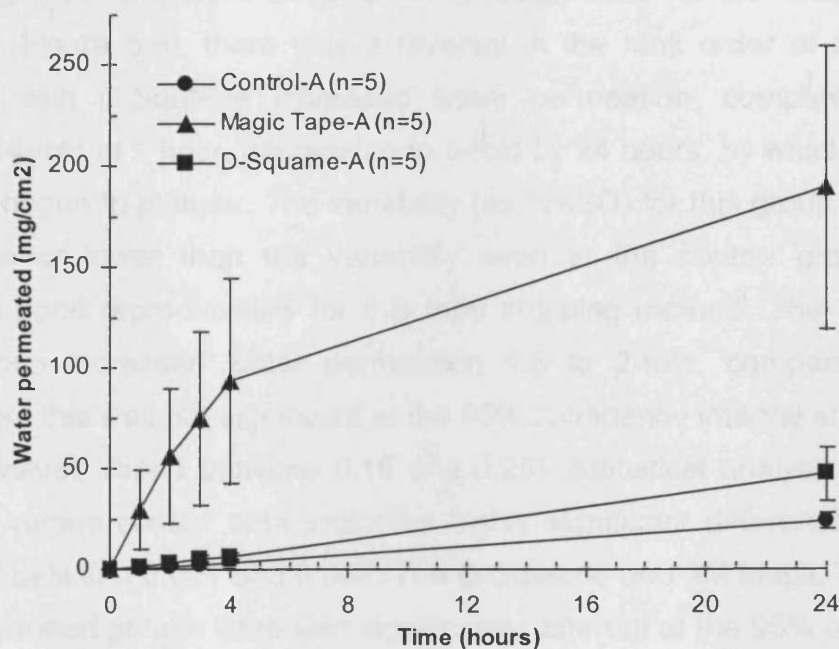


Figure 5.2 Water permeation for all groups with no hydration period

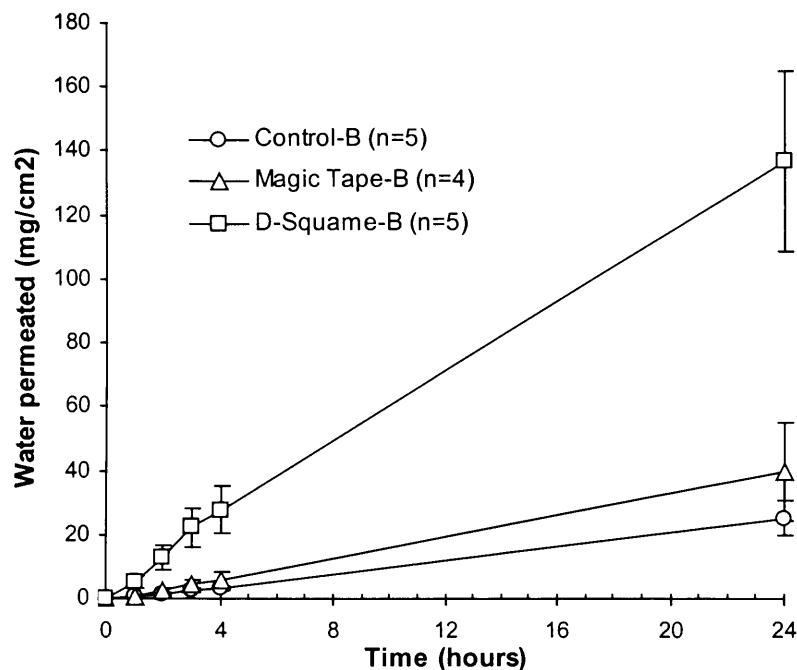


Figure 5.3 Water permeation for all groups with a 24 hour hydration period

For the groups that were mounted in diffusion cells for 24 hours prior to stripping (Figure 5.3), there was a reversal in the rank order of the tapes. Stripping with D-Squame increased water permeation, compared to the control, 14-fold at 1 hour, decreasing to 5-fold by 24 hours, by which point the rate had begun to plateau. The variability (as %RSD) for this group appeared the same or lower than the variability seen in the control group which indicated good reproducibility for this tape stripping method. The 3M Magic Tape group increased water permeation 1.6 to 2-fold, compared to the control, but this was not significant at the 95% confidence interval at any time-point (p-values varied between 0.16 and 0.25). Statistical analysis of the D-Squame versus control data indicated highly significant differences with p-values of between 0.001 and 0.007. The D-Squame and 3M Magic Tape data for the hydrated groups were also significantly different at the 95% confidence interval at all time-points.

Water permeability coefficients were calculated for all cells but, given the identical dose for all cells, comparisons were identical to those above. However, for reference, the control groups ranged between 0.4 and 1.0×10^{-3}

cm/h (at 1 and 24 hours, respectively), and these were in the normal range for water permeability coefficients (Bronaugh et al, 1986).

In conclusion, D-Squame was significantly better than 3M Magic Tape for tape stripping skin membranes that had been mounted in diffusion cells for 24 hours, and the results indicated good removal of SC for D-Squame, with relatively little variability. As all *in vitro* tape stripping in our laboratory is performed at 24 or 48 hours, D-Squame immediately became the sole tape used. Comparison of D-Squame stripping *in vitro* with published data for *in vivo* stripping was considered the next important investigation.

5.3 Tape stripping following application of a clobetasol propionate formulation

5.3.1 Introduction

Weigmann et al. (1999) measured clobetasol propionate levels in stratum corneum tape strips using TESA film type 5529 (Beiersdorf AG, Hamburg, Germany) following application of three formulations (0.05% active). This *in vivo* study was performed on 6 healthy volunteers (23 to 29 years of age), and analysis was by HPLC. This study appeared suitable for comparison with those obtainable *in vitro* using D-Squame discs. The formulations assessed included Temovate Cream, 0.05% (Glaxo Wellcome Inc., USA) and it is believed that this is the same as the product that is marketed in the UK as Dermovate Cream, 0.05%, with an identical list of excipients.

Clobetasol propionate (CAS No. 25122-46-7, Figure 5.4) is a potent synthetic corticosteroid (see section 4.3.1), with a M_w of 466.97 and a m.p. of 197.5-199°C. It was supplied as a white powder with a yellow cast (Sigma-Aldrich, UK).

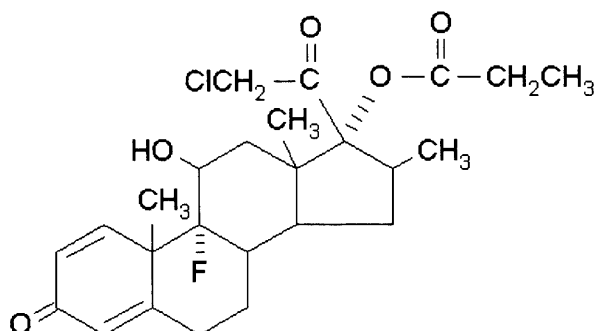


Figure 5.4 Structure of clobetasol propionate (Sigma-Aldrich)

5.3.2 Materials and equipment

Water was distilled in all glass apparatus and solvents and buffer salts were of AnalaR grade or better (BDH). HPLC solvents were of HiPerSolv grade (BDH), including acetonitrile of far-UV grade. D-Squame skin sampling discs were purchased directly from CuDerm Corporation (Dallas, USA). Clobetasol propionate (purity 98.6%) was from Sigma and Dermovate cream (0.05% clobetasol propionate, lot C008231, Glaxo) from a local pharmacy. Weight measurements were made on a Sartorius BP211D analytical balance. Sample preparation was performed using the following; Vortex Genie 2 vortexer (Scientific Industries, USA), Ultrawave U300H ultrasonic bath (Ultrawave, Cardiff, UK), Stuart Scientific Gyro-Rocker (Fisher, UK), and Eppendorf 5415C centrifuge.

5.3.3 Analytical method development and validation

Due to the frequent problem of interference with the assay during tape strip analysis by HPLC, due either to components of the strip material or skin derived peaks, it was deemed appropriate to first assess the assay described by Weigmann et al (1999) to confirm suitability for the analysis of D-Squame stripped samples.

The HPLC equipment was as described in section 3.2.2.10. A Genesis C18, 4 μm , 150x4.6mm column protected with Upchurch 0.5 μm pre-column filters

was used. Quantitation was at 240 nm, with scans 200-360nm also collected, and the injection volume was 50 μ l (Pushloop).

Initial conditions used a mobile phase (MP) consisting of 6/4 (v/v) acetonitrile/water (MP A). The retention of clobetasol propionate (CP) under these conditions was 8.8 minutes. Four D-Squame discs were used to strip my forearm and combined in a single vial prior to extraction with 500 μ l MP A (as used by Weigmann et al), with vortexing and sonication. Acetonitrile based extraction solvents have been found, in my experience, to be very efficient at extracting D-Squame discs. Analysis of this placebo extract produced a peak co-eluting with CP equivalent to 1.7 μ g/ml. However, inspection of the scan data (using Spectacle, see section 4.3.3.8) showed that the peak was not CP. Blank samples of D-Squame (containing no skin) were then extracted and analysed, which showed that the interfering peak was from the D-Squame discs. If TESA film type 5529 had been available, a sample would then have been extracted to assess for interference with our sensitive HPLC system. As that was not possible, a 2 cm length sample of 3M Magic Tape was extracted as above and analysed. No co-eluting peaks were observed, although peaks were present 1 minute either side of CP. This indicated that the problem was tape specific and that the assay required modification before D-Squame samples could be analysed.

Assay development focused on elution using a methanol/water mobile phase, and optimum separation of CP from D-Squame peaks was achieved using a gradient elution program (Table 5.2). The inclusion of an acetonitrile rinse period following CP elution allowed the most efficient removal of tape strip material remaining on the column. Mobile phase B, 7/3 (v/v) methanol/water, did not efficiently extract tape strips and, therefore, MP A was used. The retention time of CP was ~7.5 minutes.

Five level linear calibration plots (0.016 – 5 μ g/ml) were constructed (within PC1000) using CP standard solutions prepared in MP A. Calibration plot correlation coefficients, r , were always 1.0000 and the software calculated reliability values $\geq 99.999\%$. An example 5 level calibration (Figure 5.5) and a

chromatogram (Figure 5.6, extracted epidermis sample) are shown below. The limit of quantitation was 10 ng/ml and any peaks below this value were classed as a zero result. Clobetasol propionate stability in MP A was good, with 1.0% degradation (calculated from the reduction in calibration gradient) after 2 weeks.

Mode: Reprocessed Data
Original Results: C:\TSP\DG_4_00\Data\Standards1.RES
Reprocessed Results: C:\TSP\DG_4_00\Data\Standards1.RMS

Page 1

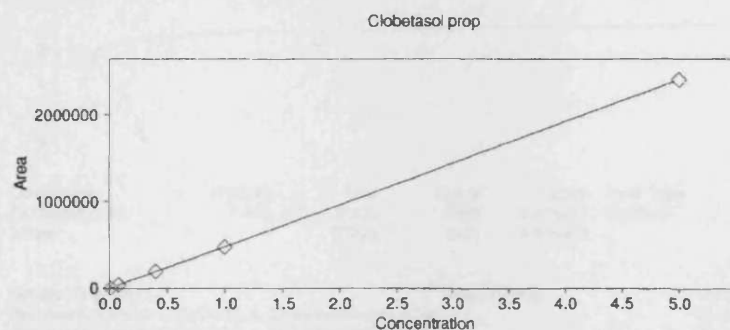
Reported On: 31-08-05 16:10:45

Calibration Report

Calculation Type: External Standard (Area)
Number of Calibration Levels: 5
Fit Type: Linear Fit
Weighting: None

Signal 1: UV6000LP A 240 nm

Vial Name	Vial	Injections
Calibration 01	A01	1
Calibration 02	A02	1
Calibration 03	A03	1
Calibration 04	A04	1
Calibration 05	A05	1



AREA = B * CONC + C
B = 4.8018e+05, C = 1.5264e+03, RELIABILITY = 99.999%, CORR COEFF = 1.0000

Component	RT(min)	Linear Coeff	Const Coeff	%Rel	Corr
Clobetasol prop	7.579	4.80180e+05	1.52644e+03	99.999	1.0000

System: Reprocess Analyst: dmg PC1000 Ver 3.5.1
Acquisition Method: C:\TSP\DG_4_00\Methods\dg2s.AQM 16-10-00 11:42:46
Calculation Method: C:\TSP\DG_4_00\Methods\dg2.CAM 08-11-00 14:08:24
Report Method: C:\TSP\DG_4_00\Methods\dg1.RPM 11-10-00 16:04:36

Figure 5.5 Typical clobetasol propionate calibration

Mode: Acquired Data
Original Results: C:\TSP\DG_4_00\Data\Epidermis1.RMS

Page 1
Reported On: 06-09-05 12:17:02

Analysis Report

Name: Cell 3
Description: epidermis
Type: Sample
Injection Volume: 50.0 μ L

Vial: C10

Injection: 1 of 1

Injected On: 18-10-00 15:54:39

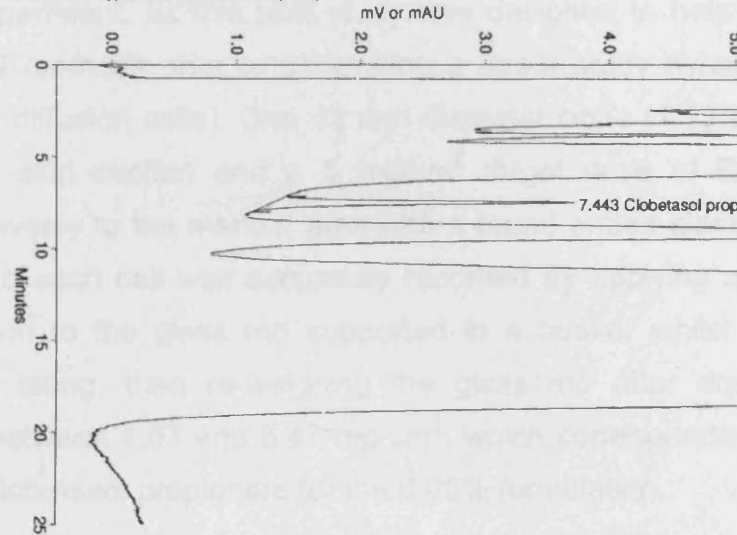
Acquisition Log
Column Pressure (PSI): 2387
Noise (microAU): 4e+01
Run-Time Messages: None

Column Temperature (C): N/A

Pump Flow Stability: 1.7

Drift (microAU/min): 2e+02

Signal 1: UV6000LP A 240 nm
Calculation Type: External Standard (Area)



Component	RT(min)	Area	Height	ug/ml	Peak Type
Clobetasol prop	7.443	37205	2421	0.074302	Modified
Totals		37205	2421	0.074302	

System: Reprocess
Acquisition Method: C:\TSP\DG_4_00\Methods\dg2g.AQM
Calculation Method: C:\TSP\DG_4_00\Methods\dg2.CAM
Report Method: C:\TSP\DG_4_00\Methods\dg1.RPM

Analyst: dmg

PC1000 Ver 3.5.1

13-10-00 16:00:14

08-11-00 14:08:24

11-10-00 16:04:36

Figure 5.6 Chromatogram of an extracted epidermis sample

Table 5.2 HPLC gradient elution program

Time (min)	% MP B (7/3 methanol/water)	% MP C (methanol)	% MP D (acetonitrile)
0	85	15	0
8	85	15	0
9	25	15	60
15	25	15	60
16	85	15	0
25	85	15	0

5.3.4 Pilot *in vitro* stripping study

5.3.4.1 Methods

Three sections (~2 x 2 cm) of skin from a single donor (female, abdominal, 50 years, surgical sample) were placed on a paper towel and each skin section labelled. Skin samples were not mounted in diffusion cells for this short time-scale experiment, as this pilot study was designed to help develop suitable analytical methods prior to performing a larger study (where skin would be dosed in diffusion cells). One 12 mm diameter circle (1.13 cm²) was marked on each skin section and a 5 mg/cm² target dose of Dermovate cream applied evenly to the marked area with a round ended glass rod. The weight applied to each cell was accurately recorded by applying a slight excess of formulation to the glass rod supported in a beaker whilst in the analytical balance, taring, then re-weighing the glass rod after dosing. The doses ranged between 4.63 and 5.47 mg/cm², which corresponded to 2.31 to 2.74 µg/cm² clobetasol propionate for the 0.05% formulation.

The following procedures were performed on a single section of skin 30, 60 and 90 minutes after dosing. The skin surface was wiped with dry cotton buds. The dosed area of the skin surface was sequentially stripped with eleven D-Squame discs. The remaining stratum corneum and epidermis was separated from the dermis (for the dosed area) using a simple heat separation technique that involved heating the skin sample, stratum corneum down, in a glass vial for 75 seconds (heat setting 5 on a Bibby B212 stirrer hotplate, hotplate surface temperature ~85°C), then removing the upper layers from the dermis using forceps. The surrounding, non-dosed, area of skin was then wiped, as Weigmann et al (1999) found significant lateral migration for some formulations. Samples were placed in glass vials and extracted with volumes of MP A (Table 5.3). Samples were shaken overnight on a gyro-rocker (Stuart Scientific), prior to vortexing and sonication (3 x 15 minutes). 200 µl samples of each extract were centrifuged (4 minutes at 10,000 rpm) prior to injection. The dermis was not analysed as only extremely

low levels of clobetasol propionate were expected to have reached the dermis in the time-scales assessed.

Table 5.3 Sample handling and extraction volumes

Compartment	Volume of MP A added (ml)
Wipe (dosed area)	3.00
Strip 1	0.50
Strips 2-11	2.00
Remaining SC and epidermis	1.00
Dermis	N/A, samples frozen
Surrounding skin wipe	1.00

5.3.4.2 Results and discussion

The recovery of applied clobetasol in each analysed compartment for each cell is presented in Table 5.4. Overall recovery for the three cells was $96 \pm 17\%$ of the applied dose. The reasons for the unexpectedly wide variations in recovery were not clear at that stage.

Table 5.4 Recovery of clobetasol propionate in each compartment, $\mu\text{g}/\text{cm}^2$ (% applied dose)

Compartment	Section 1 (30 min)	Section 2 (60 min)	Section (90 min)
Wipe (dosed area)	2.86 (117)	1.61 (69.5)	1.91 (69.8)
Strip 1	0.078 (3.19)	0.063 (2.72)	0.073 (2.65)
Strips 2-11	0.147 (6.03)	0.124 (5.35)	0.126 (4.60)
Rem. SC and epidermis	0.070 (2.87)	0.054 (2.33)	0.065 (2.40)
Dermis	*N/A	*N/A	*N/A
Surrounding skin wipe	0	0	0
Total in strips 2-11 and rem. SC and epidermis	0.195 (8.89)	0.178 (7.69)	0.191 (6.99)
Overall recovery	3.15 (129)	1.85 (79.9)	2.17 (79.5)

*N/A – not analysed

Recoveries of clobetasol propionate in strips 2-11 ranged from 4.6 to 6.0% of the applied dose, with the majority of the applied doses recovered in the surface wipes. The results of this pilot study were very different to those reported by Weigmann et al (1999), where approximately $1.80 \mu\text{g}/\text{cm}^2$ (64% of the applied dose), $1.60 \mu\text{g}/\text{cm}^2$ (57%) and $1.25 \mu\text{g}/\text{cm}^2$ (45%) was recovered in strips 2-11 at 30 minutes, 2 hours and 6 hours, respectively for Temovate cream. Rapid penetration of such significant proportions of the applied dose would generally be considered surprising for a molecule of M_w 467 Daltons and, unfortunately, the contents of the surface wipe and strip 1 were not determined in that study. The reported wiping procedure used a swab to prepare a field of 3 x 3 cm for stripping, and their data would suggest that the wipe efficiency was poor, unless very different skin penetration occurred when applied to the forearm *in vivo*. No mention was made of the application of any occlusive layer, which can greatly increase the permeation of corticosteroids, but would carry the risk of site cross-contamination. The variation in results for both of the 0.05% cream formulations assessed by Weigmann et al (1999) was not particularly large (~25%) indicating that their methods appeared reproducible for the creams. However, a 0.05% lotion was also assessed and much lower levels were found in the skin. Despite some additional migration of this formulation to surrounding (non-dosed) areas, it could be the case that the lower amounts in the skin might be due to an improved wiping efficiency for the liquid formulation. Whether the methods used by Weigmann et al (1999) allowed true quantification of drug concentrations in the stratum corneum is clearly debatable.

5.3.5 *In vivo* tape stripping following application of Dermovate and assessment of formulation variability

In order to further assess whether the results of the *in vitro* investigation described above were predictive of *in vivo* results performed under the same conditions, small *in vivo* studies were performed on the forearms of two volunteers, a colleague and myself. We had both previously been prescribed

topical corticosteroids and therefore the short term application of Dermovate was considered to be of no risk.

5.3.5.1 *In vivo* tape stripping experiment 1

In the first assessment, two 12 mm circles were marked on my right forearm (underside), 8 (active section) and 11 cm (control section) from the elbow. The active section received a 6.42 mg dose of Dermovate (2.84 $\mu\text{g}/\text{cm}^2$ clobetasol propionate). 30 minutes after dosing, both areas were wiped, tape stripped 11 times (D-Squame) then the dosed area plus an ~1 cm border wiped again with two ethanol moistened cotton buds. The wiping and stripping procedures were performed by myself, as I am left handed. The samples were extracted as described in section 5.3.4.1, except that the wipe (dosed area) was extracted with 5 ml MP A, then analysed as described in section 5.3.3.

The control samples for all analysed compartments contained small peaks that co-eluted with clobetasol propionate. The assay development was performed using D-Squame strips taken from my arm, and no interference was observed for the optimised assay. Weigmann et al (1999) found significant migration of applied active to sampling sites 2 cm from the dosed area, and this matched the site spacing used in this study. The co-eluting peaks were of too low an absorbance for spectral scans to confirm whether they were clobetasol propionate. In the absence of confirmed identity, the effect of subtraction of this interference from the active section data is presented below (Table 5.5). Recoveries of applied active in the assessed compartments were similar to those observed *in vitro* (section 5.4.3.2).

Table 5.5 Recovery of clobetasol propionate in each compartment, $\mu\text{g}/\text{cm}^2$ (% applied dose)

Compartment	Active Section, 30 min	Active minus peak in controls
Wipe (dosed area)	2.04 (71.8)	1.99 (70.2)
Strip 1	0.079 (2.77)	0.038 (1.36)
Strips 2-11	0.195 (6.85)	0.092 (3.24)
Terminal ethanol wipe	0.250 (8.79)	0.250 (8.79)*
Strips 2-11 + term. wipe	0.342 (15.6)	0.342 (12.0)*
Overall recovery	2.56 (90.2)	2.38 (83.6)

* - terminal wipe not performed for the control section

5.3.5.2 *In vivo* tape stripping experiment 2

Three 12mm circles were marked on a colleague's forearm, 8, 11 and 14 cm from the elbow for sections 1, 2 and 3, respectively. Sections 1 and 2 were dosed with 4.97 and 5.55 mg Dermovate, respectively, whilst section 3 remained undosed. The wiping and stripping procedure described above was performed on section 1 30 mins after dosing, on section 3 (control) at 45 mins, and on section 2 at 60 mins.

Samples from section 1 were extracted and analysed for active as above. All the section 1 samples were re-extracted to ensure that the extraction procedure was of high efficiency. Only the re-extracted wipe contained additional material, 7.1% of that in the first extract and, as the cotton buds were not dry when transferred to the next extraction solution, carryover of the original extraction solution would account for much or all of this material. Of greater concern was the recovery of $2.687 \mu\text{g}/\text{cm}^2$ (122% of the applied dose) in the first wipe extract, with $0.080 \mu\text{g}/\text{cm}^2$ (3.6%) and $0.154 \mu\text{g}/\text{cm}^2$ (6.2%) in strip 1 and strips 2-11, respectively. These amounted to 132% of the applied dose and such high recovery was unexpected. The high variability observed in all of the Dermovate work lead me to believe that the homogeneity of the

active within the formulation needed to be assessed, and further analysis of samples from this study was therefore abandoned.

5.3.5.3 Assessment of homogeneity of Dermovate formulation

Six samples of Dermovate (5.29 – 7.14 mg), removed from different sections of a 5 cm length of cream, were extracted into either 5 ml MP A or MP B. One sample per extraction solvent was analysed following centrifugation (5 mins at 12,000 rpm) and one sample following filtration (0.2 µm polypropylene syringe filter, Whatman, UK). The recovery was very similar for both methods (< 1% difference, but slightly higher for centrifuged samples) and therefore remaining samples were simply centrifuged prior to analysis. Recoveries are presented in Table 5.6, which shows large variations in the active content, despite average recoveries of close to 100%. This demonstration of inhomogeneity of the formulation explained the highly variable recoveries observed in the stripping experiments.

The formulation was then inspected under a microscope (Vickers Instruments, 10/0.25 lens, 10x eyepiece (both manufactured by C Baker, London)). Crystals of various sizes, randomly and infrequently dispersed, were clearly visible and it was highly likely that these crystals were clobetasol propionate. The presence of crystals may mean that the formulation was saturated and that gradual dissolution may replenish levels in the liquid phase following loss due to skin absorption.

Table 5.6 Recovery (% of theoretical content) of clobetasol propionate (CP) in each cream extract (A samples extracted with MP A, B with MP B)

Sample number (amount)	Recovery of CP (%) for MP A extracts	Recovery of CP (%) for MP B extracts
1 A (5.85 mg)	114.4	-
2 A (5.61 mg)	72.4	-
3 A (5.05 mg)	121.4	-
4 B (7.14 mg)	-	72.8
5 B (5.29 mg)	-	73.5
6 B (5.63 mg)	-	126.6
Mean	102.7	91.0
SD	26.5	30.9
SE	15.3	17.8

It was reasonable to conclude that the Dermovate cream formulation was not homogeneous. However, although this was not ideal, it may have little effect on its in-use efficacy where a larger dose is distributed over a greater area.

Despite the expected variation in recovery, one further *in vivo* experiment was performed, as the formulation variability was expected to mainly influence recovery in the wipe, and may not materially affect levels in the strips if the formulation bulk phase was saturated with active.

5.3.5.4 *In vivo* tape stripping experiment 3

Three forearm sites were dosed as described in experiment 2 (section 5.3.5.2), with active sites receiving 5.46 and 5.41 mg doses. Sampling, extraction (MP A) and analysis were as previously described. Once again, limited interference was observed in control samples, and data are presented before and after subtraction of background levels (Table 5.7).

Table 5.7 Recovery of clobetasol propionate in each compartment, $\mu\text{g}/\text{cm}^2$ (% applied dose)

Compartment	Section 1 30 min	Section 1 minus peak in control sample	Section 2 60 min	Section 2 minus peak in control sample
Wipe (dosed area)	4.01 (166)	3.86 (161)	1.61 (67.1)	1.46 (60.8)
Strip 1	0.088 (3.66)	0.073 (3.04)	0.079 (3.29)	0.064 (2.66)
Strips 2-11	0.138 (5.71)	0.090 (3.74)	0.145 (6.06)	0.097 (4.07)
Terminal ethanol wipe	0.168 (6.96)	0.104 (4.32)	0.140 (5.84)	0.076 (3.18)
Strips 2-11 + term. wipe	0.306 (12.67)	0.195 (8.06)	0.285 (11.90)	0.173 (7.25)
Overall recovery	4.40 (182)	4.13 (171)	1.97 (82.3)	1.69 (70.7)

Very high variability in the wipe recoveries was observed for the two active sites. Levels in the strips were similar to those observed for the *in vitro* assessment (section 5.3.4.2).

5.3.6 Conclusions

The results published by Weigmann et al (1999) were very different to those obtained in the studies described here, both *in vitro* and *in vivo*, and possible reasons for this were discussed above.

The D-Squame discs assessed here appeared to perform similarly under both *in vitro* and *in vivo* conditions. If one assumes that the small 'co-eluting' peaks found in the control sites were due to migration of clobetasol propionate, then recovery of active in strips 2-11 ranged between 4.6 and 7.0% for all *in vitro* and *in vivo* sites. If exposure time was taken into account, the pilot *in vitro* study data were generally slightly higher than the *in vivo* results, but within 1% of the applied dose. Levels in strip 1, typically regarded principally as surface material, were very similar for all experiments (0.063 – 0.088 $\mu\text{g}/\text{cm}^2$) indicating that the wipe efficiency was high both *in vivo* and *in vitro*.

The wide variability in recovery of applied clobetasol propionate was due to the poor homogeneity of distribution of active in the formulation. Further analysis of the distribution data would be of questionable validity as the effect of such variation in distribution on skin permeation is unknown. No further work was performed using this formulation.

5.4 Weight of tissue removed by D-Squame

As an additional way to compare the stripping performance of D-Squame *in vitro* versus *in vivo*, the total weight of tissue removed by 10 strips was investigated.

Henn et al (1993) removed between approximately 0.4 and 1.4 mg/cm² for human subjects *in vivo* using 10 D-Squame discs, and the average at 20 strips was 1.30 ± 0.34 mg/cm². A reasonably linear (r=0.996) cumulative weight removal was reported for D-Squame, but this was less so for the Cellux tape also assessed.

5.4.1 Methods

Weight of tissue removed by the 10 strips was determined by pre-weighing a 20 ml vial containing the sheet of 10 D-Squame strips. The skin was then stripped by application of each disc to pre-marked area of the skin surface, pressing with a gloved thumb (using moderate pressure), prior to rapid removal with the aid of forceps. Each D-Squame disc plus adhering skin was replaced in the vial together with the empty D-Squame backing sheet. The vial was then re-weighed and the difference in weight corresponded to the weight of tissue removed.

5.4.2 *In vivo* versus *in vitro* assessment 1

For forearm skin *in vivo*, 10 strips removed 0.76 mg (0.60 mg/cm^2). A previously frozen sample of abdominal skin was then stripped *in vitro* at room temperature (0.66 mg , 0.52 mg/cm^2). The low weights of tissue removed were clearly similar, but were at the limits of accuracy for the analytical balance (5-place Sartorius BP211D), and indicated that accurate measurement of individual strips would not be possible with the available equipment.

5.4.3 *In vivo* versus *in vitro* assessment 2

A subsequent assessment compared skin that had been mounted in a diffusion cell for 24 hours prior to stripping to a different forearm site *in vivo*. More sets of strips were removed than for the first assessment. The skin used *in vitro* was abdominal tissue (surgical, Asian) and a PBS receptor phase was used. The cell was placed in a waterbath (37°C) as described earlier for 24 hours prior to the cell being dismantled and the skin immediately stripped (no surface wipe was performed). A total of eighty strips were removed for the *in vitro* tissue and 20 strips *in vivo* (Figure 5.7).

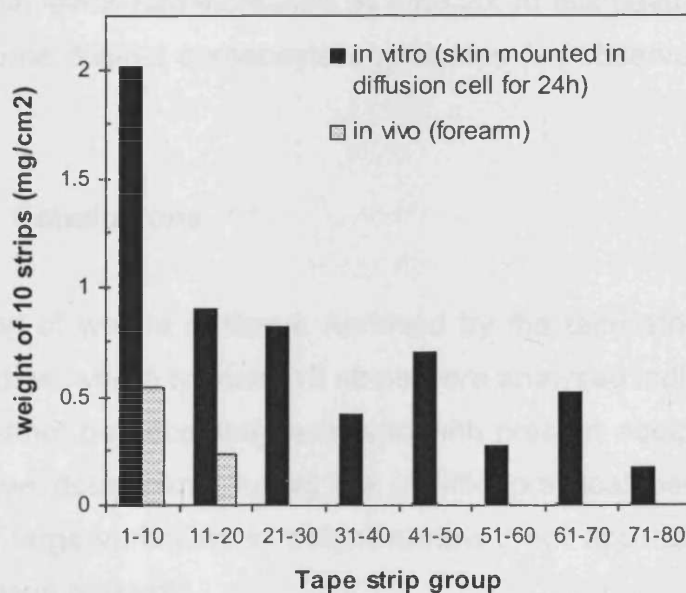


Figure 5.7 Weight of tissue removed by D-Squame *in vitro* and *in vivo*

The weight of tissue removed for the skin that had been mounted in the diffusion cell for 24 hours was vastly different to the *in vivo* result and the weights seen in assessment 1. This was somewhat surprising, as visually, the amount of tissue removed by strips 1-10 looked similar for all *in vivo* and *in vitro* groups, perhaps indicating that water content may greatly affect the weight removed. However, when vials were re-weighed 5 days later, no water loss had occurred. In fact, a slight increase in weight was observed for each group (typically 5-20 mg). This may have been due to a weighing errors or perhaps indicated that D-Squame strips plus skin is hygroscopic in nature. However, the lack of weight reduction for the *in vitro* strips 1-10 group could indicate that the high weight removed might not have been due to high water content. It was observed that the nature of tissue removed *in vitro* changed by approximately strip 35. Before that point, either all or some of the strip appeared to contain distinct corneocyte aggregates whereas, after strip 35, only a constant ill-defined layer was visible. The variability in weights removed for each group after strip 30 may have been due to the observed occasional removal of tiny sections of the entire epidermis.

For the forearm strips (*in vivo*), mild pain was reported during the first 10 strips and pain levels had increased by strip 20. At this point, strips still visibly contained some distinct corneocyte aggregates (as observed for the *in vitro* stripping).

5.4.4 Conclusions

The recording of weight of tissue removed by the tape strips in our *in vitro* stripping studies, where typically 10 strips were analysed individually or in 3 or 4 groups, cannot be accurately achieved with present equipment. Even with more sensitive equipment, it may be of little practical benefit, due to the possibility of large variations in weight removed not accurately reflecting the amount of tissue present.

A promising technique that has been developed *in vivo* since this work was performed uses a spectroscopic method to determine the amount of SC removed (Weigmann et al, 2003). Absorbance in the visible range allowed determination of the absolute mass of corneocyte aggregates on the strips removed, and identical results were achieved in two institutions performing clinical investigations (Weigmann et al, 2003). This approach was not investigated in our laboratory as it required non-available equipment, and interference will probably occur for compounds that absorb in the visible range (such as hairdyes).

5.5 Skin surface biopsies (SSB)

An alternative *in vivo* technique that sequentially removes the surface layers of the stratum corneum was optimised by Marks et al (1971). This technique uses a rapidly bonding cyanoacrylate adhesive and glass slides to remove skin surface biopsies (SSB) from volunteers following topical treatment. It is reported that up to five SSB can be removed per site before the viable epidermal layer is reached (Dykes, 1997).

It is well known that many prescription and illicit drugs can be measured many weeks to months after use through analysis of hair samples (reviewed by Villain et al, 2004). Systemically absorbed drugs and their metabolites become incorporated and trapped in the keratin matrix. Extraction of hair samples followed by analysis using highly sensitive techniques can provide a time-line of drug abuse or abstinence that will be accepted in a court of law, providing chain of custody procedures and analytical competency has been assured. A local company, Tricho-Tech Ltd, Cardiff, UK, pioneered this work in the UK.

Incorporation of systemically absorbed drugs into keratin in the skin might be expected to occur in the same manner as for hair. The differences in surface area between skin and hair would mean that only drugs that are absorbed in large quantities would be expected to be measurable in skin surface samples. A study into how an orally administered antifungal drug, terbinafine, reached

the stratum corneum was performed by Lever et al (1990) using SSB. Terbinafine was detected in the stratum corneum as early as 24 hours for three of five patients, and in all patients by day 3. The authors concluded that the rapid distribution of terbinafine in the stratum corneum indicated epidermal diffusion, rather than just inclusion in outwardly moving corneocytes.

The measurement of orally administered drugs in SSB has only been investigated to a limited extent, and mainly with antifungal drugs. Therefore, in collaboration with Professor R Marks, Dr P Dykes, and their colleagues at Cutest systems Ltd, Cardiff, UK, the following study was performed. Prof. Marks and two other volunteers at Cutest took oral doxycycline, an antibiotic, prior to removal of SSB. The SSB were collected from Cutest, extracted and analysed following development of a suitable analytical assay. The amount of tissue removed from a site visually decreased with each SSB, although the amounts appeared much greater than that removed by a tape strip.

Doxycycline (doxycycline hydrochloride hemiethanolate hemihydrate, CAS No. 24390-14-5, Figure 5.8) is a tetracyclic broad spectrum antibiotic used to treat bacterial infections, including pneumonia, acne and inhalational anthrax (after exposure). It is also used to prevent malaria. It works by preventing the growth and spread of bacteria. A typical oral dose is 100 mg every 12 hours for the first 24 hours then 100 mg/day, and doxycycline has a high oral bioavailability (95%), a long half-life (16 h), and is widely distributed throughout the body and into tissues and secretions (Goodman and Gilman's The Pharmacological Basis of Therapeutics, 9th Edition). Doxycycline has a M_w of 512.94 and is a yellow powder.

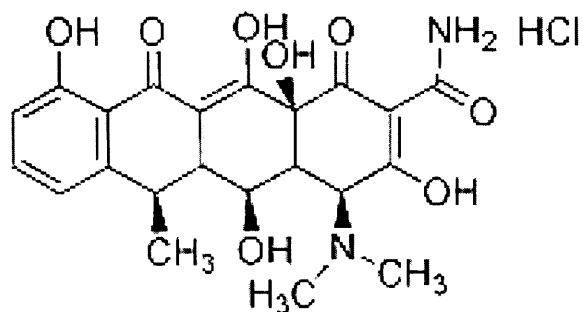


Figure 5.8 Structure of doxycycline hyclate (Sigma-Aldrich)

5.5.1 Materials and equipment

Solvents and equipment were as described in section 5.3.2. Doxycycline hyclate (purity >99%) was from Sigma.

5.5.2 Analytical method development and sample analysis

It was clear that a highly sensitive assay for doxycycline would be required and initial efforts focused on HPLC analysis with detection by UV-Vis absorbance. Fluorescence detection was subsequently assessed, as this frequently provides specific and sensitive methods for suitable compounds.

5.5.2.1 Analysis using UV-Vis detection

The first method assessed was based upon that described by Axisa et al (2000). The initial HPLC equipment was as described in section 3.2.2.10 and used a very sensitive TSP UV6000 PDA UV-Vis detector. A Genesis C18, 4 μm , 150x4.6mm column protected with a C18 security guard pre-column (Phenomenex) was used throughout with a 50 μl injection volume (Pushloop). The initial mobile phase (MP) was 50/50 (v/v) acetonitrile/water + 0.15% trifluoroacetic acid (TFA), with a detection wavelength of 350 nm (at a 10 Hz data rate) plus scans from 200 to 648 nm (at 1 Hz). Injection of a 2.1 $\mu\text{g/ml}$ solution of doxycycline in 50/50 acetonitrile/water produced a peak with a short retention time (2.05 min), and a spectral plot of the peak absorbance is shown in Figure 5.9. No absorbance was present above 420 nm so scanning

settings were reduced to 200 to 448 nm, and a second wavelength, the lambda maximum at 269 nm, was specified at the 10 Hz data rate.

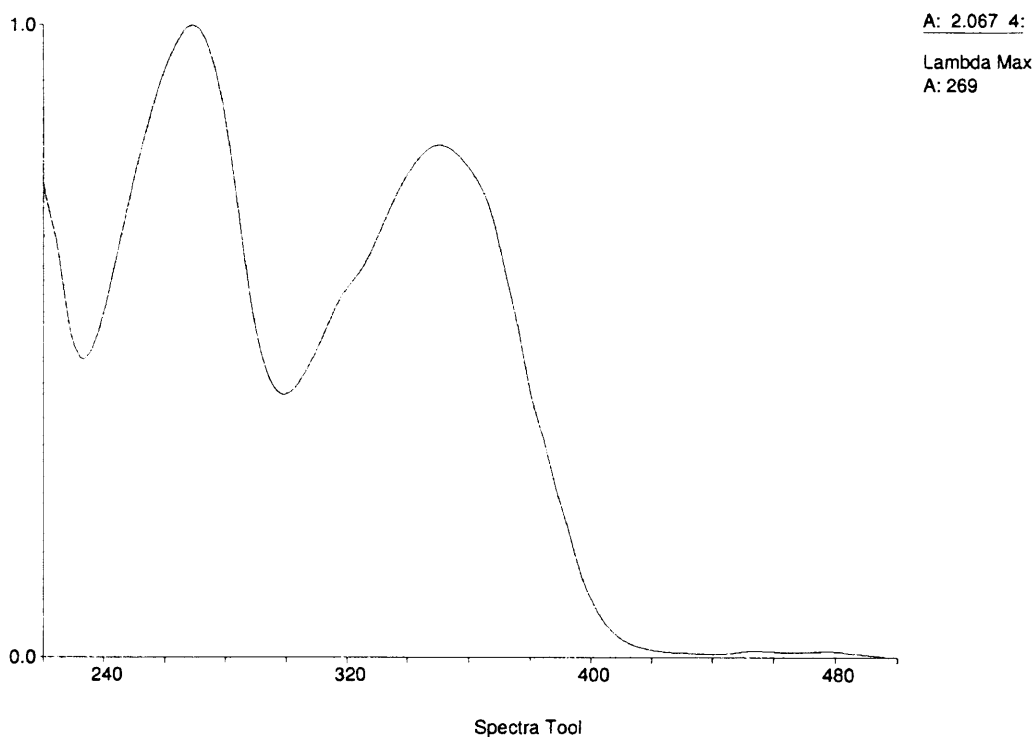


Figure 5.9 Spectral analysis of doxycycline peak (220 to 500 nm)

The injection of a 0.21 $\mu\text{g/ml}$ solution produced relatively large peaks at both 269 and 350 nm, with blank solvent injections showing no co-eluting peaks.

A suitable extraction method for the skin surface biopsies (SSB) was developed. For all assessed SSB the area of skin was traced onto a sheet of paper to allow subsequent measurement of SSB area, if required. The list of SSB provided is presented in Table 5.8.

Table 5.8 Identification of skin surface biopsies

Subject	SSB at 24 hours*	SSB at 48 hours*
1	Site A, SSB 1, 2 Site B, SSB 1, 2	Site E, SSB 1, 2, 3 Site F, SSB 1, 2, 3
2	Site C, SSB 1, 2, 3	Site G, SSB 1, 2 Site H, SSB 1, 2, 3
3	Site D, SSB 1, 2, 3	Site I, SSB 1, 2, 3

* - hours after cessation of oral dosing

The first extraction process used acetone (4-5 ml) to wash the entire SSB (Site B, SSB 1) off the slide and into a 20 ml vial. The acetone was removed under an air stream and the resultant cloudy layer on the base and sides of vial extracted with 1 ml 50/50 (v/v) acetonitrile(ACN)/water (as used by Axisa et al to extract biological tissues). The vial was vortexed and sonicated for 25 min, when the adhesive residues formed a discrete drop. A 200 µl extract sample was centrifuged and analysed. The secondary wavelength (269 nm) was of no value due to the presence of multiple interfering peaks. The absorbance at 350 nm showed several very small peaks in the vicinity of doxycycline (2.05 min) with the largest peak at the correct retention time and equivalent to approximately 35 ng/ml doxycycline (i.e. 35 ng in the entire SSB). An additional sample of the extract was spiked with 42 ng/ml doxycycline and analysed. Recovery was high at ~122%. It was clear that further separation of peaks was necessary through increased retention.

The mobile phase was changed to 30/70 (v/v) acetonitrile/water + 0.15% TFA, and this produced a retention time of ~5.8 min. A gradient wash incorporating additional acetonitrile was included to ensure removal of adhesive and skin derived peaks (Table 5.9) prior to the next injection.

Table 5.9 HPLC gradient elution program 1

Time (min)	% MP B (3/7 acetonitrile/ water + 0.15% TFA)	% MP D (acetonitrile)
0	100	0
7	100	0
9	30	70
20	30	70
22	100	0
30	100	0

Analysis of the above extract (Site B, SSB 1) showed a shift in the peak that previously co-eluted with doxycycline, with a retention time of 6.10 min (~0.3 min after doxycycline). No peak was present for doxycycline itself.

A modified extraction process was used for Site E, SSB 1; 1 ml 50/50 ACN/water + 0.15% TFA MP was used, and reduced vortexing limited clumping of the adhesive, ensuring a greater contact area with the extraction solvent. Analysis of this sample showed no detectable doxycycline.

Site F, SSB 1 was similarly extracted but with TFA excluded. Again, no doxycycline was detectable upon analysis.

5.5.2.2 Analysis using fluorescence detection

The next analytical method assessed was based upon conditions reported by Vienneau et al (1997) to measure tetracycline using fluorescence detection, where they used doxycycline as an internal standard. A different HPLC system was used for this work and consisted of: LDC membrane degasser, CM3500 and 3200 pumps, AS3000 autosampler, SM5000 PDA UV detector, FL2000 fluorescence detector (downstream of SM5000) and SN4000 controller. The HPLC program was PC1000 ver. 3.0.1 (TSP). The same column and injection volume as above was used. The initial fluorescence detector settings were: excitation 374 nm, emission 512 nm, rise time 1.0 sec, 10 Hz data rate, PMT voltage 600 V, lamp state on. The SM5000 detector wavelengths were 350 and 269 nm (10 Hz data rate, no concurrent scan possible). The SM5000 detector is approximately six times less sensitive than the UV6000 detector used in section 5.5.2.1, which is of significance regarding limits of detection.

Prior to assessing the mobile phase used by Vienneau, the optimal acetonitrile based MP (30/70 ACN/water + 0.15% TFA) used for the analysis by UV was used. The retention time of doxycycline in this system was 5.1 min using UV detection. No peak was present in the fluorescence (FL) signal for a 2.1 µg/ml injection. The sample was re-injected and emission wavelength scans (420 – 600 nm) were performed using a fixed excitation wavelength of 374 nm. No significant emission was found. A similar excitation scan (260 – 420 nm) was performed using a fixed emission wavelength of 512 nm with identical results. It was concluded that little, or no, fluorescence occurs under acidic MP conditions.

The MP used by Vienneau, 40/60 (v/v) methanol/buffer, the buffer containing 0.1M sodium acetate, 0.025M disodium EDTA and 0.035M calcium chloride, adjusted to pH 6.5 with sodium hydroxide (aq), was then assessed. Solutions of doxycycline prepared in MP buffer showed low solubility ($\ll 130 \mu\text{g/ml}$), and a saturated sample was centrifuged prior to analysis. The retention time was 4.1 min but, surprisingly, the FL response was only one third of that by UV (350 nm) even though the SM5000 detector was being used. An emission scan was performed (as above) which showed a virtual plateau between 512 and 532 nm (max 524 nm, 1.6 fluorescence units). The excitation scan therefore used a fixed emission wavelength of 524 nm, and showed excitation was maximal between 388 and 392 nm. However, this only raised the response to 2.0 fluorescence units, and the response and signal:noise ratio was still less than half that for UV detection at 350 nm.

Fluorescence detection was therefore abandoned as UV-Vis detection using the UV6000 system offered much greater sensitivity. The benefits of the FL assay for some researchers would be one of selectivity.

5.5.2.3 Further analysis using UV-Vis detection

The optimised assay in section 5.5.2.1 was used to analyse further SSB extracts. Fresh standard solutions in 50/50 ACN/water were prepared, the lowest of which was $0.055 \mu\text{g/ml}$, with a detection limit of $\sim 0.02 \mu\text{g/ml}$. This was significantly improved compared to that achieved by Axisa et al (125 ng/ml) for a $200 \mu\text{l}$ injection (4 times greater).

The SSB extraction procedure was simplified through the removal of the acetone wash step. The SSB were broken into small fragments between two plastic weighing boats, then transferred to a 20 ml vial for extraction with 50/50 ACN/water. Vials were shaken (no vortexing) and received two 15 min sessions of sonication, then a sample was centrifuged prior to analysis.

Site G, SSB 1 and 2 were extracted and analysed, with no doxycycline detected. Very small peaks were present 0.3 min prior to doxycycline retention time (5.7 min) and 0.4 min after.

Site H, SSB 2 (a small biopsy) was directly spiked by the addition of 20 μ l 2.77 μ g/ml doxycycline in 50/50 ACN/water and the spike left in contact with the skin for 4 min. The applied solvent lifted the skin/adhesive from the glass slide and the SSB was carefully transferred to a vial. A small portion of the spike remained on the glass slide. 500 μ l 50/50 ACN/water was added to the small SSB and the usual extraction procedure followed. A 200 μ l sample was analysed and 87% of the maximum 107 ng/ml spike was recovered at the correct retention time (Figure 5.10). This spiking recovery indicated that the skin/adhesive mixture did not irreversibly adsorb available doxycycline.

It was concluded that the assessed SSB contained no detectable doxycycline. The results and the dosing regimen were discussed with Prof. Marks. Doxycycline tablets were taken for only 2 days prior to cessation (and removal of SSB 24 and 48 h later) and it is probable that this was the reason for the absence of doxycycline in the SSB.

Mode: Acquired Data
 Original Results: C:\TSP\DG_12_03\Data\w_initial7.RMS
 Notes:
 SSB RM 2B2 spiked (20ul -2.77ug/ml) and skin/glue transferred to vial +
 500ul 50/50 (no acetone wash)

Page 1
 Reported On: 05-09-05 12:30:31

Analysis Report

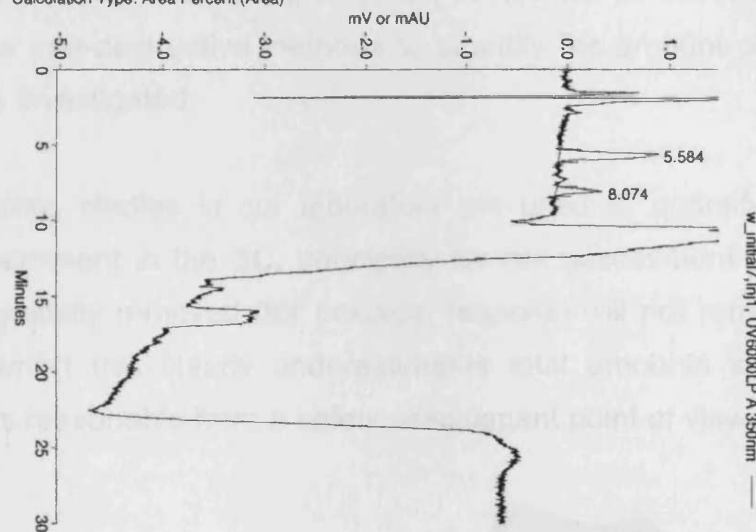
Name: w_initial7
 Type: Sample
 Injection Volume: 50.0 µL

Vial: A07

Injection: 1 of 1
 Injected On: 15-05-03 15:05:24

Acquisition Log
 Column Pressure (PSI): 1390
 Noise (microAU): 2e+01
 Run-Time Messages: None
 Column Temperature (C): N/A
 Drift (microAU/min): -4e+01
 Pump Flow Stability: 3.2

Signal 1: UV6000LP A 350 nm
 Calculation Type: Area Percent (Area)



Component	RT(min)	Area	Height	Area%	Peak Type
Unident0001	5.584	26419	970	76.51	Modified
Unident0002	8.074	8112	470	23.49	Modified
Totals		34531	1440	100.00	

Figure 5.10 Chromatogram showing a spiked SSB (doxycycline retention time 5.58 min)

5.6 Overall conclusions

The tape stripping methods investigated both in this chapter and by other workers confirmed that there is wide variability in results depending upon the techniques used. The decision by the FDA not to accept dermatopharmacokinetic studies as proof of bioequivalence appears wise with the current status of tape stripping methods.

Variations in stripping efficiency appeared to occur principally in the type of tape used, the application method, skin hydration, the presence of residual formulation on the surface and formulation components present in the SC.

The recent introduction of a new spring-loaded pressure application device by CuDerm Corp. (Figure 5.11) allows consistent application of $\sim 225 \text{ g/cm}^2$ pressure to a D-Squame disc following application to the skin surface. The effect of this device on stripping variability *in vitro* will be assessed in the near future. New non-destructive methods to quantify the amount of SC removed will also be investigated.

Tape stripping studies in our laboratory are used to quantify approximate levels of permeant in the SC, principally for risk assessment purposes. The 10 strips typically removed (for practical reasons) will not remove the entire SC and, whilst this clearly underestimates total amounts in the SC, this approach is reasonable from a safety assessment point of view.



Figure 5.11 D-Squame pressure device (CuDerm Corp., USA)

5.7 References

Axisa, B., Naylor, A.R., Bell, P.R. and Thompson, M. (2000). Simple and reliable method of doxycycline determination in human plasma and biological tissues. *J. Chromatogr. B Biomed. Sci. Appl.*, **744**, 359-65.

Bronaugh R.L., Stewart, R.F. and Simon, M. (1986). Methods for in vitro percutaneous absorption studies VII: use of excised human skin. *J. Pharm. Sci.*, **75**, 1094-1097.

Depuis, D., Rougier, A., Roguet, R., Lotte, C. and Kalopissis, G. (1984). In vivo relationship between horny layer reservoir effect and percutaneous absorption in humans and rat. *J. Invest. Dermatol.*, **82**, 353-356.

Dreher, F., Modjtahedi, B.S., Modjtahedi, S.P. and Maibach, H.I. (2005). Quantification of stratum corneum removal by adhesive tape stripping by total protein assay in 96-well microplates. *Skin Res. Technol.* **11**, 97-101.

Dykes, P.J., Hill, S. and Marks R. (1997). Pharmacokinetics of topically applied metronidazol in two different formulations. *Skin Pharmacol.*, **10**, 28–33.

Goodman and Gilman's *The Pharmacological Basis of Therapeutics*, 9th Edition (1995). Hardman, J.G., Gilman A.G. and Limbard L.E. (eds). McGraw-Hill, New York, USA.

Henn, U., Surber, C., Schweitzer, A. and Bieli, E. (1993). D-Squame adhesive tapes for standardized stratum corneum removal, in *Prediction of Percutaneous Penetration*, Vol. 3B, pp. 477-481. STS Publishing, Cardiff, UK.

Lever, L.R., Dykes, P.J., Thomas, R. and Finlay, A.Y. (1990). How orally administered terbinafine reaches the stratum corneum. *Journal of Dermatological Treatment*, **1**, 23-25.

Marks, R. and Dawber, R.P.R. (1971). Skin surface biopsy: an improved technique for the examination of the horny layer. *Br. J. Derm.*, **84**, 117–123.

Ohman, H. and Vahlquist, A. (1994). In vivo studies concerning a pH gradient in human stratum corneum and upper epidermis. *Acta. Derm. Venereol.* **74**, 375-379.

Pershing, L.K., Silver, B.S., Kruger, G.G., Shah, V.P. and Skelly, J.P. (1992). Feasibility in measuring the bioavailability of topical betamethasone dipropionate in commercial formulations using drug content in skin and a skin blanching bioassay. *Pharm. Res.*, **9**, 45-51.

Pinkus, H. (1951). Examination of the epidermis by the tape strip method of removing the horny layers I. Observations on thickness of the horny layer, and on mitotic activity after stripping. *J. Invest. Dermatol.*, **16**, 383-386.

SCCNFP (2003). Basic criteria for the in vitro assessment of dermal absorption of cosmetic ingredients, SCCNFP/0750/03. SCCNFP, Brussels.

Shah, V.P., Flynn, G.L., Yacobi, A., Maibach, H.I., Bon, C., Fleischer, N.M., Franz, T.J., Kaplan, S.A., Kawamoto, J., Lesko, L.J., Marty, J.P., Pershing, L.K., Schaefer, H., Sequeira, J.A., Shrivastava, S.P., Wilkin, J. and Williams, R.L. (1998). Bioequivalence of topical dermatological dosage forms - methods of evaluation of bioequivalence. *Pharm. Res.*, **15**,167-171.

Surber, C., Schwarb, F.P. and Smith, E.W. (1999) Tape-stripping technique, in *Percutaneous absorption: drugs – cosmetics – mechanisms – methodology*, 3rd Ed. Bronaugh, R.L and Maibach H.I. (eds) pp 395-409. Marcel Dekker, New York, USA.

Tregear, R.T. (1966). *Physical Functions of Skin*. p 94. Academic press, New York.

Tsai, J-C., Weiner, N.D., Flynn, G.L. and Ferry, J. (1991a). Properties of adhesive tapes used for stratum corneum stripping. *Int. J. Pharm.*, **72**, 227-231.

Tsai, J-C., Cappel, M.J., Weiner, N.D., Flynn, G.L. and Ferry, J. (1991b). Solvent effects on the harvesting of stratum corneum from hairless mouse skin through adhesive tape stripping in vitro. *Int. J. Pharm.*, **68**, 127-133.

Vienneau, D.S. and Kindberg,, C.G. (1997). Development and validation of a sensitive method for tetracycline in gingival crevicular fluid by HPLC using fluorescence detection. *J Pharm Biomed Anal*, **16**, 111-117.

Villain, M., Cirimele, V. and Kintz, P. (2004). Hair analysis in toxicology. *Clinical Chemistry and Laboratory Medicine*, **42**, 1265-1272.

Weigmann, H.J., Lademann, J., Pelchrzim, R.V., Sterry, W., Hagemeister, T., Molzahn, R., Schaefer, M., Lindscheid, M., Schaefer, H. and Shah, V.P. (1999). Bioavallibility of clobetasol propionate – quantitation of drug concentrations in the stratum corneum by dermatopharmacokinetics using tape stripping. *Skin Pharmacol. Appl. Skin Physiol.*, **12**, 46-53.

Weigmann HJ, Lindemann U, Antoniou C, Tsikrikas GN, Stratigos AI, Katsambas A, Sterry W and Lademann J. (2003). UV/VIS absorbance allows rapid, accurate, and reproducible mass determination of corneocytes removed by tape stripping. *Skin Pharmacol. Appl. Skin Physiol.*, **16**, 217-227.

Weigmann, H.J., Jacobi, U., Antoniou, C., Tsikrikas, G.N., Wendel, V., Rapp, C., Gers-Barlag, H., Sterry, W. and Lademann, J. (2005) Determination of penetration profiles of topically applied substances by means of tape stripping and optical spectroscopy: UV filter substance in sunscreens. *J. Biomed. Opt.*, **10**, 14009 (7 pages).

Chapter 6

Estimation of evaporative loss for volatile permeants

6.1 Introduction

When studying the *in vitro* percutaneous absorption of compounds it is often desirable to achieve full mass balance i.e. recovery of all the applied material. In this situation, in addition to the measurement of permeated compound, analysis of skin distribution, including amounts remaining on the surface, plus amounts on the diffusion cell donor chamber, requires quantitation. The various published guidelines for such studies (SCCNFP, 2003; OECD test guideline 428, 2004) indicate that average recovery should range between 100 ± 20 and $100 \pm 10\%$ of the applied dose, dependent upon the particular guideline, and any deviations should be justified.

However, in practice, it is not always possible to achieve full recovery. Problems can arise when analysing compounds formulated at very low concentrations, for example 0.1%, applied under in-use conditions, where levels in the various compartments can be below the limits of detection for the analytical technique. Instability of the applied compound can also result in poor recovery and this should always be considered.

One of the most frequent occasions where mass balance is unlikely to be achieved is for volatile compounds, including fragrances (where at least limited volatility is a prerequisite). However, simply stating that recovery was low due to volatility reduces confidence in the measured absorption values. The ideal solution would be to measure the evaporative loss directly for each diffusion cell, in a manner that does not alter the evaporation rate. The rate of fragrance evaporation has been observed to affect the amount absorbed through the skin, as evaporative loss decreases skin exposure, therefore experimental conditions should alter the evaporation as little as possible compared to in-use unoccluded conditions (Yourick et al, 1999). Whilst the

assessment of recovery of applied material can be performed using a second set of measurements under completely occluded conditions, this increases study costs greatly, and even complete occlusion may not prevent evaporation for some materials. Skin penetration can also be considerably enhanced under occlusive conditions so that concentrations in the various compartments may not reflect unoccluded conditions, limiting the validity of this approach.

Potential techniques for measurement of evaporative loss suitable for use in our laboratory, ideally using existing diffusion cells, were therefore investigated.

6.2 Published reports on assessment of evaporative loss

Reifenrath and Robinson (1982) reported the *in vitro* evaporation and penetration characteristics of several mosquito repellents. They used a complex evaporation-penetration cell that positioned a vapour trap (containing 200 mg sorbent) 6.5 mm above the skin surface. Airflow of 30 ml/min was used to draw dried air through 4 inlet tubes and capture evaporating repellent in the trap, which was changed at hourly intervals. The evaporated and permeated amounts plus levels in and on the skin surface were quantified. Total recoveries at 12 hours ranged between 79 and 101% of the applied dose, and recoveries in the trap between 0.5 and 20%. The authors commented that, for one of the repellents, a previous study using the trap positioned 1.5 mm above the skin surface had measured more than double the amount evaporated 1 hour after application. This suggests that airflow dynamics in such cells are important determinants of evaporation, and hence availability for skin penetration, for volatile compounds.

Frantz et al (1995) used a similar trapping technique (although the cell was different) for 2-ethyl-1,3-hexanediol (EHD), a moderately volatile alcohol, and a reference compound N,N-diethyl-*m*-toluamide (DEET). They also assessed skin penetration under occluded conditions using a glass stopper instead of

the trap. Airflow over the skin surface for the trapping method was 600 ml/min. EHD and DEET were applied to the skin as solutions in ethanol (15 μ l). Total recoveries for human skin (n=3) using the trapping method were 82 ± 2 and $83 \pm 3\%$ of the applied dose for EHD and DEET, compared to 75 ± 9 and $76 \pm 4\%$ under occluded conditions. Permeated amounts were 1.7 and 1.4-fold greater (EHD and DEET, respectively) for the occluded groups than the trapping method groups. Occlusion also doubled skin levels for EHD but not for DEET. The trapping method used did not raise recoveries to levels required by some guidelines. Interestingly, the recoveries in the occluded groups were lower, and it was suggested that the missing EHD and DEET were due to loss of these volatile compounds when the glass stopper was removed at the end of experiment (Frantz et al, 1995). This could certainly be a particular problem for very volatile compounds assessed under occluded conditions as a control for in-use unoccluded studies.

Lockley et al (2002) reported capture of evaporating 2-ethoxyethanol in a study measuring percutaneous penetration and metabolism. Activated carbon filter discs (exact details not provided) were placed over the donor chamber and captured the rapidly evaporating compound, with $\sim 90\%$ of the applied dose recovered at 1 hour, decreasing to $\sim 70\%$ at 8 hours, for 2-ethoxyethanol applied in methanol (31 μ l/cm² dose) to human skin. However, this capture method was reported to enhance permeation of 2-ethoxyethanol (applied in methanol) compared to unoccluded cells, with 7.5% of the applied dose absorbed, compared to 4.5% under unoccluded conditions.

Kasting and Saiyasombati (2001) produced a physicochemical based model for estimating evaporation and absorption rates of perfumes. The model was derived from an approach used to describe pesticide evaporation from soil (Kasting and Saiyasombati, 2001). Parameters such as airflow over the skin surface and vapour pressure measurements at skin surface temperature are required, although programs are available that can estimate vapour pressures. There were correlation coefficients, r^2 , of 0.74 and 0.52, for

calculated evaporation rates for two variations of the developed models when compared with published *in vivo* data (using a trapping method with a 5 l/h airflow). The model appears to be of limited practical value to *in vitro* studies.

6.3 Experimental methods for capturing evaporating material

6.3.1 Introduction

The fragrance material methyl eugenol (ME, CAS No. 93-15-2, 4-allyl-1,2-dimethoxy benzene, Figure 6.1) is a volatile compound found at low levels in many essential oils and acts in nature as an insect attractant. It has been found to be a rodent carcinogen (Burfield, 2004; National Toxicology Program, 2002) but it is believed that ME is unlikely to present a human cancer risk at current levels of exposure (IFRA, 2002).

ME is a colourless to pale yellow liquid (m.p. -4°C , b.p. 255°C), M_w 178.2, with a light clove-carnation odour. It thickens when exposed to air and readily evaporates at room temperature (National Toxicology Program, 2002). The skin penetration of ME from ethanolic solution had previously been measured in our laboratory. Overall recovery of ME in all compartments was low at $41 \pm 3\%$ of the applied dose, probably due to evaporation, as little ME remained on or in the skin at 48 hours, with nearly all ($39 \pm 3\%$ of the applied dose) of the recovered material found in the receptor phase. ME was, therefore, an ideal candidate for investigation of volatile compound evaporation during skin penetration experiments.

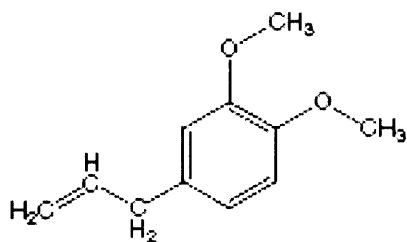


Figure 6.1 Structure of methyl eugenol (National Toxicology Program, 2002)

6.3.2 Materials and equipment

Radiolabelled methyl eugenol (ME, (ring-¹⁴C)) was from NEN (Boston, MA, USA). The specific activity was 6.98 mCi/mmol at a concentration of 0.95 mCi/ml in ethanol. Unlabelled ME (purity 97.9%) was provided by International Flavors and Fragrances Inc. (Union Beach, NJ, USA).

Ethanol (96% (v/v), AnalaR) was from Merck Ltd (Lutterworth, UK). Details of general solvents, scintillation counting materials and equipment are provided in section 3.2.1. A detailed description of the liquid scintillation counter is provided in section 4.2.1.

Anasorb CSC (coconut shell charcoal) sorbent sample tubes (2 section, 50/100 mg, 6 x 70 mm) were supplied by SKC Ltd. (Blandford Forum, UK). Activated charcoal for gas adsorption, disposable plastic syringes, filter paper discs (Whatman), parafilm (Nesco) and high vacuum silicone grease (Dow Corning) were obtained from Merck Ltd.

6.3.3 General methods

6.3.3.1 Vehicle preparation

Two 1% solutions of ME in ethanol (96% v/v) were prepared. Both solutions contained ¹⁴C-ME and unlabelled ME at a total concentration of 1% (w/v), but

the activity of the solutions varied. ME vehicle 1 contained 56 $\mu\text{Ci/ml}$, whilst ME vehicle 2 contained 8 $\mu\text{Ci/ml}$. Both vehicles were prepared by adding, with ethanol washings, 0.2 mCi of radiolabel (equivalent to 5.11 mg ME) to either a 20 ml vial (ME vehicle 1) or a 25 ml volumetric flask (ME vehicle 2) containing previously measured quantities of unlabelled ME (35.01 and 245.26 mg, respectively). Ethanol was added to produce total volumes of 4 and 25 ml, respectively. Final concentrations were 1.002 and 1.001% (w/v) for ME vehicles 1 and 2, respectively.

Each test vehicle was assessed for radiolabel activity and homogeneity of distribution. Vehicles were diluted with ethanol prior to counting ($n=5$) and the measured mean DPM/ μg was 12017 (0.17%RSD) for vehicle 1 and 1708 (0.24%RSD) for vehicle 2.

6.3.3.2 Skin preparation

Heat separated epidermal skin membranes were used, prepared as described in section 3.2.2.3.

6.3.3.3 Diffusion cells and receptor phase

Diffusion cells are described in detail in section 3.2.2.4. Any trapping devices added to the donor chamber will be described in the relevant section below. The receptor phase for skin permeation experiments was 50/50 ethanol/water (96% v/v ethanol), as this was used in the earlier work. This receptor phase would not be selected under ideal circumstances due to the likelihood of increasing permeation of an applied material, although that would not be expected to have materially affected the investigations into evaporative loss reported here.

6.3.4 Evaporative loss trapping method 1

6.3.4.1 Trapping device and diffusion cell preparation

One diffusion cell (area 1.32 cm^2 , volume 3.51 ml) was prepared containing a heat separated epidermal membrane (see above). Prior to dosing the skin surface with fragrance solution, a trapping device (Figure 6.2) was prepared consisting of the following. An SKC CSC 100/50 mg sorbent sample tube (a glass tube containing two sections of sorbent and separated by foam plugs and glass wool) was connected to the luer end of a trimmed (up to the 1 ml volume mark) section of a 5 ml plastic syringe using parafilm. The sorbent tube was left open to the environment at the top end to prevent complete occlusion. The plastic syringe was of the same diameter as the donor chamber, and they were connected (following dosing) using an airtight seal by application of silicone grease followed by parafilm then adhesive tape (3M Magic Tape).

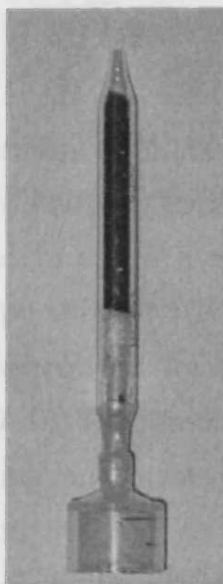


Figure 6.2 Trapping device 1

6.3.4.2 ME application and measurement of skin permeation

A $195 \mu\text{l}/\text{cm}^2$ dose of 1% ME in ethanol (ME vehicle 1) (target dose $200 \mu\text{l}/\text{cm}^2$) was applied to the skin surface at time zero. The ME dose was $1956 \mu\text{g}/\text{cm}^2$. The dose was applied by weight (as described in section 3.4.2.7) as the ethanol solution could not accurately be transferred using an air displacement pipette. Immediately following dosing the trapping device above was applied.

Receptor phase samples ($200 \mu\text{l}$) were taken 2, 4, 5.5, 21, 24, 28 and 48 hours after dosing and counted for ^{14}C by liquid scintillation counting (LSC).

6.3.4.3 Recovery of applied ME from the skin, diffusion cell and trapping device

Following removal of the 48 hour receptor phase sample, the diffusion cell and attached trapping device was dismantled and the following compartments analysed.

The skin surface was wiped with dry cotton buds. The wipes were placed in a 20 ml vial and extracted with industrial methylated spirit (IMS, 6 ml). The epidermal membrane was secured onto a small disc of thin plastic using cyanoacrylate adhesive and tape stripped 10 times using D-Squame adhesive tape discs. The tape strips were grouped (placed in the same vial) as follows: strip 1-3, strips 4-6 and strips 7-10. The remaining epidermis was then placed into a glass vial and the strips and skin extracted with OptiSolve tissue solubiliser (1 and 3 ml, respectively). The filter paper skin support was extracted into IMS (3 ml). The donor chamber was wiped with dry cotton buds, (extracted with IMS, 6 ml), and then soaked in IMS (15 ml). The syringe section was extracted using IMS (6 ml). The sorbent tube was dismantled and the following sections extracted with IMS (3 ml throughout): glass wool, 100

mg sorbent section, 50 mg sorbent section plus foam plugs and empty glass tube.

Suitable volumes of the above samples were analysed for ^{14}C by LSC.

6.3.4.4 Results for trapping method 1

The permeation of ME through the epidermal membrane was extremely rapid, with the receptor phase containing 25% of the applied dose by 2 hours and 70% by 4 hours. The amount permeated reached a maximum (87%) by 21 hours and then remained constant to 48 hours. The very rapid permeation suggested that the membrane was damaged, when compared to less than 2% permeated at 2 hours for the earlier unoccluded study.

Recovery of ME from the skin membrane, donor chamber and trapping device increased recovery to 93% of the applied dose. It is possible that the missing 7% could have evaporated during cell dismantling procedures. The majority of the additional ME was found on the syringe and in the joining grease. Very little ME was found on or in the skin membrane (0.8% of the applied dose).

A negligible amount of ME was retained by the sorbent tube ($<0.1\ \mu\text{g}$, 0.005%), although it is possible that very little reached the tube due to combination of rapid permeation and condensation on the plastic syringe lower down the trap.

It is likely that, despite the sorbent tube being open to the environment, the trapping device was producing occlusive conditions, with condensation visible. A repeat experiment with a slightly modified device was carried out to confirm whether the membrane used in this experiment was damaged.

6.3.5 Evaporative loss trapping method 2

6.3.5.1 Trapping device and diffusion cell preparation

As described in section 6.3.4.1 except that the syringe section used in the trapping device was increased in length (up to the 5 ml volume mark) to provide a larger chamber above the skin surface.

6.3.5.2 ME application and measurement of skin permeation

As described in section 6.3.4.2 except the dose was $199 \mu\text{l}/\text{cm}^2$ ($1996 \mu\text{g}/\text{cm}^2$ ME), and samples were taken at 1, 2, 3, 7, 19 and 24 hours.

6.3.5.3 Recovery of applied ME from the skin, diffusion cell and trapping device

As described in section 6.3.4.3 except as listed below.

The cell was dismantled at 24 hours, and the syringe extracted in lower and upper sections for practical reasons. A combined donor cap and skin surface wipe soaked up remaining donor solution, the two charcoal sections in the sorbent tube were combined for extraction.

6.3.5.4 Results for trapping method 2

The permeation of ME through the epidermal membrane is shown in Figure 6.3. Permeation was low at 24 hours (7.1% of the applied dose) compared to the earlier unoccluded study, where average permeation at 24 hours for the same tissue donor was $33 \pm 3\%$ of the applied dose (mean \pm SE, n=4).

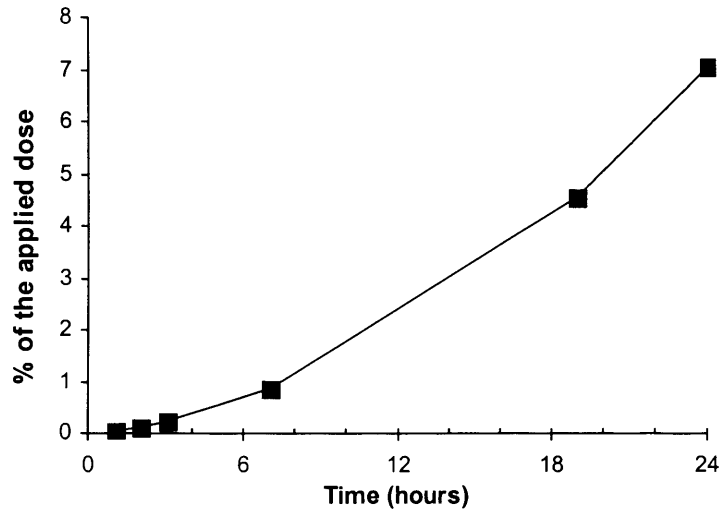


Figure 6.3 Permeation of ME through an epidermal membrane with trapping device 2 in place throughout

Occlusive conditions formed by the trapping device might have been expected to increase the amount permeated due to reduction in evaporative loss. However, the reduced permeation rate may be due to the retention of application vehicle on the skin surface, as this would have reduced the thermodynamic activity of ME compared to the unoccluded situation, where the ME concentration would have increased during ethanol evaporation. These conditions may also have changed the hydration of the skin membrane compared to the unoccluded situation.

The majority of the applied ME (83%) was recovered in the combined skin surface and donor chamber wipe that soaked up remaining surface solution. The tape strips contained 5% of the applied dose and the remaining epidermis 1%. This did not match the unoccluded study, where levels were much lower at 0.3 and 0.4% of the applied dose, respectively, due to evaporative loss of surface amounts.

The sorbent tube again contained negligible amounts of ME, but other compartments, such as the syringe and sealing grease wipe, increased overall recovery to 105%.

This trapping device was clearly acting purely as an occlusive chamber, and offered no practical benefit over simply occluding donor chambers with a greased coverslip. The sorbent tube, whilst open to the air at the top, probably provides a considerable resistance to airflow as it is designed to be used with an airflow pump.

6.3.6 Evaporative loss trapping method 3

6.3.6.1 Trapping device and diffusion cell preparation

As described in section 6.3.5.1 except as indicated below.

This method included a 3.5 hour period where a cotton wool pad was attached to the donor chamber using silicone grease, which allowed the ethanol vehicle to evaporate. The trapping device described in section 6.3.5.1 was then applied for the remainder of the experiment.

6.3.6.2 ME application and measurement of skin permeation

As described in section 6.3.4.2 except the dose was $197 \mu\text{l}/\text{cm}^2$ ($1971 \mu\text{g}/\text{cm}^2$ ME), and samples were taken at 1, 2, 3, 4, 5, 7, 24, 30 and 48 hours.

6.3.6.3 Recovery of applied ME from the skin, diffusion cell and trapping device

As described in section 6.3.5.3 except as listed below.

The cotton applied pad after dosing was extracted with IMS (10 ml).

6.3.6.4 Results for trapping method 3

The permeation of ME through the epidermal membrane (Figure 6.4) showed an unusual profile during the early stages, presumably due to the presence of

the cotton wool pad, during vehicle evaporation. The permeation rate increased greatly following application of the sorbent trapping device and, at 48 hours, was 56% of the applied dose, 1.3-fold greater than for the same tissue donor in the earlier unoccluded study ($44 \pm 2\%$ of the applied dose), indicating enhancement occurred under these partially occlusive conditions.

Inclusion of ME measured in all other compartments increased total recovery to 86% of the applied dose. The additional 30% was mainly located in the donor chamber to syringe sealing grease (8.3%) and associated parafilm (7.2%), lower section of the syringe (4.0%) and donor chamber soak (2.8%). The amounts in the parafilm indicated that either vaporised ME was absorbed by the sealing grease and then diffused through it, or that incomplete coverage of sealing grease allowed the ME to reach the parafilm, which it then diffused into. The cotton wool pad applied for the first 3.5 hours contained only 0.8% of the applied dose, possibly indicating insufficient retention of ME vapour.

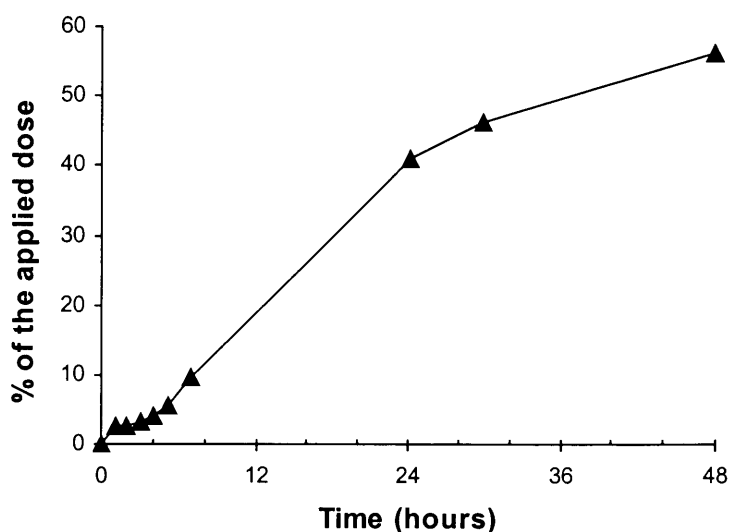


Figure 6.4 Permeation of ME through epidermal membrane using trapping method 3

Recoveries of applied ME on the skin surface, in the tape strips and remaining epidermis were 1.4, 1.6 and 0.4%, respectively. These were similar to the

unoccluded study, except for the tape strips, which were 6-fold greater in this experiment. The sorbent tube again contained negligible amounts of ME.

The amount of ME permeated under trapping method 3 was greater than for unoccluded cells, but of the same order. Overall recovery was not ideal, at 86%, probably due to loss during vehicle evaporation. There would also be concerns about the usefulness of this method for more volatile fragrances due to the expected increased loss thorough the cotton wool pad during the vehicle evaporation phase. Further modification of the trapping method was therefore required.

6.3.7 Evaporative loss trapping methods 4

6.3.7.1 Trapping device and diffusion cell preparation

As described in section 6.3.6.1 except as indicated below.

Six cells were prepared using a new skin donor (not previously assessed with ME). The cells were split into three groups of two cells and the following trapping methods were compared.

Group 1: following dosing with ME, a cotton wool pad was attached to the donor chamber using silicone grease for a 3.5 hour period. The ethanol vehicle had visually evaporated 3 hours after application. The trapping device described in section 6.3.5.1 was then applied for the remainder of the experiment. This technique matched that used in section 6.3.6.

Group 2: as for group 1 except that the cotton wool pad was replaced (for the 3.5 hour period) by a gauze pad filled with activated charcoal, which might be expected to adsorb evaporated fragrance.

Group 3: as for group 2 except that a gauze pad filled with activated charcoal was applied for the entire experimental time-frame (48 hours).

6.3.7.2 ME application and measurement of skin permeation

As described in section 6.3.4.2 except that the ME donor vehicle 2 was applied and the average dose (mean \pm SE) was $203 \pm 3 \mu\text{l}/\text{cm}^2$ ($2028 \pm 27 \mu\text{g}/\text{cm}^2$ ME). Receptor phase samples were taken at 2, 4, 10, 24, 29.25 and 48 hours.

6.3.7.3 Recovery of applied ME from the skin, diffusion cell and trapping device

As described in section 6.3.5.3 except as listed below.

The extraction solvent IMS was substituted by methanol due to unavailability. ME and silicone sealing grease dissolve easily in methanol, so it was an ideal solvent. No skin surface tape strips were taken; instead the entire epidermal membrane was simply dissolved after wiping. A combined vial containing the donor chamber wipe, sealing grease and parafilm was prepared for groups 1 and 2. For group 3, a separate donor chamber flange wipe was performed in addition to a grease plus donor chamber wipe. The gauze pads containing activated charcoal were extracted with methanol (10 ml). Following calculation of results, two of the four cells that used a charcoal containing pad (one cell per group) were re-extracted using chloroform (10 ml), and this desorbed ~100-fold greater amounts of ME from the charcoal, suggesting that earlier sorbent tube measurements were probably lower than the true value.

6.3.7.4 Results for trapping methods 4

The permeation of ME through the epidermal membranes varied greatly (Figure 6.5). Recoveries of ME in the various compartments are presented in Table 6.1.

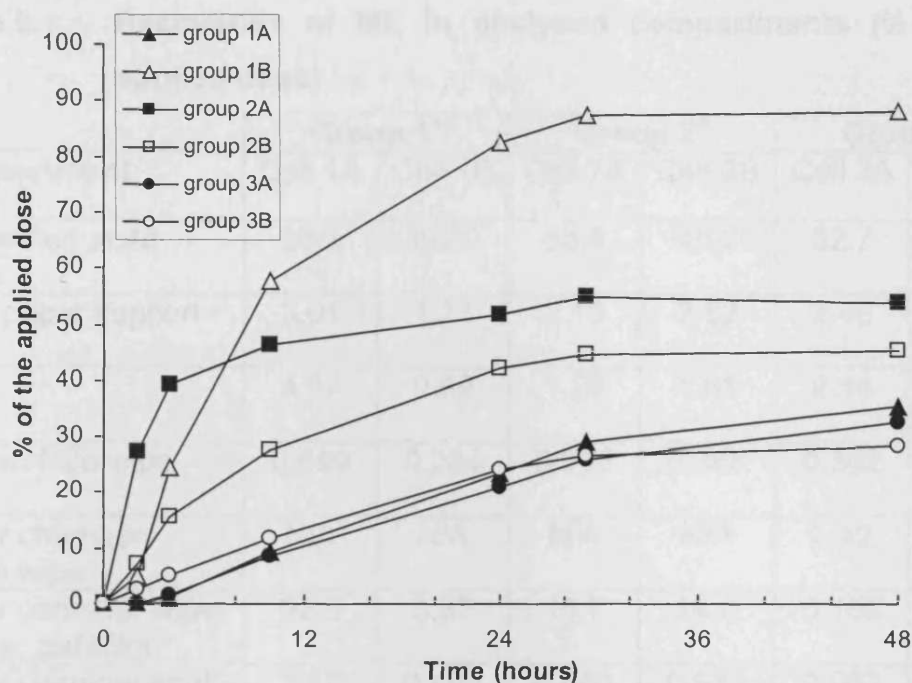


Figure 6.5 Permeation of ME through epidermal membrane using trapping methods 4; group 1 used a cotton pad then sorbent trap, group 2 used a charcoal filled gauze pad then sorbent trap, group 3 solely used a charcoal filled gauze pad

Table 6.1 Recoveries of ME in analysed compartments (% of the applied dose)

Compartment	Group 1 ^a		Group 2 ^b		Group 3 ^c	
	Cell 1A	Cell 1B	Cell 2A	Cell 2B	Cell 3A	Cell 3B
Permeated at 48 hours	35.2	88.1	53.8	45.2	32.7	28.4
Filter paper support	3.01	1.73	2.13	2.52	2.46	2.54
Skin	4.57	0.69	1.25	1.81	2.14	2.48
Skin surface wipe	0.699	0.284	0.202	0.368	0.302	0.069
Donor chamber flange wipe	N/A	N/A	N/A	N/A	2.42	4.18
Donor chamber wipe, grease, parafilm	22.5	3.37	15.7	14.0	0.106	0.239
Donor chamber soak	2.62	0.402	0.550	0.933	0.963	1.03
Lower syringe section	1.89	0.175	1.24	1.75	N/A	N/A
Upper syringe section	0.643	0.026	0.341	0.652	N/A	N/A
Sorbent tube	0.003	0.010	0.001	0.005	N/A	N/A
Cotton wool pad	0.408	0.684	N/A	N/A	N/A	N/A
Charcoal filled gauze pad	N/A	N/A	0.010	0.766 ^d	0.710	15.2 ^d
Total recovery	71.5	95.5	75.2	67.9	41.8	54.2

^a – cotton wool pad applied for 3.5 hours followed by sorbent trap device

^b – gauze pad containing activated charcoal applied for 3.5 hours followed by sorbent trap device

^c – gauze pad containing activated charcoal throughout

^d – these samples were re-extracted with chloroform, improving recovery

Group 1 cells: the epidermal membrane in cell 1B was almost certainly damaged as the permeation rate was rapid and 88% of the applied dose had permeated by 48 hours. In comparison, cell 1A showed a relatively low rate of ME permeation, and only 35% had permeated by 48 hours. For the cell assessed under the same conditions in section 6.3.6, 56% had permeated at the same time-point. The difference may be due to inter-donor variation in

skin permeability and/or a lack of reproducibility in the method used. Compartment data for cell 1B was of little significance due to the very high amounts permeated. Cell 1A showed higher values than usual in the skin, and the trapping device contained ~27%. Total recovery at 71.5% was still low and the permeation profile was affected by the occlusive conditions.

Group 2 cells: the permeation profiles were fairly similar to unoccluded cells performed in an earlier study, although total amounts permeated were higher. Unfortunately the trapping method did not improve overall recoveries to an acceptable level.

Group 3 cells: the permeation of ME for these cells showed good reproducibility, but the profiles were very different to the unoccluded situation, with permeation profiles more similar in shape to the occlusive conditions in section 6.3.5, despite the vehicle having evaporated in this case. By 48 hours the amounts permeated were reasonable, at ~30%, but skin levels may have been slightly elevated and overall recoveries were low. The recovery of 15% of the applied dose in the charcoal after chloroform extraction produced a recovery value of 54% for cell 3B, and cell 3A would be expected to reach similar levels if that procedure had been followed. However, the trapping method was clearly not a good model for the unoccluded situation.

6.3.8 Conclusions

The results of the above experimental investigations showed that the method of trapping evaporating material greatly affected permeation and distribution of applied fragrance.

None of the methods assessed provided passive collection of evaporating material and altered skin penetration compared to the unoccluded situation. They also added considerable complexity to the experimental design. A different approach was, therefore, required.

6.4 Simultaneous collection of evaporating material from several cells

The possibility of simultaneous collection of evaporating fragrance from several cells was investigated in the following manner. The waterbath in which diffusion cells were placed (Figure 6.6) was covered with a perspex sheet of matching dimensions (53 x 33 cm).

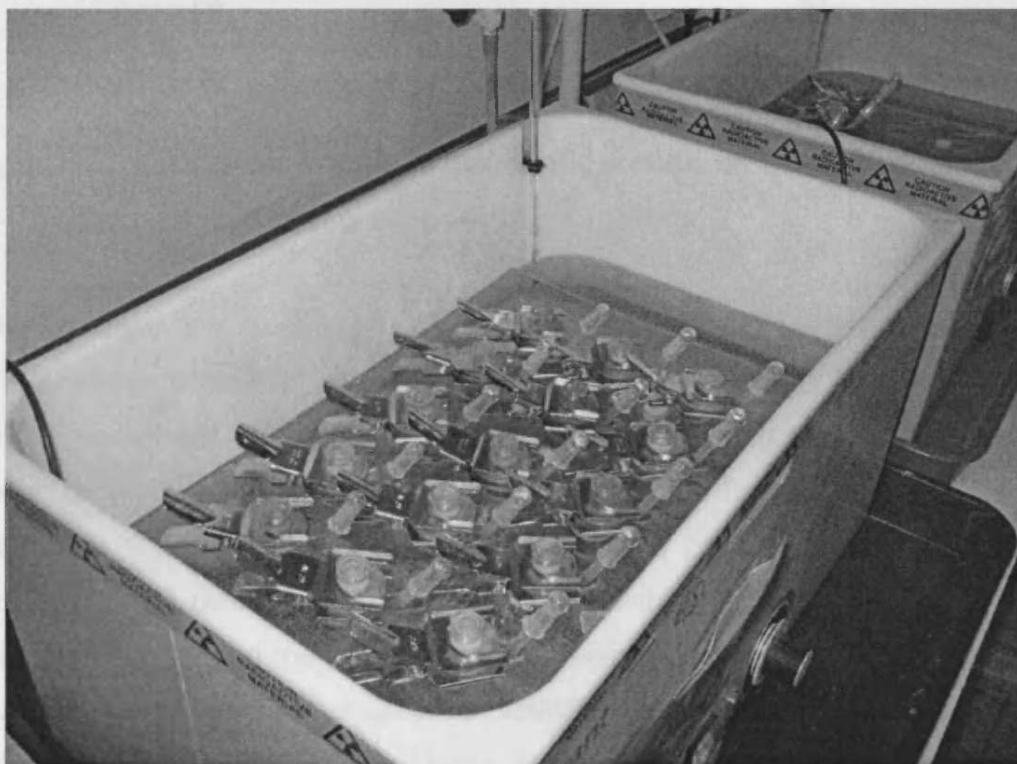


Figure 6.6 A typical experimental set-up (occluded cells in this case)

Flexible sealing strips were attached to the perspex sheet with three 0.75 cm gaps on one side (to function as air inlets), and three similar gaps on the opposite edge (air outlets). Gaps were also created for the stirrer bed cable and a hole drilled through the perspex to allow use of the thermometer. Plastic tubing was inserted into the air outlets and SKC Anasorb sorbent tubes attached. These were then connected to a low vacuum via a double liquid trap (containing water).

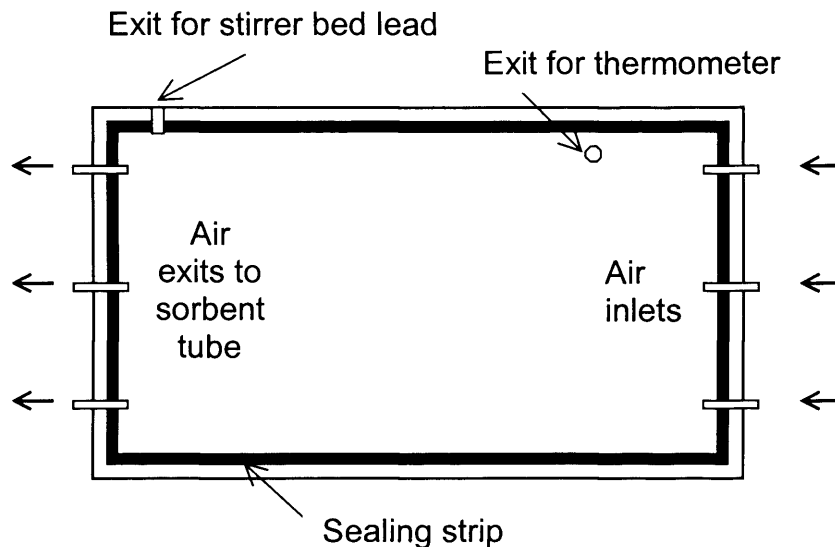


Figure 6.7 Diagram showing the configuration of the waterbath cover for collecting evaporating fragrance

Shortly after the waterbath was turned on (37°C setting), significant condensation problems began to occur, with large droplets of water forming on the perspex. Despite an increase in vacuum setting (to improve airflow) water droplets soon entered the sorbent tubes, which would make them ineffective. Modification of the perspex sheet to provide a slope (for water droplets to run down) did not prevent water entering the sorbent tubes. The very high humidity in the waterbath would also probably have greatly affected skin permeation and evaporation of volatile compounds. This approach was therefore rejected without quantitative assessment using diffusion cells.

6.5 Methods of estimating evaporative loss

6.5.1 Introduction

In light of the difficulties encountered in trapping evaporating material without altering skin penetration, an experimental method of estimating evaporative loss under conditions as similar to those for an unoccluded skin penetration study appeared attractive. The volatile fragrance material methyl eugenol (ME

test vehicle 2) continued to be used for this work, but the applied dose was reduced to a more realistic in-use value of 20 $\mu\text{l}/\text{cm}^2$.

6.5.2 Materials and equipment

As described in section 6.3.2 plus polytetrafluoroethylene (PTFE) sheet (1.5 mm thick, 600 x 300 mm) was obtained from RS Components Ltd. (Corby, UK), and glass coverslips (20 x 20 mm) were from Merck.

6.5.3 Evaporative loss method 1

6.5.3.1 Diffusion cell preparation and ME dosing

Six diffusion cells were prepared containing glass coverslips instead of a skin membrane. The cells were not greased, and receptor chambers were filled with water. The cells were placed in a waterbath (at 37°C) as described previously and a 1 cm^2 square of filter paper placed on the exposed coverslip surface. 20 μl of 1% ME in ethanol (vehicle 2) was applied to the filter paper in each cell using a 25 μl Hamilton syringe.

6.5.3.2 Cell sampling

One diffusion cell was dismantled at each of the following time-points after dosing: 5 minutes, 30 minutes, 1, 3, 6 and 24 hours.

The filter paper was placed in a vial, extracted with IMS (10 ml), and a sample (~200 μl accurately weighed) counted for ^{14}C . The coverslip and donor chamber were wiped with IMS wetted cotton buds, the wipes extracted (1 ml IMS) and a sample counted as above.

6.5.3.3 Results for evaporative loss method 1

Evaporation of the applied ME from the filter papers was relatively low, with the 24 hour sample still containing 88.6% of the applied dose. Very little of the fragrance was recovered from the coverslip and donor chamber wipe. These recoveries indicated that the filter paper was either sequestering the fragrance or that some surface adsorption process was occurring. This method was not predictive of evaporation from the skin surface, and overall recoveries of applied fragrance are presented in Table 6.2.

Table 6.2 Recovery of ME from filter paper and diffusion cell for evaporative loss method 1 (% of the applied dose)

Time	Filter paper (%)	Donor chamber and coverslip (%)	Total recovery (%)
5 minutes	100.47	0.04	100.51
30 minutes	90.84	0.24	91.08
1 hour	92.91	0.49	93.40
3 hours	98.47	0.04	98.51
6 hours	95.26	0.12	95.39
24 hours	88.60	0.14	88.74

6.5.4 Evaporative loss method 2

6.5.4.1 Diffusion cell preparation and ME dosing

Seven diffusion cells were prepared as described in section 6.5.3.1, except that filter paper squares were not applied to the coverslip surface. The ME solution was applied directly to the coverslip.

6.5.4.2 Cell sampling

One diffusion cell was dismantled at each of the following time-points after dosing: 5 minutes, 30 minutes, 1, 3, 4.5, 24 and 48 hours.

The coverslip was wiped with four IMS dampened cotton buds, the wipes extracted with IMS (5 ml), and a sample (~200 μ l accurately weighed) counted for ^{14}C . The donor chamber was wiped with two IMS wetted cotton buds, the wipes extracted (5 ml IMS) and a sample counted as above.

6.5.4.3 Results for evaporative loss method 2

Recovery of applied ME from the coverslip surfaces and diffusion cell donor chambers were very variable (Table 6.3). The overall trend appeared to be that ME was gradually lost via evaporation, but the technique was not reproducible. The wiping process may have been responsible for the poor recoveries at early time-points. A soaking process may improve recoveries but the coverslips were fragile and difficult to handle.

Table 6.3 Recovery of ME from coverslip surface and diffusion cell for evaporative loss method 2 (% of the applied dose)

Time	Coverslip wipe (%)	Donor chamber wipe (%)	Total recovery (%)
5 minutes	71.50	4.23	75.72
30 minutes	13.08	4.94	18.02
1 hour	40.41	0.78	41.18
3 hours	4.28	0.85	5.13
4.5 hours	30.37	2.50	32.88
24 hours	2.63	0.08	2.70
48 hours	1.52	0.24	1.76

6.5.5 Evaporative loss method 3

6.5.5.1 Diffusion cell preparation and ME dosing

Six diffusion cells were prepared as described in section 6.5.4.1, except that a square section (approximately 25 x 25 mm) of PTFE sheet replaced the coverslip. The PTFE sheet was the thinnest available (1.5 mm). The ME solution (20 μ l) was applied directly to the PTFE sheet.

6.5.5.2 Cell sampling

One diffusion cell was dismantled at each of the following time-points after dosing: 37 minutes, 65 minutes, 2, 5, 24 and 48 hours.

The PTFE sheet was carefully removed from the diffusion cell and the underside wiped with tissue to remove any adhering receptor phase. The PTFE sheet was then placed in a glass beaker and IMS (10 ml) added. The beaker was agitated and the PTFE sheet turned over several times with forceps. The wash solution was transferred to a vial, then the PTFE sheet washed again with IMS (5 ml). The donor chamber was similarly washed once with IMS (15 ml). Samples (~1 ml accurately weighed) of the two PTFE wash solutions and donor chamber wash were counted for ^{14}C .

6.5.5.3 Results for evaporative loss method 3

The combined recovery of applied ME at each time-point from the PTFE surfaces and diffusion cell donor chambers up to 24 hours is shown in Figure 6.8. Little additional material was lost between 24 and 48 hours (Table 6.4). The initial assessment of this method of estimating evaporative loss (from skin during penetration studies) was very encouraging, and subsequent comparison with skin penetration measurements showed the value of this method. It should be noted that this method probably overestimates the loss through evaporation, as the surface material is not reducing through absorption.

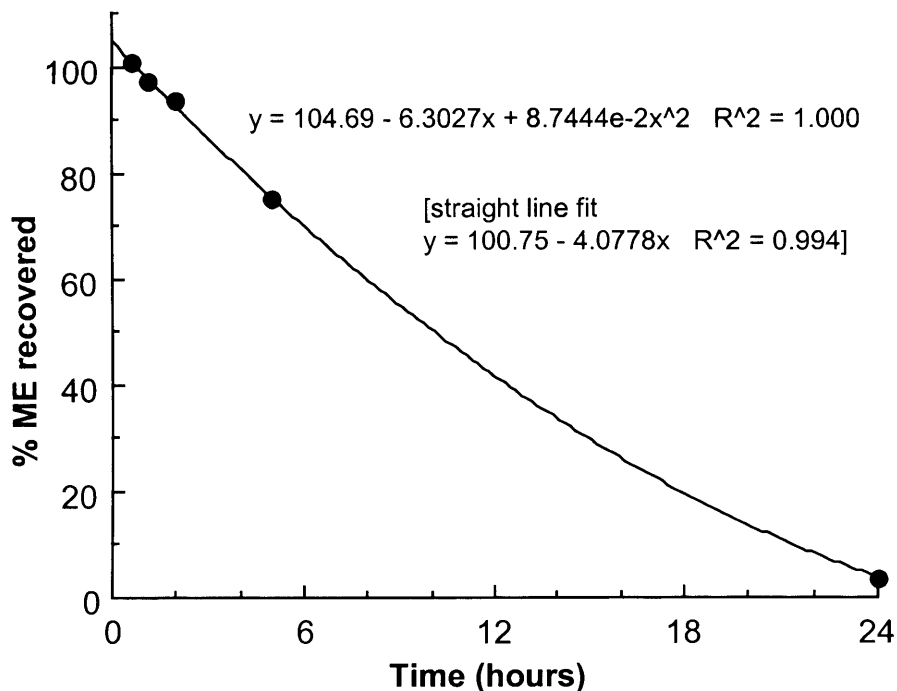


Figure 6.8 Combined recovery of ME up to 24 hours for evaporative loss method 3 (% of the applied dose)

Table 6.4 Recovery of ME from PTFE surface and diffusion cell for evaporative loss method 3 (% of the applied dose)

Time	PTFE wash 1 (%)	PTFE wash 2 (%)	DC wash 1 (%)	Total recovery (%)
37 minutes	98.13	2.49	0.36	100.98
65 minutes	95.72	1.01	0.29	97.01
2 hour	91.13	1.02	1.32	93.47
5 hours	73.86	0.77	0.45	75.08
24 hours	2.15	0.04	1.58	3.77
48 hours	1.76	0.04	0.19	1.99

6.6 Comparison of the final estimation of evaporative loss method with fragrance material skin permeation

The developed method for estimating evaporative loss using PTFE sheet mounted in a diffusion cell was subsequently used for several contract studies in our laboratories. The results of three such studies are currently being

prepared for publication. Comparison of skin permeation versus evaporative loss for two fragrance materials are discussed below.

The human skin permeation and distribution of the fragrances were performed using in-use $5 \mu\text{l}/\text{cm}^2$ doses of fragrance in 7/3 (v/v) ethanol/water (unoccluded). The evaporative loss was estimated from a $5 \mu\text{l}$ dose applied to the PTFE containing cells.

6.6.1 Fragrance 1 (very volatile)

Recovery of applied fragrance in the skin penetration study at 24 hours was low at $14.1 \pm 0.4\%$. The permeation profile is shown in Figure 6.9 and the estimation of evaporative loss in Figure 6.10. The distribution of fragrance in all analysed compartments for the skin penetration study is presented in Figure 6.11. Evaporative loss was clearly confirmed as the reason that the rate of permeation through the skin began to plateau after a short period of time and fully explained the poor overall recovery.

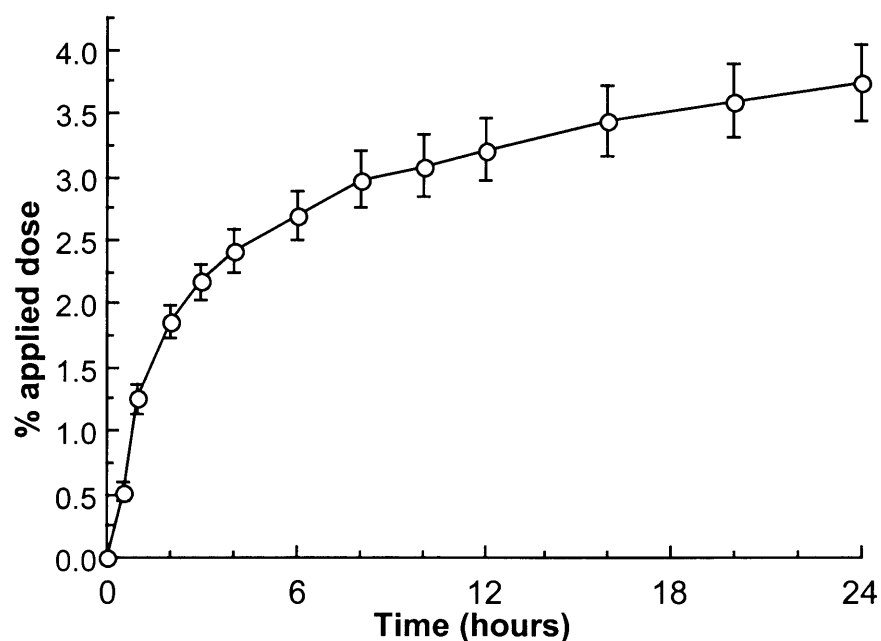


Figure 6.9 Permeation of fragrance 1 through human skin *in vitro* (n=12, mean \pm SE)

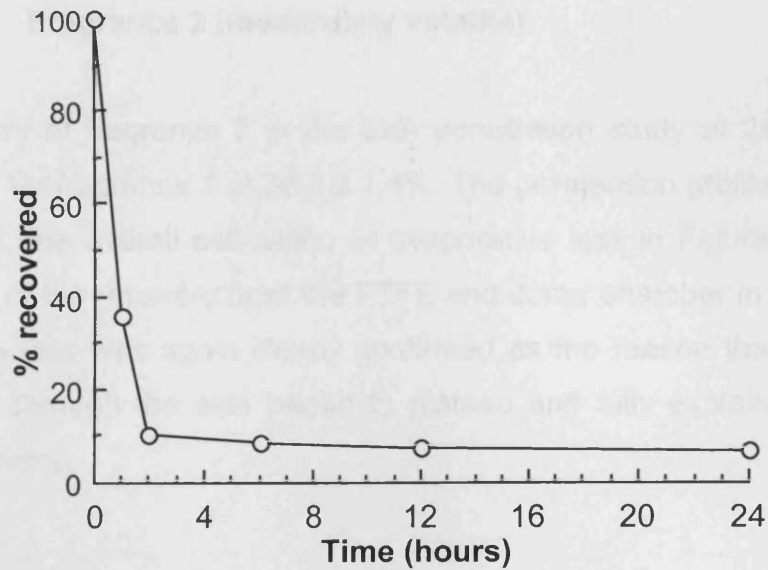


Figure 6.10 Estimation of evaporative loss for fragrance 1 using PFTE sheets mounted in diffusion cells

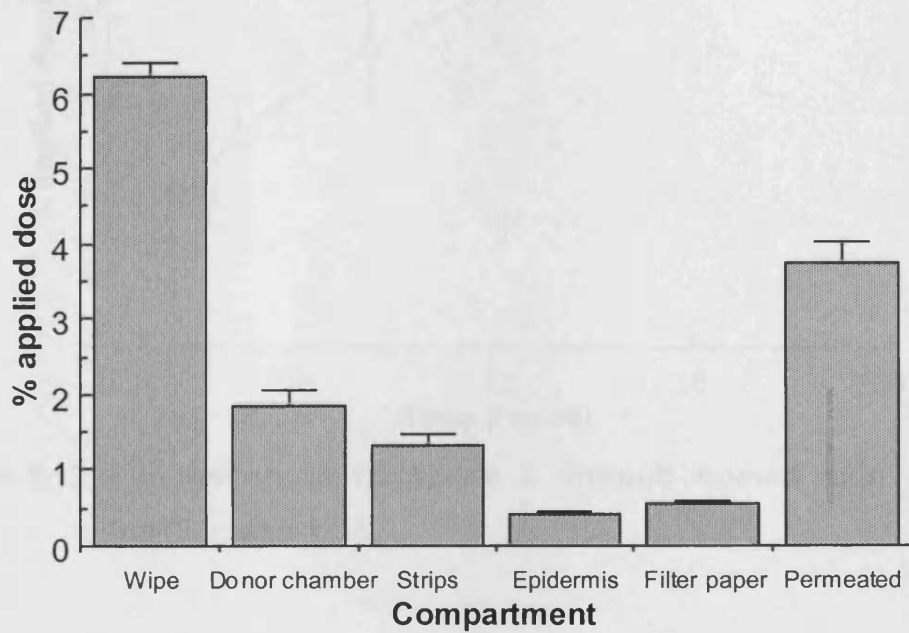


Figure 6.11 Recovery of fragrance 1 in all compartments (n=12, mean \pm SE)

6.6.2 Fragrance 2 (moderately volatile)

The recovery of fragrance 2 in the skin penetration study at 24 hours was higher than for fragrance 1 at $36.3 \pm 1.4\%$. The permeation profile is shown in Figure 6.12, the overall estimation of evaporative loss in Figure 6.13 and a breakdown of the recovery from the PTFE and donor chamber in Figure 6.14. Evaporative loss was again clearly confirmed as the reason that the rate of permeation through the skin began to plateau and fully explained the poor overall recovery.

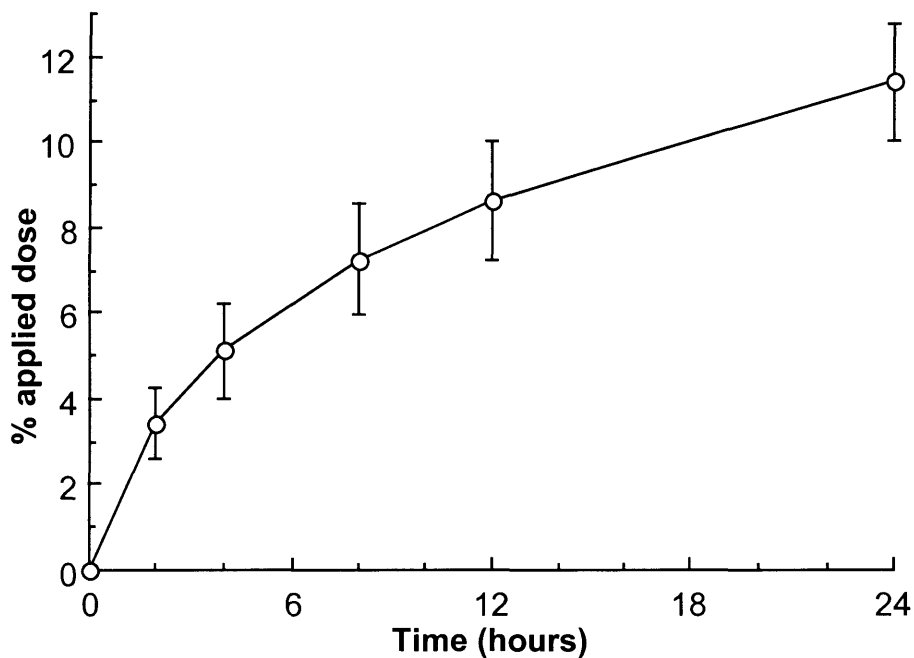


Figure 6.12 Permeation of fragrance 2 through human skin *in vitro* (n=12, mean \pm SE)

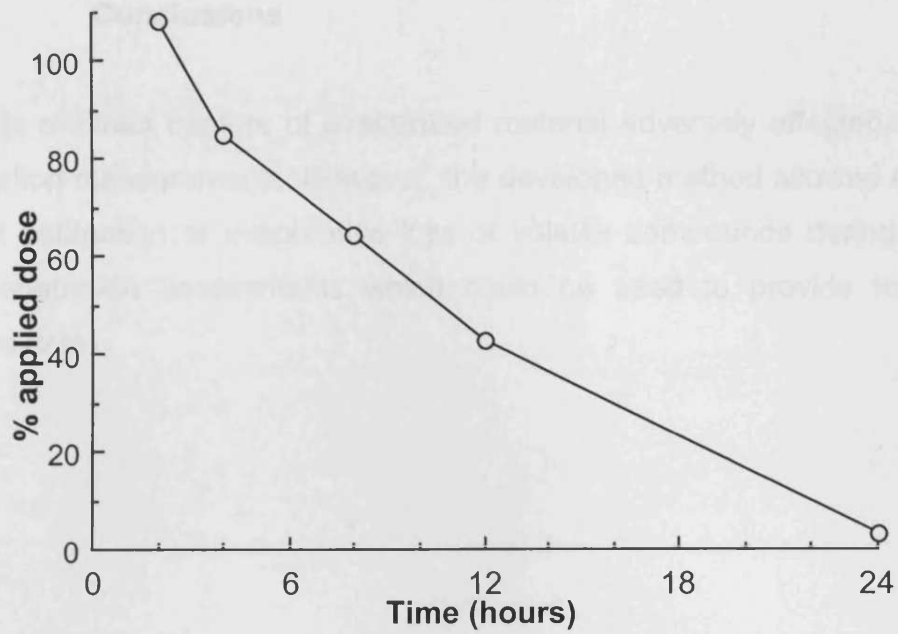


Figure 6.13 Estimation of evaporative loss for fragrance 2 using PFTE sheets mounted in diffusion cells

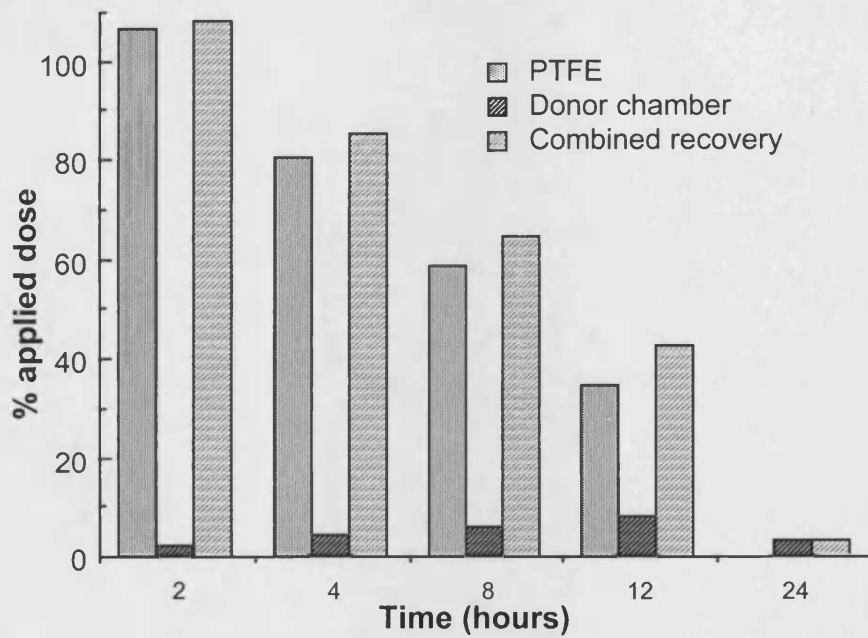


Figure 6.14 Recovery of fragrance 2 from PFTE sheets and the diffusion cell donor chambers

6.7 Conclusions

Methods of direct capture of evaporated material adversely affected the skin penetration measurements. However, the developed method allowed effective indirect estimation of evaporative loss of volatile compounds during *in vitro* skin penetration assessments which could be used to provide full mass balance data.

6.8 References

Burfield (2004). Opinion document to NAHA: a Brief Safety Guidance on Essential Oils. Updated from a document written for IFA, Sept 2004. Through; http://www.naha.org/articles/brief_safety%20guidance%20.htm, accessed 061005.

IFRA (2002). Notification of IFRA standards no. 2, 36th Amendment to the IFRA Code of Practice. Through; http://www.ifraorg.org/Enclosures/News/36th%20Amendment_IFRA%20Code%20of%20Practice.pdf, accessed 061005.

Frantz, S.W., Ballantyne, B., Beskitt, J.L., Tallant, M.J. and Greco, R.J. (1995) Pharmacokinetics of 2-ethyl-1,3-hexanediol. III. In vitro skin penetration comparisons using the excised skin of humans, rats, and rabbits. *Fundam. Appl. Toxicol.*, **28**, 1-8.

Kasting, G.B and Saiyasombati, P. (2001). A physico-chemical properties based model for estimating evaporation and absorption rates of perfumes from skin. *Int. J. Cosm. Sci.*, **23**, 49-58.

National Toxicology Program (2002), Methyleugenol CAS No. 93-15-2. Through; <http://ntp.niehs.nih.gov/ntp/roc/elevnth/profiles/s109meth.pdf>, accessed 061005.

Lockley, D.J., Howes, D. and Williams, F.M. (2002). Percutaneous penetration and Metabolism of 2-Ethoxyethanol. *Toxicol. Appl. Pharm.*, **180**, 74–82.

OECD test guideline 428 (2004). OECD guideline for the testing of chemicals; Skin absorption: *in vitro* method. OECD, Paris.

Reifenrath, W.G. and Robinson, P.B. (1982). *In vitro* skin evaporation and penetration characteristics of mosquito repellents. *J. Pharm. Sci.*, **71**, 1014-1018.

SCCNFP (2003). Basic criteria for the *in vitro* assessment of dermal absorption of cosmetic ingredients, SCCNFP/0750/03. SCCNFP, Brussels.

Yourick, J.J., Hood, H.L. and Bronaugh, R.L. (1999). Percutaneous absorption of fragrances. Chapter 39 in, *Percutaneous Absorption*, 3rd Edition, Bronaugh R.L. and Maibach H.I. (Eds), Marcel Dekker, Inc., New York. p673-684.

Chapter 7

Comparison between the pre-study water permeability of human skin membranes and subsequent permeation of alternative test compounds

7.1 Introduction

Work reported in Chapter 3 identified a possible correlation between water permeability, measured in the membrane integrity check, and test compound permeation (DEET) for some retarder dosed cells (see section 3.5). The correlation was closest when the retarder was co-administered with DEET ($r^2 = 0.92$), with higher water permeability closely indicative of higher DEET permeation. The corresponding control group did not show correlation ($r^2 = 0.09$), i.e. high water permeability did not indicate that high DEET permeation would subsequently be observed. Whether this finding was of any significance was not clear, as there are few published reports of correlation between water permeability and test compound permeation (see below). Therefore, a comparison between measured water permeability and test compound permeation in several studies in our laboratories was performed.

7.2 Review of published data

Bronaugh et al (1986) reported that skin samples of higher pre-study water permeability (compared to less permeable control samples from the same donor) showed higher permeation for all of the seven varied compounds assessed ($n=5$ for each compound). The degree of correlation between the two measurements appeared to vary widely (Figure 7.1, Bronaugh 1989, same data as Bronaugh et al, 1986), but was reasonably close for five permeants. The increase in pre-study water permeability was significantly different at the 95% confidence level (t test, $p < 0.05$) to the increase in permeation of test compound for cortisone and dichloro-diphenyl-trichloroethane (DDT). Cortisone permeation was far lower than predicted by

the water permeability, whereas DDT was much greater than expected. Bronaugh et al (1986) concluded that permeability measurements were a good indicator of general changes in barrier integrity for both polar and non-polar test compounds. The very limited reporting of data and experimental methods for this section of their work limited exploration of the correlation between water permeability and test compound permeation in their study.

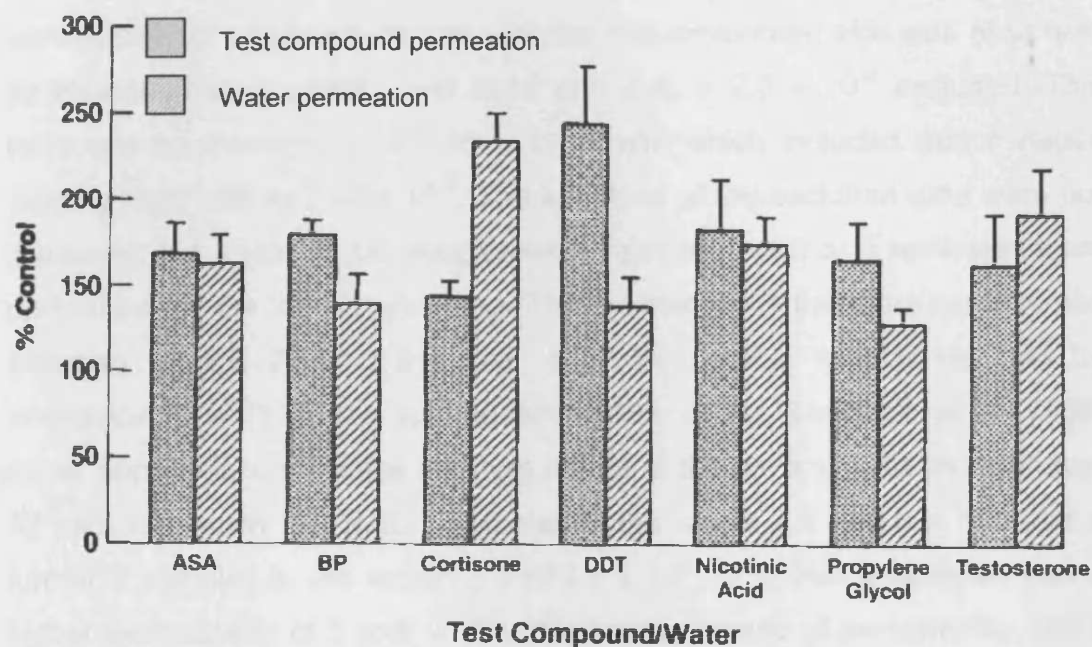


Figure 7.1 Water permeation as an indicator for permeation of other compounds (% increase compared to control samples of skin from the same donor with lower water permeability; modified from Bronaugh, 1989); ASA is acetylsalicylic acid, BP benzo(a)pyrene and DDT dichloro-diphenyl-trichloroethane

A typical water permeability coefficient rejection value is 2.5×10^{-3} cm/h and this was first suggested by Bronaugh et al (1986). This value was chosen as historically most k_p values ranged from 0.5 to 2.5×10^{-3} , and therefore skin with values above this were arbitrarily considered to be damaged (Bronaugh et al, 1986). However, there is evidence that this value is too limiting, and may reject samples within the normal permeability range. Williams et al (1992)

suggested that permeability coefficients *in vitro* might follow more closely a log-normal rather than normal distribution. Watkinson et al (1998) showed the distribution of water permeabilities for a total of ~800 determinations performed in two laboratories. The inter-laboratory profiles were reported to be virtually indistinguishable (Watkinson et al, 1998). No natural k_p cut-off point at 2.5×10^{-3} cm/h was apparent, and this value would reject 16% of samples, with ~5% of samples between 2.5 and 6×10^{-3} cm/h. The water permeability of previously frozen samples of dermatomed skin was assessed by Bronaugh et al (1986), and cells with a $k_p > 2.5 \times 10^{-3}$ excluded. This produced an average k_p of 1.55×10^{-3} cm/h, which included donor values ranging from 0.69 to 2.42×10^{-3} . The k_p values of the excluded data were not disclosed, but a total of 16 samples were rejected and 2 or 3 replicates were performed for the 33 donors listed. The rejected cells therefore represented between 14 and 20% of the total, a similar number to that reported by Watkinson et al (1998). A subsequent section of the Bronaugh et al (1986) paper appeared to show the arbitrary nature of the set limit with an estimated 32 samples within the limit, 7 samples in the range 2.5 to 3.0×10^{-3} and a further 7 samples in the region 3.2 to 4.1×10^{-3} . A further 6 samples had a higher permeability of 5 to 6×10^{-3} . Given this spread of permeability, there appears little evidence that skin membranes with a $k_p > 2.5 \times 10^{-3}$ are necessarily significantly damaged.

A strong correlation ($r^2 = 0.82$) between concurrent water and lidocaine flux through dermatomed ($150 \mu\text{m}$) human skin was reported by Kushla and Zatz (1991). Skin was obtained from cadavers, amputated limbs and following an abdominoplasty. Sites varied between leg (3 donors), midline chest (2 donors) and abdominal (1 donor, elective surgery). Tritiated water and ^{14}C -lidocaine were simultaneously applied, and the resulting flux plotted (Figure 7.2, source Kushla and Zatz, 1991). Two distinct regions are visible in the graph. Four of the six donors showed average lidocaine flux of between approximately 125 and $150 \mu\text{g}/\text{cm}^2\text{h}$, and these fluxes did not correlate with the corresponding water flux, which ranged between approximately 1.6 and $3.6 \text{ mg}/\text{cm}^2\text{h}$. The remaining two donors showed significantly higher lidocaine and water fluxes.

However, average water flux for these donors was high (approximately 5.1 and 6.2 mg/cm²h), perhaps indicating poor membrane integrity, which may explain the higher lidocaine flux. When measuring the permeation of water in membrane integrity tests the average water flux for an individual donor is typically well below 2.5 mg/cm²h, although this is usually for breast and abdominal tissue. The tissue samples used in the above study were predominately from amputated legs, and the effect of disease state on the tissue permeability is unknown. Thirty percent of the cells prepared used skin from a female, age 92 years, race: Caucasian, site: leg, and a further thirty percent were from a female, age 54 years, race: Black, site: leg. This all suggested that the reported strong correlation between water flux and lidocaine flux might, in fact, be an experimental artefact due to unusual skin samples.

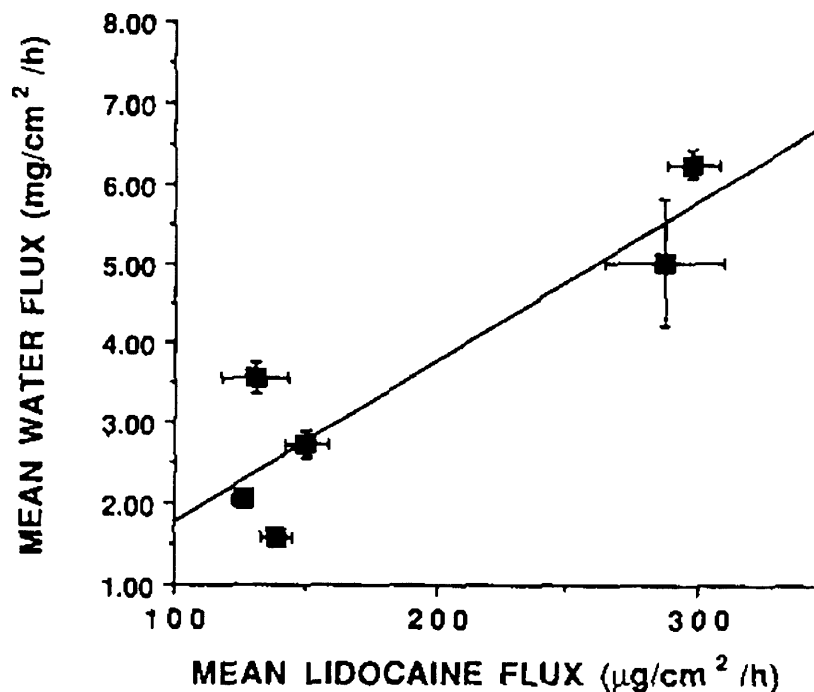


Figure 7.2 Water flux versus lidocaine flux for six skin donors (mean \pm SE; n typically = 4; Kushla and Zatz, 1991)

A recent review (Levin and Maibach, 2005) has explored the correlation between transepidermal water loss (TEWL) and percutaneous absorption

measurements. TEWL is the normal water loss from the skin in the absence of sweat gland activity (Chilcott et al, 2002). The review summarised that both TEWL and percutaneous absorption rates increased when the barrier function was compromised but that “experiments to discern a quantitative and/or qualitative correlation between the two indicators have resulted in controversy” (Levin and Maibach, 2005). The majority of the data reviewed was for *in vivo* studies and they all showed a quantitative correlation between TEWL and test compound absorption. However, this correlation was not observed in two *in vitro* studies. A hairless mouse study showed a correlation ($r = 0.72$ to 0.86) for compounds with $\log K_{o/w}$ -3.7 to 2.7 , but no correlation ($r = 0.01$) for a compound of high lipophilicity ($\log K_{o/w}$ 3.9). A human and pig skin study (Chilcott et al, 2002) showed no correlation between TEWL and tritiated water permeation for human skin and pig skin, or TEWL and lipophilic sulfur mustard permeation for human skin. The lack of any correlation between TEWL and water permeation is perhaps most surprising, as TEWL is used by some workers as a membrane integrity test instead of the more commonly used measurement of tritiated water permeation. Indeed, Chilcott et al (2002) went on to state that “TEWL rates cannot be used as a tool to evaluate epidermal membrane integrity prior to *in vitro* percutaneous absorption experiments using epidermal membranes or full-thickness skin”.

7.3 Comparison of water permeability and test compound permeation for studies in our laboratory

Many contract studies performed in our laboratory have used a tritiated water membrane integrity check prior to assessment of the *in vitro* skin penetration of a test compound. The results of the membrane integrity check are used in one of two ways depending upon the study protocol. Membranes (in diffusion cells) are either rejected if water permeability is above a pre-determined value (and are therefore not dosed with test compound), or all cells are dosed with test compound and the initial membrane integrity check provides assistance in determining whether a cell should be considered an outlier, should the test compound permeation appear abnormal.

Where a k_p rejection value was set, the value of 2.5×10^{-3} cm/h was most often used, despite the possible limitations of this value (see above). It should be noted that many cells exhibit water permeability slightly greater than this, although obviously damaged membranes may have a water permeability approaching 100×10^{-3} cm/h. For studies where cells with a $k_p > 2.5 \times 10^{-3}$ cm/h had been dosed with test compound, the validity, or otherwise, of the normal k_p cut-off may become apparent on examination of the test compound permeation data.

The study data discussed below was performed with the assistance, at various times, of the following colleagues; Sally I. Brain, Kenneth A. Walters and Keith R. Brain. The identity of each test compound cannot be disclosed for reasons of confidentiality, but pertinent information is provided including approximate molecular weight and approximate lipophilicity (where known).

7.3.1 Methods of measurement of water permeability and test compound permeation

The tritiated water membrane integrity for the data below was typically performed by applying 500 μ l of tritiated water (2 μ Ci/ml) to the skin surface, removing a receptor phase sample 1 hour later, and counting it for 3 H. The calculated water permeability coefficient values, k_p , are presented as values $\times 10^{-3}$ (cm/h). The measured values may slightly underestimate k_p due to the lag time prior to steady state, which may also be greater for full thickness skin than epidermal membranes.

Test compound permeation was measured by removing receptor phase samples at various time-points and analysing either via HPLC analysis or liquid scintillation counting for radiolabelled (14 C) permeants.

7.3.2 Methods of comparison

The comparison approaches used in section 3.5 appeared to have validity but were slightly modified here. To allow easy comparison between studies, the permeation data for each study were normalised, as test compound permeation can vary by several orders of magnitude depending upon the permeant and the application conditions. The normalisation process presents the data for each test group as the percent of the average permeated for that group. This process does not change the variability in the data, with %RSD unchanged.

Where finite doses of test material (typically 5 mg/cm²) were applied to the skin surface, the % of the applied dose permeated data were used, as this corrects for the unavoidable small variations in the applied dose. Either the final time-point data was used (24 or 48 hours) or, where the permeation rate may have begun to plateau (usually due to donor depletion), data from the previous time-point were used. For infinite dose studies, % of the applied dose is not relevant and amounts permeated were used (typically µg/cm²).

Comparisons were performed in Microsoft Excel 97 (Windows XP) and Microsoft Excel X (Mac OS X). The data were assessed in two ways for each test group (i.e. for cells dosed with the same test compound and vehicle/formulation):

- (i) Linear regression analysis was performed on normalised values of test compound permeated (% of the average for the group) versus measured water permeability for each individual cell. Correlation coefficient squared, r^2 , gradient and y-axis intercept were noted.
- (ii) Simple comparison of the %RSD in the normalised permeation data before and after dividing by the measured water permeability for each individual cell. A decrease in %RSD indicated correlation with water permeability.

For comparison type (i), the generated linear regression correlation coefficient squared, r^2 , gradient and y-axis intercept values were used together to determine whether test compound permeation and water permeability were in agreement. The sole use of r^2 does not provide suitable confirmation of experimental correlation. A generated example of this (Figure 7.3) shows that, despite an r^2 of precisely 1, a tripling of the skin membrane water permeability coefficient from 0.5 to 1.5×10^{-3} cm/h increased test compound permeation by a minimal amount (99.5 increased to 100.5%). Therefore, where r^2 indicated that the linear regression was a good fit, the gradient was inspected to confirm whether the test compound permeation and water permeability were actually in agreement.

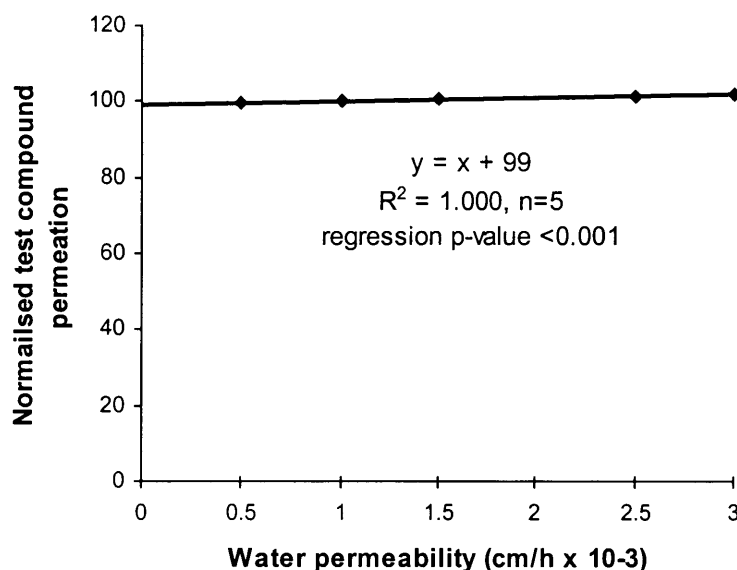


Figure 7.3 Generated example of test compound permeation versus water permeability showing no correlation despite the linear regression coefficient, $r^2 = 1.000$

Visual examples of comparison type (i) for experimental data presented in section 3.5 are shown below. Figure 7.4 shows good correlation ($r^2 = 0.92$, gradient = 63) between water permeability and DEET permeation for cells where retarder and DEET were co-administered. The control group (Figure 7.5) shows no such correlation ($r^2 = 0.09$, gradient = 13).

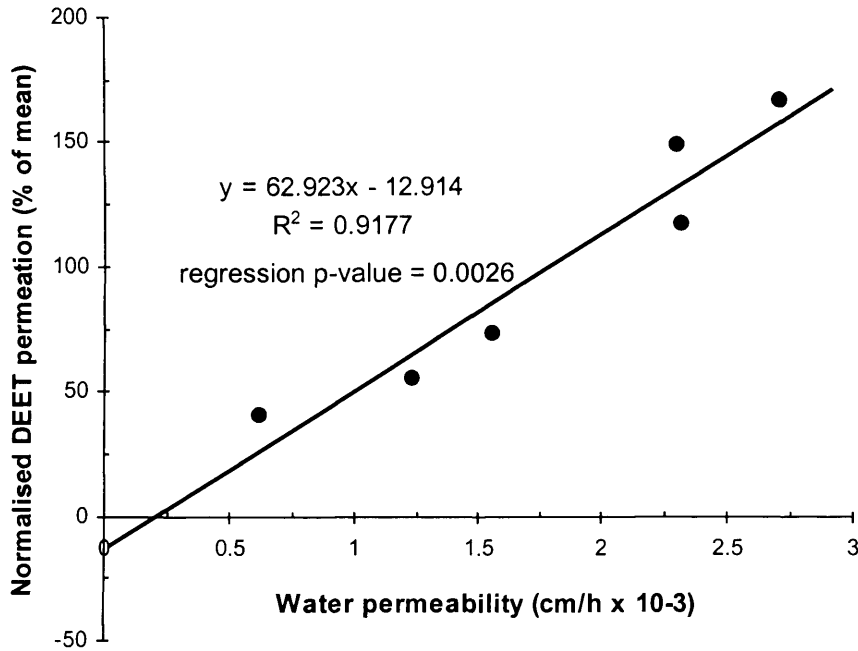


Figure 7.4 Comparison of DEET permeation to water permeability for co-administered retarder/DEET (see section 3.5), six replicates; good correlation observed

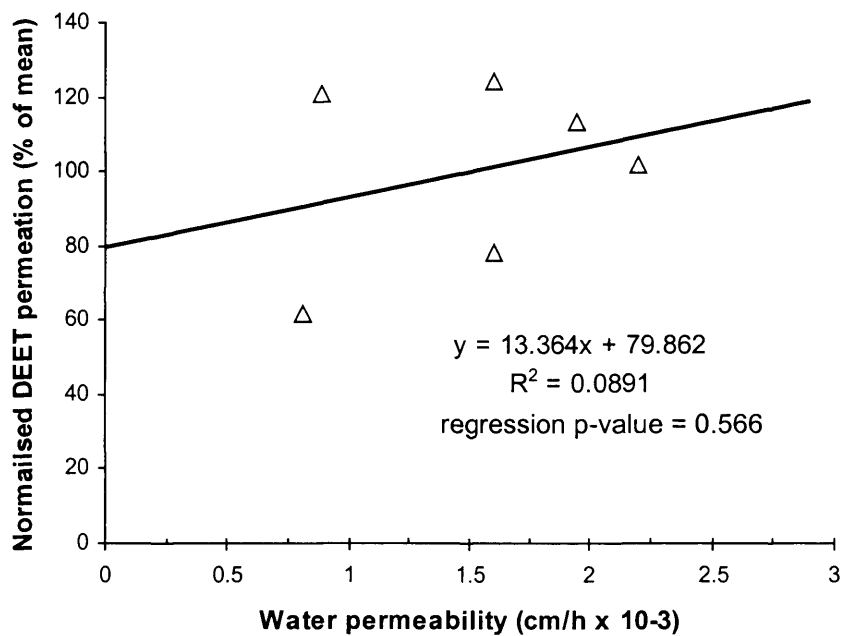


Figure 7.5 Comparison of DEET permeation to water permeability for DEET dosed control cells (see section 3.5), six replicates; no correlation observed

An example of comparison type (ii) for the same data (Table 7.1), shows that division of the normalised permeation data by k_p decreased the %RSD from 52% to 17% for the co-administered retarder/DEET group (indicating correlation), but the %RSD increased from 25 to 45% for the control group (indicating no correlation).

Table 7.1 Comparison of data variability with and without correction for water permeability, six replicates (data from section 3.5)

Replicate	Retarder/DEET group			DEET control group		
	Perm*	k_p **	Perm/ k_p	Perm*	k_p **	Perm/ k_p
1	54.9	1.24	44.3	78.4	1.60	48.9
2	166.7	2.72	61.3	113.4	1.95	58.2
3	116.6	2.32	50.2	101.7	2.20	46.3
4	40.2	0.62	64.7	61.6	0.81	76.0
5	149.1	2.30	64.7	120.7	0.88	136.9
6	72.6	1.56	46.4	124.2	1.60	77.8
Mean	100.0	1.79	55.3	100.0	1.51	74.0
SD	51.9	0.79	9.4	25.0	0.56	33.5
SE	21.2	0.32	3.8	10.2	0.23	13.7
%RSD	51.9	44.1	17.0	25.0	37.1	45.3

* - normalised DEET permeation (% of the mean for the group)

** - water permeability coefficient, k_p , ($\text{cm/h} \times 10^{-3}$)

7.3.3 Results

Analysis of data was performed preferentially for studies where large numbers of replicates (typically $n=12$) were run for each test group. Whilst calculations were performed separately for each group, it was also possible to plot test compound permeation versus water permeability for several larger groups.

7.3.3.1 Compounds of moderate to high lipophilicity

For twelve compounds that varied in molecular weight between ~150 and 270 and lipophilicity (measured or calculated $\log K_{o/w}$) between 1.4 and 7.0, no substantial correlation was found between test compound and water permeability. Correlation coefficients squared were all <0.5 and the data are

summarised in Table 7.2, including approximate molecular weight and log $K_{o/w}$. All groups used epidermal membranes prepared from, typically, 3 or 4 donors, and finite doses of test compound were applied.

Table 7.2 Comparison of test compound permeation with water permeability for 12 compounds of moderate to high lipophilicity

Test compound			Linear regression data*		
ID (n**)	Log $K_{o/w}$	M_w (approx.)	Gradient	Intercept	R^2
A (n=12)	1.4	190	5	94	0.005
B (n=12)	2.0	190	181	-102	0.477
C (n=12)	2.7	180	9	83	0.056
D (n=12)	2.9	200	73	28	0.497
E (n=12)	3.0	230	31	66	0.383
F (n=12)	3.1	150	16	66	0.411
G (n=12)	3.5	150	34	45	0.258
H (n=12)	4.8	250	51	41	0.418
I (n=12)	5.3	240	116	-7	0.313
J (n=11)	5.7	260	76	7	0.255
K (n=12)	5.9	260	63	8	0.325
L (n=12)	7.0	270	-4	106	0.001

* - linear regression analysis of normalised test compound permeation versus water permeability coefficient, k_p

** - n = number of replicates

The analysis (Table 7.2) showed that, whilst there was little evidence of a direct correlation between test compound permeation and k_p , for some groups, higher k_p did, on average, correlate with slightly higher test compound permeation. The effect of dividing the permeation data by k_p is shown in Table 7.3, and variability decreased in some groups but increased in others, with no apparent relationship with test compound lipophilicity. The magnitude of the change in data variability when applying correction for k_p appeared greatest for compounds up to a log $K_{o/w}$ of ~ 3 . Groups that showed a very poor correlation (r^2) between test compound permeation and k_p in Table 7.2 usually showed an increase in data variation when applying correction for k_p .

Table 7.3 Effect of dividing test compound permeation by the water permeability, k_p , on data set variability

Test compound			Permeation data variability (%RSD)		
ID (n*)	Log $K_{o/w}$	M_w (approx.)	Permeated	Permeated $\div k_p^{**}$	Difference ***
A (n=12)	1.4	190	21	36	+15
B (n=12)	2.0	190	74	59	-15
C (n=12)	2.7	180	34	55	+21
D (n=12)	2.9	200	43	34	-9
E (n=12)	3.0	230	36	52	+16
F (n=12)	3.1	150	38	45	+7
G (n=12)	3.5	150	24	26	+2
H (n=12)	4.8	250	44	35	-9
I (n=12)	5.3	240	32	28	-4
J (n=11)	5.7	260	53	48	-5
K (n=12)	5.9	260	49	42	-7
L (n=12)	7.0	270	40	43	+3

* - n = number of replicates

** - normalised test compound permeation divided by k_p

*** - difference in %RSD after dividing permeation data by k_p

Data for all 12 compounds were combined and plotted (Figures 7.6 and 7.7) as normalised test compound permeation versus water permeability coefficient. The linear regression coefficient was poor for the complete data set ($r^2 = 0.125$), but there was an overall trend of higher water permeability being associated with slightly higher test compound permeation, and this was marginally more prevalent ($r^2 = 0.148$) if the cells with $k_p > 2.5 \times 10^{-3}$ were excluded (Figure 7.7). However, a more significant point appeared to be that cells included with slightly elevated water permeability (k_p between 2.51 and 5.21×10^{-3}) did not correlate with increased test compound permeation ($r^2 = 0.089$). These cells were from groups C, E and F (log $K_{o/w}$ 2.7 – 3.1). The cell with the highest k_p (5.2×10^{-3}) was in the third centile of test compound permeation and it was not clear if this was significant. However, membranes with k_p 3.7 to 4.6×10^{-3} were of normal permeability for the compounds assessed, confirming the arbitrary nature of the 2.5×10^{-3} exclusion value. Several additional membranes with slightly elevated water permeability were rejected during the above studies, which was unfortunate, as they would have allowed the validity of the exclusion value to be probed further.

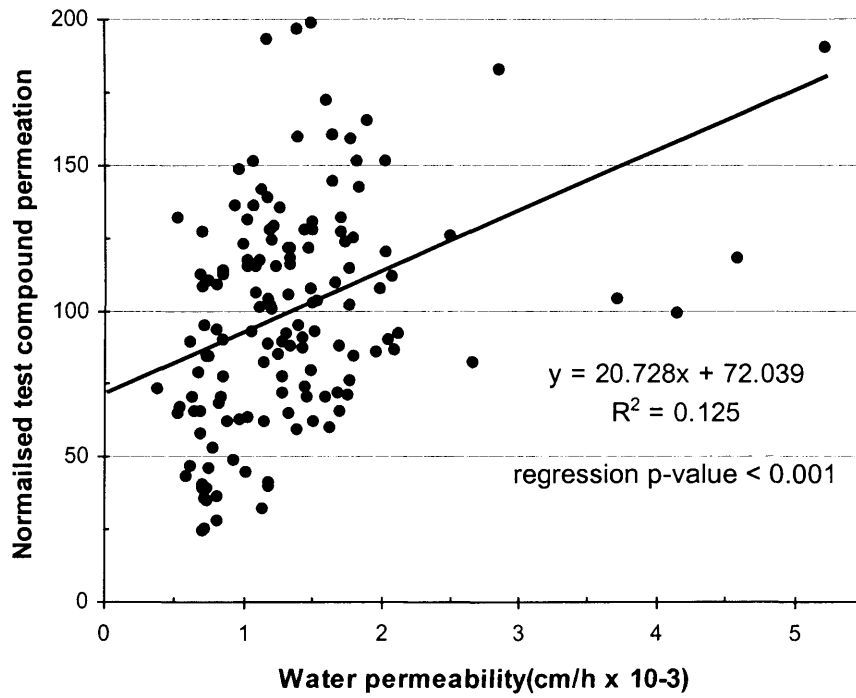


Figure 7.6 Normalised test compound permeation versus water permeability for 12 compounds; all cells (n=143)

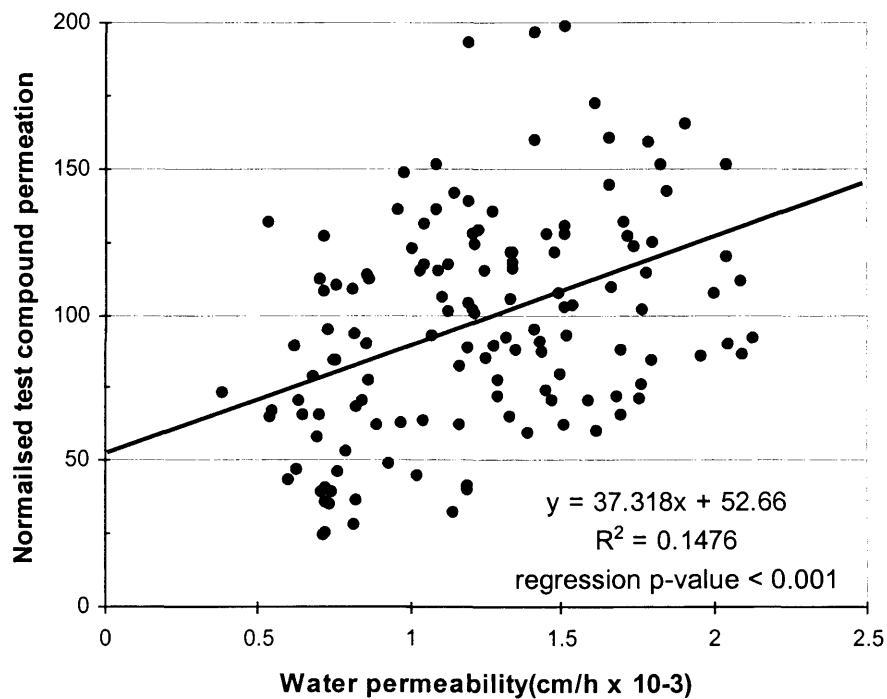


Figure 7.7 Normalised test compound permeation versus water permeability for 12 compounds; cells with water permeability $> 2.5 \times 10^{-3}$ excluded (n=136)

7.3.3.2 Compounds of low lipophilicity

Several studies have been performed for compounds of low lipophilicity where membrane integrity was also assessed. However, these studies were frequently for charged compounds, applied under in-use wash-off conditions where skin contact periods were short. The data from these studies were inspected and no correlation between test compound permeation and water k_p was observed. However, test compound permeation was typically very low, and I believe the conditions used do not make the data suitable for comparison as examples of typical low lipophilicity permeants.

7.3.3.3 Compounds applied in formulations containing a permeation enhancer

Studies have been performed where test compounds were co-applied in a vehicle containing the enhancer oleic acid (cis-9-octadecenoic acid). The results of these studies were evaluated to clarify whether there was a correlation between test compound permeation and water permeability, as possibly observed for retarder 4-F2/DEET co-administration (section 3.5).

The studies discussed here were performed with between 4 and 6 replicates per group, and a total of four groups used the same vehicle containing 2% oleic acid. In all cases the enhancer-containing vehicle delivered significantly more test compound through the skin membrane than the control vehicle (4 replicates).

The results of the data analysis (as outlined in section 7.3.2) indicated that for oleic acid enhanced permeation, there appeared to be reasonable correlation between test compound permeation and water permeability for three of the four groups (Table 7.4), but the lower number of replicates limited the value of these findings. For reference, data analysis of the control group has also been included in Table 7.4, but this group did appear particularly variable and a low

linear regression correlation coefficient, r^2 , was produced. This was possibly an experimental artefact due to the low number of replicates.

Table 7.4 Comparison of test compound permeation with water permeability for oleic acid enhanced vehicles

Group		Linear regression data*		
ID	n**	Gradient	Intercept	R ²
OA group 1	4	70	14	0.850
OA group 2	4	162	-110	0.878
OA group 3	4	43	43	0.208
OA group 4	6	94	12	0.501
Control group	4	102	-17	0.143

* - Linear regression analysis of normalised test compound permeation versus water permeability coefficient, k_p

** - number of replicates per group

Analysis of the effect of k_p correction on permeation data variability (Table 7.5) showed a reduction in variability for three of the four groups that was consistent with the linear regression analysis above.

Table 7.5 Comparison of test compound permeation with water permeability for oleic acid enhanced vehicles

Group		Permeation data variability (%RSD)		
ID	n*	Permeated	Permeated ÷ k_p **	Difference ***
OA group 1	4	48	18	-30
OA group 2	4	79	62	-17
OA group 3	4	39	46	+7
OA group 4	6	28	20	-8
Control group	4	109	114	+5

* - number of replicates per group

** - normalised test compound permeation divided by k_p

*** - difference in %RSD after dividing permeation data by k_p

Combining the data for all 18 cells (Figure 7.8) showed a closer relationship ($r^2 = 0.498$) between test compound permeation and water permeability than for other the larger comparisons in section 7.3.3.1, but the data set was relatively small.

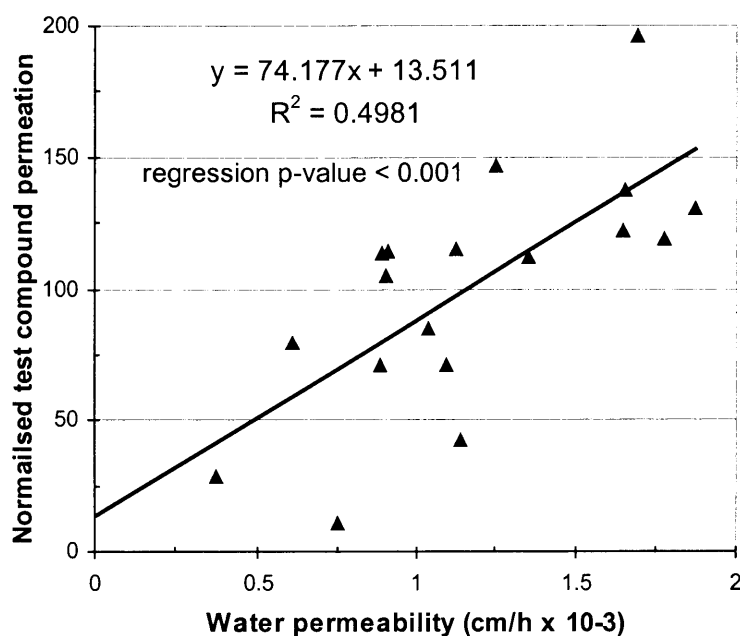


Figure 7.8 Normalised test compound permeation versus water permeability for groups using a 2% oleic acid vehicle (n=18)

7.4 Conclusions

There appeared to be little correlation between water permeability measurements (performed during membrane integrity assessments) and subsequent permeation of test compounds, for the assessed range of compounds ($\log K_{o/w} \sim 1.4 - 7$).

Further studies should be performed to clarify whether the membrane water permeability coefficient, k_p , rejection value of 2.5×10^{-3} cm/h typically used in many laboratories should be increased. The data presented here showed that membranes with higher k_p ($3.7 - 4.6 \times 10^{-3}$ cm/h) were of 'normal' permeability for compounds of $\log K_{o/w}$ 2.7 – 3.1, and a wider range of lipophilicities should be assessed.

It appears that skin barrier disruption (with enhancer compounds, such as oleic acid) or augmentation (with retarder compounds) may alter the relationship between test compound permeation and water permeability. Specifically, they may make water permeability measurements more indicative of test compound permeation, although studies with larger number of replicates may provide better evidence of this relationship.

7.5 References

Bronaugh R.L., Stewart, R.F. and Simon, M. (1986). Methods for in vitro percutaneous absorption studies VII: use of excised human skin. *J. Pharm. Sci.*, **75**, 1094-1097.

Bronaugh, R.L. (1989). Determination of percutaneous absorption by in vitro techniques, in *Percutaneous absorption: mechanisms – methodology – drug-delivery*, 2nd Ed. Bronaugh, R.L and Maibach H.I. (eds) pp. 239-258. Marcel Dekker, New York, USA.

Chilcott, R.P., Dalton, C.H., Emmanuel, A.J., Allen, C.E. and Bradley, S.T. (2002). Transepidermal water loss does not correlate with skin barrier function in vitro. *J. Invest. Dermatol.*, **118** (5), 871-875.

Kushla, G.P. and Zatz, J.L. (1991). Correlation of water and lidocaine flux enhancement by cationic surfactants in vitro. *J. Pharm. Sci.*, **80**, 1079-1083.

Levin, J. and Maibach, H (2005). The correlation between transepidermal water loss and percutaneous absorption: an overview. *J. Contr. Rel.*, **103**, 291-299.

Watkinson, A.C., Brain, K.R., Walters, K.A., Grabarz, R.S. and Sharma, R.K. (1998). Is it logical to reject skin samples based on water permeability data?, in *Perspectives in percutaneous penetration*, Vol. 6A. p62. STS Publishing, Cardiff.

Williams, A.C., Cornwell, P.A. and Barry, B.W. (1992). On the non-gaussian distribution of human skin permeabilities. *Int. J. Pharm.*, **86**, 69-77.

Chapter 8

General discussion

8.1 General discussion

The ability to safely modulate the skin penetration of an applied chemical would be beneficial in many circumstances. Penetration enhancers may allow effective delivery of drugs that cannot currently be delivered to therapeutic levels. Penetration retarders may provide additional personal protection from potentially toxic compounds such as pesticides and chemical warfare agents.

The likely modes of action of several existing, specifically designed, skin penetration enhancers were discussed in chapter 2. There are few specifically designed skin penetration retarders, and it appears that the only current commercial product is a liquid polymeric mixture to help retain topical actives on and in the skin surface.

Novel potential skin penetration retarder compounds, designed to augment the skin barrier through co-operative insertion into SC bilayers, were investigated in chapters 3 and 4 using four model permeants. Although some retardation was observed, this was not predictable and was dependent on application conditions. This raises the question of whether the skin barrier function really can be significantly, and reproducibly, improved. On the evidence reported here and by other workers, it seems unlikely that an effective generic retarder compound (designed to act through co-operative insertion into SC bilayers) could be developed. Nature clearly developed an excellent barrier for people with normal skin. However, for diseased skin, such as that seen in atopic dermatitis, there may be more opportunity to assist the compromised barrier function.

The investigation of skin sampling techniques in chapter 5 demonstrated the superiority of D-Squame discs over 3M Magic Tape for *in vitro* skin surface

tape stripping. However, a comparison of *in vitro* tape stripping using D-Squame, with published *in vivo* tape stripping data for a topical corticosteroid cream, was of limited value due to formulation inhomogeneity and limitations in the *in vivo* data. Future attempts to standardise tape stripping should use the new constant pressure application device, and methods to non-destructively assess the amount of tissue removed by each strip. As there are many variables that can have a significant influence on tape stripping efficiency, it is unlikely that any tape stripping method will ever provide unequivocal quantitative measurement of permeant content throughout the stratum corneum. However, tape stripping measurements may well provide useful semi-quantitative or qualitative assessments of permeant levels in the stratum corneum.

The limited investigations of an alternative *in vivo* skin surface sampling technique involving the removal of skin surface biopsies suggested that it is unlikely that the technique will be of much practical benefit in the detection of orally administered drugs.

The significance of estimation of the evaporative loss of volatile permeants, such as fragrances, during skin penetration studies was discussed in chapter 6. It was shown that direct capture of evaporating material significantly affected the amount that permeated through the skin membranes. Whilst the developed novel alternative model of evaporation during permeation still has limitations, it is of great practical value in identification of the cause of low recoveries for skin penetration studies assessing volatile permeants.

Correlations between pre-study skin membrane water permeability (used as a membrane integrity check in many laboratories) and subsequent test compound permeation were probed in chapter 7. Limited literature evidence suggested that skin membranes of higher pre-study water permeability would also be more permeable to subsequently applied compounds, regardless of differing physicochemical properties. This was shown to not be the case for twelve compounds of moderate to high lipophilicity. The investigations also

showed that the pre-study water permeability coefficient cut-off used to reject 'damaged' skin samples (2.5×10^{-3} (cm/h)) did not provide discrimination between normal and damaged membranes. This raised significant issues as to what should be considered 'normal' barrier function. Further investigations with compounds of a greater range of lipophilicities will be required to enable selection of an appropriate value.

In conclusion, it can be said that many issues remain in both the use of *in vitro* techniques to accurately assess *in vivo* dermal absorption of xenobiotics, and the development of barrier-modulating molecules. However, the work described in this thesis has added significantly to the available data in the area and has made useful practical contributions to the continued development of *in vitro* skin permeation technology.

